Appendix 7-B

Murray River Coal Project: Groundwater Modelling Report

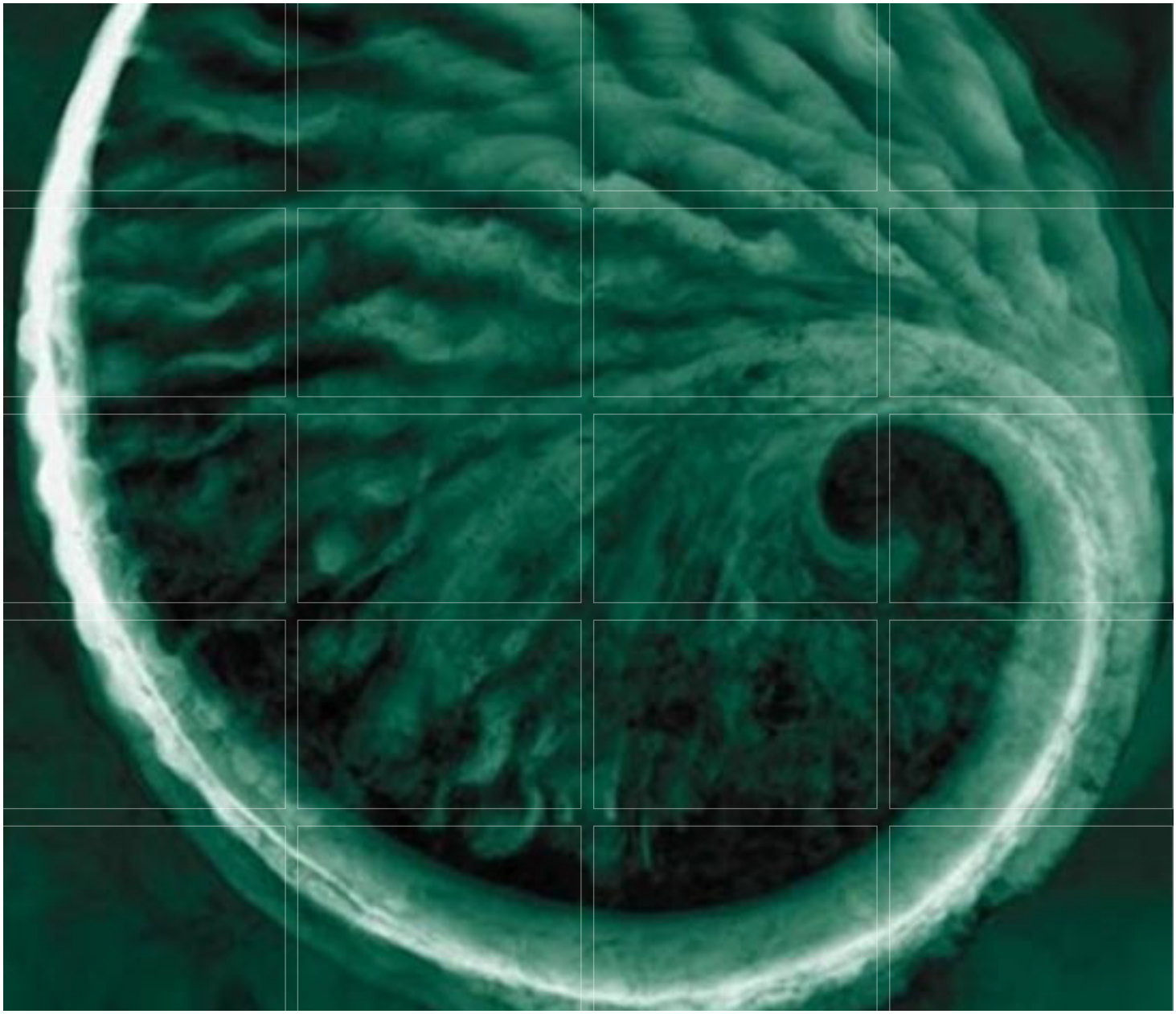

Prepared for:

hd Mining

MURRAY RIVER COAL PROJCT

Groundwater Modelling Report

July 2014

The world's leading sustainability consultancy

ERM

HD Mining International Ltd.

MURRAY RIVER COAL PROJECT
Groundwater Modelling Report

July 2014

Project #0194106-0004-0003

Citation:
ERM Rescan. 2014. *Murray River Coal Project: Groundwater Modelling Report.* Prepared for HD Mining International Ltd. by ERM Consultants Canada Ltd.: Vancouver, British Columbia.

ERM Rescan
ERM Rescan Building, 15th Floor
1111 West Hastings Street
Vancouver, BC
Canada V6E 2J3
T: (604) 689-9460
F: (604) 687-4277

EXECUTIVE SUMMARY

HD Mining International Ltd. (HD Mining) proposes to develop the Murray River Coal Project (the Project) as a 6 million ton per annum (Mtpa) underground metallurgical coal mine. The underground mine dewatering may influence groundwater levels and flow patterns within the Camp Creek Drainage Basin (CCDB) located west of Murray River. Operating the Coarse Coal Rejects (CCR) facility has a potential of impacting groundwater- and surface water quality down-gradient from the CCR Site.

All the meteorological, hydrological, geological and hydrogeological information available as of May 2014 for this project were examined and utilized to form a hydrogeological conceptual model for characterization of the regional pre-mining groundwater system at and around the Project area. The baseline model was then used to build a numerical model - the Murray River Coal Project Groundwater Model (the model). This model was constructed following the Groundwater Modelling Guidelines developed by British Columbia Ministry of Environment, and using the industry standard approaches and software Visual MODFLOW and Surfact package.

ERM constructed and developed the model to support the environmental assessment of the proposed Project. The model was calibrated to the baseline pre-mine conditions. Groundwater flow was simulated as steady-state, representing long-term average conditions; solute transport was simulated as conservative (with the output in 200 years after the mine closure), representing the long-term "worst case" effects without considering retardation and attenuation of contaminants.

Once the baseline model was set, calibrated and subjected to sensitivity analysis, ERM developed a multiple scenarios using the calibrated baseline model for predictive simulations of potential effects of the proposed underground mine dewatering and operating the CCR Piles. Those scenarios were developed to examine how changing values of different sensitive model parameters and, also, different "stress configurations" (different areas of the planned underground mine subject to dewatered, the use of liner vs. drains under CCR facilities) influence the model predictions of groundwater flow and plumes.

The model predicted rates of groundwater inflow into the mine range from 1,891 m^3/day (for base case scenario) to 12,748 m^3/day (for uppermost case scenario 2). This uppermost case value is similar to 13,152 m^3/day, a conservatively calculated value for the "first prospecting area", as provided by the No.173 Prospecting Party of China National Administration of Coal Geology.

Maximum model predicted drawdowns caused by underground mine dewatering range from 2.5 m (for base case scenario) to 19.5 m (for uppermost case scenario 2).

After the mining operations are finished, it is conservatively estimated that filling the post-mine voids with naturally infiltrating groundwater will take from 24 years (for uppermost case scenario) to 164 years (for base case scenario). Once the post-mine voids are completely filled, groundwater levels lowered by mine dewatering will start recovering. The model calculations show that it will take 40 years for water table to reach 80% recovery toward the pre-mining levels.

The minimum times for the contact groundwater water (groundwater contacting the post-mine voids) to travel between the mine and the Murray River are calculated to range from 460 to 1,200 years, depending on the model scenario.

The model pathline simulations show that groundwater flowing through the area of the CCR Piles discharges a short distance to the neighboring creeks. Due to this short distance, groundwater travel time from the edges of the CCR South Pile to the M19A Creek will be less than 10 years.

The model simulations of solute transport from the CCR Piles show that groundwater solute concentrations will reach their maximum 30 years after the start of the Piles' operations and, then, quickly decrease after the Piles' capping and closure. The maximum base case model calculated solute concentration reaching the nearby creeks is 9.4% of the concentration at the source (CCR Piles). The concentrations in other parts of the solute plume reaching the creeks are calculated to be about 3%. The maximum concentrations calculated by the other model scenarios range from 4.4% (for high permeability scenario) to 18% (for the wetter climate scenario).

The low value for high permeability scenario is explained by mixing of source water with groundwater entering the CCR Pile's footprint area from the up-gradient direction at a higher rate (compared to rates for lower permeability scenarios). The high value for wetter climate is caused by the higher rate of source loading (the rate of leachate migrating to groundwater from the bottom of CCR Pile) for that scenario, compared to the other scenarios. Those model predictions are based on a conservative assumption that a 5% of the entire area of synthetic liners (to be installed under each of the CCR Piles) will fail completely. This is considered unlikely. A 2% value is judged more realistic. Another conservative assumption is that both CCR Piles are full right at start of the 30-year long operation. In fact the South Pile may be opened only during the second half of the mine operations.

The range of the results generated from different model scenarios illustrate uncertainties associated with the model predictions, given available information and data. The report provides a discussion of the sources of uncertainty and offers recommendations for collecting additional data to reduce those uncertainties.

As the coal mine project progresses and new monitoring data are collected, the Murray River Groundwater Model can be adjusted, refined, re-calibrated and used in a predictive mode to assist in the planning of mine operations.

TABLE OF CONTENTS

LIST OF FIGURES

LIST OF TABLES

LIST OF APPENDICES

GLOSSARY AND ABBREVIATIONS

Terminology used in this document is defined where it is first used. The following list will assist readers who may choose to review only portions of the document.

AIR	Application Information Requirements
AEMC	AMEC Earth and Infrastructure
CCDB	Camp Creek Drainage Basin
CCR	Coarse Coal Rejects
CVGD28	Canadian Vertical Geodetic Datum 1928
ERM	ERM Consultants Canada Ltd.
HD Mining	HD Mining International Ltd.
K	Hydraulic conductivity
LSA	Local Study Area
MAP	Mean Annual Precipitation
masl	metres above mean sea level
mbgs	metres below ground surface
MSL	Mean Sea Level
Mtpa	Million tonnes per annum
NAD 1983	North American Datum 1983
PRC	Peace River Coalfield
Rescan	Rescan Environmental Services Ltd.
RSA	Regional Study Area
UTM	Universal Transverse Mercator System
VWP	Vibrating Wire Piezometer
WSC	Water Survey of Canada

1. INTRODUCTION

HD Mining International Ltd. (HD Mining) proposes to develop the Murray River Coal Project (the Project) as a 6 million ton per annum (Mtpa) underground metallurgical coal mine. Project-specific hydrogeology baseline studies and other geotechnical and environmental studies have been carried out since 2010 by ERM Rescan, AMEC and other consultants, to support HD Mining's designs of the Project, and to provide the results and inputs to the environmental assessment. Since the mine operations could impact groundwater (and surface water) within the mine property, ERM Rescan developed a three dimensional numerical groundwater model to help evaluate those potential impacts and to help improving mining operation plans such that the impacts are minimized.

1.1 PROJECT DESCRIPTION

The property is located approximately 12.5 km south of Tumbler Ridge, British Columbia (Figure 1.1-1), and consists of 57 coal licenses covering an area of 16,024 hectares, within the Peace River Coalfield (PRC). This area has a long history of metallurgical grade coal mining, mainly open pit type. However, HD Mining is proposing to access deeper zones of the coal field (600 to 1,000 m below surface) through underground mining techniques. It is planned that the coal deposits will be exploited for 25 years using the long-wall mining method (Rescan 2013a). Operating mine facilities will have a potential to affect groundwater system, and creeks and groundwater-dependent ecosystems within the project's property. Of particular concern with this regard are two mining related activities: underground mine dewatering proposed on the west side of Murray River and operating the Coarse Coal Rejects (CCR) facility on the east side of Murray River.

The underground mine dewatering may influence groundwater levels and flow patterns within the Camp Creek Drainage basin (CCDB) located west of Murray River. Operating the CCR facility has a potential of impacting groundwater- and surface water quality down-gradient from the CCR Site.

1.2 OBJECTIVES

The objective of this modelling study is to construct a representative groundwater model to support the environmental assessment of the Project. Figure 1.1-2 shows the regional study area (RSA) and local study area (LSA) / the numerical model domain for hydrogeology and groundwater assessment.

The Project's Application Information Requirements (AIR) specifies that a three-dimensional groundwater model needs to be constructed to simulate the hydrogeological system around the Project site and to assess the potential impacts on groundwater quantity and quality caused by:

- The underground long-walls (located on the west side of Murray River, Figure 1.1-3) during the mine operations and post-closure; and
- The proposed Coarse Coal Rejects Facility (located on the east side of the Murray River, Figure 1.1-3) during the mine operations and post-closure.

Figure 1.1-1

Project Location

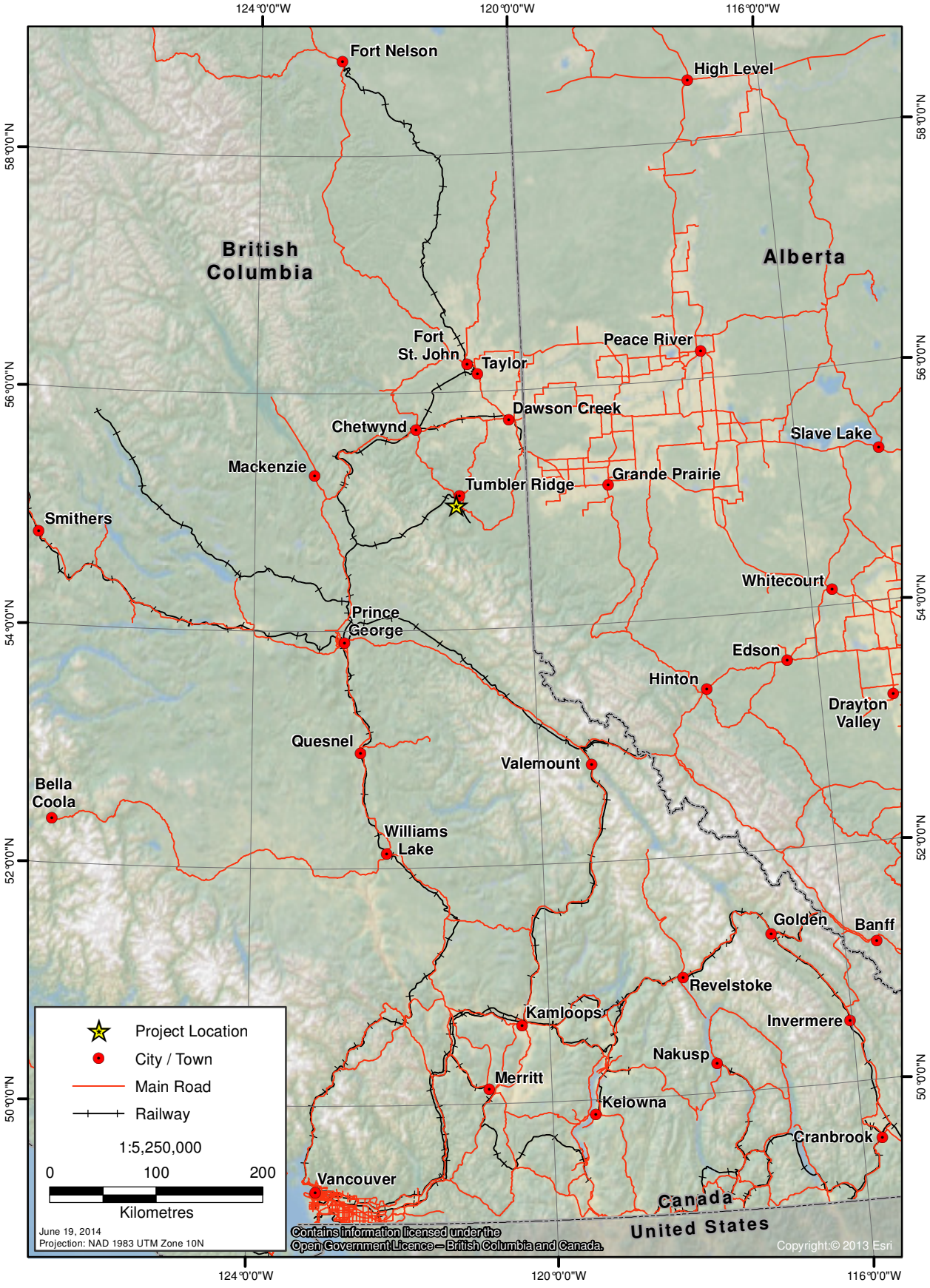

Figure 1.1-2
Groundwater Study Areas

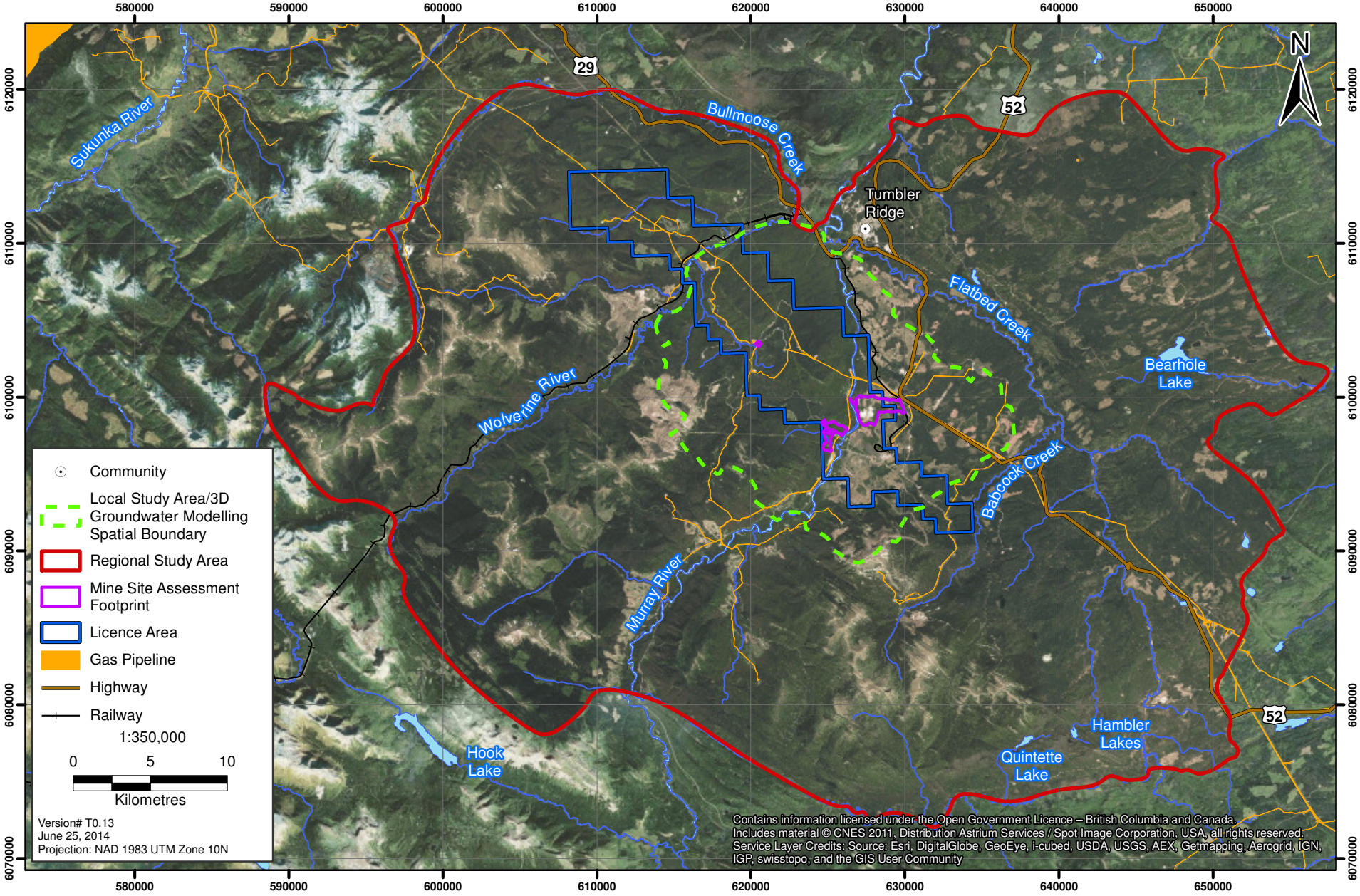

The groundwater modelling was calibrated to the baseline pre-mine conditions. The baseline model was then used in a predictive mode to evaluate the effects of the underground mine dewatering and the operations of Coarse Coal Rejects facility on groundwater quantity and quality.

1.3 METHODOLOGIES

The modelling work for the Project was conducted in accordance with the Groundwater Modelling Guidelines developed by the British Columbia Ministry of Environment (BC MOE 2012). The model was developed using the graphical user interface of the industry standard software package Visual MODFLOW Premium version 4.3 (Schlumberger 2008), together with MODFLOW-Surfact flow version 3.0 (HydroGeologic Inc. 1996). MODFLOW is a three-dimensional finite difference flow model developed by the United States Geological Survey (Harbaugh et al. 2000). It uses an equivalent porous medium approach to represent discretely fractured bedrock. This approach has been commonly accepted for simulations of groundwater flow in bedrock environments at regional scales.

The software package allows simulation of variably saturated groundwater flow and solute transport. MODFLOW has been tested thoroughly and applied successfully for decades in mining and resources development related hydrogeological analysis and environmental impact assessment (e.g. Stone and Fontaine 1998; Jones 2002; Davis 2003; Larry et al. 2005; Wels et al. 2006; Wels and Findlater 2009; Lyford et al. 2007; Gleeson and Manning 2008; Water Management Consultants 2008; Wels and Findlater 2009; BGC 2009; Cho 2009; Rescan 2009a; Rescan 2009b; Rescan 2013c).

The high-level methodologies and steps that were used to develop the models for the Murray River Coal Project include:

- collecting, reviewing and analyzing all relevant regional and local climatological, hydrological, geologic and geomorphologic, geotechnical and hydrogeological information and test data available to date;
- developing a conceptual hydrogeological model based on the available information and data;
- building a baseline numerical model founded on the conceptual model to represent the pre-mining condition on the site;
- calibrating the baseline model to multiple targets, including measured groundwater levels in monitoring wells/piezometers and observed low flows (assumed to approximate baseflows) in M20 Creek;
- identifying sensitive input parameters most influencing the model calibration and model predictions;
- running the calibrated baseline model to simulate steady-state hydrogeological conditions and baseflows under the pre-mining baseline conditions; and
- using the calibrated baseline model to assess the potential impacts of the proposed mine plan on groundwater quantity and quality (i.e., dewatering of the underground mine and operating CCR Site).

Figure 1.1-3
Underground Mine Blocks and Coarse Coal Rejects (CCR) Site Footprints

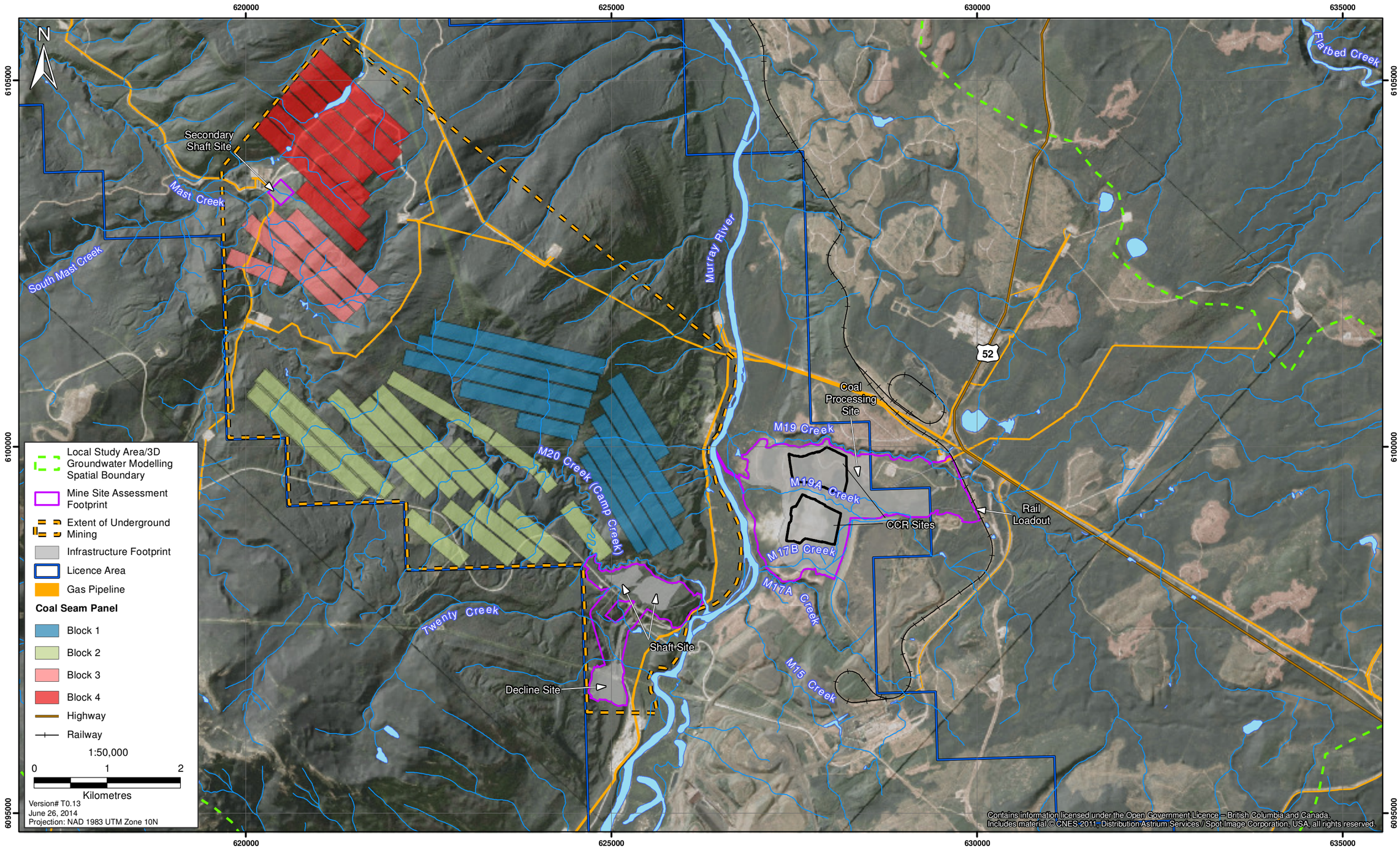

This report presents the details of the methodologies, and the inputs and outputs of the comprehensive hydrogeological modelling for the Project. The outputs from the modelling analysis were used in the Project environmental effects assessments for groundwater and surface water quantity and quality.

2. HYDROGEOLOGICAL BASELINE DATA

This chapter presents the information and test data that was available as of May 2014 for the Project and has been used in developing the hydrogeological conceptual and baseline model to characterize the hydrogeological system and to simulate the baseline groundwater flow at the current pre-mining conditions in the future mine and the CCR areas.

The following sections outline the climate and meteorological, topography and geomorphology, geology, surface hydrology and groundwater hydrology data collected and reviewed to date. More details of the information and data are available in Rescan's Murray River Coal Project: 2011 Terrain and Soils Baseline Report: 2011-2012 (Rescan 2011), 2011-2012 Cumulative Meteorology Baseline (Rescan 2013b), Hydrogeology Baseline Report (ERM Rescan 2014b), Murray River Hydrometeorology Report (Rescan 2013d) and 2011-2013 Hydrology Cumulative Baseline Report (ERM Rescan 2014a). The information in all of these reports forms the base for the Project's groundwater modelling study.

2.1 CLIMATE AND METEOROLOGY

The region around the model study area (the area) is frequently influenced by moist air from the Pacific as well as drier continental air, as it is very close to the leeward side of the Rocky Mountains' Hart Ranges. The topography plays a large role in the climate as precipitation, air temperature, snow depth, and wind speed and direction are highly variable within the region. The orographic influence due to mountains within the area, as well as the inflow of moist air from the Pacific meeting with drier continental air masses, results in a precipitation that is highly variable over the area.

Precipitation in the Project area typically falls as rain from May to September and as snow for the remaining months of the year. Annual precipitation measured at the Murray River meteorological station (elevation 1,055 masl) ranged from 387.4 mm in 2011 to 484.6 mm in 2012. At Tumbler (Denison) station, a few kilometers east of the area, annual precipitation was 544.6 mm in 2011 and 429.2 mm in 2012. Figure 2.1-1 presents mean monthly precipitation at the project site and at the regional stations around.

Snow depth data from regional stations show that it ranges from 5 to 43 cm between November and March. Snow depth is highly dependent on elevation. The greatest snow depth observed at Murray River meteorological station was 57 cm on December 24, 2012.

The mean daily maximum summer temperatures are above 15°C and the mean daily minimum winter air temperature falls well below -10°C (Rescan 2013b). Figure 2.1-2 presents mean monthly air temperatures at the project site and in the region.

Figure 2.1-1

Mean Monthly Precipitation at Murray River (2011 to 2012) and Regional Stations (1988 to 2003)

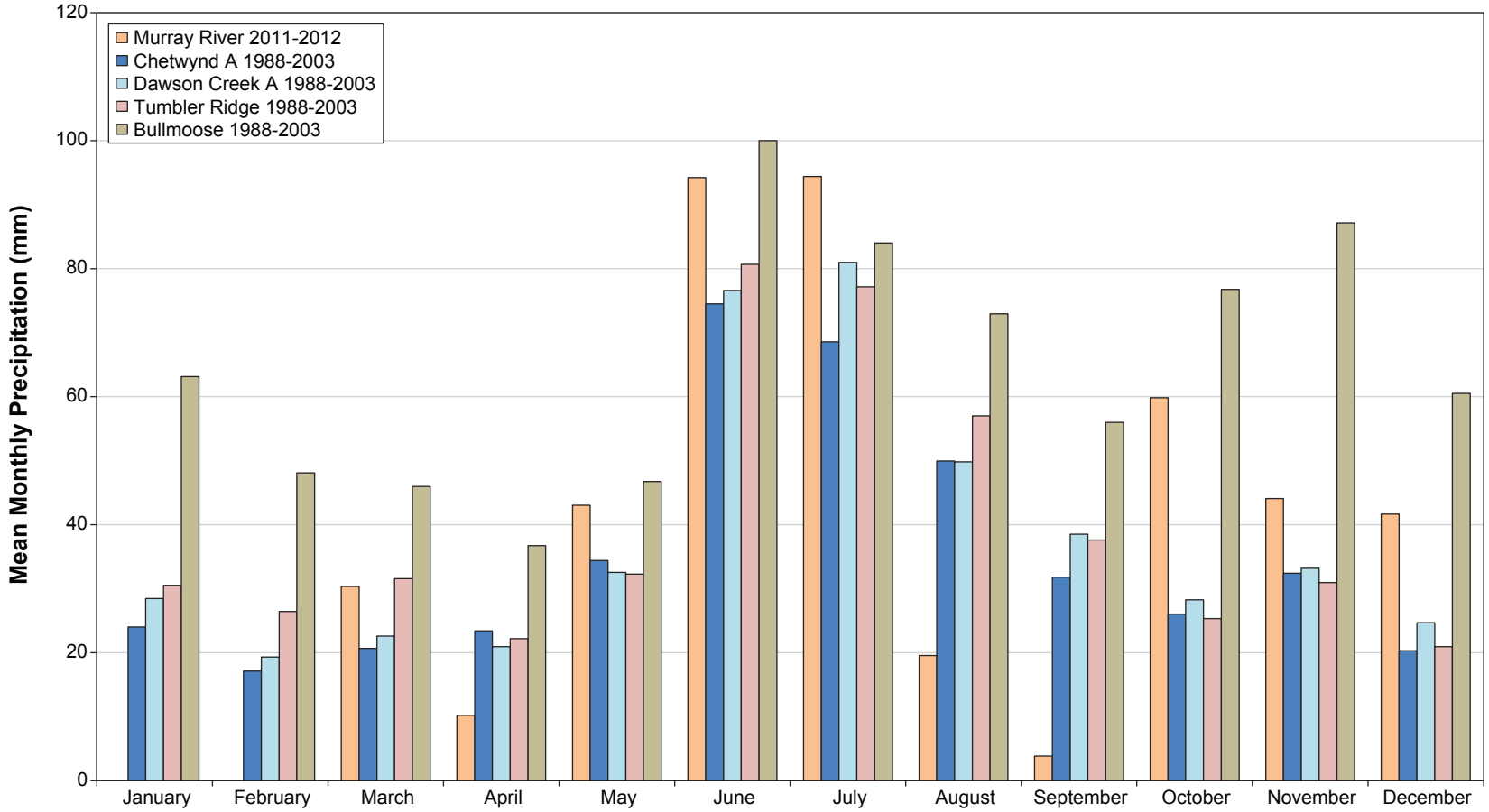

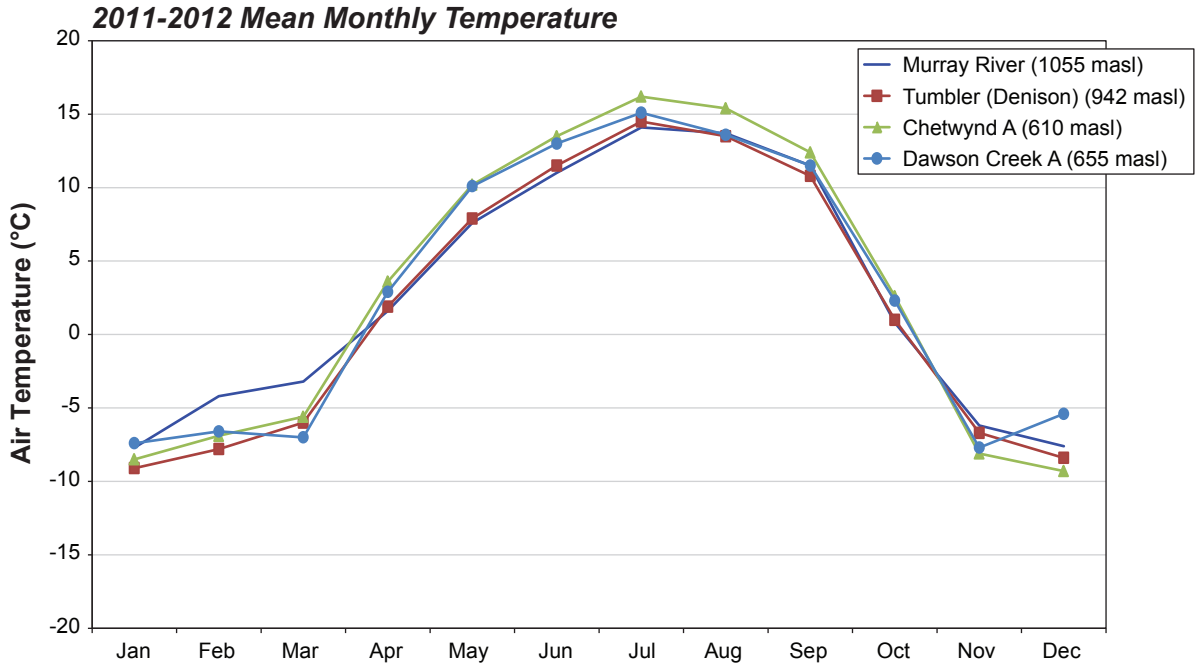
2011-2012 Mean Monthly Temperature
Air Temperature (°C)
20
15
10
5
0
-5
-10
-15
-20
Jan
Feb
Mar
Apr
May
Jun
Jul
Aug
Sep
Oct
Nov
Dec
Murray River (1055 masl)
Tumbler (Denison) (942 masl)
Chetwynd A (610 masl)
Dawson Creek A (655 masl)

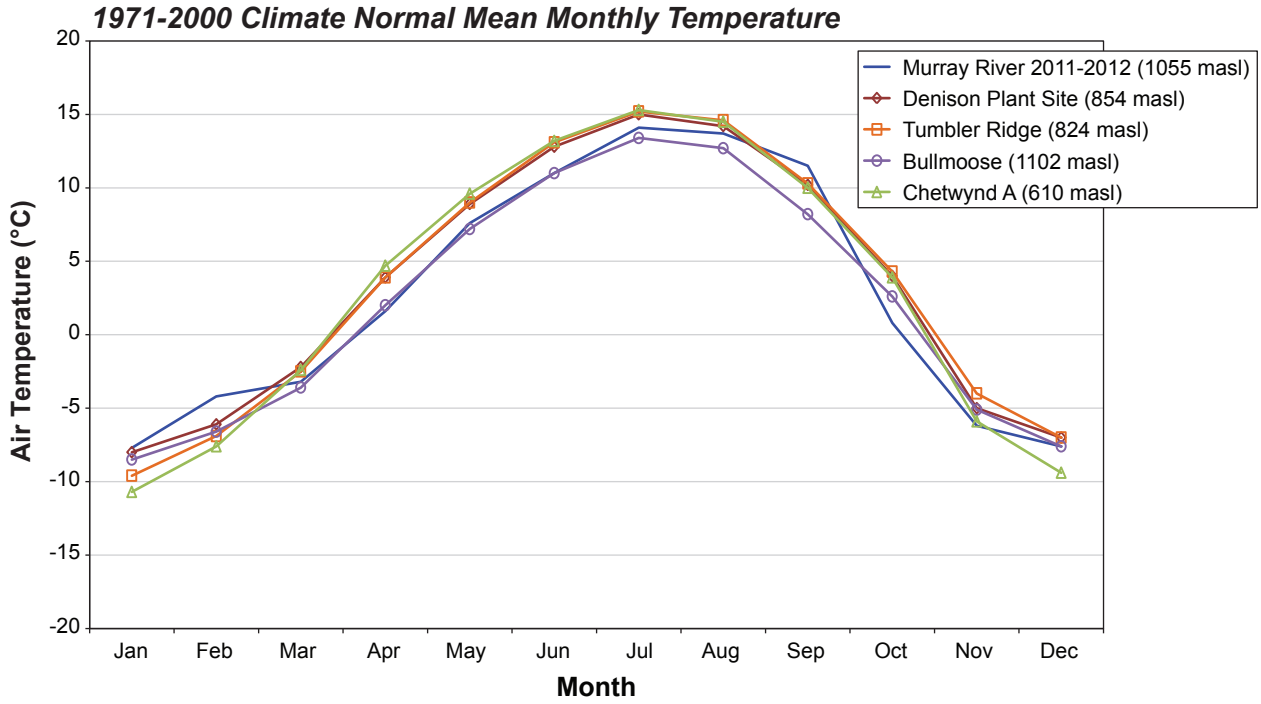
1971-2000 Climate Normal Mean Monthly Temperature
Air Temperature (°C)
20
15
10
5
0
-5
-10
-15
-20
Jan
Feb
Mar
Apr
May
Jun
Jul
Aug
Sep
Oct
Nov
Dec
Month
Murray River 2011-2012 (1055 masl)
Denison Plant Site (854 masl)
Tumbler Ridge (824 masl)
Bullmoose (1102 masl)
Chetwynd A (610 masl)

2.2 TOPOGRAPHY AND GEOMORPHOLOGY

The Project area is located in the eastern foothills of the Rocky Mountains. The highly variable topography of the area is characterized by the presence of hills and steep-sided, round-topped mountains with elongated ridges, on a regional scale characteristically oriented in the NW-SE direction. Valleys eroded along broad belts of soft rock and are generally wide; however, their bottoms and slopes are often deeply incised by rivers and streams (Rescan. 2011). In general, smooth landscapes predominate with plains and gentle slopes covering most of the area. Only a small portion of the area represents rougher landscapes, such as ridges and hummocks (Lorax Environmental 2007).

Topography of the area over the proposed underground mine on the west side of Murray River can be characterized as mountain slopes dissected by several erosional valleys occupied by the local creeks, the largest of them the M20 Camp Creek.

On the east side of Murray River, the proposed CCR facility will be constructed on terraces of the Murray River, a gently slopped area dissected by the ravines of several local creeks, M17, M19 and M19A.

2.3 GEOLOGY AND STRUCTURE OF BEDROCK FORMATIONS

The proposed mine site is located within the Peace River Coalfield (PRC) within the eastern foothills of the Canadian Rocky Mountains, in the transition area between the more faulted and tightly folded areas in the west to the less structurally complex areas in the east (Norwest 2010). The western margin of the foothills belt is usually classified as the easternmost major thrust fault that emplaced Paleozoic strata over Mesozoic strata. The eastern margin of the foothills is a series of en echelon thrust faults that separate the foothills from the gently dipping strata of the Alberta Plateau (Norwest 2010). The foothills belt is characterized by folded and faulted Mesozoic sediments. Because of diminishing structural complexity towards the east, it appears that the geology surrounding the Project area is less severely affected structurally than the adjoining coal properties to the west.

Figure 2.3-1 presents bedrock geology of the region around the project site. Figure 2.3-2 shows stratigraphic sequence of rock formations present in the region of the project site, while Figure 2.3-3 displays a stratigraphic column of rock formations identified in boring logs completed for the project site.

2.3.1 Stratigraphy

A geological report for the licensed area completed by Norwest in 2010 describes the coal-bearing deposits (the focus of Murray River Coal Project) as present in cyclical sequences that occur over a stratigraphic interval referred to as the Upper and Middle Gates, within the Lower Cretaceous Formation, at depths between 300 to 600 meters below ground surface (mbgs). Regional dip of the coal seams is towards the northwest to depths of up to 1,000 mbgs. Each cycle typically begins with laminated, medium- to fine grained sandstone at the base that is transitioning to carbonaceous shale and coal. Coal seams are thickest and more continuous in the lowermost cycle. Moosebar Formation underlies the Gates Formation and consists of marine shale, siltstone, sandstone and conglomerate.

Figure 2.3-1
Regional Geology around the Project Area

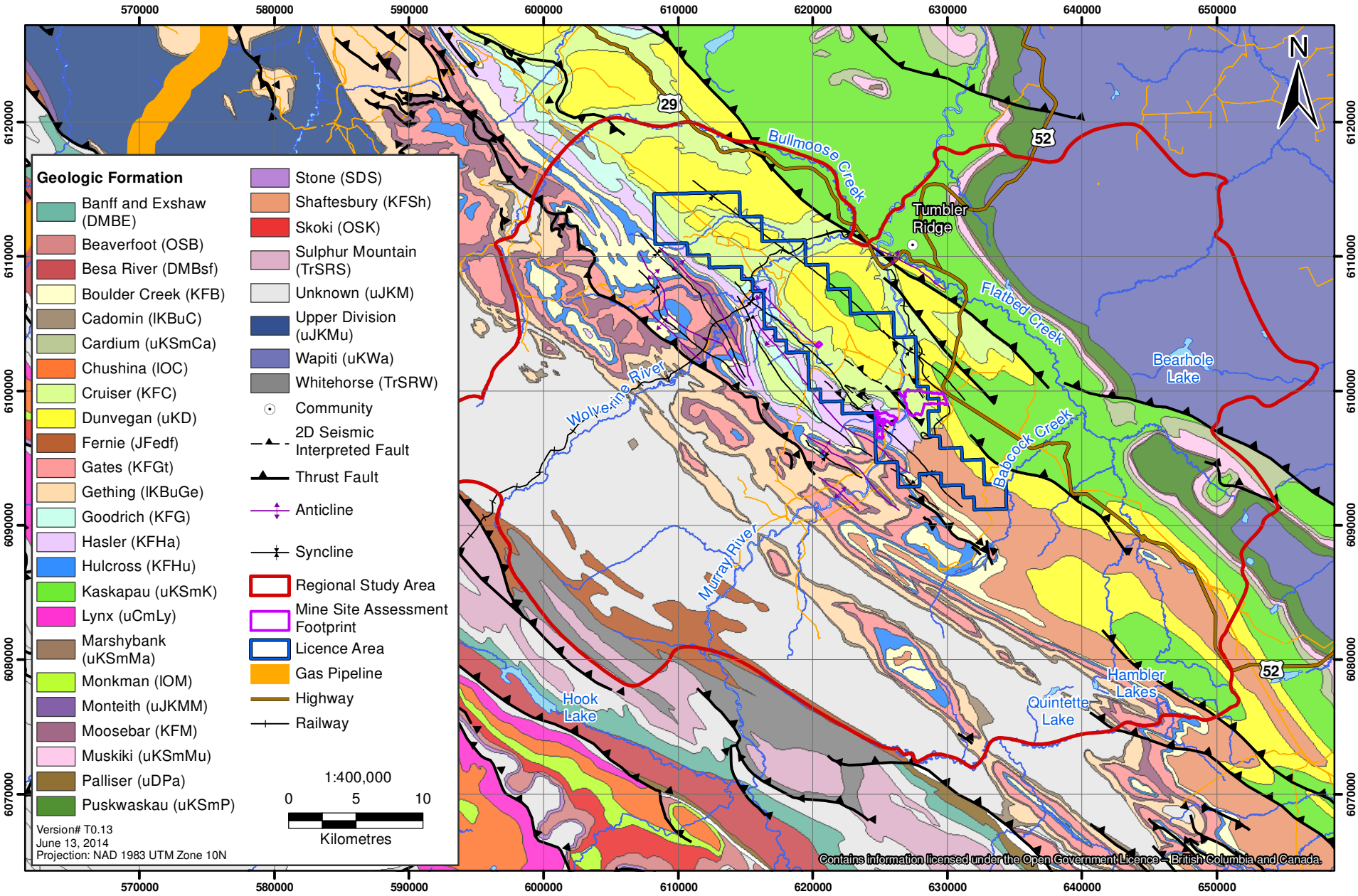

Figure 2.3-2

Regional Stratigraphic Section of Upper Jurassic-Tertiary Units of NE British Columbia

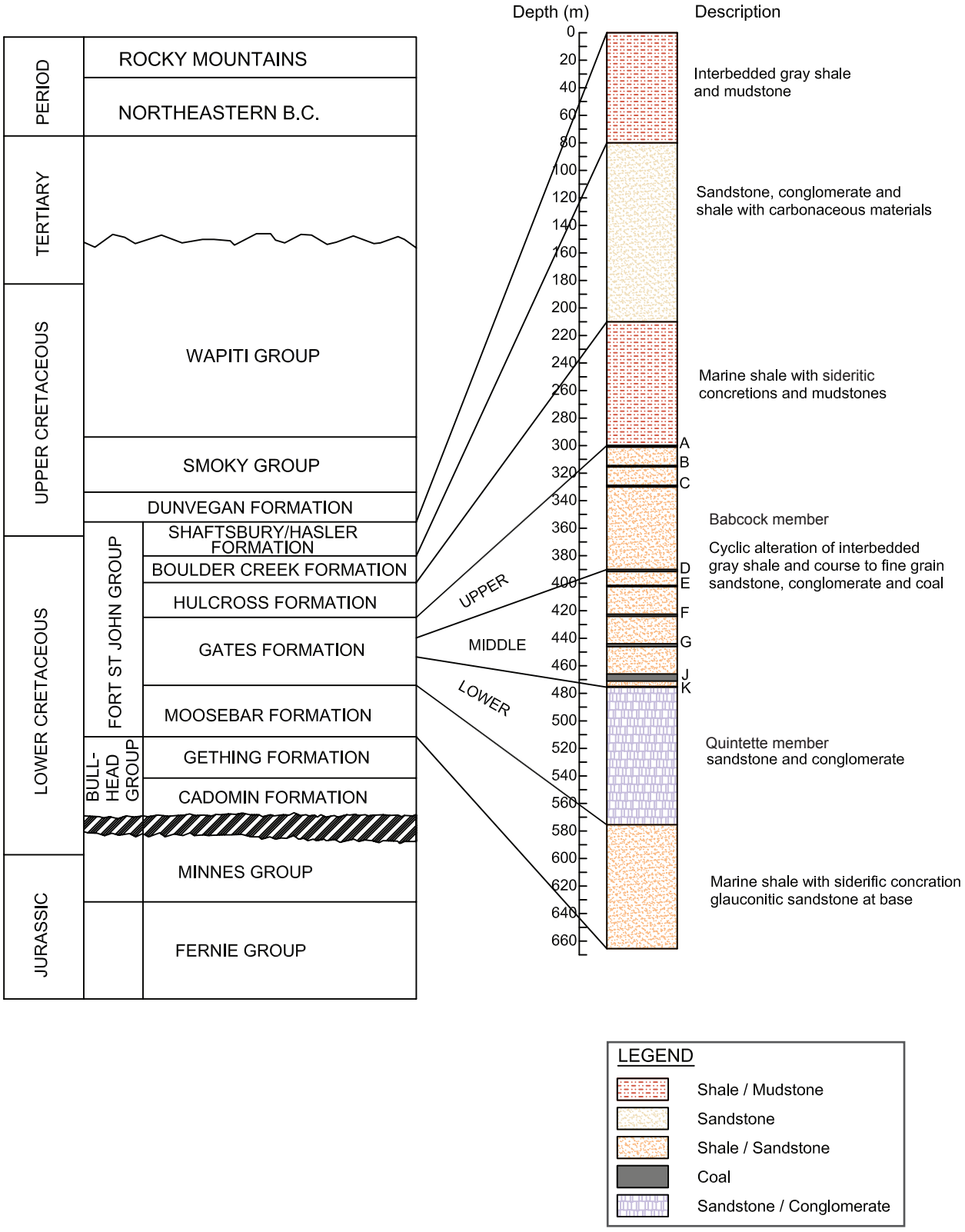

Figure 2.3-3

Idealized Stratigraphic Section for the Project

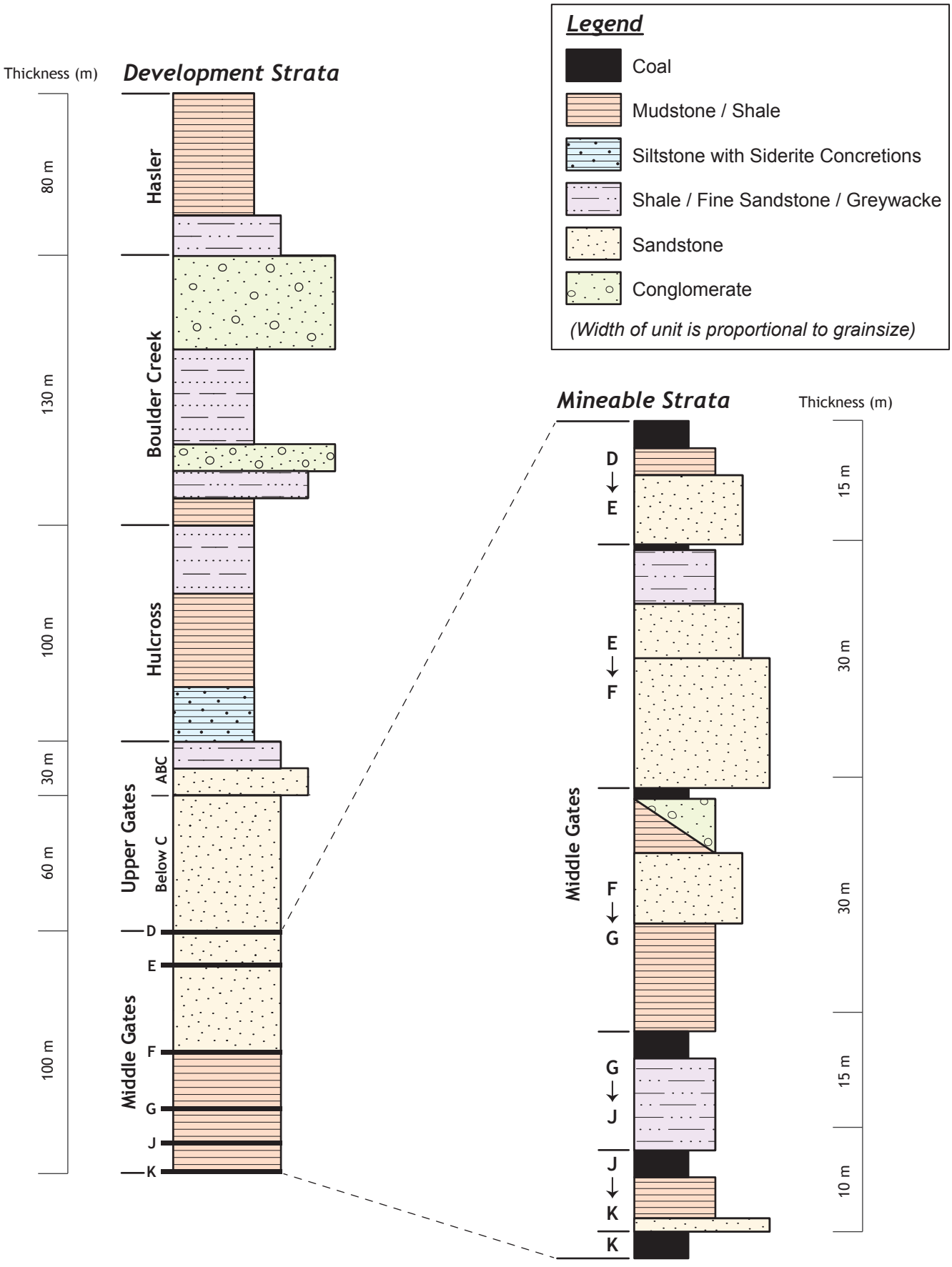

The Hulcross Formation overlies the Gates Formation and is comprised predominantly of dark grey marine shale approximately 100 m thick. The base of the Hulcross Formation is more homogeneous, arenaceous and can contain sideritic concretions. The upper portion of the Formation is dominated by thinly laminated interbeds of siltstone and very fine-grained sandstone. A few kaolinitic beds have also been observed.

The Boulder Creek Formation is a 130 m to 200 m thick sequence of shale, greywacke, and conglomerate that conformably overlies the Hulcross Formation. The upper portion of the Boulder Creek Formation is a coarsening upward sequence of massive conglomerate and conglomeratic sandstone. The middle part of this formation consists of alternating medium- to fine-grained sandstones and shale, while the lower part of the formation consists of marine and non-marine mudstone.

The lower portion of the Hasler Formation, that overlies the Boulder Creek Formation, consists of predominantly dark grey marine shale with sideritic concretions and siltstone. The upper portion of the Hasler Formation, consists of grey marine shale, siltstone and cross-bedded sandstone.

The shallowest bedrock formation present at the Murray River Coal Property is described to be Shaftsbury/Hasler Formation (Huiyong Holding Group 2011; Norwest 2010). In some parts of the Property (the area around the CCR site east of Murray River) Hasler Formation may by overlaid by a younger, Cruiser Formation. However, due to their lithological similarities (the lithology dominated by marine dark-gray silty mudstone), those two formations have not been differentiated.

2.3.2 Geologic Structure

Figure 2.3-4 presents a general, three-dimensional view of the interpreted structure of the rock formations at the proposed mine site. This figure, as well as Figures 3.2-2, 3.2-3 and 3.2-4 (presented and discussed in Section 3 below), was generated from a three-dimensional geological model developed by ERM. Discussion of that model and its sources is provided in Appendix A to this report.

Two anticlines (A1 and A2) and two synclines (B1 and B2) have been found within the Murray River Coal Property, running in a general NW to SE direction. The anticline A1 is located in the middle of almost the entire planned mine field, with the extended length of the anticlinal axis of more than 8,000 m (Huiyong Holding Group 2011).

Seismic surveys indicate the presence of thrust faults of different sizes dissecting geologic structures in NW-SE strike direction. According to seismic surveys interpretation, five large reversed faults run within the Property in parallel from NW to SE and are spaced from 1.5 to 2.5 km apart, with drop heights over 30 m (Huiyong Holding Group 2011).

Rock in the fault zones is characterized by highly developed rock fracturing, loose cementation, relatively low consolidation and higher content of mudstone (compared to adjacent rock); the fault breccia is mostly cemented by the shale and displays compression deformation marks; and the coal seams in the fault zone are ground and burnt to deterioration. Due to the impact of the faults, the adjacent rock-strata are characterized by developed rock fractures (Huiyong Holding Group 2011).

Figure 2.3-4

Geologic Structure of the Proposed Mine Area

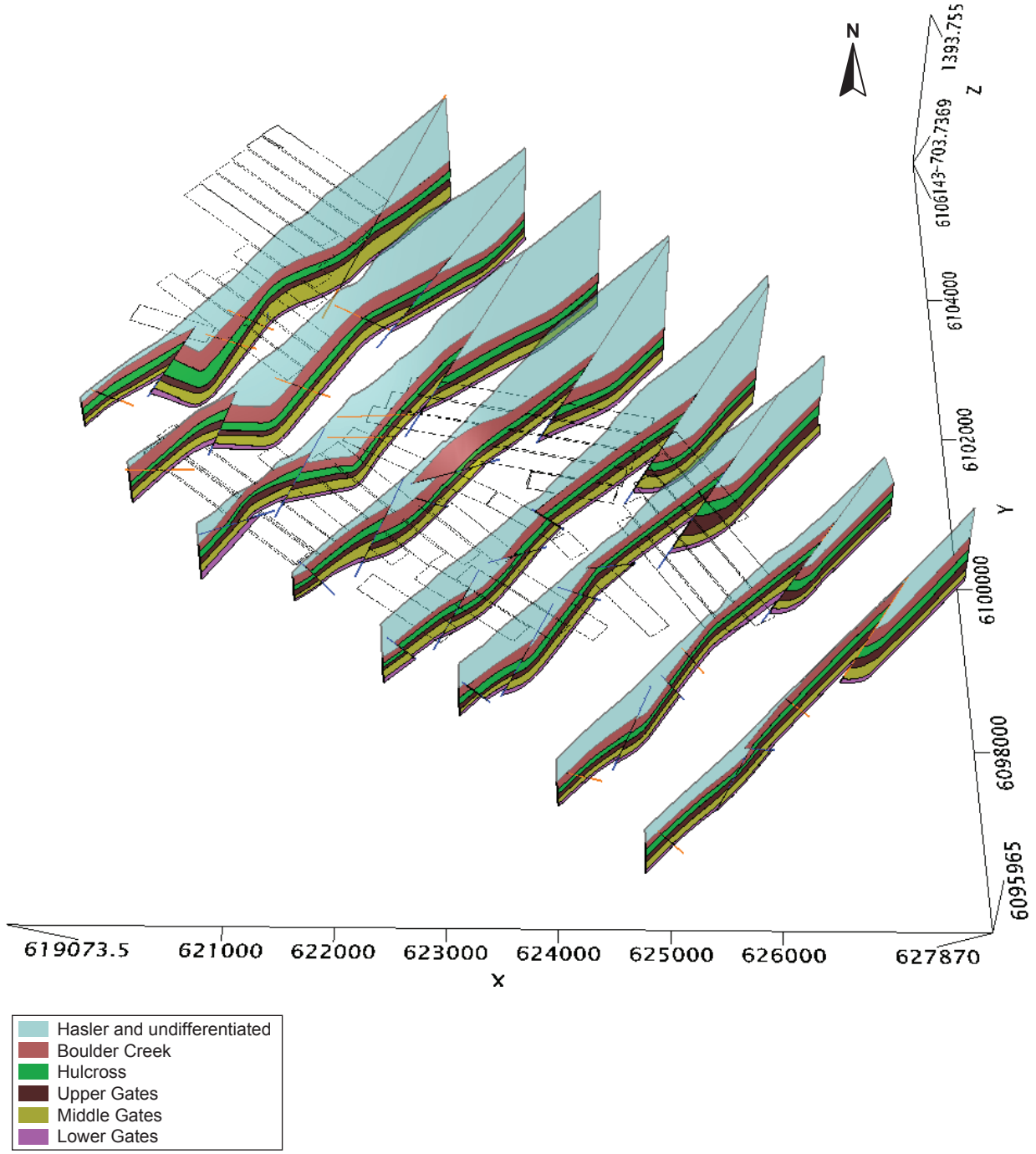

As faults in the mine area are predominately reversed faults and of limited drop height, it is our judgment that they are unlikely to provide major preferential pathways for groundwater flow across the entire rock formation (from Gates Formation, subject to the planned mining, to ground surface). There is plenty of fine grained material (in the type of sedimentary rock formations present at the project site) available to largely fill and plug the fault lines, although such faults may still provide pathways locally, between the adjacent strata.

Two interpretations indicate the presence of a notable fault zone below Murray River. Those two interpretations were developed independently from one another:

- Cross sections derived from the geologic model developed by ERM (see Figures 3.2-3 and 3.2-4 and, also, Appendix A) show the interpreted presence of significant faults under the bottom of the Murray River valley. Interpreting the presence of such faults is consistent with the frequently observed pattern of fault structures influencing development of major valleys (Garber 2011, at the weblink).
- Golder Associates (2013 – Section 5) provide that several fault zones have been interpreted from the geotechnical data collected from the vertical shaft pilot corehole BH12-VSGT-01/01B completed to a depth of 751.62 m, located about 1,200 m west of Murray River.

2.3.3 Surficial Deposits (Overburden)

2.3.3.1 Common Types of Surficial Deposits (Based on Rescan 2011)

Surficial geology in the Project area has been significantly influenced by glaciation. Most of the area outside of the bottoms of major valleys is covered by glacial till. That till typically consists of well-compacted, non-stratified mixture of sand, silt and clay. Much of the area of major valleys is covered by glaciofluvial materials deposited as blankets or veneers on river terraces. Those materials mainly consist of sand and silt with occasional lenses of gravel, and often display evidence of stratification (Rescan 2011).

Fluvial deposits dominate the relatively flat areas of the bottom of Murray River valley. These sediments generally contain a high proportion of sand and gravel, are typically well-sorted and display stratification (Rescan 2011).

Colluvial materials are products of mass-wasting typically occurring on moderate to steep slopes. They are commonly derived from unconsolidated Quaternary deposits, are generally poorly sorted and contain a wide range of particle sizes (Rescan 2011).

Accumulations of organic material are present in areas of intense groundwater seepage, or in wetland depressions. Such depressions are commonly present east of Murray River near the watershed boundary.

As a result of mining activities around the project area, large portions of the land are disturbed and covered by a variety of anthropogenic materials. West of Murray River, Shikano Pits of the Quintette Coal Mine (SRK 2012) resulted in creation of large quarries and waste dumps. However, those quarries and dumps are located a few kilometers from the proposed Murray River Coal Mine. One

exception is the Quintette Coal Mine's waste dump located a short distance up-gradient from the planned CCR facility.

2.3.3.2 Surficial Deposits within the M20 Creek Drainage Area

Thickness of the surficial sediments varies from thin veneers over the higher slopes and steeper terrain, to as much as 15 m in lower slope positions.

Monitoring well MW05-4 of the Hermann Mine Project located on a terrace in the M20 Creek's valley bottom, encountered 42 m of surficial sediments, consisting of dense, silty sand moraine with some gravelly horizons and stiff clay layers near the bottom of the sequence. These soils in this Creek's valley bottom provide some confinement to the underlying groundwater flow regime in bedrock, but do not prevent its discharge up to the Creek. The quantity of groundwater flow through the surficial sediments that mantle the upper slopes in the area are likely limited to small amounts by the thin, low permeability soil profile (Lorax Environmental 2007).

2.3.3.3 Surficial Deposits around CCR Site

A thick strata of silty clay is present below a thin veneer of glaciofluvial sandy sediments at the middle and bottom terraces around the CCR Site (Rescan. 2013c). At some distance between the CCR Site and Murray River, this clay formation ends and glacial till formation occurs instead. Both silty clay and glacial till rest on mudstone inter-bedded with sandstone. This bedrock formation is exposed along the banks of Murray River near the CCR Site.

Table 2.3-1 provides thickness of unconsolidated sediments on top of bedrock as documented in boring logs completed during installation of the hydrogeology baseline study monitoring wells.

Table 2.3-1. Thickness of Unconsolidated Sediments on Top of Bedrock

Borehole / Monitoring Well Name	Thickness of Unconsolidated Sediments (m)	Borehole / Monitoring Well Name	Thickness of Unconsolidated Sediments (m)
MW-H2A	16	MW-H24B	1.5
MW-H3A	30	MW-H24C	8.8
MW-H5	>30.5	MW-H25A	57
MW-H13	57	MW-H26A	28
MW-H15	7	MW-H27	30.5
MW-H16	10	MW-H28	12.5
MW-H17	4.6	MW-H29	3
MW-H18	4.6	MW-H30	16.5
MW-H19	1	MW-H31	>32
MW-H20	7	MW-H32	10.7
MW-H21	40	MW-PNB	>50
MW-H22	>25	VWP-H7	6
MW-H23	>25	VWP-H12	12

2.4 SURFACE HYDROLOGY

The model study area is located within the Hydrologic Zone 7. Two largest streams within this area are Murray River flowing through the center of the model domain area and Wolverine River present along the northwest boundary of the model domain. Numerous small tributary streams and creeks drain the surrounding mountainous areas. Long-term hydrological records are available at Water Survey of Canada (WSC) stations for Murray River and other large streams/rivers in the region. However, very little hydrological information is available on small watersheds (ERM Rescan 2014a). In 2011, Rescan established a network of five hydrometric monitoring stations to fill the gap. The automated stations recorded stream water level data at ten minute intervals during the open water season. This network, as shown on Figure 2.4-1, was expanded to seven stations in 2012 (Rescan 2013d). Figure 2.4-2 shows the location of an important (for this modelling project) hydrometric station MH-2 and boundaries of the M20 Creek's drainage area that this station is monitoring.

The annual flow hydrograph pattern in the area is related to the seasonal distribution of precipitation and temperature (see Figure 2.4-3). Rivers in this area are predominantly fed by spring snowmelt (freshet) that is often augmented by rain-on-snow events during the melt period. High flow discharges occur from mid-April through July, with a low flow period during winter and early spring (see Figures 2.4-3, 2.4-4, 2.4-5 and 2.4-6). Large streams (e.g., Murray River) flow year-round; while small streams (e.g., Twenty Creek) can be ephemeral (Rescan 2013a).

Discharge data collected at Water Survey of Canada Hydrometric Station 07FB006 (Murray River above Wolverine River) over a period of 32 years were used to calculate annual low flows in Murray River. Those annual low flows are considered an approximation of baseflow – the part of river discharge that is representing discharge of groundwater. Average annual low flow for this 32 year period was calculated to be 8.3 m^3/sec. This value was used in calculations of the overall recharge in the groundwater model study area (see discussion in Section 4.4 – Recharge).

In addition to Murray River, discharge measurements were collected for four creeks within the groundwater model study area: M20 Creek (hydrometric stations MH-2 and MH-4), Twenty Creek (MH-3), Mast Creek (MH-5), M17 Creek (MH-6) and M19 Creek (MH-7). MH-2 and MH-4 are the only hydrometric stations with enough data collected to date to allow calculation of low-flow discharge.

The low flow value of 0.01 m^3/sec calculated for 2012 for the lower M20 Creek (MH-2, Figure 2.4-6) is used in the model calibration as the approximation of the long-term low flow in the Creek (Rescan 2013d, Table 3.3-15).

2.5 GROUNDWATER HYDROLOGY DATA

2.5.1 Groundwater Levels

ERM Rescan has been collecting groundwater level measurements between 2011 and 2014 from 30 monitoring wells and 4 vibrating wire piezometers as part of a hydrogeological baseline study (Figure 2.5-1; Rescan 2014b). Measurements from most of those wells have already been taken quarterly during these years, thus generating information about seasonal variability in groundwater levels. Twenty seven of them are located in the proposed underground mine area and seven of them are located at CCR Site. Twelve of those monitoring points are completed in surficial sediments (overburden), the rest are completed in bedrock (sixteen in Hasler Formation and six in Boulder Creek Formation).

Figure 2.4-1
Hydrometric Station Locations

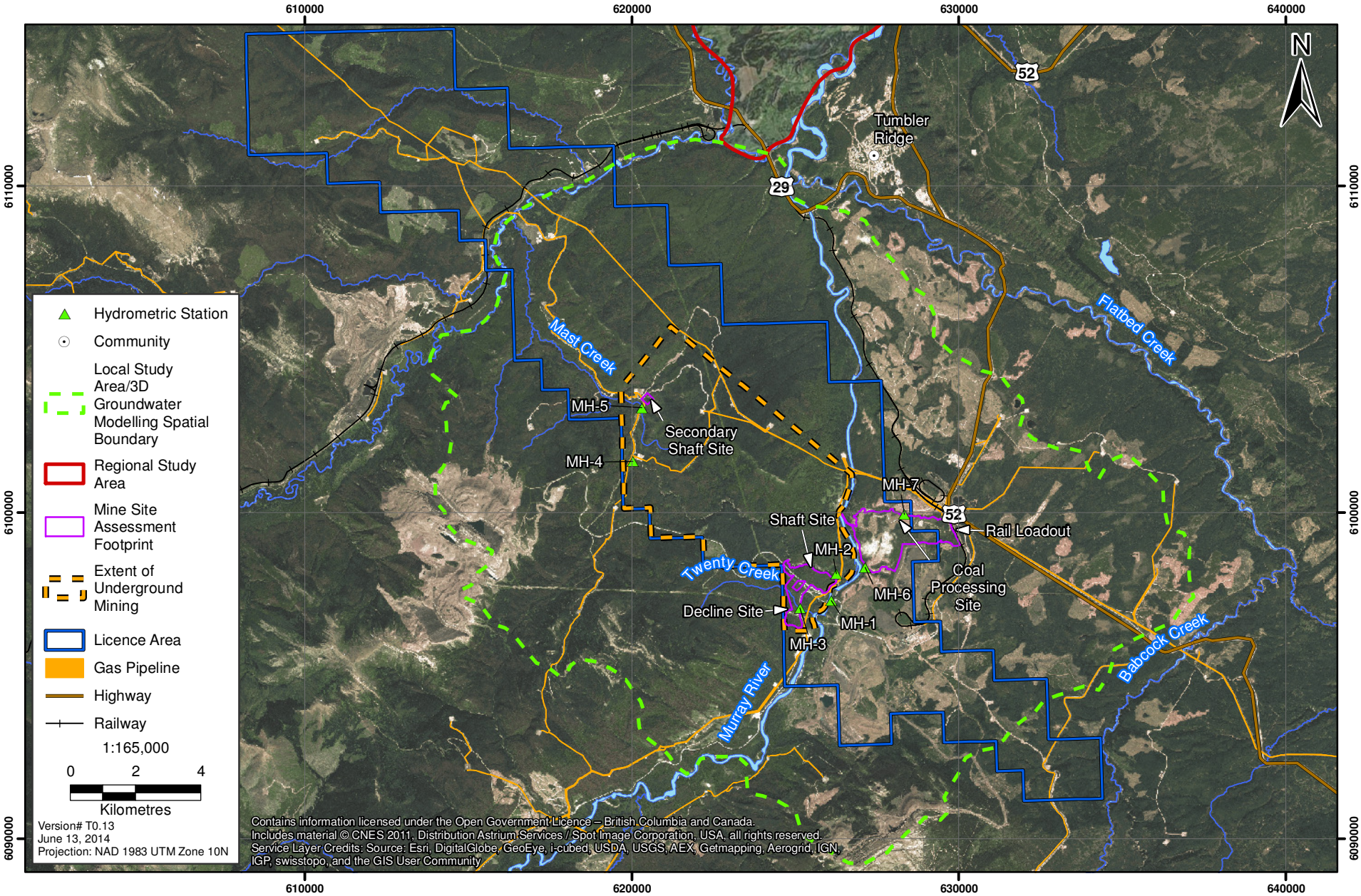

Figure 2.4-2
Drainage Boundary for Camp Creek Hydrometric Monitoring Stations MH-2 and MH-4

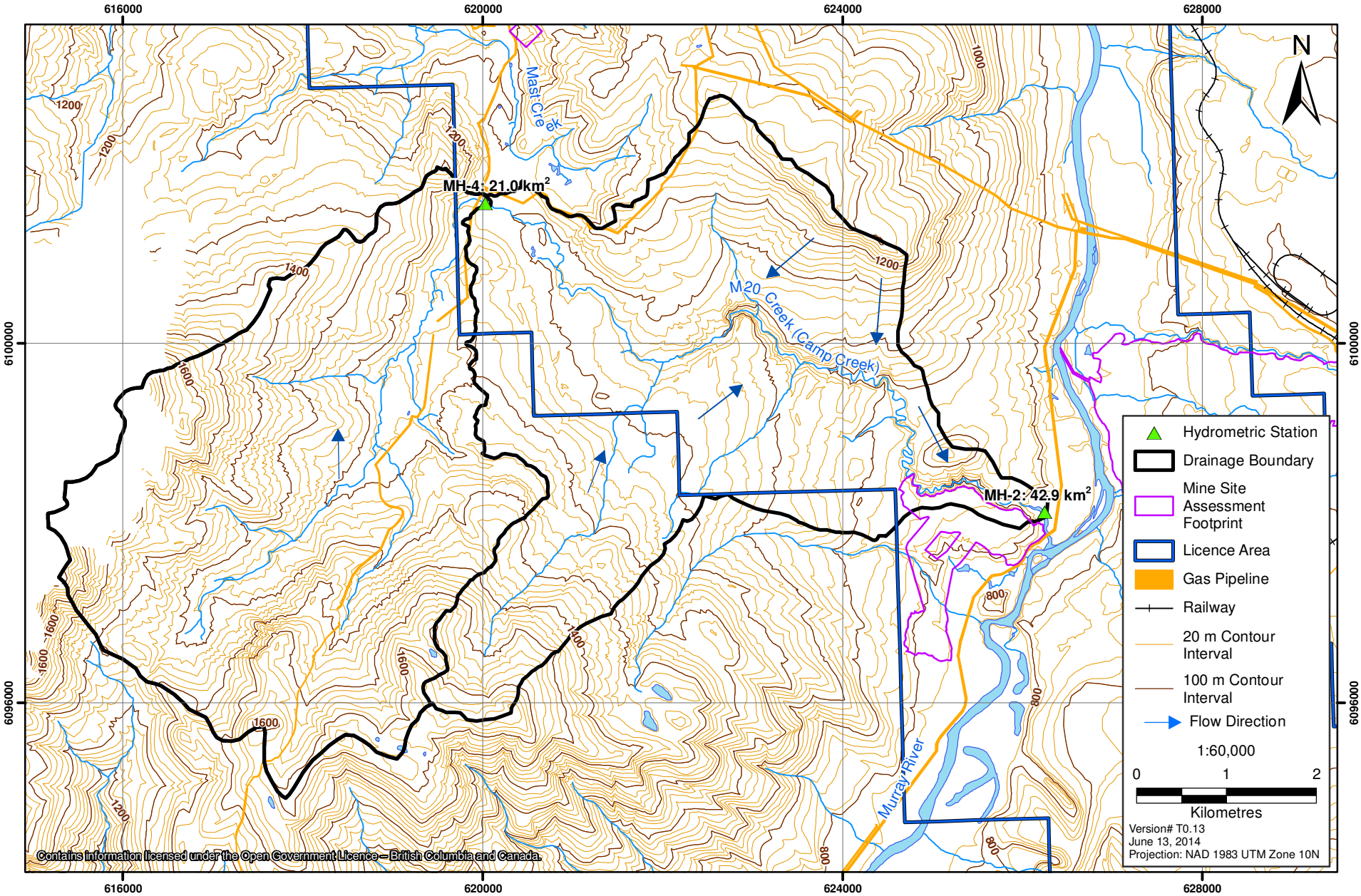

Figure 2.4-3

Annual Hydrograph at Hydrometric Monitoring Station MH-2 for 2013

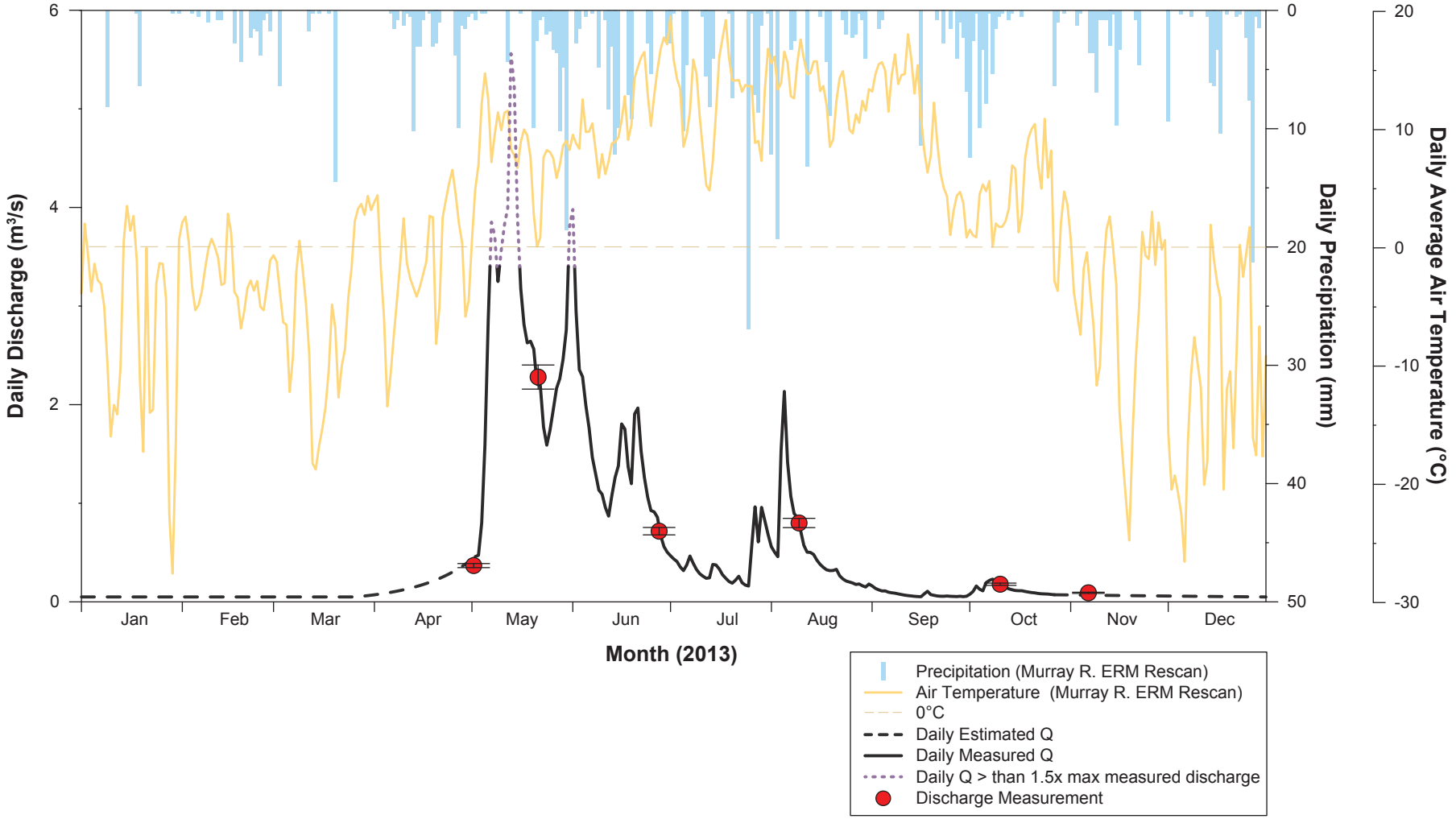

Figure 2.4-4

Adjusted MH-1 Hydrograph
(based on WSC 07FB006 Hydrograph)

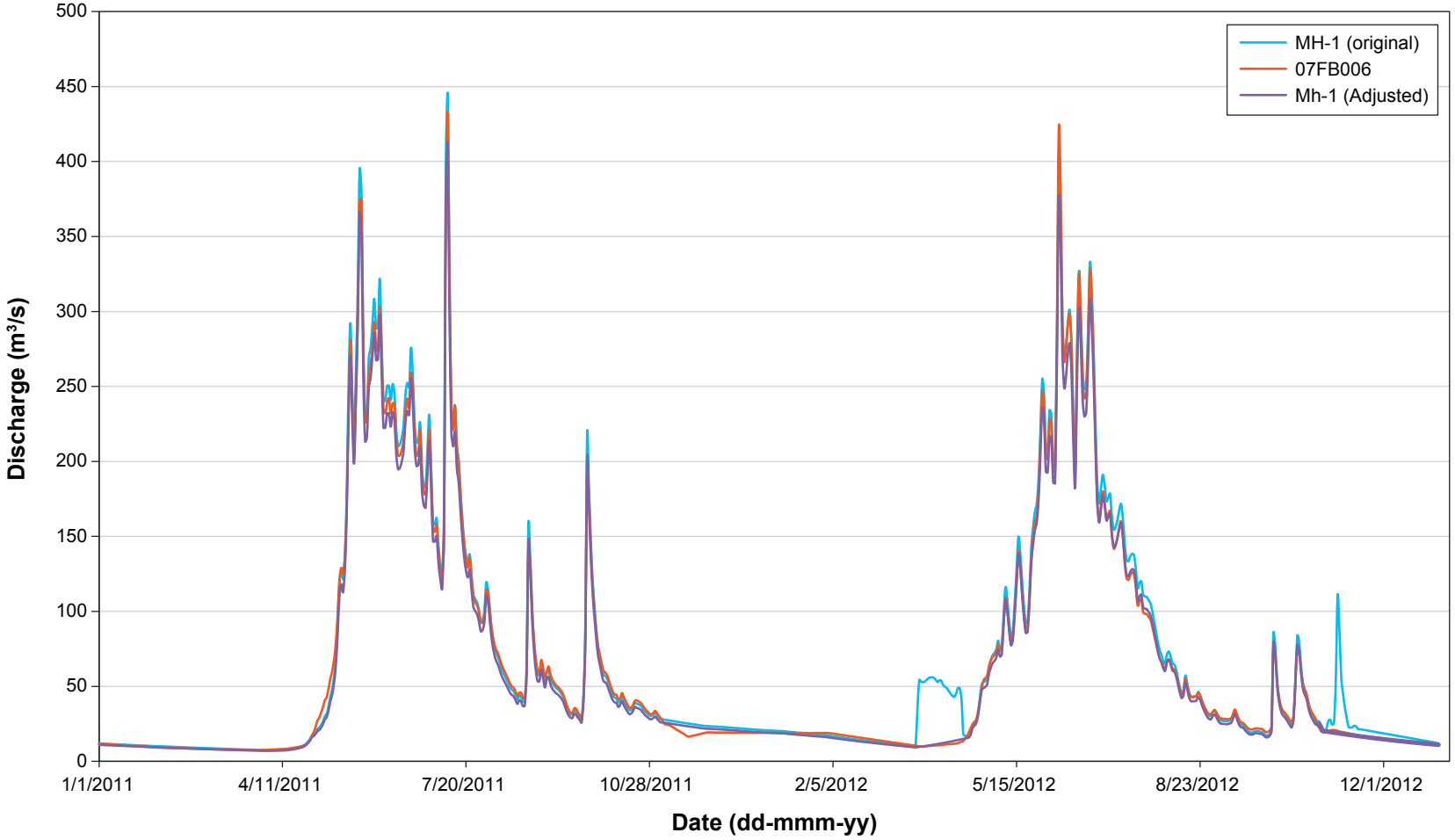

Figure 2.4-5

Typical Annual Murray River Discharge Hydrograph near the Project Area

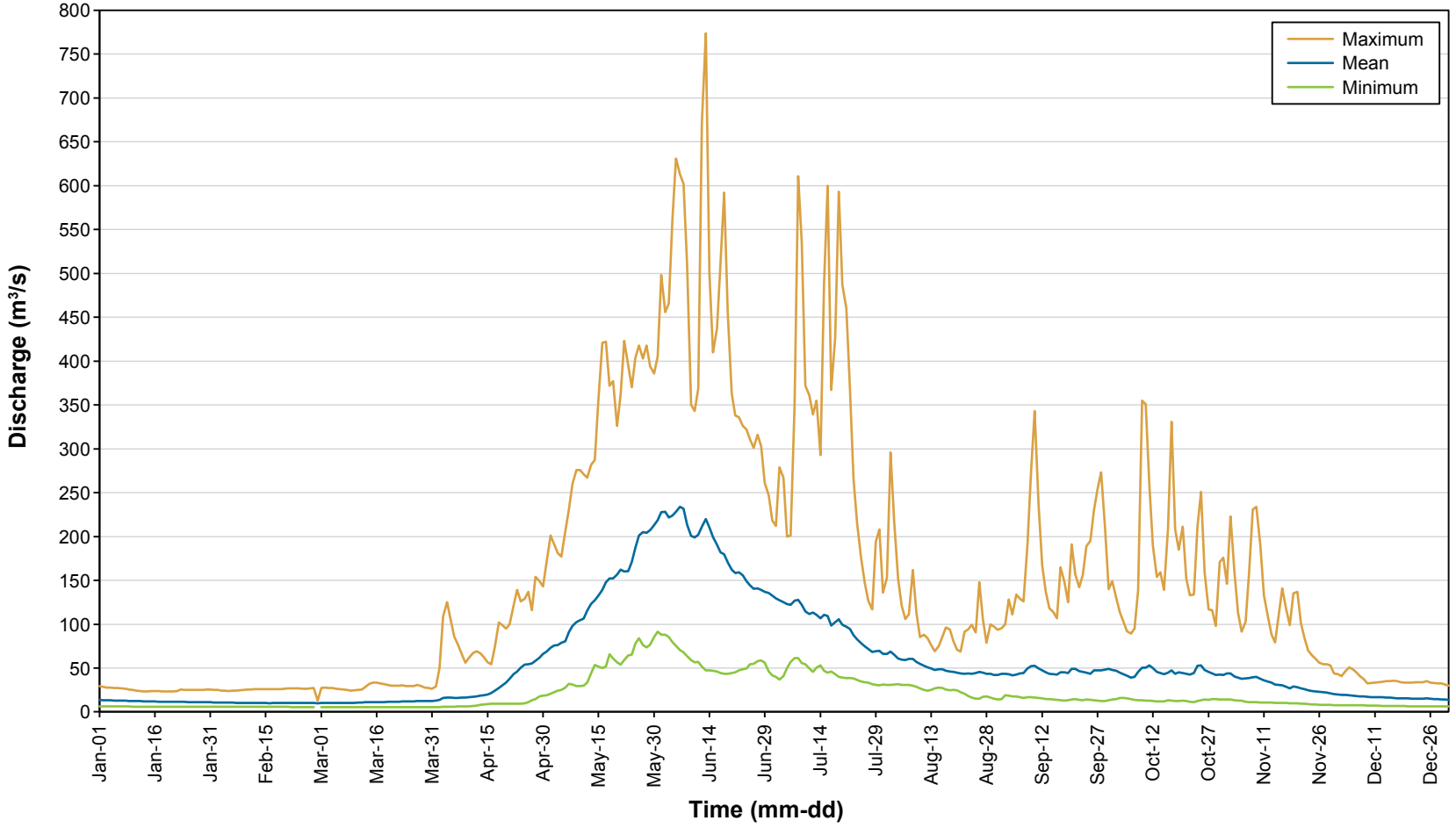

Note: based on the 1977 – 2010 records of Water Survey of Canada Station Murray River Above Wolverine (07FB006).

Figure 2.4-6

Annual Hydrograph at Hydrometric Monitoring Station MH-2, 2011 to 2013

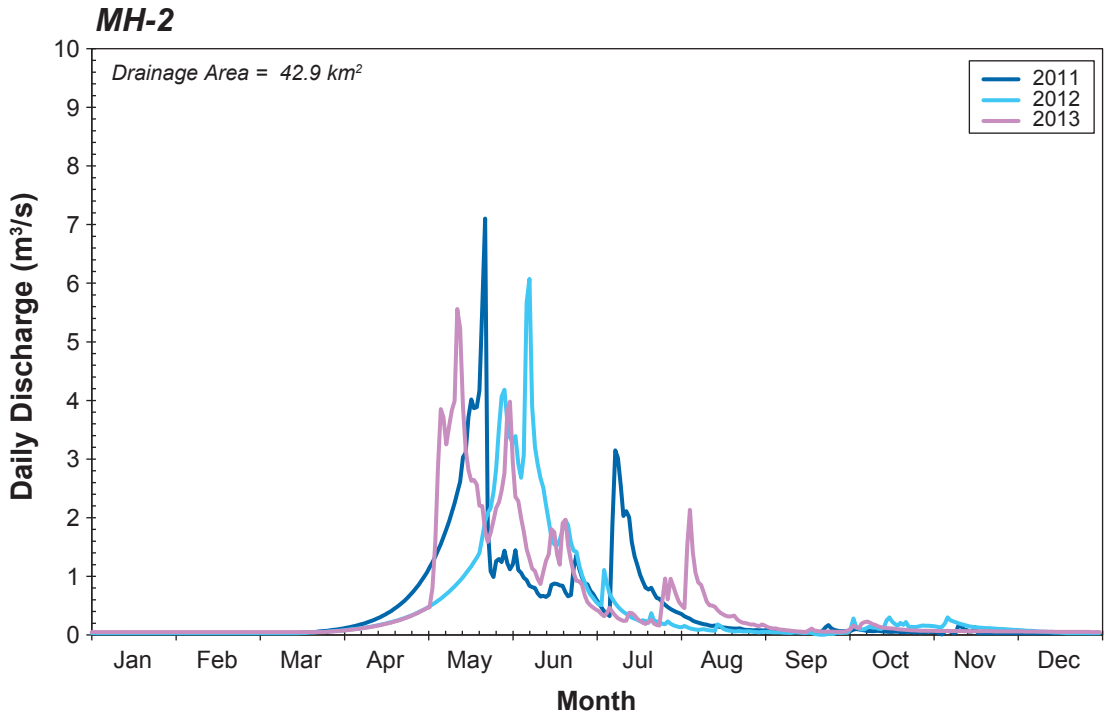

Figure 2.5-1
Groundwater Monitoring Network and Potentiometric Surface Map

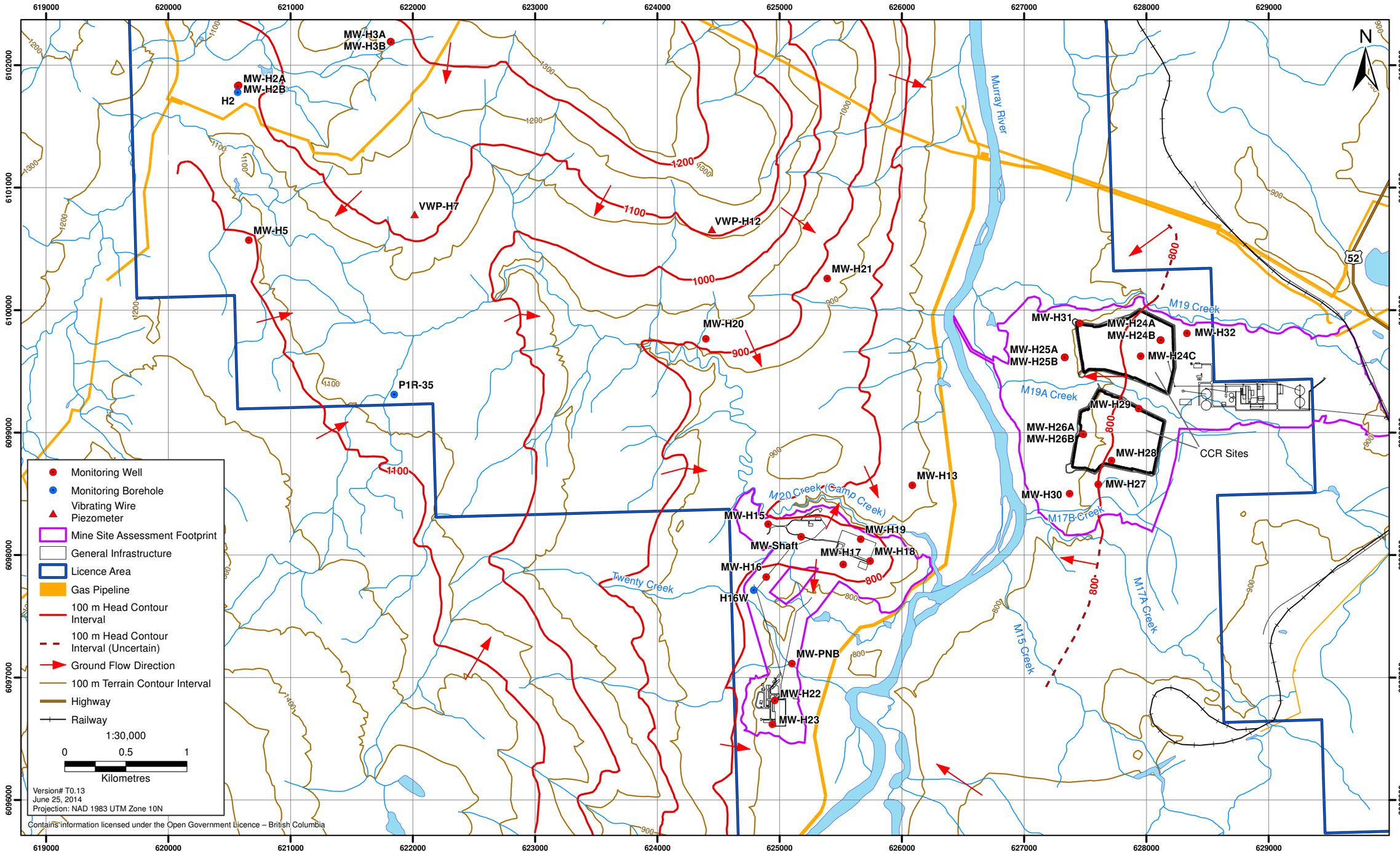

In addition, three strategically located (with regard to the proposed mining area) boreholes, P1R-35 (671 m deep), H2 (872 m deep) and H16W (955 m deep) were subject to several pump tests and packer tests, providing measurements of hydraulic head and hydraulic conductivity of deeper rock formations. Those tests and measurements were completed within three different depth intervals for each of those boreholes (AMEC 2010; AMEC 2012). The rock formations subject to the proposed mining were focus of those tests and measurements.

Several other monitoring wells were constructed in close vicinity of the Murray River Coal Project's area. ERM-Rescan reviewed available information from two adjacent mining projects: Hermann Mine Project (Lorax Environmental 2007) and Quintette Mine Project (SRK 2012). Data of sufficient completeness for use in the model calibration was found for four Herman wells and three Quintette wells. All those are relatively shallow wells with a single set of water level measurements collected in 2005 (Quintette) and 2010 (Herman). As such, measurements from those two projects are not quite synchronous with measurements collected from Murray River Coal Project's wells (2005 and 2010 vs. 2011-2013). In addition, those single measurements do not document seasonal variations in water levels. However, qualitative comments are provided in the reports stating that such variations are relatively small, particularly compared to a large range of elevations at which the wells were installed over the project areas.

Inclusion of this additional data from adjacent mining projects in the groundwater model database improves an aerial coverage of monitoring points over the model domain.

All the groundwater level data collected to date as part of the hydrogeological baseline study are presented in Table 2.5-1.

Table 2.5-2 shows the wells with water level and hydraulic conductivity data used for groundwater model construction. Not all wells shown in Table 2.5-1 were included in the Table 2.5-2 database, while that database used several other wells that were not constructed and monitored as part of hydrogeology baseline study (and are not shown in Table 2.5-1).

The wells that are part of baseline study and were not included in the model database are:

- H2B, H3B, H24B, H25B and H26B – those are the shallower of the pairs of well nests. Water levels measured in shallow wells are in general similar to water levels in deeper wells in the well nest. It was judged that data collected from deeper wells are more representative of the hydrogeological conditions of the larger area and it is more appropriate for use in a sub-regional scale groundwater model. In addition, we followed the rule of trying not to concentrate targets in a small area and, thus, creating a spatial bias in the process of calibration;
- H29 - borehole used to construct this well was drilled to a depth 90 m below a van Ruth plug that was installed below the well. Water level measurements in that well are considered anomalous and less reliable than in other monitoring wells around;
- VWP-H7 and VWP-H12 – data collected using vibrating piezometer are considered much less reliable than collected from standard monitoring wells;
- TH12-03 – this well is located very close to another well included in the model database: MW-H22.

The wells that were included in the model database but are not part of baseline study (and are not listed in Table 2.5-1) are:

- P1R35, H2, H16W – those are deep boreholes that were tested/monitored outside of the hydrogeology baseline study (AEMC 2010; AMEC 2012);
- BD11-011/0012/0013, MW05-1a, MW05-2b, MW05-3a and MW05-4a – those are the wells that were constructed and monitored as part of neighboring Quintette and Hermann mine projects (Lorax Environmental 2007; SRK 2012).

2.5.2 Hydraulic Gradients

Existing water level data confirm that groundwater migrates from areas of high elevation (within recharge zones) toward valleys where it discharges to creeks and rivers (Figure 2.5-1). Lateral hydraulic gradients for shallow groundwater mimic the steepness of mountain slopes. On the other hand, gradients for deep bedrock groundwater are expected to be influenced less by the terrain's topography and more by: the location relative to major recharge / discharge areas; lithology and structural features of geologic formations. For instance, deep groundwater levels measured in well H16W located close to Murray River are significantly higher than River stage (831.5 masl at depth of 876 mbgs and 815.4 masl at depth of 256 mbgs in well H16W vs. Murray River stage of 735 masl), indicating a groundwater discharge area.

Limited data collected from seven paired shallow groundwater monitoring sites (nested deeper and shallower wells constructed within the Camp Creek drainage basin and the CCR Site) show a presence of steep downward vertical gradients within the high-ground recharge areas, and very low upward- to no vertical gradients at the CCR Site. It is important to note that the CCR Site's wells are all relatively shallow, too shallow to document the presence of strong upward vertical gradients expected within major discharge areas. However, such well-defined upward gradient is documented in a deep well H16W, which is located close to River and within regional discharge zone.

The presence of a flowing well in the upper reaches of the M20 Creek (P1R-35) illustrates that strong upward gradients are likely to be present close to the creeks and rivers – particularly when the bottoms of the valleys are filled with low permeability sediments.

2.5.3 Hydraulic Conductivities

In total, twenty one monitoring wells installed as part of Murray River Coal Project hydrogeology baseline study were subject to slug testing (Rescan 2014b). In addition, packer tests (falling-head) were conducted in packer zones along 26 intervals in nine boreholes as drilling advanced through bedrock horizons during the baseline hydrogeology study. The methodology of those tests is described in the hydrogeology baseline study report (Rescan 2014b). All those tests provide information about hydraulic conductivities of relatively shallow formations – less than 100 meters below ground surface.

Table 2.5-1. Groundwater Level Data Collected as Part of Hydrogeology Baseline Study

Well ID	Coordinates		Top of Casing	Stick-up	Top of Casing	Screen Interval		Date	Time	Water Level				Remarks
	Northing (m)	Easting (m)	Elev. (masl)	Height (m)	Elevation (masl)	Top (mbg)	Bottom (mbg)			mbsu	mbg	masl	Annual Mean	
	Zone 10U (NAD83)													
MW-H2A	6,101,837	620,575	1,104.341	0.76	1,104.341	83.00	88.00	10-Jul-11	na	9.350	8.590	1,094.991		
MW-H2A	6,101,837	620,575	1,104.341	0.76	1,104.341	83.00	88.00	18-Oct-11	na	9.640	8.880	1,094.701		
MW-H2A	6,101,837	620,575	1,104.341	1.19	1,104.341	83.00	88.00	13-May-12	na	10.818	9.628	1,093.523		
MW-H2A	6,101,837	620,575	1,104.341	1.19	1,104.341	83.00	88.00	23-Aug-12	na	10.695	9.505	1,093.646		
MW-H2A	6,101,837	620,575	1,104.341	1.19	1,104.341	83.00	88.00	6-Nov-13	10:00	10.877	9.687	1,093.464	1,093.957	Pressure transducer installed November 2013
MW-H2B	6,101,831	620,567	1,103.370	0.35	1,103.370	9.90	12.90	10-Jul-11	na	5.770	5.420	1,097.600		
MW-H2B	6,101,831	620,567	1,103.370	0.35	1,103.370	9.90	12.90	18-Oct-11	na	7.690	7.340	1,095.680		
MW-H2B	6,101,831	620,567	1,103.370	0.47	1,103.370	9.90	12.90	13-May-12	na	6.192	5.722	1,097.178		
MW-H2B	6,101,831	620,567	1,103.370	0.47	1,103.370	9.90	12.90	23-Aug-12	na	7.140	6.670	1,096.230		
MW-H2B	6,101,831	620,567	1,103.370	0.47	1,103.370	9.90	12.90	6-Nov-13	10:00	7.225	6.755	1,096.145	1,096.363	
MW-H3A	6,102,191	621,818	1,215.710	0.45	1,215.700	183.00	193.00	7-Jul-11	na	26.700	26.250	1,189.000	1,189.000	difficult/unsafe site access during trip after this date
MW-H3B	6,102,191	621,821	1,215.700	0.45	1,215.700	4.50	8.80	7-Jul-11	na	1.830	1.380	1,213.870	1,213.870	difficult/unsafe site access during trip after this date
MW-H5	6,100,571	620,658	1,102.530	0.68	1,102.500	27.50	30.50	9-Jul-11	na	na	na	na		
MW-H5	6,100,571	620,658	1,102.530	0.68	1,102.500	27.50	30.50	18-Oct-11	na	na	na	na		
MW-H5	6,100,571	620,658	1,102.530	0.68	1,102.500	27.50	30.50	12-May-12	na	na	na	na		
MW-H5	6,100,571	620,658	1,102.530	0.68	1,102.500	27.50	30.50	22-Aug-12	na	na	na	na		
MW-H5	6,100,571	620,658	1,102.530	0.83	1,102.650	27.50	30.50	6-Nov-13	11:30	-2.1	-2.930	1,104.750	1,104.750	flowing artesian, pressure gauge reads 3.0 psi
MW-H13	6,098,569	626,086	821.580	1.27	822.070	66.00	69.00	14-Oct-11	na	52.710	51.440	769.360		
MW-H13	6,098,569	626,086	821.580	1.27	822.070	66.00	69.00	11-May-12	na	54.950	53.680	767.120		
MW-H13	6,098,569	626,086	821.580	0.78	821.580	66.00	69.00	22-Aug-12	na	54.688	53.908	766.892	767.791	
MW-H15	6,098,253	624,907	854.397	1.17	854.347	94.00	100.00	13-Oct-11	na	52.630	51.460	801.717		
MW-H15	6,098,253	624,907	854.397	1.17	854.347	94.00	100.00	14-May-12	na	55.992	54.822	798.355		
MW-H15	6,098,253	624,907	854.397	1.22	854.397	94.00	100.00	23-Aug-12	na	55.214	53.994	799.183		
MW-H15	6,098,253	624,907	854.397	1.22	854.397	94.00	100.00	25-Oct-12	na	55.488	54.268	798.909		
MW-H15	6,098,253	624,907	854.397	1.22	854.397	94.00	100.00	19-Dec-12	na	54.880	53.660	799.517		
MW-H15	6,098,253	624,907	854.397	1.22	854.397	94.00	100.00	23-Jul-13	na	53.745	52.525	800.652		
MW-H15	6,098,253	624,907	854.397	1.22	854.397	94.00	100.00	11-Nov-13	9:30	48.885	47.665	805.512	799.722	
MW-H15	6,098,253	624,907	854.397	1.22	854.397	94.00	100.00	9-Feb-14	8:30	50.805	49.585	803.592		
MW-H16	6,097,821	624,891	839.467	0.86	839.467	67.50	70.50	14-May-12	na	61.748	60.888	777.719		
MW-H16	6,097,821	624,891	839.467	0.86	839.467	67.50	70.50	21-Aug-12	na	61.580	60.720	777.887	777.803	
MW-H16	6,097,821	624,891	839.467	0.86	839.467	67.50	70.50	8-Feb-14	16:30	> 60.58	-	-		
MW-H17	6,097,925	625,520	829.960	0.66	829.960	5.50	8.50	10-May-12	na	5.528	4.868	824.432		
MW-H17	6,097,925	625,520	829.960	0.66	829.960	5.50	8.50	22-Aug-12	na	5.552	4.892	824.408		
MW-H17	6,097,925	625,520	829.960	0.66	829.960	5.50	8.50	25-Oct-12	na	5.740	5.080	824.220		
MW-H17	6,097,925	625,520	829.960	0.66	829.960	5.50	8.50	20-Dec-12	na	5.852	5.192	824.108		
MW-H17	6,097,925	625,520	829.960	0.66	829.960	5.50	8.50	23-Jul-13	na	5.706	5.046	824.254		
MW-H17	6,097,925	625,520	829.960	0.66	829.960	5.50	8.50	11-Nov-13	10:00	5.905	5.245	824.055	824.284	
MW-H17	6,097,925	625,520	829.960	0.66	829.960	5.50	8.50	9-Feb-14	13:00	5.630	4.970	824.330		Pressure Transducer records available from July 2013
MW-H18	6,097,953	625,740	831.697	0.82	831.697	10.50	13.50	10-May-12	na	11.956	11.136	819.741		
MW-H18	6,097,953	625,740	831.697	0.82	831.697	10.50	13.50	22-Aug-12	na	11.747	10.927	819.950		
MW-H18	6,097,953	625,740	831.697	0.82	831.697	10.50	13.50	25-Oct-12	na	11.828	11.008	819.869		
MW-H18	6,097,953	625,740	831.697	0.82	831.697	10.50	13.50	20-Dec-12	na	11.821	11.001	819.876		
MW-H18	6,097,953	625,740	831.697	0.82	831.697	10.50	13.50	23-Jul-13	na	11.707	10.887	819.990		
MW-H18	6,097,953	625,740	831.697	0.82	831.697	10.50	13.50	11-Nov-13	10:25	11.720	10.900	819.977	819.885	
MW-H18	6,097,953	625,740	831.697	0.82	831.697	10.50	13.50	9-Feb-14	13:45	10.595	9.775	821.102		
MW-H19	6,098,131	625,663	833.344	0.77	833.344	5.70	8.70	10-May-12	na	4.420	3.650	828.924		
MW-H19	6,098,131	625,663	833.344	0.77	833.344	5.70	8.70	22-Aug-12	na	4.134	3.364	829.210		
MW-H19	6,098,131	625,663	833.344	0.77	833.344	5.70	8.70	25-Oct-12	na	4.366	3.596	828.978		
MW-H19	6,098,131	625,663	833.344	0.77	833.344	5.70	8.70	20-Dec-12	na	4.511	3.741	828.833		
MW-H19	6,098,131	625,663	833.344	0.77	833.344	5.70	8.70	23-Jul-13	na	4.090	3.320	829.254		
MW-H19	6,098,131	625,663	833.344	0.77	833.344	5.70	8.70	11-Nov-13	10:15	4.428	3.658	828.916	829.040	
MW-H19	6,098,131	625,663	833.344	0.77	833.344	5.70	8.70	9-Feb-14	13:50	4.290	3.520	829.054		

(continued)

Table 2.5-1. Groundwater Level Data Collected as Part of Hydrogeology Baseline Study (continued)

Well ID	Coordinates		Top of Casing Elev. (masl)	Stick-up Height (m)	Top of Casing Elevation (masl)	Screen Interval		Date	Time	Water Level				Remarks
	Northing (m)	Easting (m)				Top (mbg)	Bottom (mbg)			mbsu	mbg	masl	Annual Mean	
	Zone 10U (NAD83)													
MW-H20	6,099,766	624,397	954.200	0.67	954.075	37.80	40.80	14-Oct-11	na	25.980	25.310	928.095		
MW-H20	6,099,766	624,397	954.200	0.67	954.075	37.80	40.80	11-May-12	na	26.638	25.968	927.437		
MW-H20	6,099,766	624,397	954.200	0.80	954.200	37.80	40.80	22-Aug-12	na	26.740	25.945	927.460	927.664	
MW-H21	6,100,259	625,390	917.000	1.30	915.700	50.70	53.70	8-Jul-11	na	25.830	24.530	889.870		
MW-H21	6,100,259	625,390	917.000	0	917.000	50.70	53.70	14-Oct-11	na	25.310	25.310	891.690		
MW-H21	6,100,259	625,390	917.000	0	917.000	50.70	53.70	11-May-12	na	26.638	26.638	890.362		
MW-H21	6,100,259	625,390	917.000	0	917.000	50.70	53.70	22-Aug-12	na	26.020	26.020	890.980	25.989	
MW-H22	6,096,815	624,960	784.422	0.85	784.422	22.10	25.10	11-May-12	na	19.558	18.708	764.864		
MW-H22	6,096,815	624,960	784.422	0.85	784.422	22.10	25.10	21-Aug-12	na	20.540	19.690	763.882		
MW-H22	6,096,815	624,960	784.422	0.85	784.422	22.10	25.10	28-Oct-12	na	21.730	20.880	762.692		
MW-H22	6,096,815	624,960	784.422	0.85	784.422	22.10	25.10	19-Dec-12	na	22.022	21.172	762.400		
MW-H22	6,096,815	624,960	784.422	0.85	784.422	22.10	25.10	21-Jul-13	na	19.680	18.830	764.742		
MW-H22	6,096,815	624,960	784.422	0.85	784.422	22.10	25.10	6-Nov-13	15:50	21.510	20.660	762.912	763.460	
MW-H22	6,096,815	624,960	784.422	0.85	784.422	22.10	25.10	8-Feb-14	12:30	21.715	20.865	762.707		
MW-H23	6,096,618	624,942	785.698	0.78	785.698	22.10	25.10	11-May-12	na	20.937	20.157	764.761		
MW-H23	6,096,618	624,942	785.698	0.78	785.698	22.10	25.10	21-Aug-12	na	22.361	21.581	763.337		
MW-H23	6,096,618	624,942	785.698	0.78	785.698	22.10	25.10	28-Oct-12	na	23.496	22.716	762.202		
MW-H23	6,096,618	624,942	785.698	0.78	785.698	22.10	25.10	19-Dec-12	na	23.773	22.993	761.925		
MW-H23	6,096,618	624,942	785.698	0.78	785.698	22.10	25.10	21-Jul-13	na	21.480	20.700	764.218		
MW-H23	6,096,618	624,942	785.698	0.78	785.698	22.10	25.10	6-Nov-13	15:40	23.294	22.514	762.404	763.056	
MW-H23	6,096,618	624,942	785.698	0.78	785.698	22.10	25.10	8-Feb-14	9:00	23.440	22.660	762.258		Pressure Transducer records available from July 2013
MW-H24A	6,099,756	628,116	832.000	0.90	832.000	44.85	47.90	1-Nov-12	na	19.720	18.820	812.280		
MW-H24A	6,099,756	628,116	832.000	0.90	832.000	44.85	47.90	18-Dec-12	na	16.025	15.125	815.975		
MW-H24A	6,099,756	628,116	832.000	0.90	832.000	44.85	47.90	7-May-13	na	16.462	15.562	815.538		
MW-H24A	6,099,756	628,116	832.000	0.90	832.000	44.85	47.90	31-Jul-13	na	16.200	15.300	815.800		
MW-H24A	6,099,756	628,116	832.000	0.90	832.000	44.85	47.90	7-Nov-13	8:55	16.345	15.445	815.655	815.771	
MW-H24B	6,099,756	628,119	832.000	0.40	832.000	5.55	8.60	1-Nov-12	na	5.956	5.556	826.044		
MW-H24B	6,099,756	628,119	832.000	0.40	832.000	5.55	8.60	18-Dec-12	na	5.973	5.573	826.027		
MW-H24B	6,099,756	628,119	832.000	0.40	832.000	5.55	8.60	7-May-13	na	2.842	2.442	829.158		
MW-H24B	6,099,756	628,119	832.000	0.40	832.000	5.55	8.60	31-Jul-13	na	4.860	4.460	827.140		
MW-H24B	6,099,756	628,119	832.000	0.40	832.000	5.55	8.60	7-Nov-13	8:55	5.898	5.498	826.102	827.442	
MW-H24B	6,099,756	628,119	832.000	0.40	832.000	5.55	8.60	10-Feb-14	15:45	4.800	4.400	827.200		
MW-H24C	6,099,625	627,954	825.000	0.92	825.000	9.23	12.28	31-Jul-13	na	2.515	1.595	822.485		
MW-H24C	6,099,625	627,954	825.000	0.92	825.000	9.23	12.28	10-Nov-13	9:15	3.415	2.495	821.585		
MW-H24C	6,099,625	627,954	825.000	0.92	825.000	9.23	12.28	13-Feb-14	12:45	3.200	2.280	821.800	821.957	
MW-H25A	6,099,615	627,334	766.000	0.70	766.000	58.95	62.00	1-Nov-12	na	1.315	0.615	764.685		
MW-H25A	6,099,615	627,334	766.000	0.70	766.000	58.95	62.00	18-Dec-12	na	0.700	0.000	765.300		
MW-H25A	6,099,615	627,334	766.000	0.70	766.000	58.95	62.00	7-May-13	na	0.890	0.190	765.110		
MW-H25A	6,099,615	627,334	766.000	0.70	766.000	58.95	62.00	31-Jul-13	na	2.744	2.044	763.256		
MW-H25A	6,099,615	627,334	766.000	0.70	766.000	58.95	62.00	5-Nov-13	10:00	2.765	2.065	763.235	764.555	
MW-H25A	6,099,615	627,334	766.000	0.70	766.000	58.95	62.00	13-Feb-14	9:15	2.570	1.870	763.430		MW-H25B purged/sampled previous day (2 m away)
MW-H25B	6,099,615	627,332	766.000	0.70	766.000	1.55	4.60	1-Nov-12	na	0.840	0.140	765.160		
MW-H25B	6,099,615	627,332	766.000	0.70	766.000	1.55	4.60	18-Dec-12	na	0.790	0.090	765.210		
MW-H25B	6,099,615	627,332	766.000	0.70	766.000	1.55	4.60	7-May-13	na	0.842	0.142	765.158		
MW-H25B	6,099,615	627,332	766.000	0.70	766.000	1.55	4.60	31-Jul-13	na	0.776	0.076	765.224		
MW-H25B	6,099,615	627,332	766.000	0.70	766.000	1.55	4.60	8-Nov-13	14:00	0.840	0.140	765.160	765.197	
MW-H25B	6,099,615	627,332	766.000	0.70	766.000	1.55	4.60	12-Feb-14	14:00	0.670	-0.030	765.330		ice at indicated water level, approx. 10 cm thick
MW-H26A	6,098,990	627,478	792.000	0.78	792.000	29.84	32.89	29-Oct-12	na	0.822	0.042	791.178		

(continued)

Table 2.5-1. Groundwater Level Data Collected as Part of Hydrogeology Baseline Study (completed)

Well ID	Coordinates Northing (m) Zone 10U (NAD83)	Coordinates Easting (m) Zone 10U (NAD83)	Top of Casing Elev. (masl)	Stick-up Height (m)	Top of Casing Elevation (masl)	Screen Interval Top (mbg)	Screen Interval Bottom (mbg)	Date	Time	Water Level mbsu	Water Level mbg	Water Level masl	Annual Mean	Remarks
MW-H26A	6,098,990	627,478	792.000	0.78	792.000	29.84	32.89	18-Dec-12	na	0.800	0.020	791.200		
MW-H26A	6,098,990	627,478	792.000	0.78	792.000	29.84	32.89	7-May-13	na	1.265	0.485	790.735		
MW-H26A	6,098,990	627,478	792.000	0.78	792.000	29.84	32.89	31-Jul-13	na	1.175	0.395	790.825		
MW-H26A	6,098,990	627,478	792.000	0.78	792.000	29.84	32.89	7-Nov-13	10:30	1.367	0.587	790.633	790.920	
MW-H26A	6,098,990	627,478	792.000	0.78	792.000	29.84	32.89	10-Feb-14	11:10	1.490	0.710	790.510		Pressure Transducer records available from July 2013
MW-H26B	6,098,987	627,485	792.000	0.65	792.000	1.55	4.60	1-Nov-12	na	2.258	1.608	789.742		
MW-H26B	6,098,987	627,485	792.000	0.65	792.000	1.55	4.60	18-Dec-12	na	1.810	1.160	790.190		
MW-H26B	6,098,987	627,485	792.000	0.65	792.000	1.55	4.60	7-May-13	na	1.307	0.657	790.693		
MW-H26B	6,098,987	627,485	792.000	0.65	792.000	1.55	4.60	31-Jul-13	na	1.476	0.826	790.524		
MW-H26B	6,098,987	627,485	792.000	0.65	792.000	1.55	4.60	7-Nov-13	10:30	1.935	1.285	790.065	790.469	
MW-H26B	6,098,987	627,485	792.000	0.65	792.000	1.55	4.60	11-Feb-14	11:15	1.705	1.055	790.295		Pressure Transducer records available from July 2013
MW-H27	6,098,578	627,607	810	0.47	810	34.58	37.63	31-Jul-13	na	10.365	9.895	799.635		
MW-H27	6,098,578	627,607	810	0.47	810	34.58	37.63	8-Nov-13	12:15	10.436	9.966	799.564		
MW-H27	6,098,578	627,607	810	0.47	810	34.58	37.63	10-Feb-14	9:15	10.510	10.040	799.490	799.563	
MW-H28	6,098,772	627,715	819	0.70	819	13.92	16.97	31-Jul-13	na	12.591	11.891	806.409		
MW-H28	6,098,772	627,715	819	0.70	819	13.92	16.97	8-Nov-13	16:15	12.798	12.098	806.202		
MW-H28	6,098,772	627,715	819	0.70	819	13.92	16.97	12-Feb-14	10:10	11.520	10.820	807.480	806.697	
MW-H29	6,099,198	627,938	826	0.70	826	8.26	11.31	31-Jul-13	na	5.578	4.878	820.422		
MW-H29	6,099,198	627,938	826	0.70	826	8.26	11.31	9-Nov-13	na	5.788	5.088	820.212	820.317	
MW-H29	6,099,198	627,938	826	0.70	826	8.26	11.31	10-Feb-14	10:00	5.260	4.560	820.740		
MW-H30	6,098,501	627,372	793	0.73	793	11.46	14.51	31-Jul-13	na	13.644	12.914	779.356		
MW-H30	6,098,501	627,372	793	0.73	793	11.46	14.51	8-Nov-13	13:20	10.140	9.410	782.860		
MW-H30	6,098,501	627,372	793	0.73	793	11.46	14.51	11-Feb-14	11:25	9.160	8.430	783.840	782.019	
MW-H31	6,099,893	627,456	798	0.68	798	27.37	30.42	31-Jul-13	na	15.703	15.023	782.297		
MW-H31	6,099,893	627,456	798	0.68	798	27.37	30.42	9-Nov-13	17:00	16.738	16.058	781.262	781.780	
MW-H32	6,099,810	628,333	840	0.37	840	27.08	30.13	31-Jul-13	na	10.771	10.401	829.229		
MW-H32	6,099,810	628,333	840	0.37	840	27.08	30.13	10-Nov-13	16:10	11.195	10.825	828.805		
MW-H32	6,099,810	628,333	840	0.37	840	27.08	30.13	13-Feb-14	10:45	9.270	8.900	830.730	829.588	
MW-PNB	6,097,114	625,101	778.853	1.27	778.983	45.50	48.50	6-Jul-11	na	13.050	11.780	765.933		
MW-PNB	6,097,114	625,101	778.853	1.27	778.983	45.50	48.50	15-Oct-11	na	13.070	11.800	765.913		
MW-PNB	6,097,114	625,101	778.853	1.14	778.853	45.50	48.50	11-May-12	na	14.820	13.680	764.033		
MW-PNB	6,097,114	625,101	778.853	1.14	778.853	45.50	48.50	21-Aug-12	na	14.057	12.917	764.796		
MW-PNB	6,097,114	625,101	778.853	1.14	778.853	45.50	48.50	19-Dec-12	na	15.206	14.066	763.647		
MW-PNB	6,097,114	625,101	778.853	1.14	778.853	45.50	48.50	7-May-13	na	14.102	12.962	764.751		
MW-PNB	6,097,114	625,101	778.853	1.14	778.853	45.50	48.50	21-Jul-13	na	13.575	12.435	765.278		
MW-PNB	6,097,114	625,101	778.853	1.14	778.853	45.50	48.50	6-Nov-13	16:00	14.678	13.538	764.175	764.846	
MW-PNB	6,097,114	625,101	778.853	1.14	778.853	45.50	48.50	8-Feb-14	14:45	14.615	13.475	764.238		
MW-Shaft	6,098,150	625,176	846.032	0.90	846.032	2.10	5.10	9-Jul-11	na	3.275	2.375	842.757		
MW-Shaft	6,098,150	625,176	846.032	0.90	846.032	2.10	5.10	22-Aug-12	na	4.445	3.545	841.587		
MW-Shaft	6,098,150	625,176	846.032	0.90	846.032	2.10	5.10	25-Oct-12	na	4.785	3.885	841.247		
MW-Shaft	6,098,150	625,176	846.032	0.90	846.032	2.10	5.10	20-Dec-12	na	3.985	3.085	842.047		
MW-Shaft	6,098,150	625,176	846.032	0.90	846.032	2.10	5.10	23-Jul-13	na	4.235	3.335	841.797		
MW-Shaft	6,098,150	625,176	846.032	0.90	846.032	2.10	5.10	11-Nov-13	9:45	4.330	3.430	841.702	841.697	
MW-Shaft	6,098,150	625,176	846.032	0.90	846.032	2.10	5.10	9-Feb-14	11:00	3.815	2.915	842.217		
VWP-H7-1MPa	6,100,872	622,015	1,131.500	na	na	92.50		4-Apr-11	na	na	-11.099	1142.60		
	6,100,872	622,015	1,131.500	na	na	92.50		13-May-12	na	na	-0.292	1131.79		
	6,100,872	622,015	1,131.500	na	na	92.50		24-Aug-12	na	na	2.880	1128.62		
VWP-H7-2MPa	6,100,872	622,015	1,131.500	na	na	207.50		4-Apr-11	na	na	-0.740	1132.24		
	6,100,872	622,015	1,131.500	na	na	207.50		13-May-12	na	na	4.076	1127.42		
	6,100,872	622,015	1,131.500	na	na	207.50		24-Aug-12	na	na	6.640	1124.86		
VWP-H12-1MPa	6,100,659	624,446	1,120.800	na	na	116.00		4-Apr-11	na	na	15.609	1105.19		
	6,100,659	624,446	1,120.800	na	na	116.00		24-Aug-12	na	na	24.190	1096.61		
VWP-H12-2MPa	6,100,659	624,446	1,120.800	na	na	210.00		4-Apr-11	na	na	78.288	1042.51		
	6,100,659	624,446	1,120.800	na	na	210.00		24-Aug-12	na	na	81.660	1039.14		
TH12-03*	6,096,785	624,886	783.804	0.79	783.804	na	na	25-Aug-12	na	20.018	19.228	763.786	763.786	

Note: na indicates record not available or not applicable

Table 2.5-2. Wells with Water Level and Hydraulic Conductivity Data Used for Groundwater Model Construction

Well Name	Easting m	Northing m	Ground Elevation masl	Top of Casing Elevation masl	Elevation of Screen's Midpoint masl	Measured Groundwater Elevation masl	Depth to Monitoring Point mbgs	Measured Hydraulic Conductivity m/sec	Date of Measurement	Source	Formation	Notes
1	2	3	4	5	6	7	8	9	10	11	12	13
MW-H2A	620575	6101837	1103.581	1104.341	1018.54	1094.21	85.04	1.5E-07	2011 - 2012	Rescan 2013c	Hasler Formation	Mudstone / Siltstone
MW-H3A	621818	6102191.4	1215.26	1215.71	1027.25	1189.01	188.01		7-Jul-11	Rescan 2013c	Boulder Creek Formation	Sandstone
MW-H5	620658	6100571	1101.85	1102.53	1072.82	1102.53	29.03	2.0E-06	2011 - 2012	Rescan 2013c	Overburden	Sand and Gravel
MW-H13	626086.4	6098569	820.31	821.58	752.81	767.46	67.5		2011 - 2012	Rescan 2013c	Hasler Formation	Shale
MW-H15	624907	6098253	853.23	854.40	756.18	799.74	97.05		2011 - 2013	Rescan 2013c plus July 2013 field event data	Boulder Creek Formation	Sandstone
MW-H16	624891	6097821	836.61	837.47	769.60	777.80	67.01	6E-9 to 3E-8	May, Aug 2012	Rescan 2013c	Boulder Creek Formation	Sandstone
MW-H17	625520	6097925	829.30	829.96	822.30	824.28	7	2.0E-06	2012 - 2013	Rescan 2013c plus July 2013 field event data	Overburden	Silty Sand/Shale bedrock interface
MW-H18	625740	6097953	830.88	831.70	818.88	819.69	12	2.0E-06	2012 - 2013	Rescan 2013c plus July 2013 field event data	Hasler Formation	Shale
MW-H19	625663	6098131	832.57	833.34	825.37	829.04	7.2	5.0E-09	2012 - 2013	Rescan 2013c plus July 2013 field event data	Hasler Formation	Shale
MW-H20	624396.9	6099765.8	953.53	954.20	914.11	927.75	39.43	1.5E-08	2011 - 2012	Rescan 2013c	Boulder Creek Formation	Sandstone
MW-H21	625390.3	6100258.8	915.70	917.00	864.80	891.05	50.9		2011 - 2012	Rescan 2013c	Hasler Formation	Mudstone
MW-H22	624960	6096815	783.57	784.42	759.97	763.72	23.6	1.0E-06	2012 - 2013	Rescan 2013c plus July 2013 field event data	Overburden	Silty Sand
MW-H23	624942	6096618	784.92	785.70	761.30	763.29	23.62	3.0E-05	2012 - 2013	Rescan 2013c plus July 2013 field event data	Overburden	Sand
MW-H24A	628116	6099756	831.10	832.00	784.80	814.90	46.3	7.0E-08	2012 - 2013	Rescan 2013c plus July 2013 field event data	Hasler Formation	Siltstone/Sandstone interface
MW-H24C	627954	6099625	824.08	825.00	813.38	822.49	10.7	1.1E-06	06/31/13	June-July 2013 field event data	Hasler Formation	Mudstone
MW-H25A	627334	6099615	765.30	766.00	704.80	764.59	60.5	4E-7 to 6E-9	2012 - 2013	Rescan 2013c plus July 2013 field event data	Hasler Formation	Mudstone / Sandstone
MW-H26A	627478	6098990	791.22	792.00	758.02	790.98	33.2	2E-6 to 7E-8	2012 - 2013	Rescan 2013c plus July 2013 field event data	Hasler Formation	Mudstone / Sandstone
MW-H27	627607	6098578	809.53	810.00	772.03	799.64	37.5	2.0E-07	7/31/2013	Rescan July 2013 field event data	Hasler Formation	Mudstone / Sandstone
MW-H28	627715	6098772	818.30	819.00	801.80	806.41	16.5	2.0E-07	7/31/2013	Rescan July 2013 field event data	Hasler Formation	Mudstone / Sandstone
MW-H30	627372	6098501	792.27	793.00	779.27	779.36	13	3.6E-09	7/31/2013	Rescan July 2013 field event data	Overburden	Silty clay
MW-H31	627456	6099893	797.32	798.00	768.32	782.30	29	2.4E-08	7/31/2013	Rescan July 2013 field event data	Overburden	Silty clay
MW-H32	628333	6099810	839.63	840.00	811.13	829.23	28.5	2.4E-09	7/31/2013	Rescan July 2013 field event data	Hasler Formation	Siltstone / Sandstone
MW-PNB	625101	6097114	777.58	778.85	730.71	765.49	46.87		2011 - 2013	Rescan 2013c plus July 2013 field event data	Overburden	Glacial till
MW-Shaft	625176	6098150	845.13	846.03	841.61	841.89	3.52		2011 - 2013	Rescan 2013c plus July 2013 field event data	Overburden	Glacial till
P1R-35 - Test Zone 1	621852	6099308	1083	N/A	447.5	1097.7	635.5	4.5E-10	2010	AMEC 2010	Gates	Sandstone / Mudstone
P1R-35 - Test Zone 3	621852	6099308	1083	N/A	590.0	1098.9	493	3.0E-08	2010	AMEC 2010	Hulcross	Sandstone / Mudstone
P1R-35 - Test Zone 4	621852	6099308	1083	N/A	769.5	1098.8	313.5	2.9E-08	2010	AMEC 2010	Hasler / Boulder Creek	Sandstone / Mudstone
H2 - Test Zone 1	620584	6101836.4	1111.9	N/A	375	1094	737	4.5E-09	2012	AMEC 2012	Hulcross / Gates	Sandstone / Mudstone
H2 - Test Zone 2	620584	6101836.4	1111.9	N/A	720	1134	392	1.8E-09	2012	AMEC 2012	Hasler / Boulder Creek	Sandstone / Mudstone
H16W - Test Zone 1	624789	6097713	835.5	N/A	-40	831.5	876	6.1E-09	2012	AMEC 2012	Gates	Sandstone / Mudstone
H16W - Test Zone 3	624789	6097713	835.5	N/A	580	815.4	256	2.7E-08	2012	AMEC 2012	Hasler	Sandstone / Mudstone
BD11-011	628313	6091327	1420.18	?	1383.61	1417	36.57		2011	SRK 2012, Appx B-1, Table 8.2	Overburden	Glacial till
BD11-012	628585	6091997	1281.63	?	1271.51	1273	10.12		2011	SRK 2012, Appx B-1, Table 8.2	Overburden	Glacial till / bedrock contact
BD11-014	625953	6091270	1256.44	?	1226.75	1228	29.69		2011	SRK 2012, Appx B-1, Table 8.2	Overburden	Glacial till / bedrock contact
MW05-1a	618240	6096769.9	1422.46	1423.06	1320.49	1416.26	101.97	8.2E-08	Dec-05	Lorax Environmental 2007	Bedrock	Siltstone
MW05-2b	617523.4	6097674.6	1262.82	1263.42	1237.22	1261.22	25.60	6.7E-07	Dec-05	Lorax Environmental 2007	Bedrock	Sandstone
MW05-3a	618902.2	6097617.5	1291.58	1292.18	1191.60	1299.21	99.98	6.4E-06	Dec-05	Lorax Environmental 2007	Bedrock	Siltstone
MW05-4a	618477.7	6098334.4	1201.44	1202.04	1121.28	1201.44	80.17	1.1E-07	Dec-05	Lorax Environmental 2007	Bedrock	Siltstone

Notes:

masl - meters above sea level

N/A - not applicable

AMEC 2010. Memorandum: Packer Testing to Assess Bedrock Permeability Tumbler Ridge, B.C., From T. Kostya, AMEC to J. Luo, Canadian Dehua International Mines Group Inc.

AMEC 2012. Single Well Response Tests: Proposed Murray River Underground Coal Mine, Tumbler Ridge, BC. Submitted to Canadian Dehua International Mines Group Inc. by AMEC Environment and Infrastructure, Kamloops, BC.

Lorax Environmental 2007. Application for an Environmental Assessment Certificate for the Hermann Mine Project submitted by Western Canadian Coal to Bob Hart (British Columbia Environmental Assessment Office) February 2007. Volume 2: Main Document - Part 2, Section 8 – Groundwater, Section 12 – Terrain and Soils.

Rescan 2013. Murray River Coal Project: 2011 to 2012 Hydrogeology Baseline Report. Prepared for HD Mining International Ltd. by Rescan Environmental Services Ltd.: Vancouver, British Columbia, May 2013.

SRK 2012. Quintette Groundwater Technical Assessment Report - Appendix 4-7-A Groundwater Technical Data – Report prepared for Teck Coal Corporation, March 2012.

In February 2010, AMEC conducted (AMEC 2010) a series of packer tests conducted on borehole P1R35. The results of those tests are particularly relevant for this modelling project as the formations subject to testing were coal seams of the Gates Formation. Hydraulic conductivity results were 2.1 x 10^{-7} m/sec for coal sections of Gates Formation with coal seams F, G and I, and 3.0 x 10^{-8} m/sec for sandstone and mudstone at the bottom of coal seam D.

Nine shallow piezometers installed as part of Hermann Mine Project were subject to hydraulic testing in 2005. That project is adjacent to Murray River Coal Project area on its western / southwestern side. The calculated values of hydraulic conductivity ranged from 1.2 × 10^{-9} to 6.4 × 10^{-6} m/s, with the geometric mean of the results equal 1.8 × 10^{-7} m/s (Lorax Environmental 2007 – Table 8.3-2). All those tested piezometers were installed in shallow bedrock (mostly siltstone but also sandstone – no stratigraphic designation was provided in the report) and one in moraine deposits.

A considerable amount of hydraulic testing was conducted as part of Quintette Mine Project, adjacent to the Murray River Coal Project area, on eastern side of Murray River and south of CCR Site. The average hydraulic conductivity calculated from thirty five tests conducted on boreholes located in Mount Babcock and Shikano Pit areas is reported to be 1.5 x 10^{-7} m/sec (SRK 2012). All those bores are less than 200 meter deep, most of them completed in Gates Formation (siltstone, mudstone, sandstone and coal seams), some in Hulcross Formation (mudstone, shale, clay) and in Boulder Creek Formation (sandstone, mudstone).

In April and August 2011, AMEC installed two observation wells and conducted pumping and recovery tests, step-drawdown test (borehole H2 only), and constant head test in two deep exploration boreholes H2 and H16W. Conductivity estimates were collected at six vertical intervals at depths covering Hasler, Boulder Creek, Hulcross and Gates formations. The packers were used to isolate different depth intervals of the boreholes ranging from 20 to 950 mbgs. The obtained values of hydraulic conductivity are consistently low, in the range of 4 x 10^{-10} m/sec to 3 x 10^{-8} m/sec (AMEC 2012).

AMEC (2013) conducted packer testing of three deep boreholes completed at the Bullmoose North property located approximately 30 km west of Tumbler Ridge, BC, where construction of an underground coal mine is proposed. Packer tests were performed using triple and dual packer configurations along test intervals ranging between 6 and 107 m. Packer tests were performed only in the Gates and Boulder Creek formations. Hulcross and Hassler transmissivities were conservatively assumed to be equal to the measurement accuracy of the applied packer test methodology (1 x 10^{-8} m/sec). Hydraulic conductivities measured in Boulder Creek formation ranged between <1 x 10^{-8} and 6.2 x 10^{-7}, while hydraulic conductivities in Gates formation ranged between 2 x 10^{-8} and 4 x 10^{-7}. However, all of Gates formation hydraulic conductivities measured at greater depths (600 – 700 meters below ground surface) were less than 1 x 10^{-7}m/sec.

Golder Associates (2013a) provide information about packer testing (slug and constant rate injection) of the vertical shaft pilot hole located about 1,200 m west of Murray River. This testing conducted concurrently with the geotechnical drilling program, was carried out to a depth of 236 mbgs. A total of nine single well pressure response tests were performed on Hasler and Boulder Creek formations. The calculated hydraulic conductivity ranged from 2 x 10^{-9} to 6 x 10^{-6} m/sec showing a trend of values decreasing with depth (Golder Associates 2013a, Table 19).

Golder Associates (2013b) conducted packer testing of twelve boreholes drilled at Wapiti River project located near Tumbler Ridge, BC, where the underground development is proposed. The tests used wireline packer system. The boreholes ranged in depth from 258 m to 1,092 m. Several rock formations underlying the project site were targeted for testing bulk hydraulic conductivity ranging from Hasler (the shallowest) to Gething (the deepest). The following values of hydraulic conductivity were obtained for different formations:

- Hasler: from 1×10^{-9} m/sec to 2×10^{-9} m/sec;
- Boulder Creek: from 2×10^{-12} m/sec to 2×10^{-8} m/sec;
- Hulcross: from 3×10^{-11} m/sec to 7×10^{-10} m/sec; and
- Gates: from 1×10^{-10} m/sec to 3×10^{-8} m/sec.

Figure 2 of that report (Golder Associates 2013b) shows a weak trend of decreasing hydraulic conductivity with depth below ground surface.

The available values of measured hydraulic conductivities (see Figures 3.1-1a and 3.1-1b) show that the bedrock permeability appears to be generally decreasing with depth. Table 2.5-2 provides the measured hydraulic conductivities for monitoring points included in the model calibration database (also see discussion in Section 5 – Model Calibration).

3. HYDROGEOLOGICAL CONCEPTUAL MODEL

A hydrogeologic conceptual model has been developed based on the available meteorological, geological and hydrological information and data as summarized in Chapter 2, and the findings of the hydrogeology baseline studies (ERM 2014b).

Figures 3.1-1a and 3.1-1b show a pattern of hydraulic conductivities changing with depth. Figures 2.3-4, 3.2-1, 3.2-2, 3.2-3, and 3.2-4 show the general geologic setting with conceptual groundwater flow directions and areas of groundwater recharge and discharge.

3.1 HYDROSTRATIGRAPHIC FEATURES AND PROPERTIES

The Project is situated within a folded and faulted series of Lower Cretaceous clastic sedimentary rocks, underlying a covering dominated by glacially-derived sediments and river sediments. The majority of the rock mass is composed of mudstones and siltstones, which are inter-bedded with sandstone and coal seams. The geometry of the strata is controlled by two principal factors: structural features (presence of synclines, antyclines, faults and dense joint sets) and erosion (presence of river and creek valleys dissecting the bedrock formations).

The bedrock is saturated except where it crops above the water table, and constitutes a fractured bedrock medium for saturated groundwater flow. Most of the formations are characterized by low hydraulic conductivity.

The Hasler formation (and other undifferentiated sediments above the Boulder Creek Formation) has hosted 40 hydraulic conductivity (K) measurements within the Local Study Area (LSA), which show K ranging from 6E-6 m/s to 9E-10 m/s (geometric mean of 8E-8 m/s). This wid range in the Hasler formation is interpreted to represent variability in joint density, where the lower measurements approach the permeability of the primary porosity.

The permeability appears to generally decrease with depth. The two K measurements in the Boulder Creek formation were 5E-9 m/s and 3E-8 m/s. Two measurements spanning the lower Boulder Creek, Hulcross, and upper Gates formations were 6E-9 m/s, and 2E-9 m/s. The extent of the Gates formation containing Coal Seams may present an exception to the K versus depth trend: K has been reported to be as high as 2E-7 m/s (AMEC 2010) within the part of Gates Formation that is containing the F, G, and I coal seams.

Due to a sizeable presence of sandstone in the stratigraphic columns of the Boulder Creek and Gates formations, they may behave as aquifers on a regional scale. The Hasler and Hulcross formations may behave as regional aquitards due to the dominance of mudstones and siltstones in these formations. However, the limited hydraulic conductivity data available for the deeper strata of the Project area is not sufficient to clearly designate bedrock formations within the project area as aquifers or aquitards.

Figure 3.1-1a

Hydraulic Conductivity vs. Depth – Shallow Wells

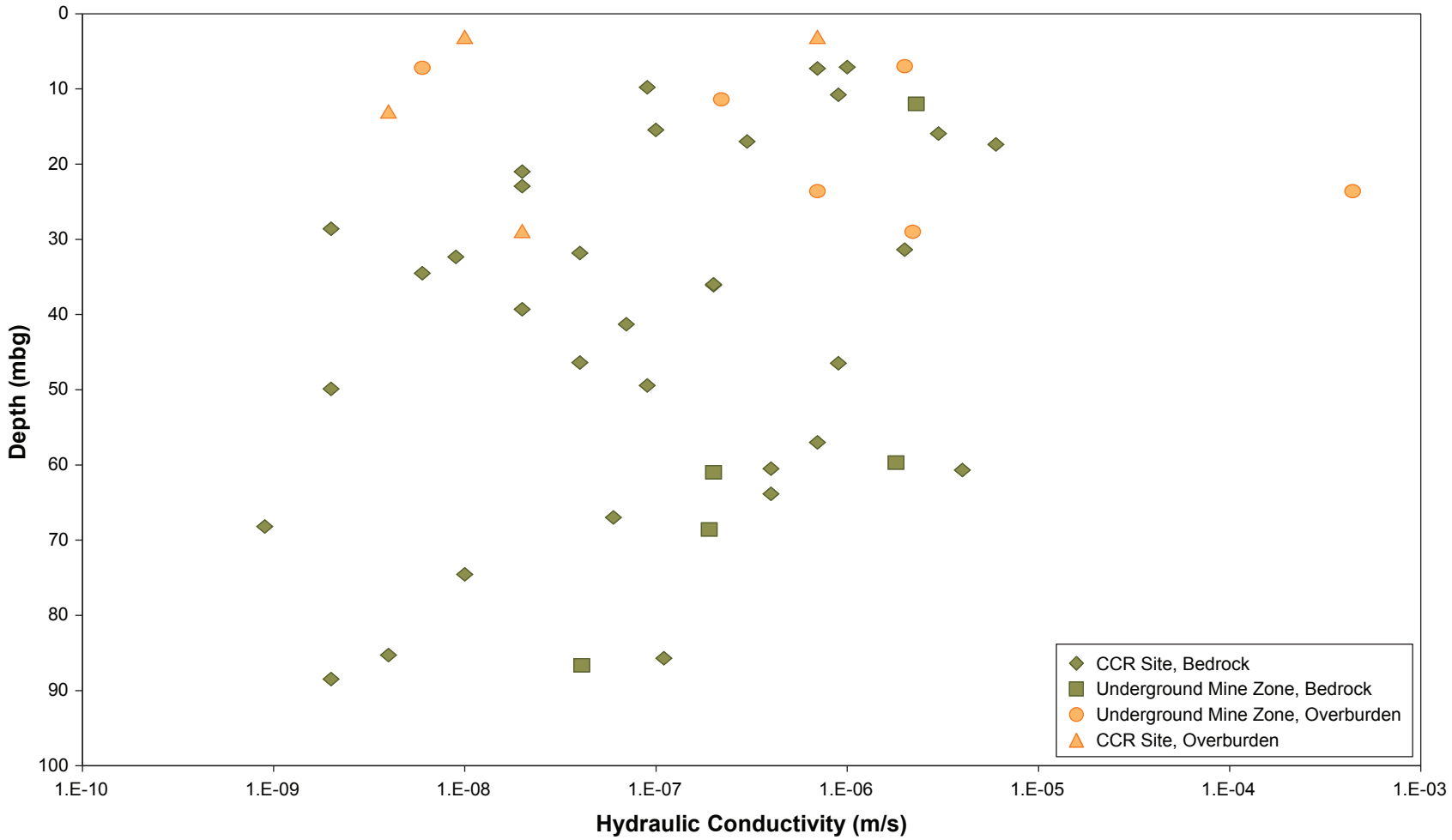

Figure 3.1-1b

Hydraulic Conductivity vs. Depth – Deep and Shallow Wells

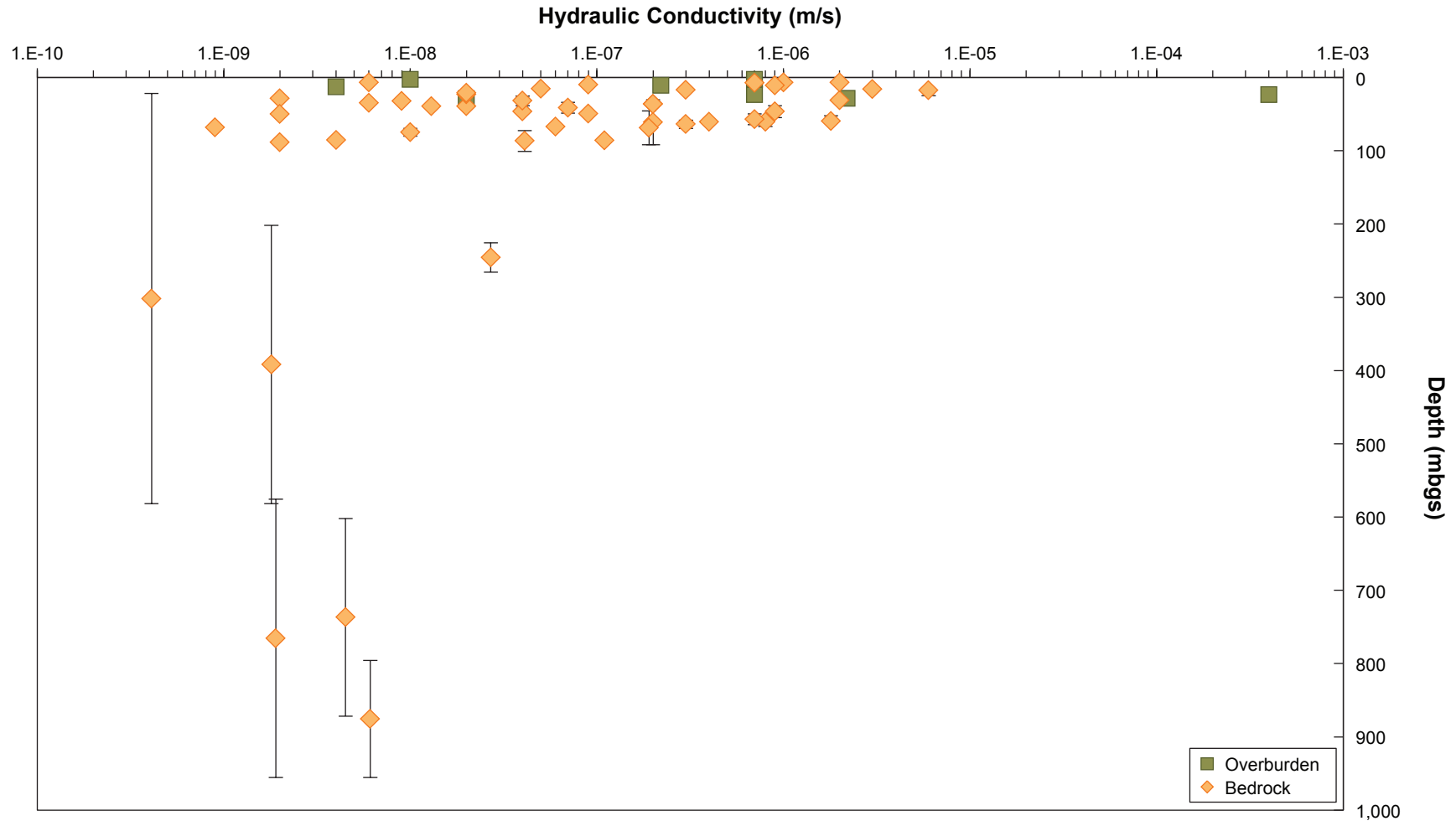

Note: Tested hydrogeologic interval is indicated by the error bar.

Surficial deposits vary greatly in thickness and lithological character from place to place. Principal deposit types include fluvial, glaciofluvial, morainal, colluvial and wetland sediments. Fluvial and glaciofluvial sediments are present mainly along the bottoms of river valleys, morainal sediments cover much of the ground surface of the hills and mountains, colluvial sediments are common along steeper slopes, while wetland sediments accumulated in terrain depressions or at the base of major slopes where locally a significant groundwater seeps can be expected.

Grain size distribution is the primary factor determining hydraulic properties of surficial sediments. Sand/gravel and clay/silt are at the opposite ends of a spectrum of high- and low-K sediments, respectively. K of gravelly sand situated in the southern part of the Underground Mine Zone have ranged as high as 4E-4 m/s, and measurements in fines within the CCR site are as low as 4E-9 m/s.

Groundwater levels in bedrock formations indicate confined conditions, except near bedrock outcrop / sub-crop areas close to deeply incised valleys. Groundwater in overburden deposits is most often present under unconfined conditions, although some wells at the CCR Site are exhibit confined conditions where a clay layer overlies a granular deposit.

3.2 GROUNDWATER FLOW REGIME (DIRECTION AND GRADIENTS)

The Project is located in a Mountain foothill area dissected by the broad valleys containing the Murray and Wolverine Rivers. Foothills within the regional study areas rise over 1000 meters above the valley bottoms: Mount Babcock 1855 masl) rises 1080 m above the Murray River (770 masl).

Such terrain results in certain consequences to a groundwater flow system. Groundwater is recharged by greater precipitation at higher elevations, while valley bottoms constitute discharge zones. Local groundwater flow systems develop above intermediate and regional flow systems, whereby localized groundwater flow discharges to small tributaries, and deeper groundwater discharges to larger streams and rivers. However, folding and faulting formations may modify these patterns.

Thus, the groundwater flow system in the project area is characterized by groundwater flowing from the upper foothills towards the Murray River, with anisotropy introduced by lithologic properties of sedimentary rocks, folds, faults and local topography (Figures 3.2-1, 3.2-2, 3.2-3 and 3.2-4). Local topography creates intermediate and shallow systems existing above regional systems (Figures 3.2-2, 3.2-3 and 3.2-4). The Camp Creek basin behaves as an intermediate catchment basin. The small watersheds containing M19a, M17b, and M19 creeks behave as local catchment basins for shallow groundwater flow in the CCR site and adjacent areas. The watersheds of Twenty Creek, M17b Creek, and other minor tributaries within the Underground Mine Zone behave as local catchment basins as well.

3.3 SPATIAL AND TEMPORAL VARIATIONS IN RECHARGE AND DISCHARGE

Recharge to groundwater is a function of a range of variables, such as precipitation, temperature, evapotranspiration, soil type, land use, and slope aspect. On a regional scale, variability in precipitation is expected to play a dominating role, whereby greater precipitation (and by extension greater recharge) is received at greater elevations due to the orographic effect.

Figure 3.2-1
Location of Cross Sections

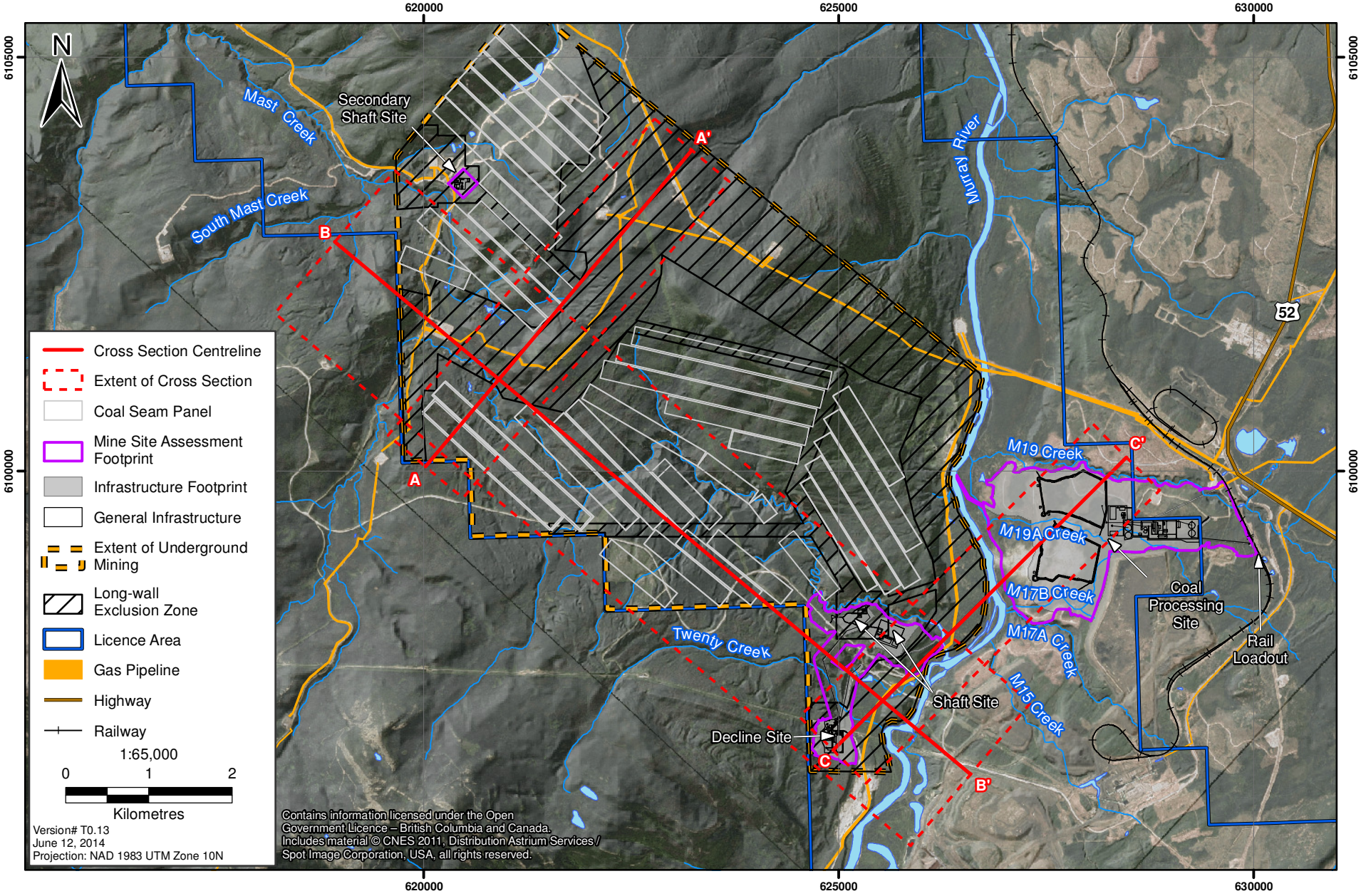

Temporal variations in natural recharge and discharge are expected to be minor. Documented seasonal variations in groundwater levels have been as high as 2 m. Given the scale of topographic relief within the LSA, these water level variations are expected to be too small to give rise to meaningful changes in hydraulic gradients or the patterns of groundwater flow. Therefore, relatively speaking, the groundwater system can be considered steady-state from the long-term average point of view.

3.4 SURFACE WATER - GROUNDWATER INTERACTIONS

All streams are fed to a varying degree by overland flow, interflow (lateral movement of water below ground surface but above the water table) and groundwater discharge. Stream flow is dominated by groundwater discharge (often referred to as base flow) during the winter or prolonged periods of low precipitation. During periods of flooding (e.g. freshet), streams may be recharging groundwater, particularly along reaches at higher elevations. Stream reaches at lower elevations are predominantly situated in groundwater discharge zones. The groundwater likely supports Wetlands found along the flood plains of the Murray River during non-peak flow periods.

3.5 GROUNDWATER ABSTRACTIONS

The only known currently operating groundwater supply wells are located in and in close proximity to Tumbler Ridge, far from the planned underground mine area. One or two groundwater supply wells are planned to be constructed near MW-H22 at the Decline Site, west of Murray River. However, the anticipated production rate (120 m^3/day) is unlikely to cause major changes in groundwater flow patterns further away from the well(s).

Groundwater will be pumped during Construction and Operation of the planned underground mine. Several predictive model simulations discussed in further sections of this report were run to estimate the pumping rates needed to keep the mine dry.

Figure 3.2-2
Cross Section A-A'

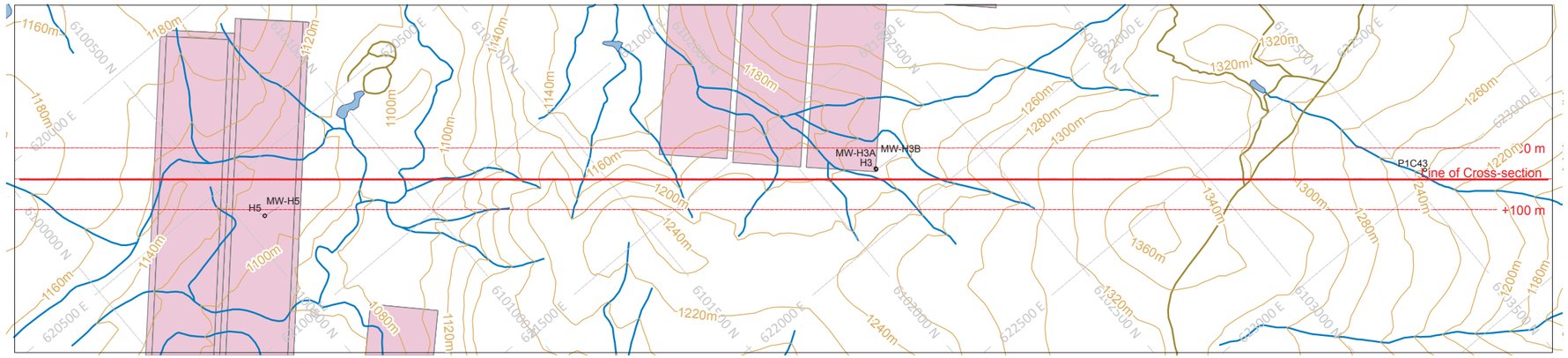

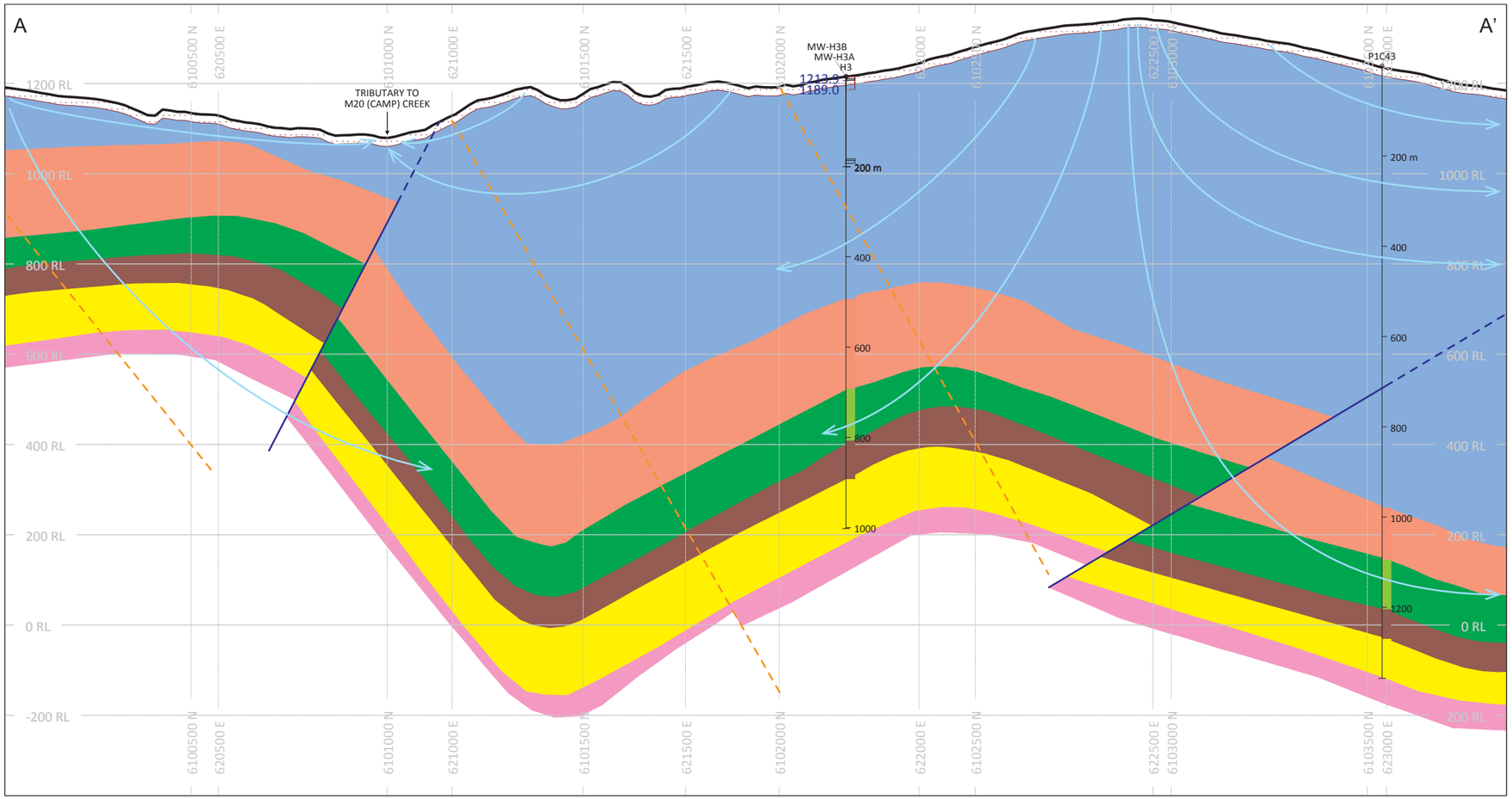

HOLES PLOTTED

TOTAL 4

H3 MW-H3A MW-H3B P1C43

- Contours
- Transportation
- Stream
- Coal Seam Panel
- Water/Wetlands
- Topography
- Groundwater Flow Line
- Overburden
- Hasler and undifferentiated
- Boulder Creek
- Hulcross
- Upper Gates
- Middle Gates
- Lower Gates
- Hydrogeology Well
- 777.8 Water Table
- Fault, Interpretted from Geophysics
- Fault, Inferred

SECTION SPECS:

REF. PT. E, N	621650 m	6101940 m
EXTENTS	5000 m	1754 m
SECTION TOP, BOT	1375 m	-378.5 m
TOLERANCE +/-	100 m	
VERTICAL EXAG.	1.5 m	

SCALE
(m)
-100 0 100 200 300 400 500
NAD83 / UTM zone 10

AZIMUTH = 45°
N
W E
S

Figure 3.2-3
Cross Section B-B'

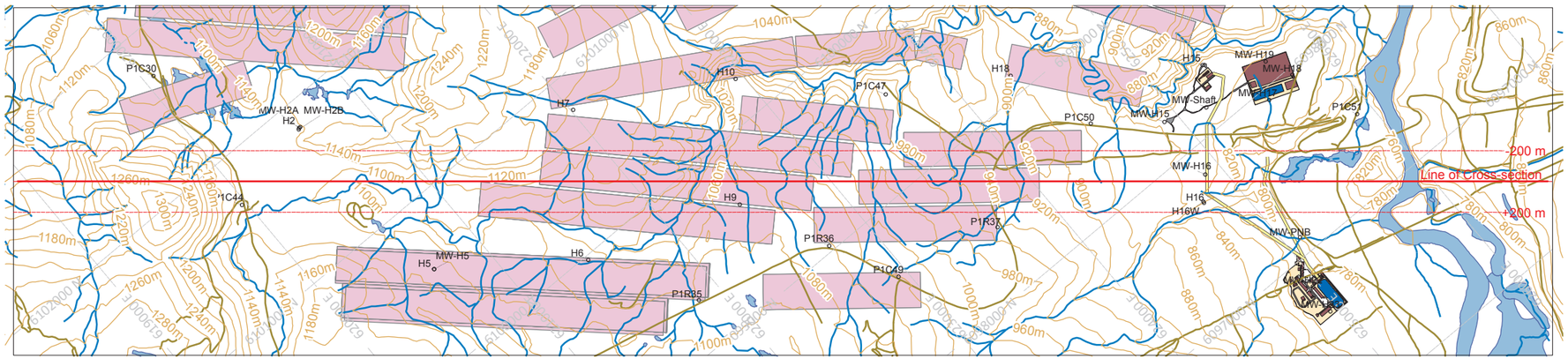

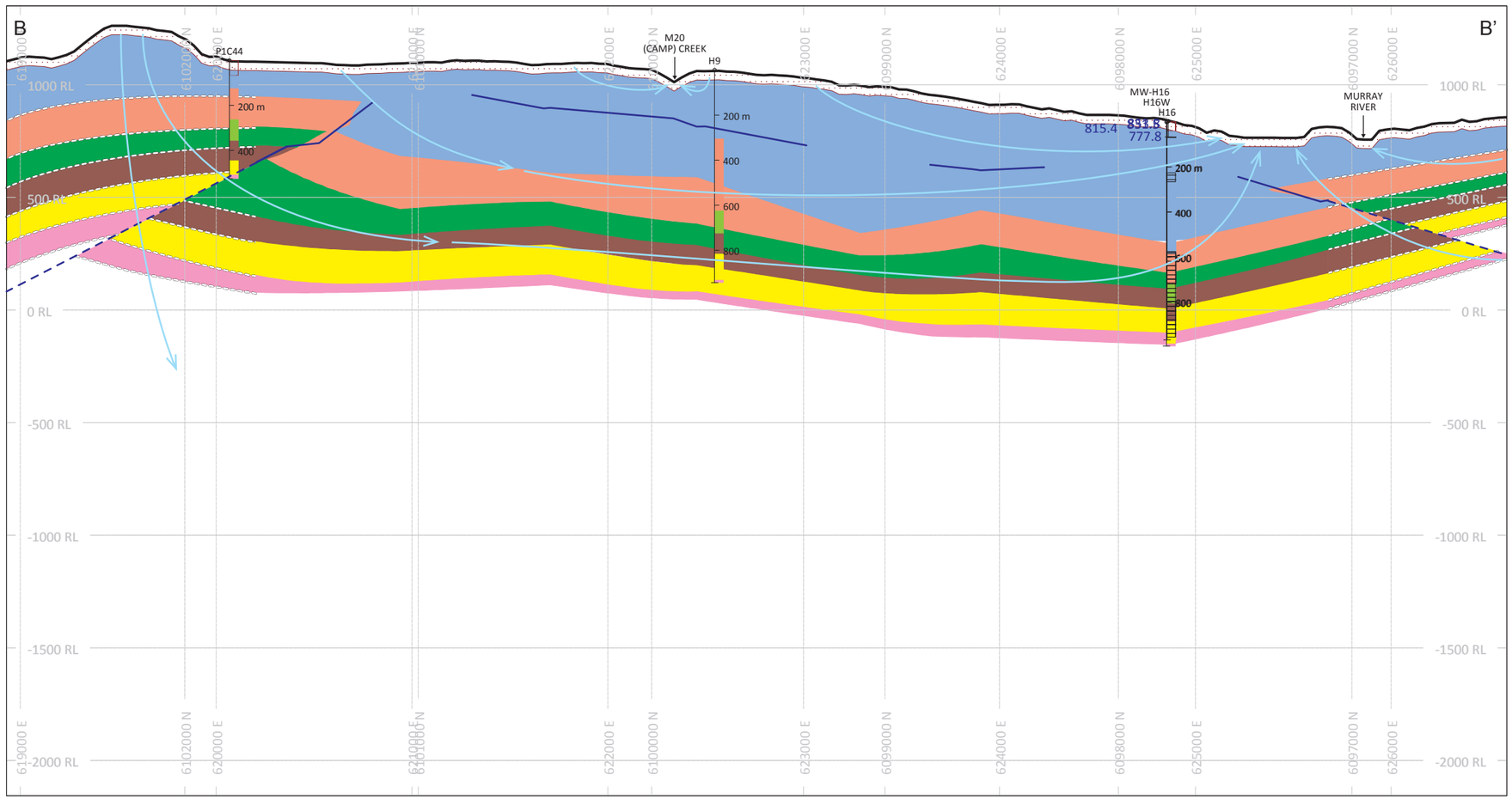

HOLES PLOTTED

TOTAL 5

H16 P1C44 | H16W | H9 | MW-H16

- Contours
- Transportation
- Stream
- Coal Seam Panel
- Water/Wetlands
- Powerline
- Conveyor
- Structure
- Concrete Paving
- Coarse Coal Reject Pile
- Pad
- Pond
- Collection Pipe
- Diversion Channel
- Topography
- Groundwater Flow Line
- Overburden
- Hasler and undifferentiated
- Boulder Creek
- Hulcross
- Upper Gates
- Middle Gates
- Lower Gates
- Hydrogeology Well
- 777.8 Water Table
- Fault, Interpretted from Geophysics
- Fault, Inferred
- Interpretted Stratigraphic Contact

SECTION SPECS:

REF. PT. E, N	622760 m	6099550 m
EXTENTS	10000 m	3508 m
SECTION TOP, BOT	1351 m	-2157 m
TOLERANCE +/-	200 m	
VERTICAL EXAG.	1.5 m	

SCALE
(m)
-200 0 200 400 600 800 1000
NAD83 / UTM zone 10

AZIMUTH = 130°
N W E S

Figure 3.2-4
Cross Section C-C'

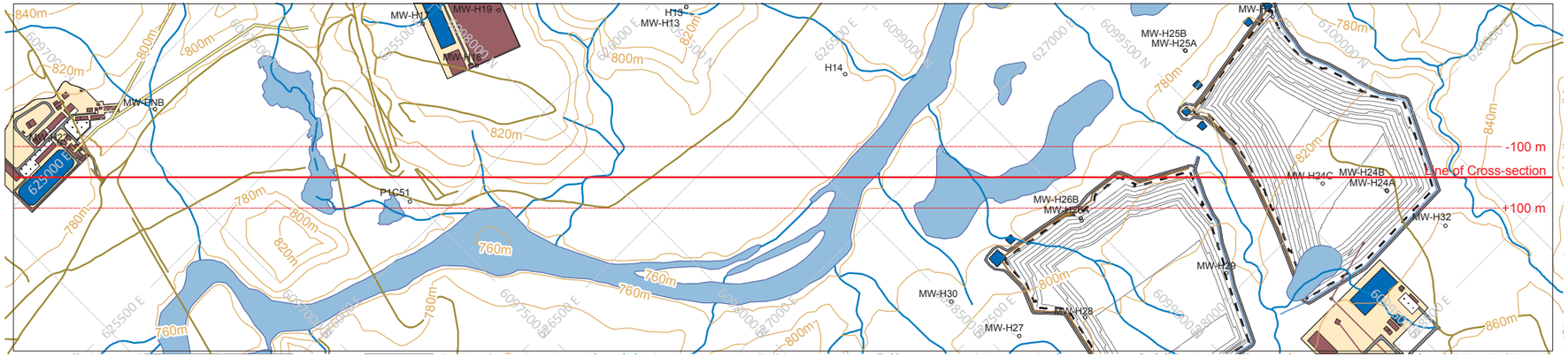

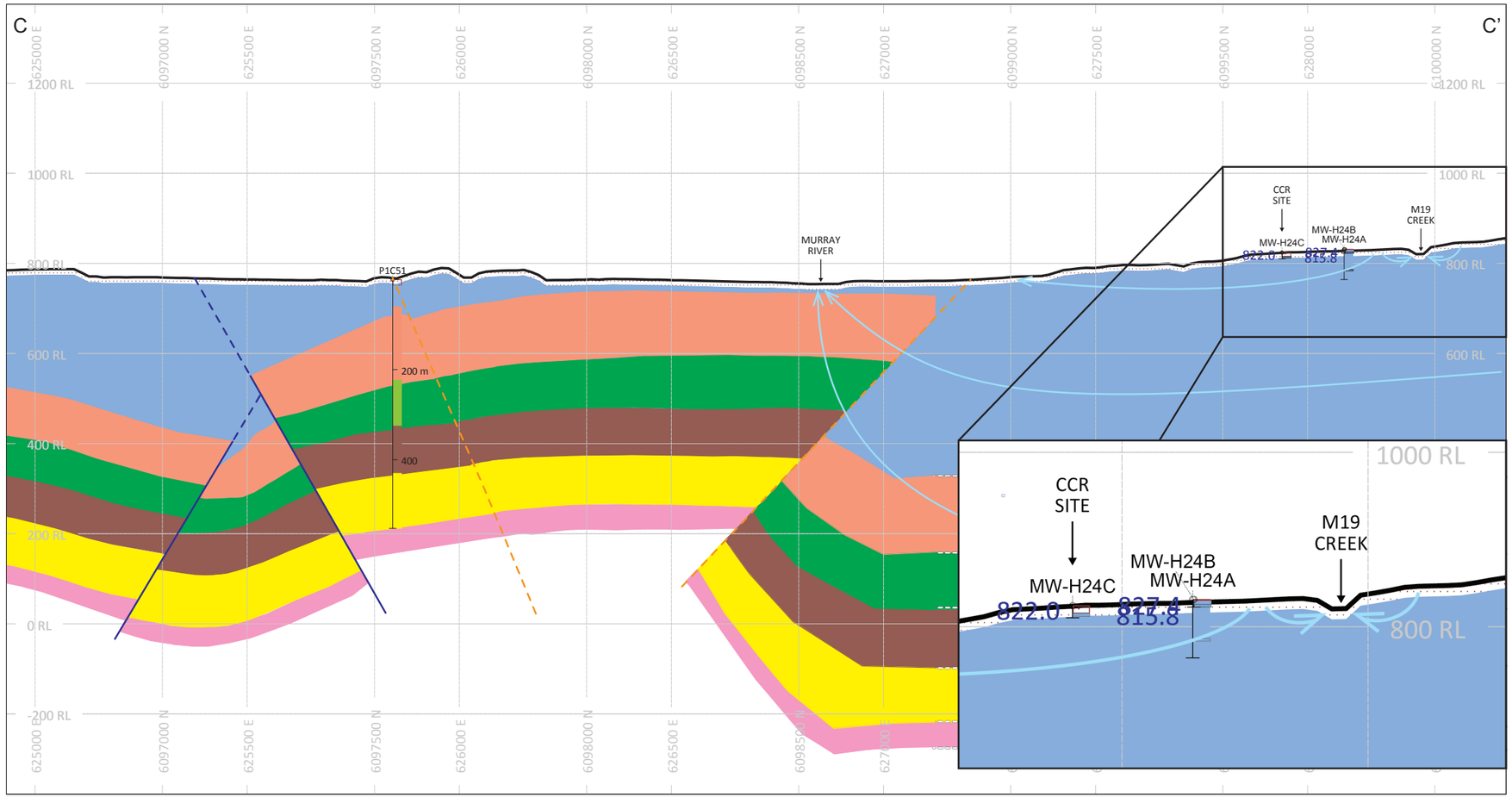

HOLES PLOTTED

TOTAL 4

MW-H24A MW-H24B MW-H24C P1C51

- Contours
- Transportation
- Stream
- Coal Seam Panel
- Water/Wetlands
- Powerline
- Conveyor
- Structure
- Concrete Paving
- Coarse Coal Reject Pile
- Pad
- Pond
- Collection Pipe
- Diversion Channel
- Topography
- Groundwater Flow Line
- Overburden
- Hasler and undifferentiated
- Boulder Creek
- Hulcross
- Upper Gates
- Middle Gates
- Lower Gates
- Hydrogeology Well
- 777.8 Water Table
- Fault, Interpretted from Geophysics
- Fault, Inferred
- Interpretted Stratigraphic Contact

SECTION SPECS:

REF. PT., E, N	626700 m	6098400 m
EXTENTS	5000 m	1754 m
SECTION TOP, BOT	1375 m	-378.5 m
TOLERANCE +/-	100 m	
VERTICAL EXAG.	1.5 m	

SCALE
(m)
-100 0 100 200 300 400 500
NAD83 / UTM zone 10

AZIMUTH = 45°
N
W E
S

4. HYDROGEOLOGICAL BASELINE NUMERICAL MODEL

4.1 MODELLING SOFTWARE CODE SELECTION AND COORDINATE SYSTEM

The model was developed using the graphical user interface of the industry standard software package Visual MODFLOW Premium, version 4.3 (Schlumberger 2008), together with MODFLOW-Surfact version 3.0 (HydroGeologic Inc. 1996).

4.2 MODEL DOMAIN

The model's domain area is about 323 km^2 and its lateral boundaries (Figure 4.2-1) were set several kilometers away from the planned mining operations. The model lateral and vertical boundaries are discussed in Section 4.5 of this report.

4.3 MODEL GRID AND LAYERS

Model grid consists of 451 rows, 455 columns and 12 layers (see: Figures 4.3-1, 4.3-2 and 4.3-3 and 4.3-4) - those are forming a total of 2,462,460 grid cells. Out of this number, only 2,402,506 cells are within the model's domain area. The 59,954 cells outside of the domain were designated inactive.

Gridlines in the central part of the grid are spaced 20 meters apart (Figure 4.3-2). The grid spacing from the central part was designed to gradually increase toward the external boundaries of the model's domain by using an expansion factor of 1.2 (the size of the next row/column is increased by a factor of 1.2, compared to the size of the previous row/column).

Two digital elevation models were used to construct the two key surfaces of the model's twelve layers: ground surface (a large database of points spaced 20 meters apart) and the top of Gates Formation (source: Huiyong Holding Group 2011 - Figure 3-2-2). Ground surface serves as the top of model Layer 1. The top of Gates Formation was set as the top of model Layer 8.

Model Layers 1 and 2 were designated to represent surficial unconsolidated deposits and the shallow weathered bedrock. They both were set as 50 m thick, with the layer bottoms running parallel to and below the ground surface. This 50 m thickness (of each layer) was modified around CCR Site to more accurately represent local lithology (as documented in thirteen boring logs available for that area).

Model Layers 3, 4 and 5 were set to represent Hasler Formation and (possibly) other, younger than Hasler formations (Goodrich, Cruiser) that may be present within the model domain area.

Model Layers 6 and 7 represent Boulder Creek and Hulcross formations, respectively. Model Layers 8 to 12 represent Gates Formation and deeper formations present within the model domain.

The tops of Hulcross and Boulder Creek formations were assumed to run parallel to Gates Formation: the top of Hulcross 80 m above the top of Gates; the top of Boulder Creek 130 m above the top of Hulcross. The thickness of Hulcross and Boulder Creek formations was assumed based on AMEC data (AMEC 2012, Figure No. 5).

Figure 4.2-1

Hydrogeological Baseline Model Domain (Plan View)

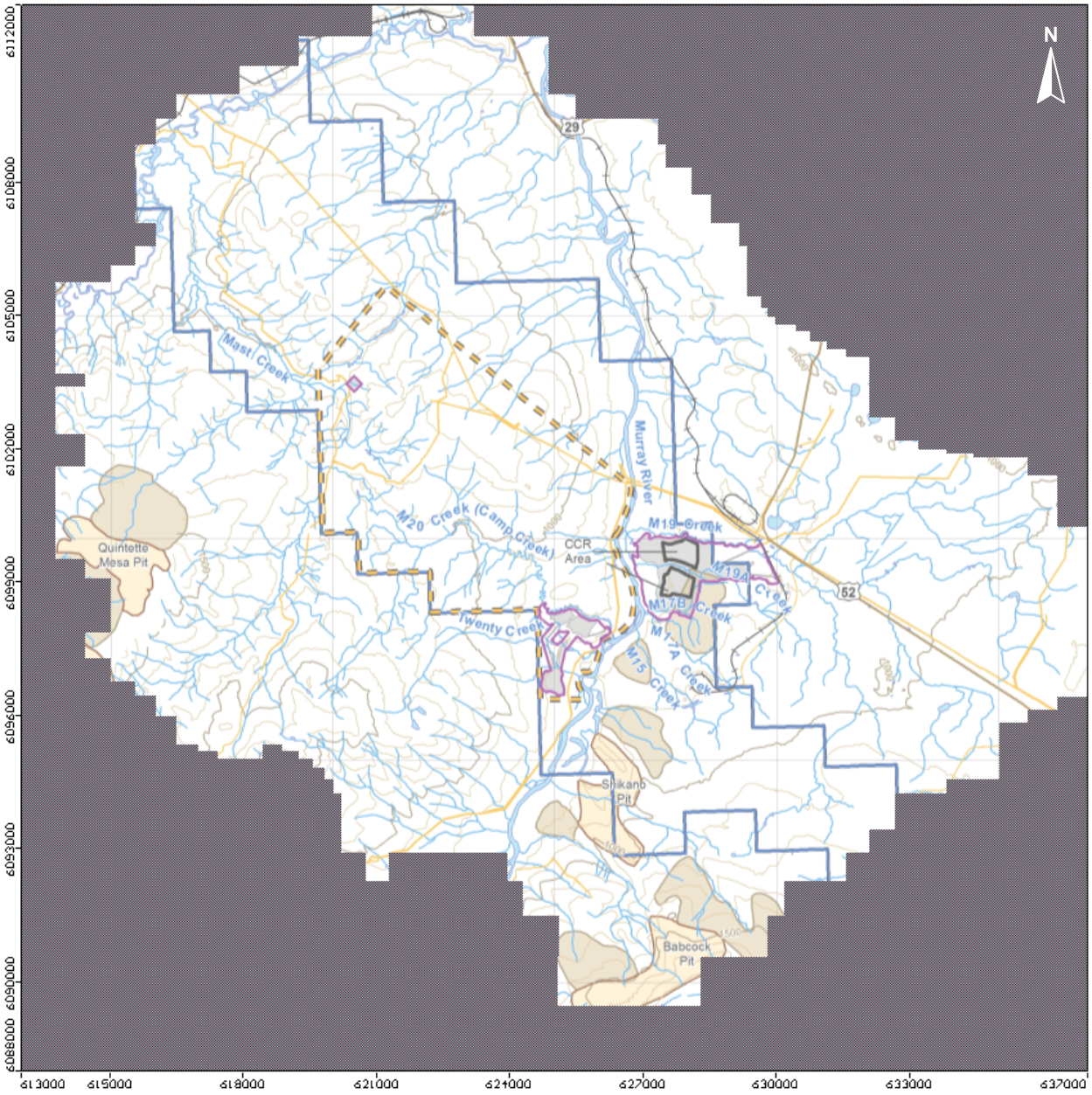

Figure 4.3-1

Hydrogeological Baseline Model Grid (Plan View, (the Entire Domain)

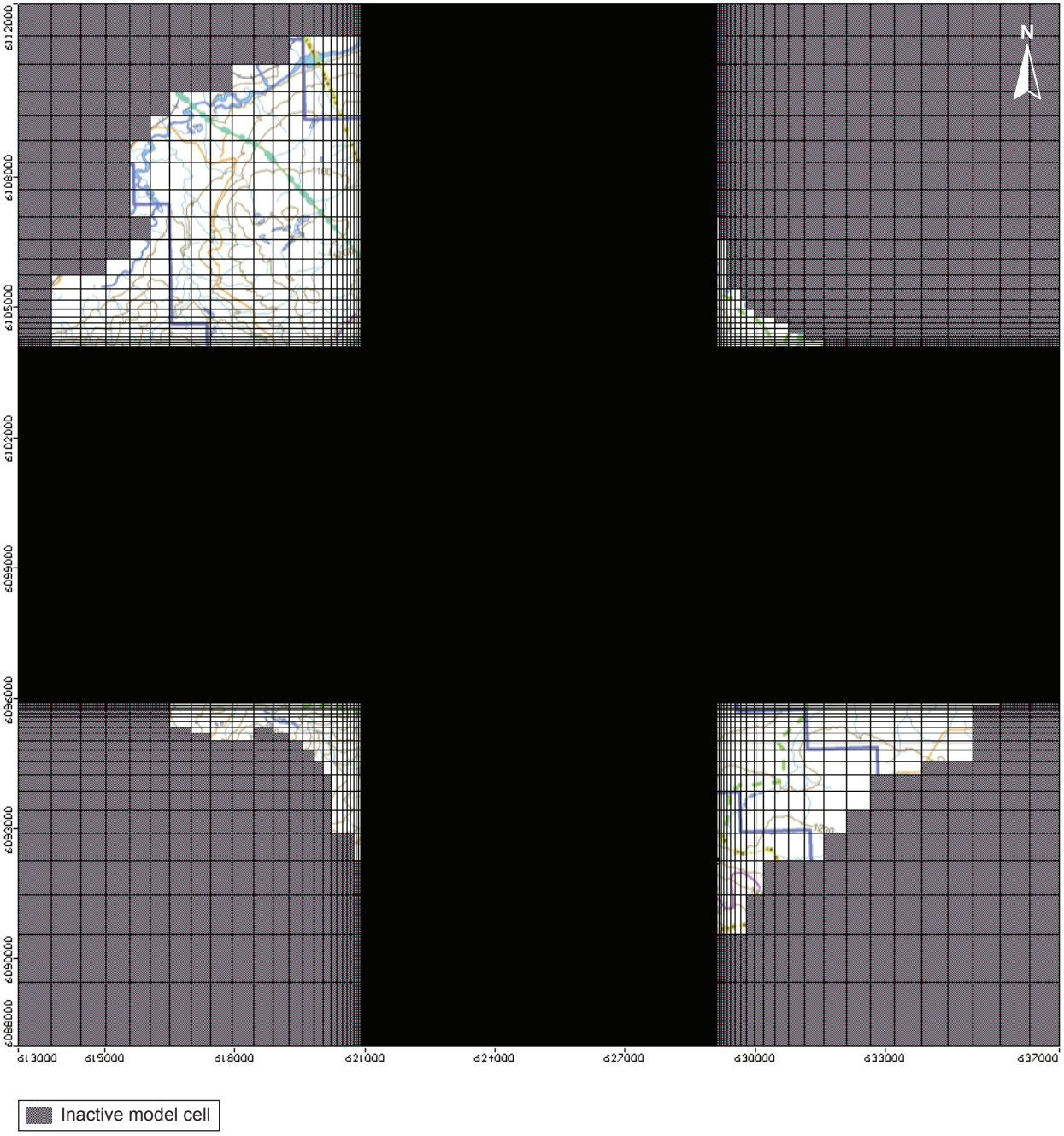

Figure 4.3-2

Hydrogeological Baseline Model Grid
(Planar View, Central Part, Underground Mine and CCR Footprints)

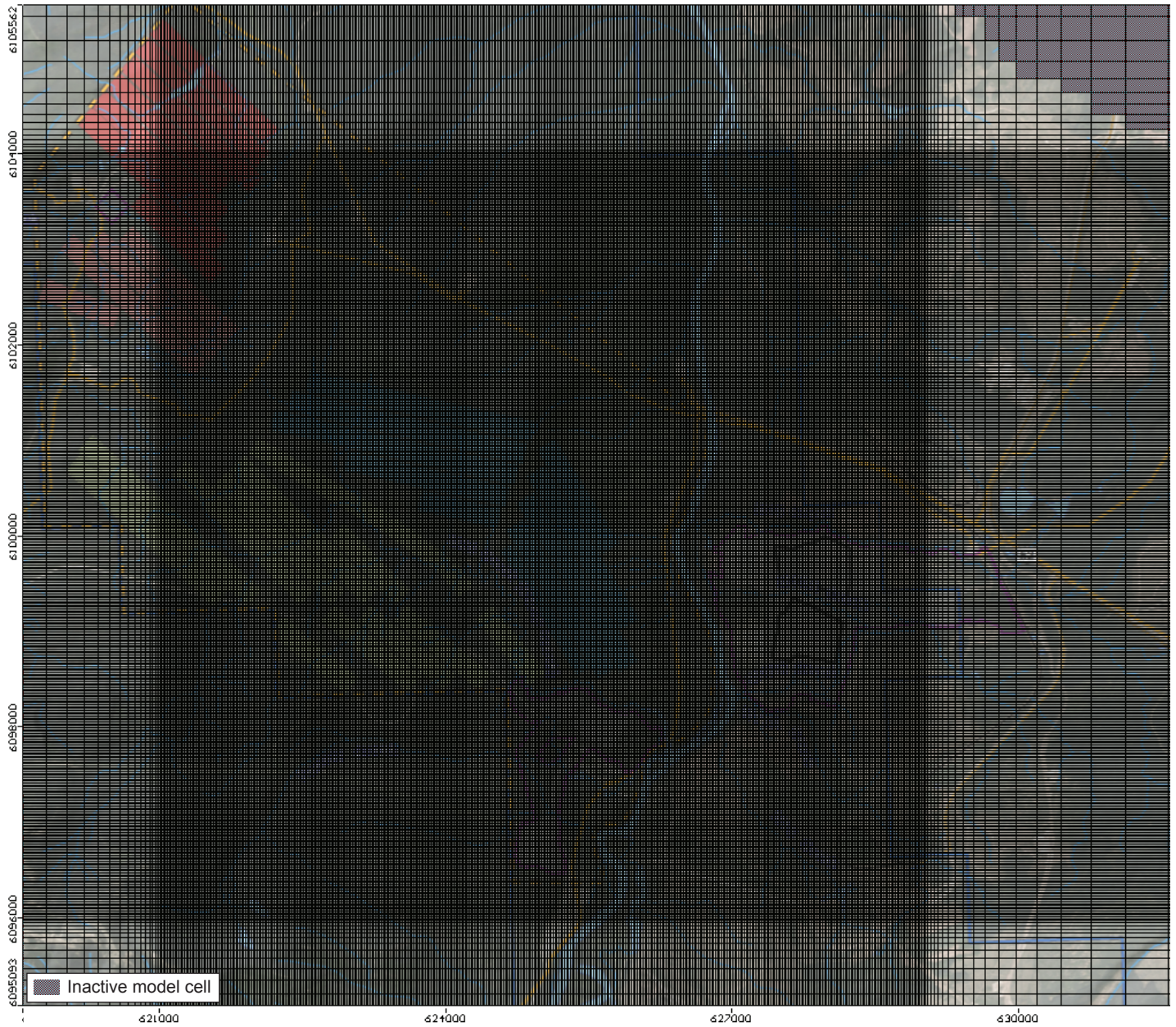

Figure 4.3-3

Hydrogeological Baseline Model Grid (Cross-section, Row 225)

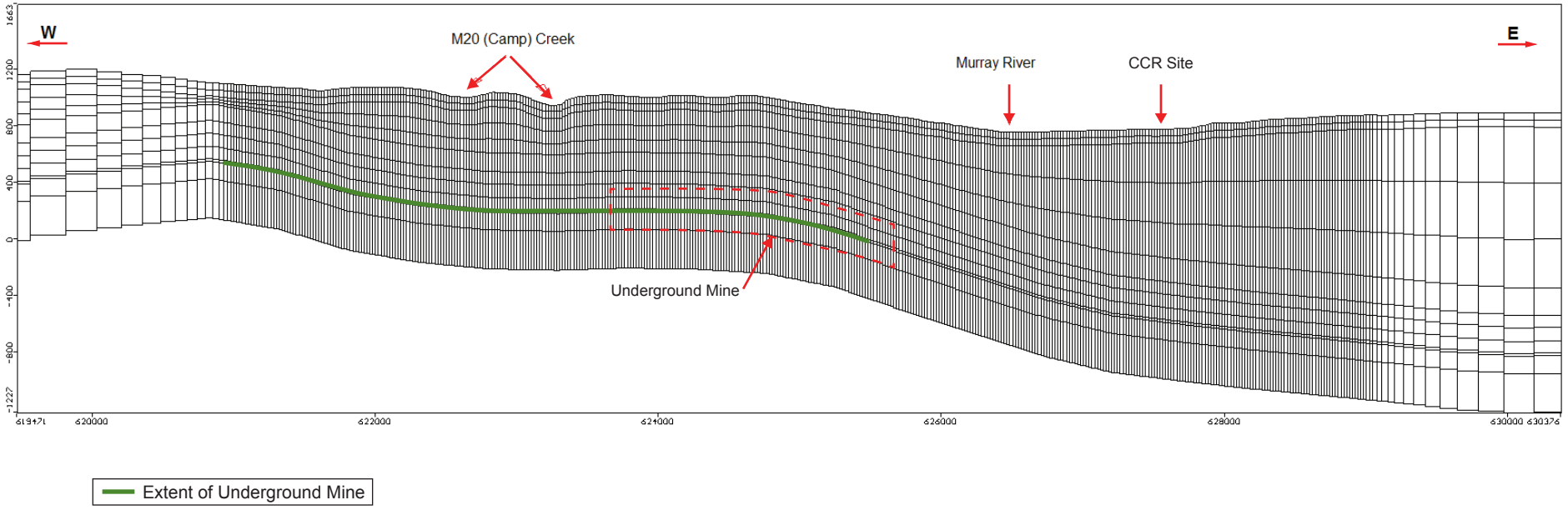

Figure 4.3-4

Hydrogeological Baseline Model Grid (Cross-section, Column 200)

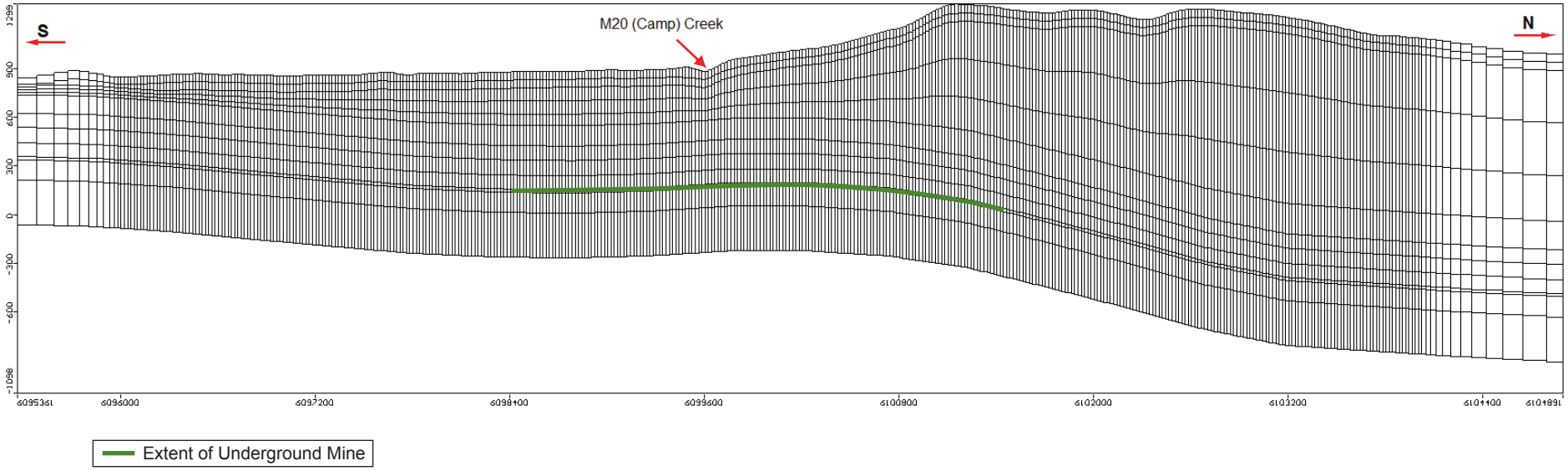

The model Layers 8 to 12 were set to represent Gates and older than Gates formations. Layer 10 represents J Coal Seam and other coal seams within Gates Formation that will be subject to mining. This layer's thickness is 20 m and represents approximately a combined thickness of all the coal seams that will be subject to underground mining.

4.4 RECHARGE

Recharge from precipitation and snow melt is assumed to account for all water entering the groundwater system in the project area. Murray River and Wolverine River are the only rivers carrying water that originated mostly from outside of the project area. However, those rivers are dominantly receiving groundwater discharge and unlikely to significantly recharge groundwater, such as to influence groundwater flow patterns on a scale of the model domain. The only exception may be periods of flooding when surface water is moving into bank storage and recharging groundwater system some distance away from the river. However, such events are of short duration and the effects of such recharge are limited to small areas and are relatively quickly reversed / dissipated.

Recharge of the modelled system via lateral inflow of groundwater from the neighbouring areas is assumed insignificant - the model domain lateral boundaries were drawn to follow either the watershed divide lines or lines of regional discharge (to Wolverine River). Recharge to the system via vertical leakage through the model's bottom is also assumed insignificant as permeability of deep bedrock is low.

The total rate of recharge over the model domain was estimated based on "low-flow" Murray River discharge rate. This discharge rate was, in turn, calculated using data collected at 07FB006 Murray River gaging station (located about 8 km north of the M20 Creek's discharge into Murray River). It was assumed that the Murray River's drainage area above that gauging station is similar in character to the area of the groundwater model domain. Since the low-flow approximates base flow (flow originating from groundwater discharge), it was used to calculate groundwater recharge per unit area and as a percentage of a long-term average precipitation (as measured at four gauging stations near the project area).

Recharge to groundwater is assumed to be primarily a function of precipitation increasing with elevation. Several other factors such as soil and vegetation types, steepness and exposition of slopes relative to cardinal directions also influence recharge. However, these were not considered directly due to difficulties in estimating in a systematic way the influences of those other factors over the area of model domain.

Precipitation tends to be correlated with elevation in mountainous regions due to the orographic effects (Loukas and Quick 1993). Data from several meteorological stations in the area around the Project site have been evaluated to characterize precipitation at the Murray River project site. The selected stations are close to the Project, located in comparable terrain and at a similar elevation (Rescan 2013d – Figure 2.2-1 and Table 2.2-1).

Rescan study (2013d provides an empirical equation that was developed to relate a long-term mean annual precipitation (MAP) to elevation of the four regional climate stations: Chetwynd A, Dawson

Creek A, Tumbler Ridge, and Bullmoose. Criteria for station selection included proximity to the Project area and length of precipitation record. The period of record for the selected stations ranged from 19-45 years.

A linear regression analysis was conducted using the mean annual precipitation points (MAP points) representing stations with the most reliable data series. The resulting equation is of the following form:

$$P = (0.696 \times E) - 19.54$$

where P is mean annual precipitation (mm) and E is median area elevation (masl). As expected, MAP was positively correlated with higher elevations (R2 = 0.9145).

Four vertical recharge zones were set dividing the model domain into areas located within at the following elevation zones: below 900 m, 900 to 1,110 m, 1,100 to 1,300 m and above 1,300 masl. Those are the same elevation divisions as presented in the SRK's Groundwater Technical Assessment Report (SRK. 2012) of Quintette Coal Mine Project, which is adjacent to the proposed Project. One additional recharge zone was set for areas of closed dumps in Quintette Project area. Those areas are expected to receive recharge that is higher than the surrounding, undisturbed land (Figure 4.4-1).

A spreadsheet program was developed for calculation of values to be applied to each of the model recharge zones. This spreadsheet incorporated the regression equation presented above, and the calculated areas and average elevation of the set recharge zones. A coefficient relating recharge to precipitation was selected such that the recharge rate over the entire model domain area equaled the "target recharge rate" (explained below).

The "target recharge rate" was estimated using a measured "low-flow" Murray River discharge rate (8.3 m^3/sec) and ratio of the areas of model domain and Murray River drainage. This Murray River "low-flow" rate was calculated utilizing data collected at a gaging station 07FB006 (located about 8 km down-gradient from the outlet of M20 (Camp) Creek). It was assumed that the groundwater model domain area (323 km^2) is similar in character to a much larger Murray River drainage area (up-gradient of the 07FB006 gaging station - 2,370 km^2). The "low-flow" approximates "baseflow" (the part of the river's flow rate that represents groundwater discharge into the river).

The following two parameters were used to calculate groundwater recharge per the entire groundwater model domain area:

- Murray River's "low-flow" (8.3 m^3/sec) and
- ratio of the area of the model domain and the area of Murray River drainage area (323 km^2/ 2,370 km^2 = 0.136)

The calculated groundwater recharge per the entire groundwater model domain area is 1.13 m^3/sec (110 mm/year) – a "target recharge rate". It represents an average recharge for the entire area of model domain. The value varies from recharge zone to recharge zone, as set in the model. The value of the coefficient factor that closes the water balance is 15% of MAP. Thus, it is calculated that 15% of mean annual precipitation ends up recharging groundwater within the model domain.

Figure 4.4-1

Hydrogeological Baseline Model Recharge Zones

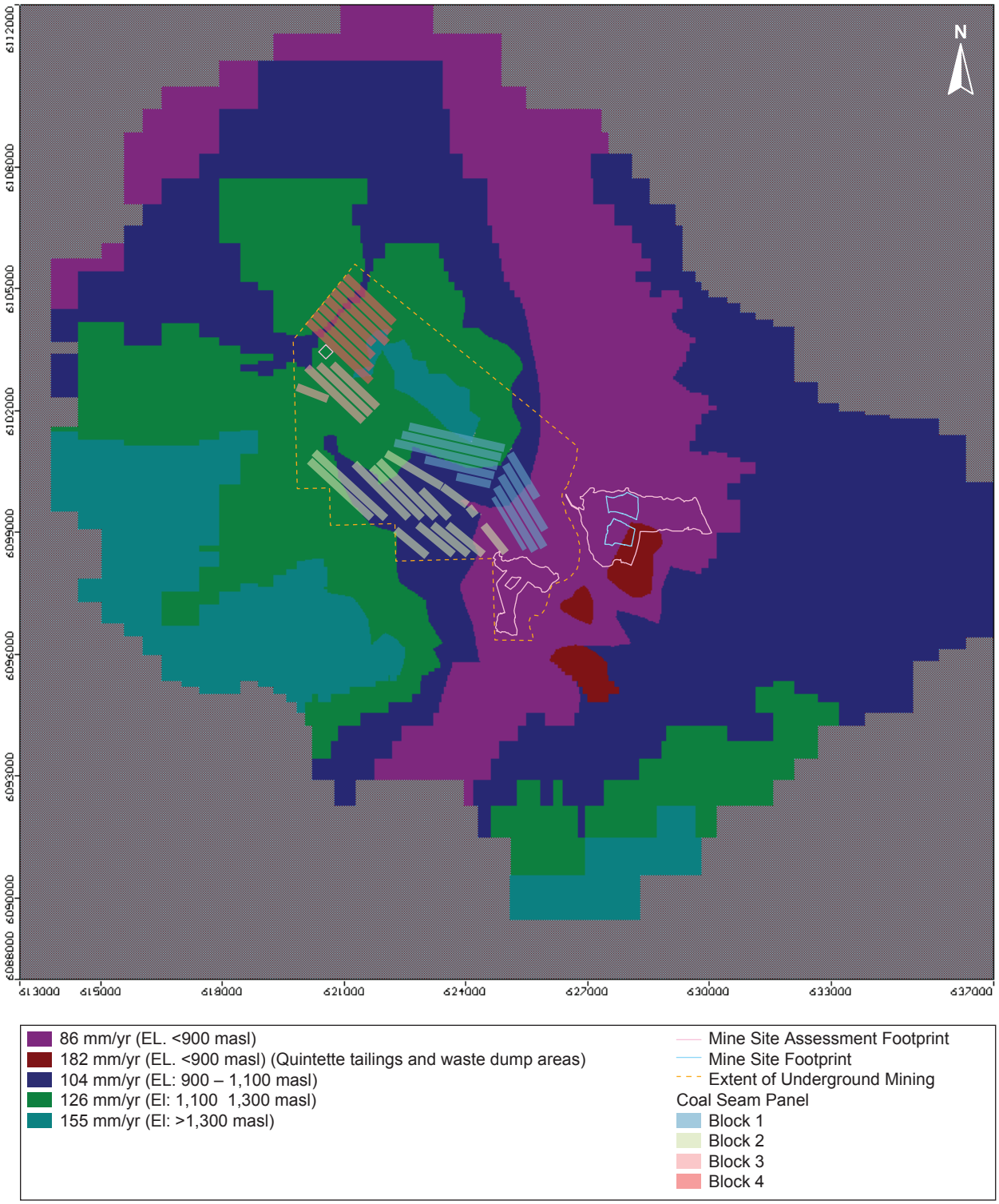

Evapotranspiration was not explicitly simulated by the model. Its component is conceptually incorporated into the calculation of groundwater recharge – it is the net result of several factors operating on water on the ground and within vadose zone.

The recharge zones set in the model are presented on Figure 4.4-1. The calculated recharge values are as follows: zone below 900 m – 86 mm/year; zone 900 to 1,110 m – 104 mm/year; zone 1,100 to 1,300 m – 126 mm/year; zone above 1,300 m – 155 mm/year; One additional recharge zone was created to represent Quintette Project's existing tailings and waste dump areas (east of Murray River and south of CCR Site). A high recharge value of 182 mm/year was assumed and assigned to those areas.

4.5 MODEL BOUNDARIES

4.5.1 External Boundaries

Figure 4.5-1 shows the flow boundary conditions assigned in the model domain. Except for northwest portion, the model's lateral boundaries were set along watershed water-divides, assuming that surface water drainage divides coincide with groundwater divides. This is justified in view of a conceptual model that considers mountain tops as the regional centers of recharge, with groundwater migrating divergently and away from such centers. This model assumes that structural features of geologic formations below such set boundaries do not significantly alter the pattern of groundwater flow from recharge centers near the mountains' tops to the valleys.

On the northwest side the lateral boundary was set along the course of Wolverine River. This River's valley constitutes a major groundwater discharge zone.

No flow boundaries are assumed at the bottom and also along the exterior boundary of the model domain (along the watershed divides). The assumption of no flow at the bottom of the model domain is justified in view of a documented general decrease in hydraulic conductivity with depth (see: SRK 2012 - Figure 5.1; ERM Rescan 2014 – Figure 4.2-1), and groundwater flow crossing the model's bottom (at over 1,000 m below ground surface) is likely insignificant.

4.5.2 River Boundaries

River boundaries were assigned in the model to represent Murray River, Wolverine River, and three tributary creeks near the CCR Site: M17, M19 and M19A (see Figure 4.5-1). Small creeks west of the Murray River are represented in the model using drain boundaries (see discussion in the next section). Using river boundary for those creeks could result in the model simulating a recharge from the creeks to groundwater at the rate larger than baseflow. Such recharge will happen in case mine dewatering caused water table to drop below the bottom of the creeks.

The river boundary condition is used to simulate interactions between groundwater and surface water in both directions. The depths and widths of the creeks set in the model were taken from Rescan's hydrologic field observation data for the gauged stations (Rescan 2013a), and estimated for the un-gauged creeks considering their catchment areas.

Figure 4.5-1

Hydrogeological Baseline Model Flow Boundaries

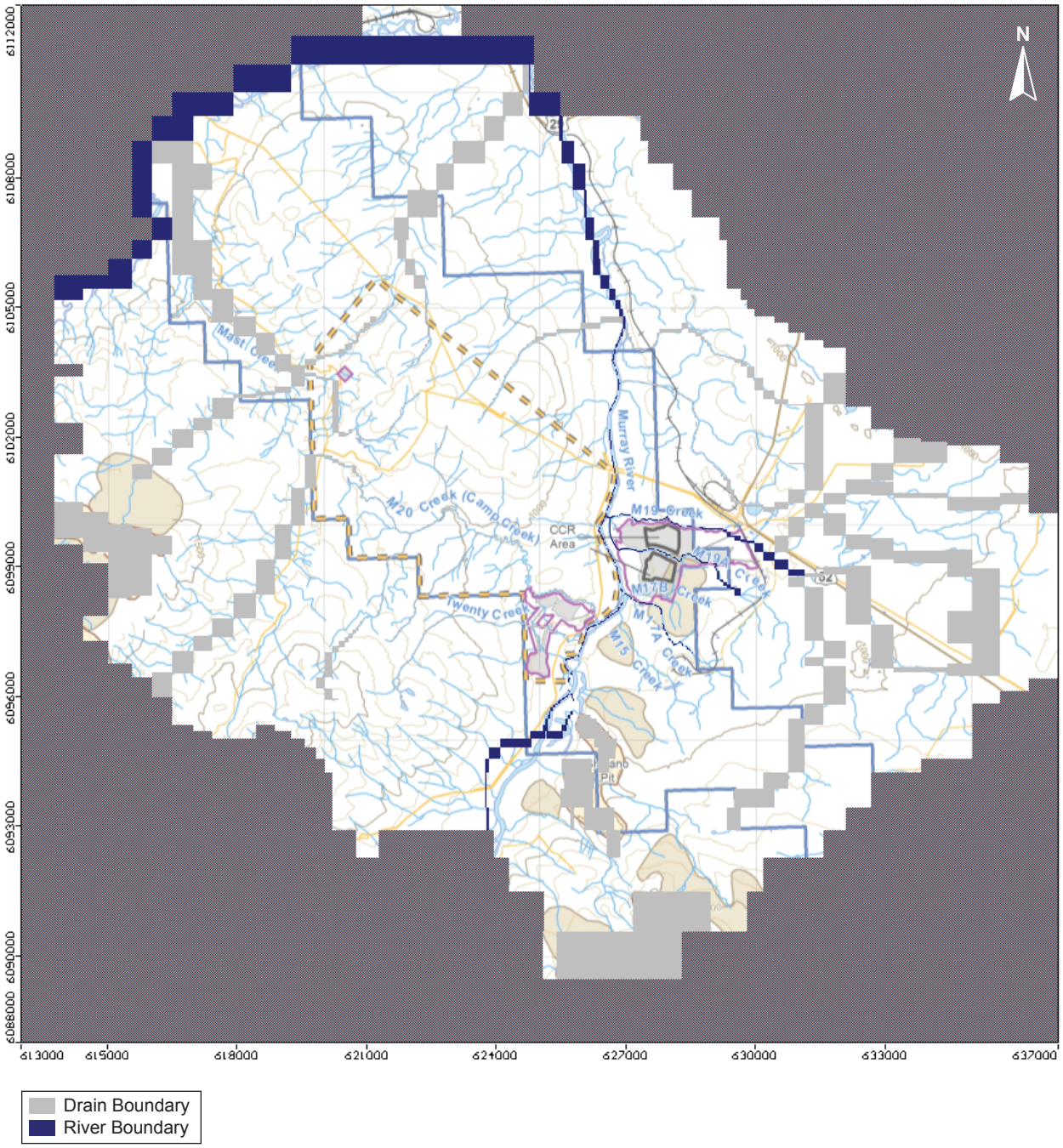

Field observations, land topography and riverbed elevations were used to estimate the streambed thicknesses of Murray River's and Wolverine River's tributaries. The thickness is judged to vary from approximately 0.4 m at the headwaters of the creeks to 2.0 m at their outlets. Murray River's width was set to 79 m (average of four width measurements completed around MH1 Gaging Station during normal and low-flow conditions) and Wolverine River's width was estimated to be 20 m. Based on the literature and experience from similar projects, hydraulic conductivity of riverbed was set at 1.0×10^{-5} m/s (Cho 2009; Rescan 2013c).

4.5.3 Drain Boundaries

Drain boundaries are applied to represent small and seasonal streams on mountain slopes. The drain boundaries are assigned at ground surface elevation (or close to) and receive groundwater seepage only when the water table close to the stream is above the drain elevation. Unlike the river boundaries, the drain boundaries do not allow recharge to the aquifer from the streams (in case water table drops below the drain elevation). Several streams draining the mountains west of the Murray River are represented in the model as drains. The value of conductance used for the drains is 0.1 m/d based on experience derived from similar projects (Rescan, 2013d; Cho 2009).

Drain boundaries are also used in the model to simulate the effects of old quarries (present within the Quintette and Herman Coal Mine project areas) on the groundwater system. This type of boundary is also used to represent wetland areas present east of Murray River. Distribution of river and drain boundaries set in the model is presented on Figure 4.5-1.

4.6 MODEL PROPERTY ZONES PARAMETRIZATION

4.6.1 Hydraulic Conductivities

All the available hydraulic conductivity information discussed above (in Section 2.5.3) was considered while designing hydraulic conductivity zones and assigning initial conductivity values. In total, fifteen hydraulic conductivity zones were set in the model (see Figures 4.6-1 to 4.6-14); Table 4.6-1 – column 1 of that table lists the zone numbers as set in the model, while column 2 numbers the zones listed in the table consecutively to show the total number of zones used in the model. The initial K values were set to closely match the field measured conductivities, and they were adjusted during the model calibration runs. The K values shown in Table 4.6-1 are the calibrated values.

Since all the hydraulic tests were single well/borehole tests (except H16W / H16A, AMEC 2012), no measurements are available to assess anisotropy or vertical hydraulic conductivity. It was assumed that the modeled system is horizontally isotropic (hydraulic property values do not vary with XY direction, $K_x = K_y$). Vertical hydraulic conductivity (K_z) was assumed to be ten times smaller than horizontal conductivity for most formations (1/10 ratio assumed in 9 out of 15 zones: 2, 3, 4, 5, 8, 9, 15, 16 and 18). SRK (2012) provides a comment that an anisotrophy ratio of 1/10 is considered a reasonable assumption for bedrock in Quintette Mine area (adjacent to the project area), but it could be as low as 1/100.

Figure 4.6-1

Hydrogeological Baseline Model Hydraulic Conductivity Zones – (Layer 1)

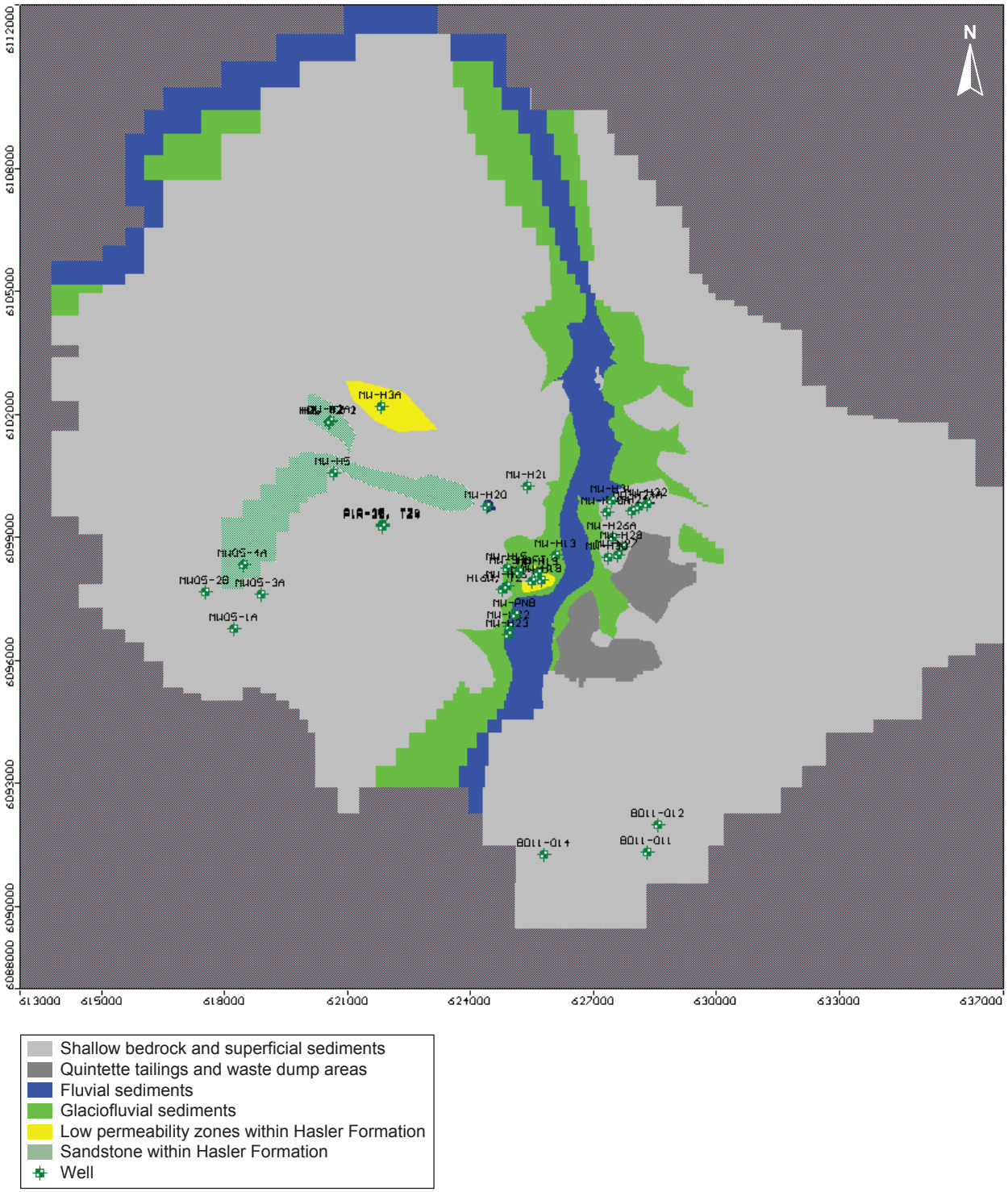

Figure 4.6-2

Hydrogeological Baseline Model Hydraulic Conductivity Zones – (Layer 2)

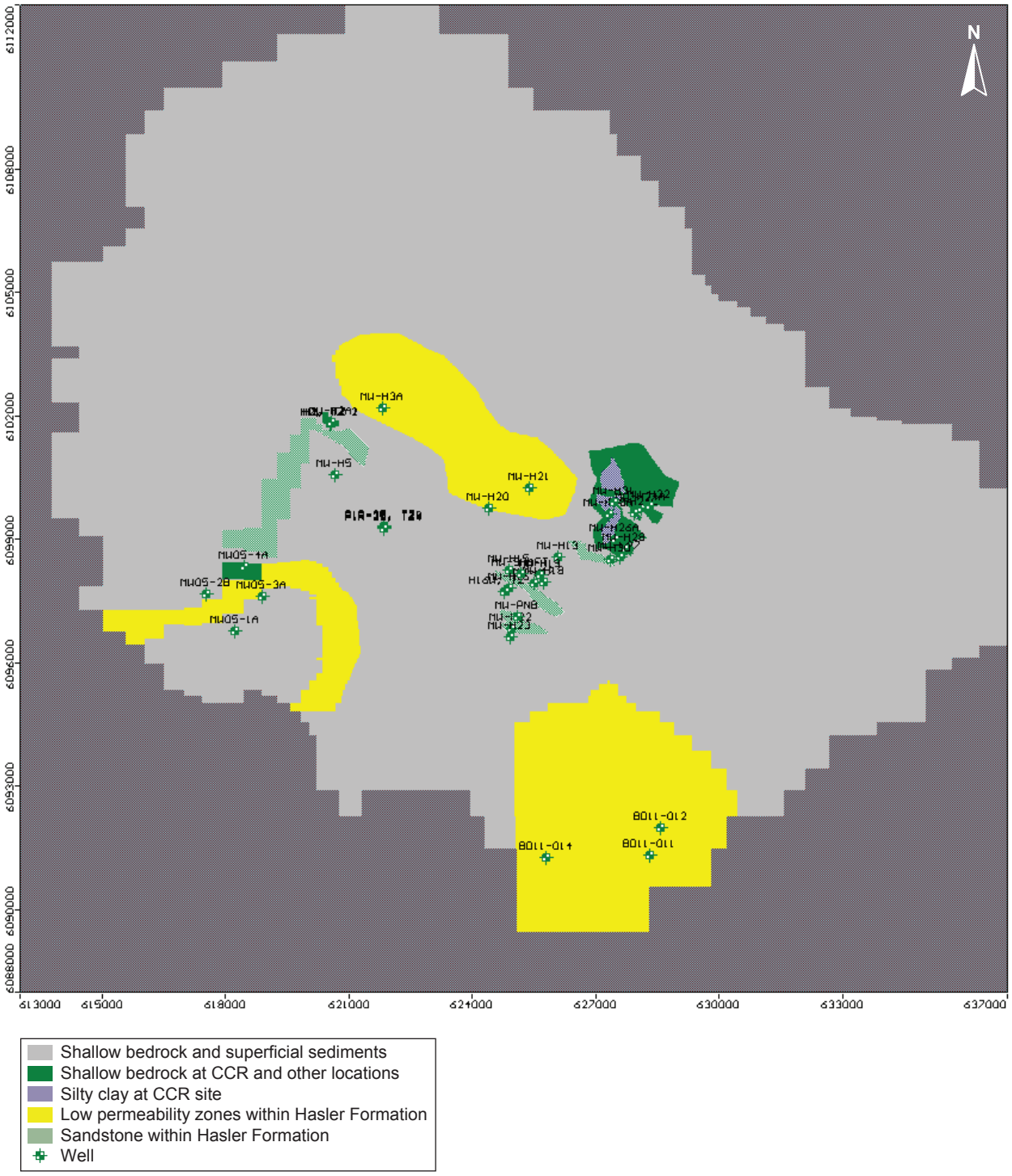

Figure 4.6-3

Hydrogeological Baseline Model Hydraulic Conductivity Zones – (Layer 3)

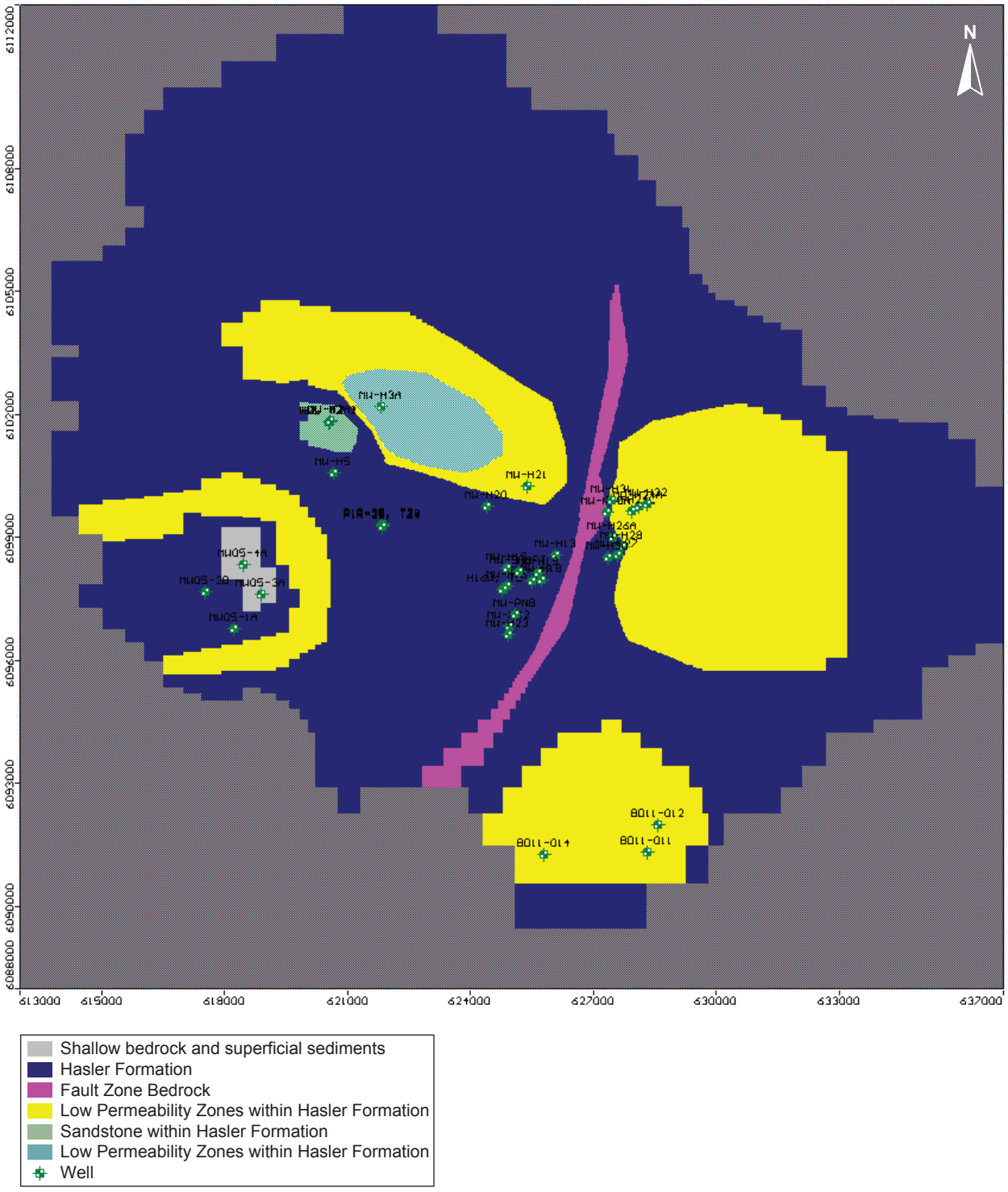

Figure 4.6-4

Hydrogeological Baseline Model Hydraulic Conductivity Zones – (Layer 4)

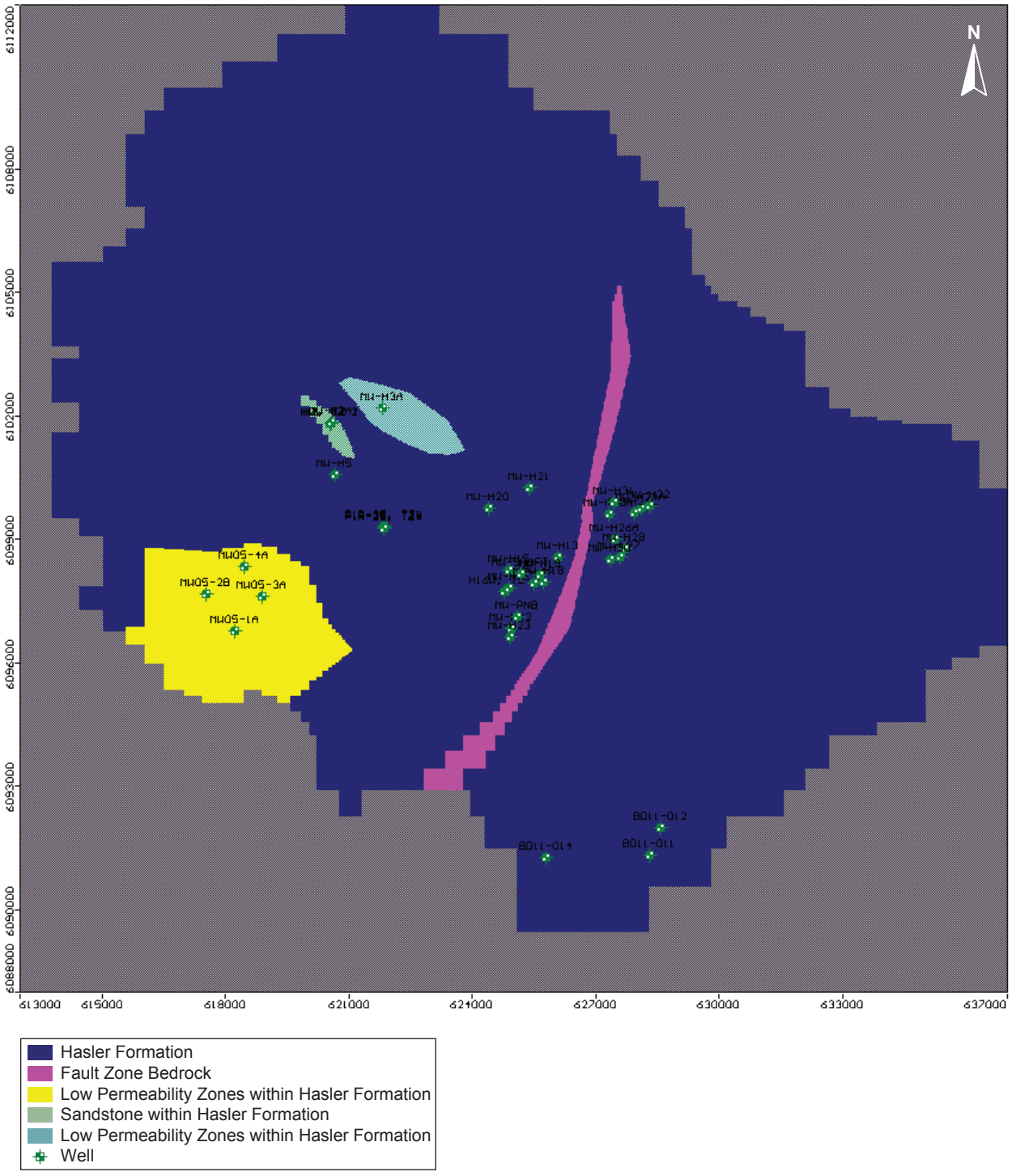

Figure 4.6-5

Hydrogeological Baseline Model Hydraulic Conductivity Zones – (Layer 5)

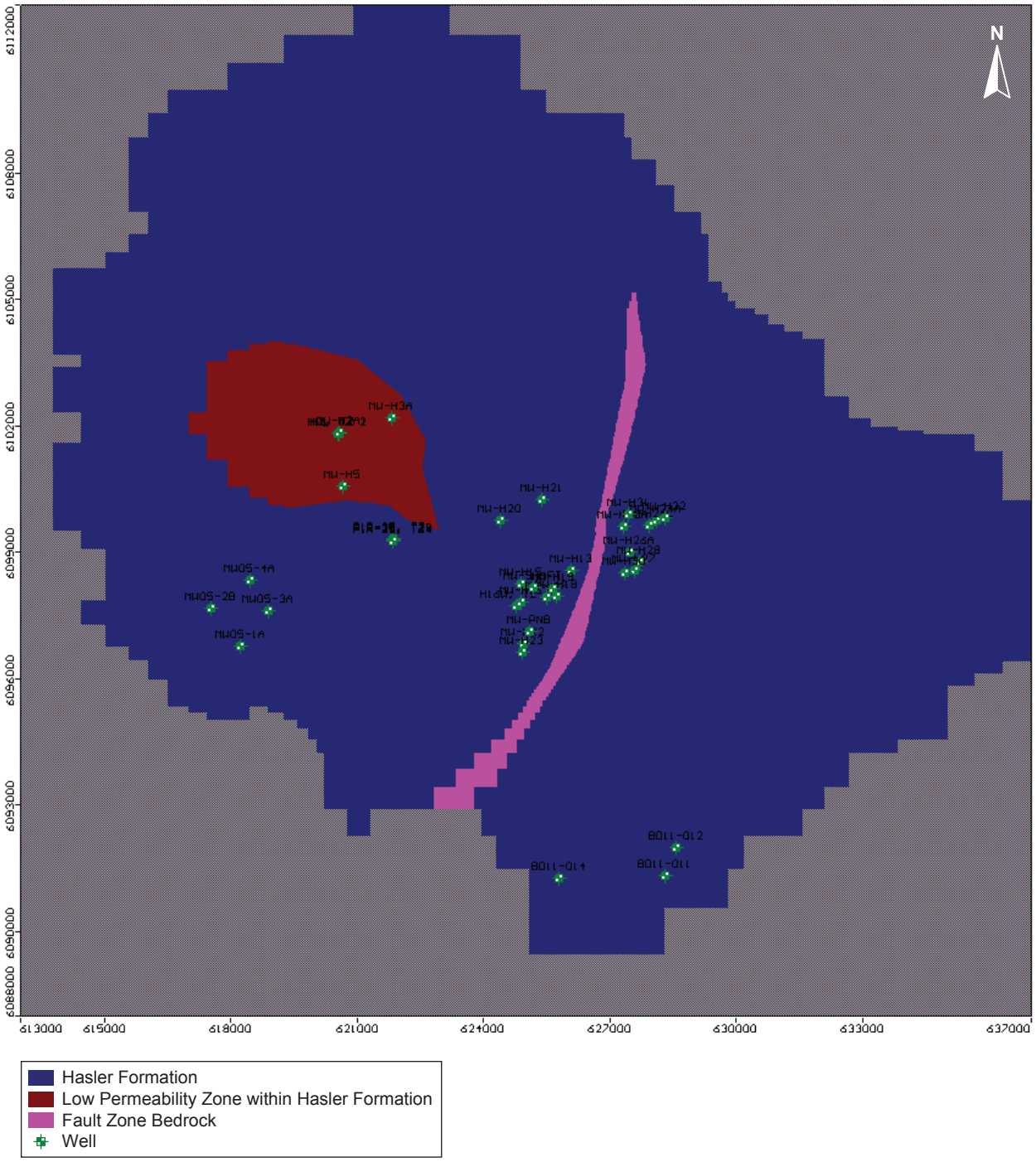

Figure 4.6-6

Hydrogeological Baseline Model Hydraulic Conductivity Zones – (Layer 6)

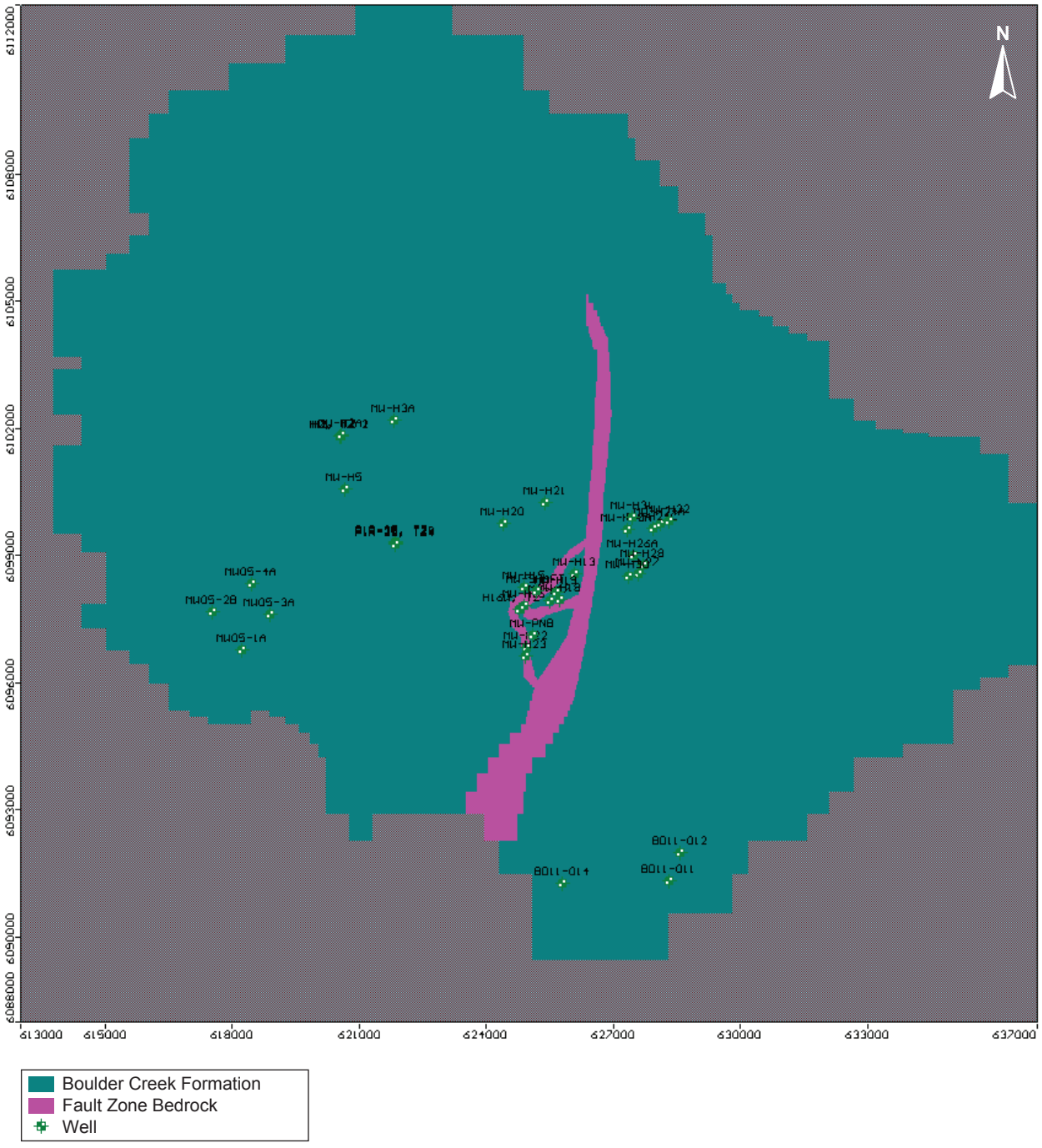

Figure 4.6-7

Hydrogeological Baseline Model Hydraulic Conductivity Zones – (Layer 7)

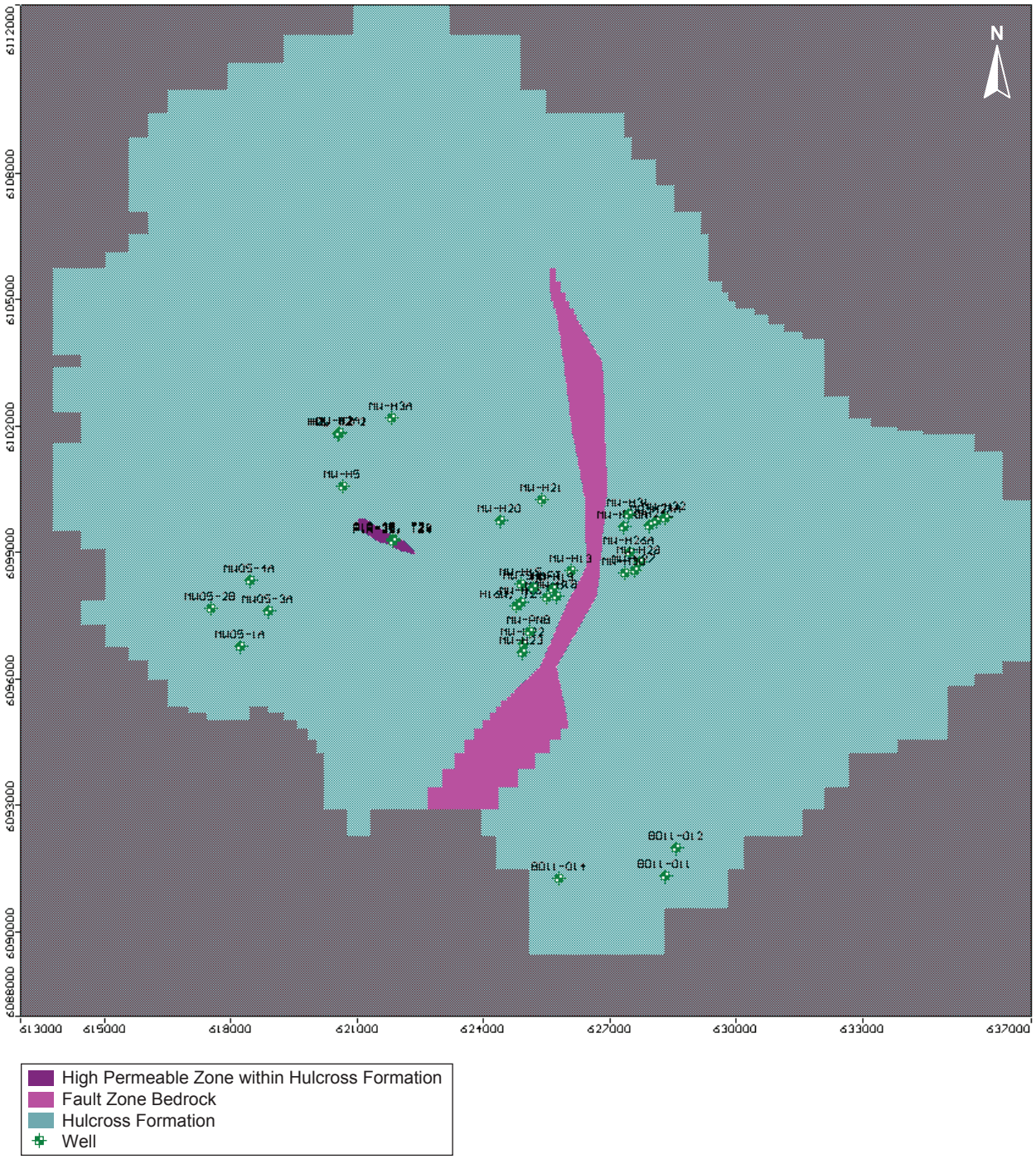

Figure 4.6-8

Hydrogeological Baseline Model Hydraulic Conductivity Zones – (Layer 8)

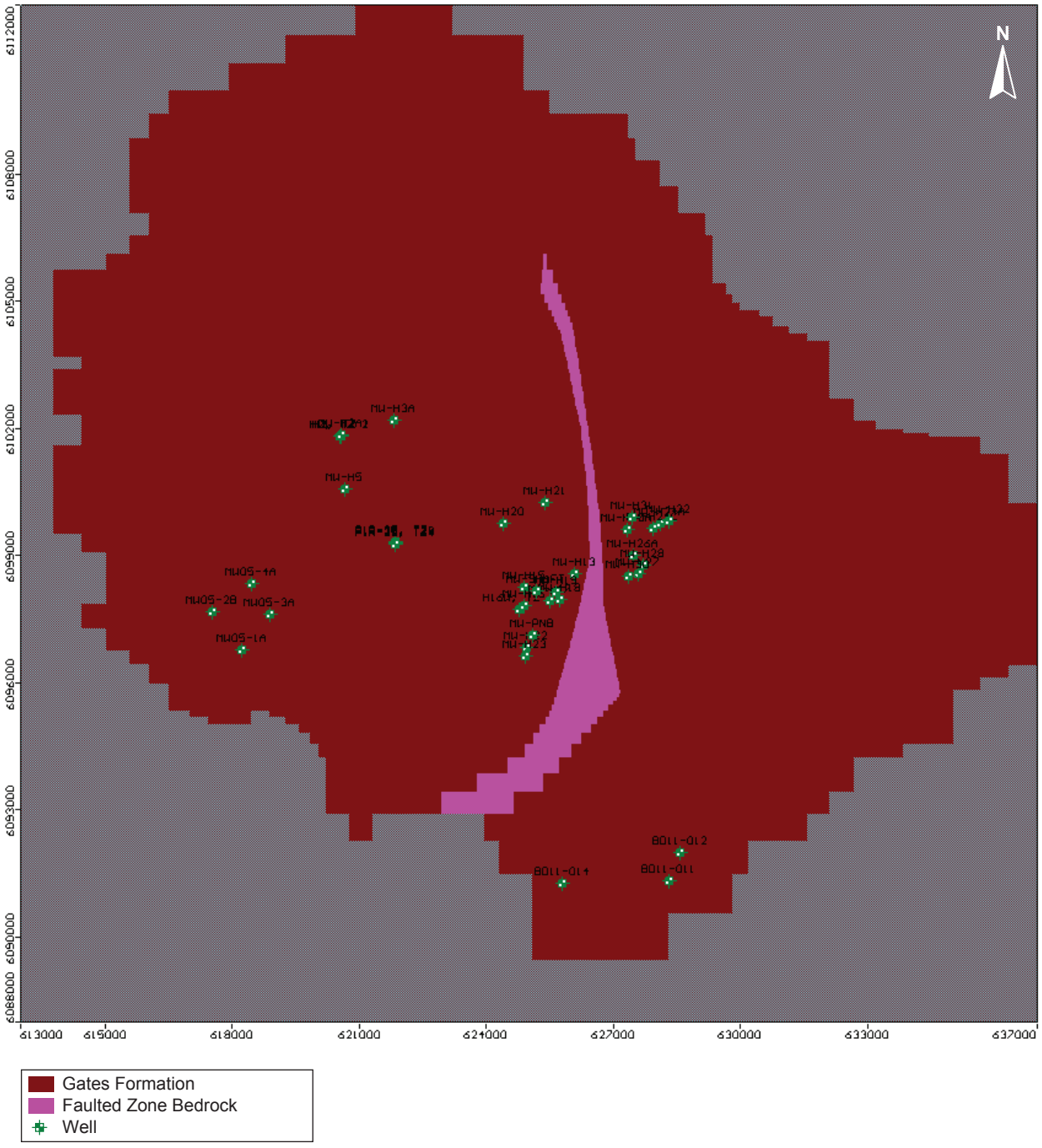

Figure 4.6-9

Hydrogeological Baseline Model Hydraulic Conductivity Zones – (Layer 9)

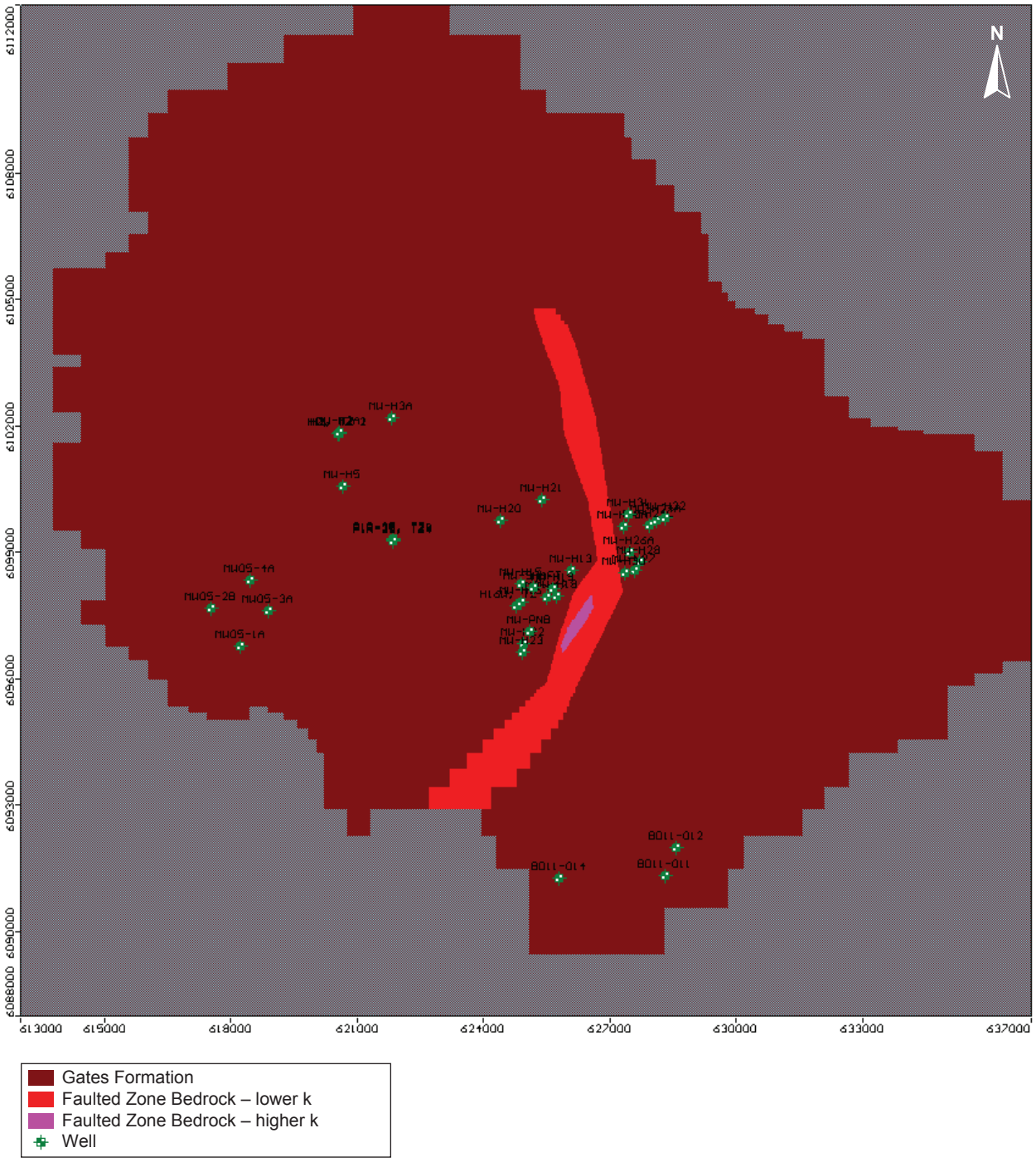

Figure 4.6-10

Hydrogeological Baseline Model Hydraulic Conductivity Zones – (Layer 10)

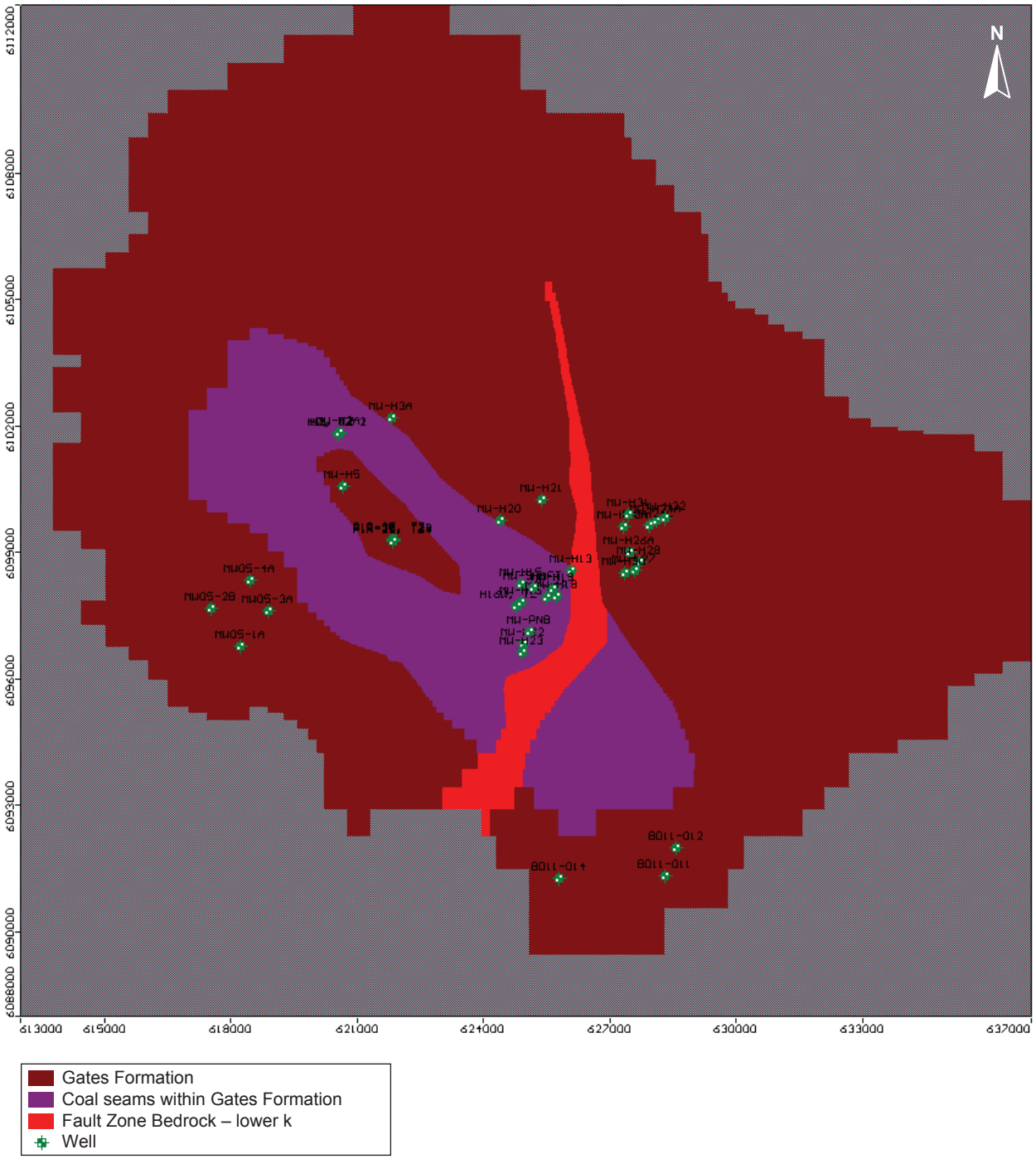

Figure 4.6-11

Hydrogeological Baseline Model Hydraulic Conductivity Zones – (Layer 11)

Figure 4.6-12

Hydrogeological Baseline Model Hydraulic Conductivity Zones – (Layer 12)

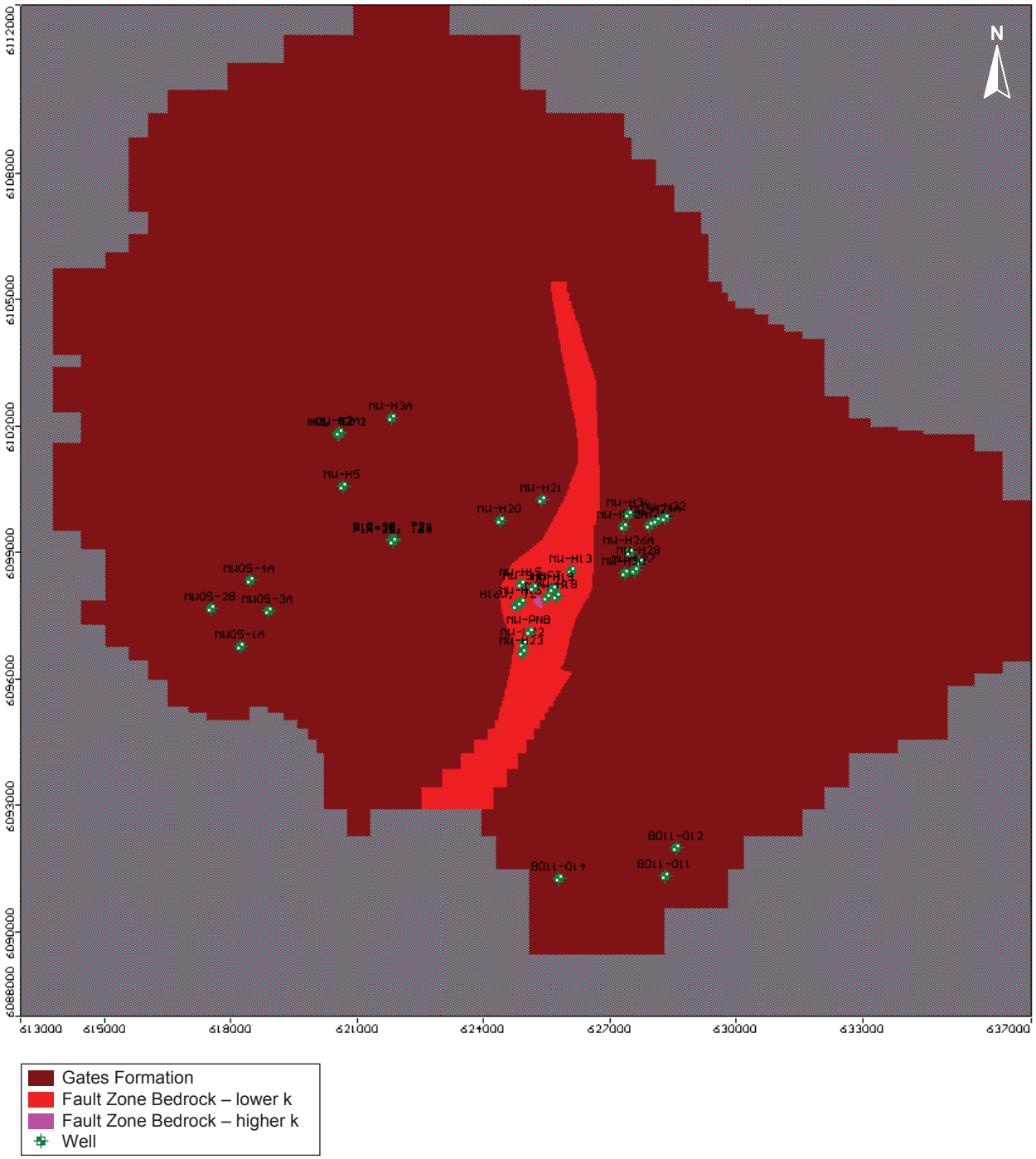

Figure 4.6-13

Hydraulic Conductivity Zones in Model Cross-section along Row 225

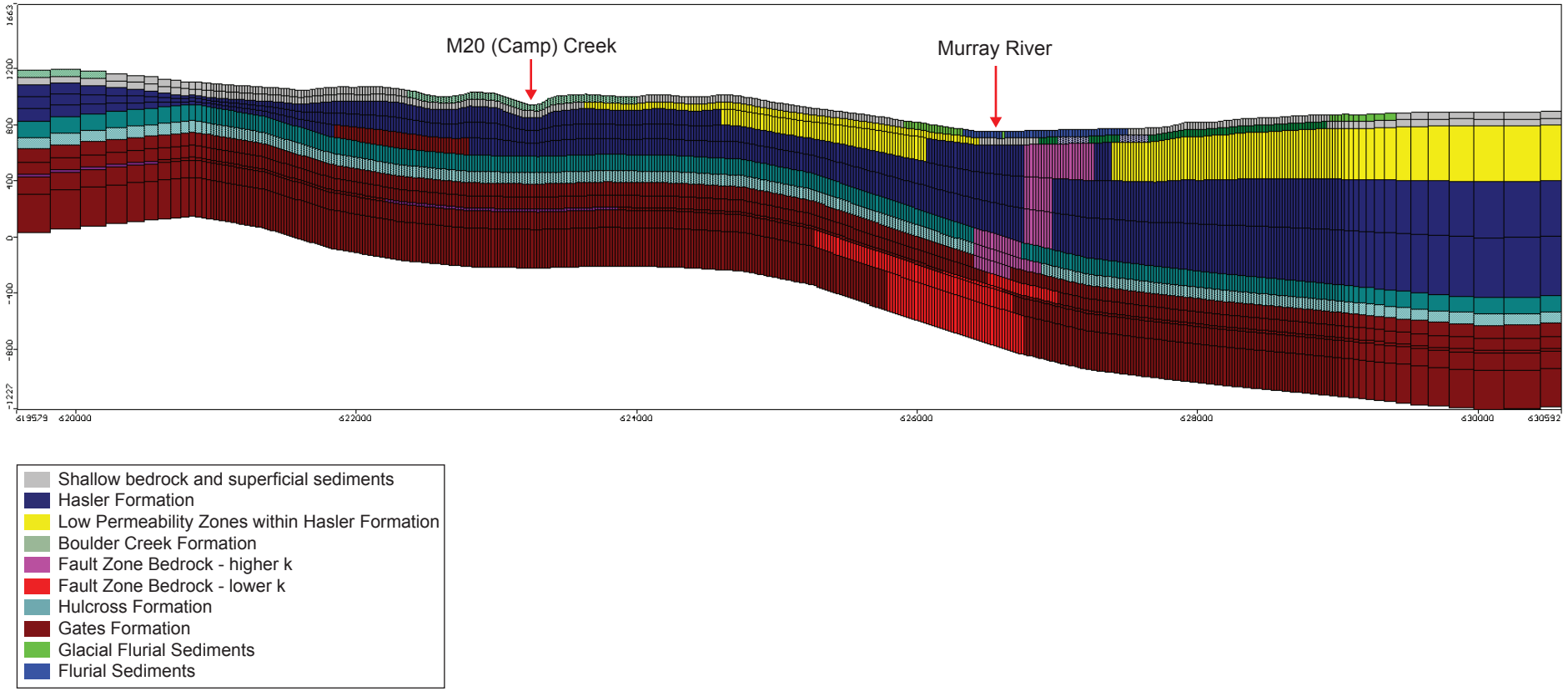

Figure 4.6-14

Hydraulic Conductivity Zones in Model Cross-section along Column 200

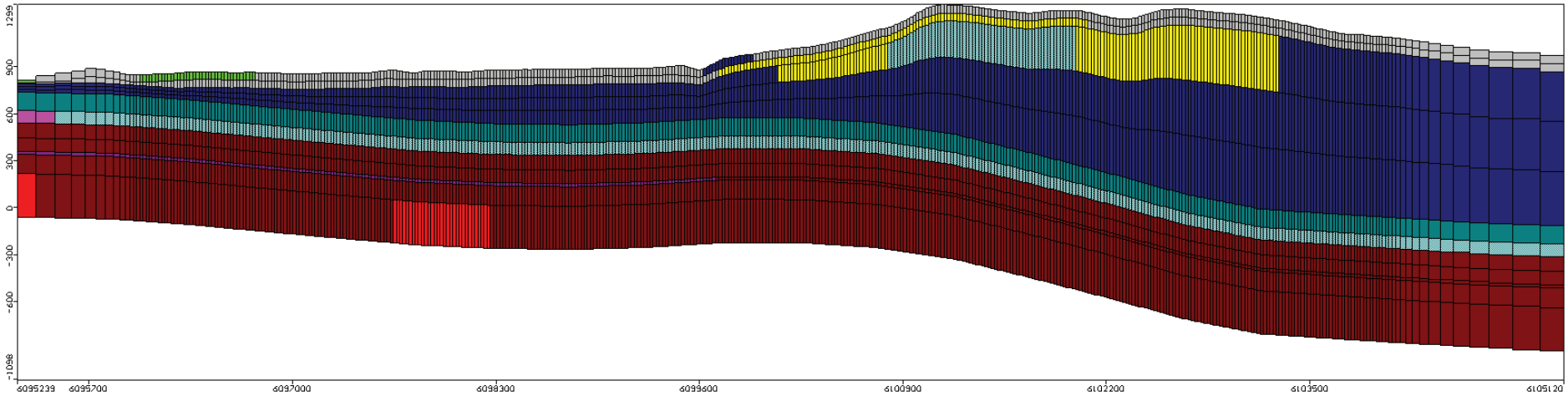

- Shallow bedrock and superficial sediments
- Hasler Formation
- Low Permeability Zones within Hasler Formation
- Boulder Creek Formation
- Fault Zone Bedrock - higher k
- Fault Zone Bedrock - lower k
- Hulcross Formation
- Gates Formation
- Glacial Flurial Sediments
- Flurial Sediments

Table 4.6-1. Hydraulic Conductivity Zones in Hydrogeology Baseline Model

Zone Number in Numerical Model	Count of Zones in the Model	Color	Model Layer	Hydraulic Conductivities			Dominant Lithology	Comments
				5 (K_x)	6 (K_y)	7 (K_z)		
1	2	3	4	[m/sec]	[m/sec]	[m/sec]	8	9
2	1		3, 4, 5	5.0E-08	5.0E-08	5.0E-09	Shale	Bedrock - Hasler Formation
3	2		2	1.1E-07	1.1E-07	1.1E-08	Shale / Siltstone / Sandstone	Shallow bedrock at CCR and other locations
4	3		6	1.0E-08	1.0E-08	1.0E-09	Shale / Conglomerate / Sandstone	Bedrock - Boulder Creek Formation
5	4		5, 8, 9, 10, 11, 12	5.0E-10	5.0E-10	5.0E-11	Sandstone / Shale / Coal	Bedrock - Gates Formation, low k zone within Hasler Formation
6	5		7, 10	5.1E-08	5.1E-08	2.6E-08	Coal	Coal seams within Gates Formation; more permeable zone within Hulcross Formation
8	6		1, 2, 3	5.0E-06	5.0E-06	5.0E-07	Siltstone / Glacial till	Shallow bedrock and superficial sediments (mainly morainal) on slopes of mountains
9	7		1	1.0E-07	1.0E-07	5.0E-08	Anthropogenic Silt / Sand	Quintette Project's tailings and waste dump areas
10	8		1	3.0E-05	3.0E-05	1.5E-05	Sands / Gravels / Silts	Fluvial sediments (along rivers)
11	9		1	1.2E-05	1.2E-05	6.0E-06	Sands / Gravels / Silts	Glaciofluvial sediments (on terraces along rivers)
13	10		9, 10, 11, 12	2.0E-09	2.0E-09	2.0E-09	Shale / Siltstone / Sandstone	Fault zone bedrock along the axis of Murray River Valley - deeper strata
14	11		3, 4, 5, 6, 7, 8, 9, 11, 12	4.0E-07	4.0E-07	4.0E-07	Shale / Siltstone / Sandstone	Fault zone bedrock along the axis of Murray River Valley - shallower strata
15	12		1, 2, 3, 4	1.0E-08	1.0E-08	1.0E-09	Shale	Low permeability zones within Hasler Formation
16	13		2	7.0E-09	7.0E-09	7.0E-10	Silty clay	Silty clay at CCR Site
17	14		1, 2, 3, 4	4.0E-05	4.0E-05	2.0E-05	Sandstone	Sandstone within Hasler Formation along upper Camp Creek, around H2, North & South Sites, MW-H5 and south of CCR Site
18	15		3, 4, 7	5.0E-09	5.0E-09	5.0E-10	Shale	Bedrock - Hulcross Formation, low permeability zones within Hasler Formation

Note: Number of hydraulic conductivity zones used in the model = 15

The anisotrophy ratio 1/2 was assigned to zones representing: coal seams (zone 6), Quintette Project's tailings and waste dump areas (zone 9), fluvial and glaciofluvial sediments (zones 10 and 11), and sandstone within Hasler Formation (zone 17). Finally, the ratio of 1:1 was assigned to zones 13 and 14 that represent the faulted and fractured bedrock along the axis of Murray River Valley. The anisotropy ratios assigned are considered to be conservative for the highly heterogeneous layered sedimentary rock formations.

4.6.1.1 Storage Parameters

Storage parameter zones set in the model are the same as the hydraulic conductivity zones - fifteen zones numbered and color-coded identically to hydraulic conductivity zones (as shown in Figures 4.6-1 to 4.6-14).

Very limited site-specific information is available regarding groundwater storage properties of rocks and sediments in the project area. AMEC (2012) reports that storage coefficient (storativity) in the Gates and Hulcross formations adjacent to borehole H16W was estimated using time-drawdown data (from pump test conducted on that borehole) to range between 3.1×10^{-4} and 2.4×10^{-5} (see discussion in AMEC 2012, Section 8.3). SRK (2012) provides that a pumping test conducted in the bedrock aquifer in the Shikano Mine North Pit (on eastern side of Murray River, south of CCR Site) produced a storage coefficient result of 1×10^{-4}, which was commonly accepted as a typical value of the confined aquifers in the area. SRK report (2012, Table 6.1) also lists specific storage (storativity divided by a groundwater bearing formation's thickness) values for till (1.0×10^{-3} 1/m) and Boulder Creek, Hulcross and Gates formations (5.0×10^{-5} to 2.0×10^{-6}). However, no sources of such values are discussed.

There is no site-specific information available regarding other groundwater storage properties: specific yield, effective porosity and total porosity.

In view of limited or not available site-specific data, the values of storage parameters were assigned to model considering experience of similar mining-related modelling reports (Dorsch and Katsube 1996; Stone and Fontaine 1998; Jones 2002; Malkki 2003; Lyford 2007; BCG 2009; Cho 2009; Rescan 2013c) and literature-provided values typical of different rock and sediment formations encountered at the project site. The following literature sources were consulted while assigning the values of storage parameters to model zones:

- Storage parameters: Domenico and Mifflin 1965; Freeze and Cherry 1979; Fetter 2001.
- Specific yield: Johnson 1967; Morris and Johnson 1967; van der Leeden et al. 1990; ASTM 1996; Fetter 2001.
- Porosity parameters: Morris and Johnson 1967; Mahajan and Walker Jr. 1978; Freeze and Cherry 1979; ASTM 1996; Fetter 2001.

Table 4.6-2 lists the values of storage properties by zone.

Table 4.6-2. Specific Storage, Specific Yield, Effective and Total Porosities in Hydrogeology Baseline Model

Number in Numerical Model	Count of Zones in the Model	Color	Model Layer	Specific Storage Ss [1/m]	Specific Yield Sy [m^3/m^3]	Effective Porosity [m^3/m^3]	Total Porosity [m^3/m^3]	Dominant Lithology	Comments
2	1		3, 4, 5	5.0E-06	0.05	0.005	0.07	Shale	Bedrock - Hasler Formation
3	2		2	5.0E-06	0.05	0.005	0.07	Shale / Siltstone / Sandstone	Shallow bedrock at CCR and other locations
4	3		6	1.0E-06	0.02	0.002	0.05	Shale / Conglomerate / Sandstone	Bedrock - Boulder Creek Formation
5	4		5, 8, 9, 10, 11, 12	1.0E-06	0.02	0.002	0.05	Sandstone / Shale / Coal	Bedrock - Gates Formation, low k zone within Hasler Formation
6	5		7, 10	1.0E-06	0.04	0.040	0.09 (*)	Coal	Coal seams within Gates Formation; more permeable zone within Hulcross Formation
8	6		1, 2, 3	1.0E-05	0.08	0.006	0.20	Siltstone / Glacial till	Shallow bedrock and superficial sediments (mainly morainal) on slopes of mountains
9	7		1	5.0E-05	0.05	0.050	0.30	Anthropogenic Silt / Sand	Quintette Project's tailings and waste dump areas
10	8		1	5.0E-05	0.25	0.200	0.30	Sands / Gravels / Silts	Fluvial sediments (along rivers)
11	9		1	5.0E-05	0.25	0.200	0.30	Sands / Gravels / Silts	Glaciofluvial sediments (on terraces along rivers)
13	10		9, 10, 11, 12	1.0E-06	0.02	0.002	0.05	Shale / Siltstone / Sandstone	Fault zone bedrock along the axis of Murray River Valley - deeper strata
14	11		3, 4, 5, 6, 7, 8, 9, 11, 12	1.0E-06	0.02	0.002	0.05	Shale / Siltstone / Sandstone	Fault zone bedrock along the axis of Murray River Valley - shallower strata
15	12		1, 2, 3, 4	5.0E-06	0.02	0.002	0.05	Shale	Low permeability zones within Hasler Formation
16	13		2	1.0E-05	0.05	0.050	0.40	Silty clay	Silty clay at CCR Site
17	14		1, 2, 3, 4	1.0E-06	0.05	0.005	0.20	Sandstone	Sandstone within Hasler Formation along upper Camp Creek, around H2, North & South Sites, MW-H5 and south of CCR Site
18	15		3, 4, 7	5.0E-06	0.02	0.002	0.10	Shale	Bedrock - Hulcross Formation, low permeability zones within Hasler Formation

Notes:

(*) - Mahajan O.P and P.L. Walker Jr. 1978 (assuming bulk density of bituminous coal = 800 kg/m^3)

Low values of effective porosity (less than 1%) were set in the model for bedrock formations (except for coal seams). Using the low values is conservative for most types of model predictive simulations - it makes the model simulate faster expansion of cones of depression, and faster movement of groundwater dissolved contaminants. Although specific yield is often used as approximation of effective porosity, it is reasonable to assume that effective porosity is somewhat lower than specific yield.

4.7 BUDGET ZONES

Several budget zones were set in model layers 1 and 10 (L1 and L10) to allow water mass balance tracking for different parts of the model domain (Figure 4.7-1). Ten zones were set in baseline model's layer 1 (L1), each for a different creek within the model domain, to allow documenting the model-calculated groundwater discharges to different creeks.

4.8 SIMULATION PERIOD, INITIAL CONDITIONS, AND TIME STEPPING

All model boundary elements were set for a 100 year simulation (36,500 days) to allow sufficient flexibility in setting up model transient simulations.

Initial heads (groundwater levels) for the initial steady-state baseline flow model simulations were set in all model layers equal to ground surface elevations.

4.9 FLOW SOLVER AND MODEL CONVERGENCE PARAMETERS

The pre-conditioned conjugate gradient (PCG4) solver in the MODFLOW-Surfact flow package version 3.0 was used for simulations of variably-saturated flow in the aquifer system, and the solver used the efficient and rigorous Newton-Raphson linearization approach in solving the non-linear governing equations for unsaturated flow (HydroGeologic 1996). The flow solver parameters and the convergence criteria were set as follows:

- The number of maximum outer iterations: 500;
- The number of maximum inner iterations: 50;
- Head change criterion: 0.2 m; and
- Relative closure criterion: 0.1 m.

The other parameters of the solver, such as the damping factor, were kept at their default values from the numerical code (HydroGeologic 1996; Harbaugh et al. 2000; Schlumberger 2008). The absolute head change and residual criteria were set sufficiently small to achieve satisfactory and accurate flow solution. The damping factor was applied to help solving the problem of groundwater flow in the domain characterized by the presence of steep terrains.

Figure 4.7-1

Hydrogeological Baseline Model
Budget Zones (Layer 1)

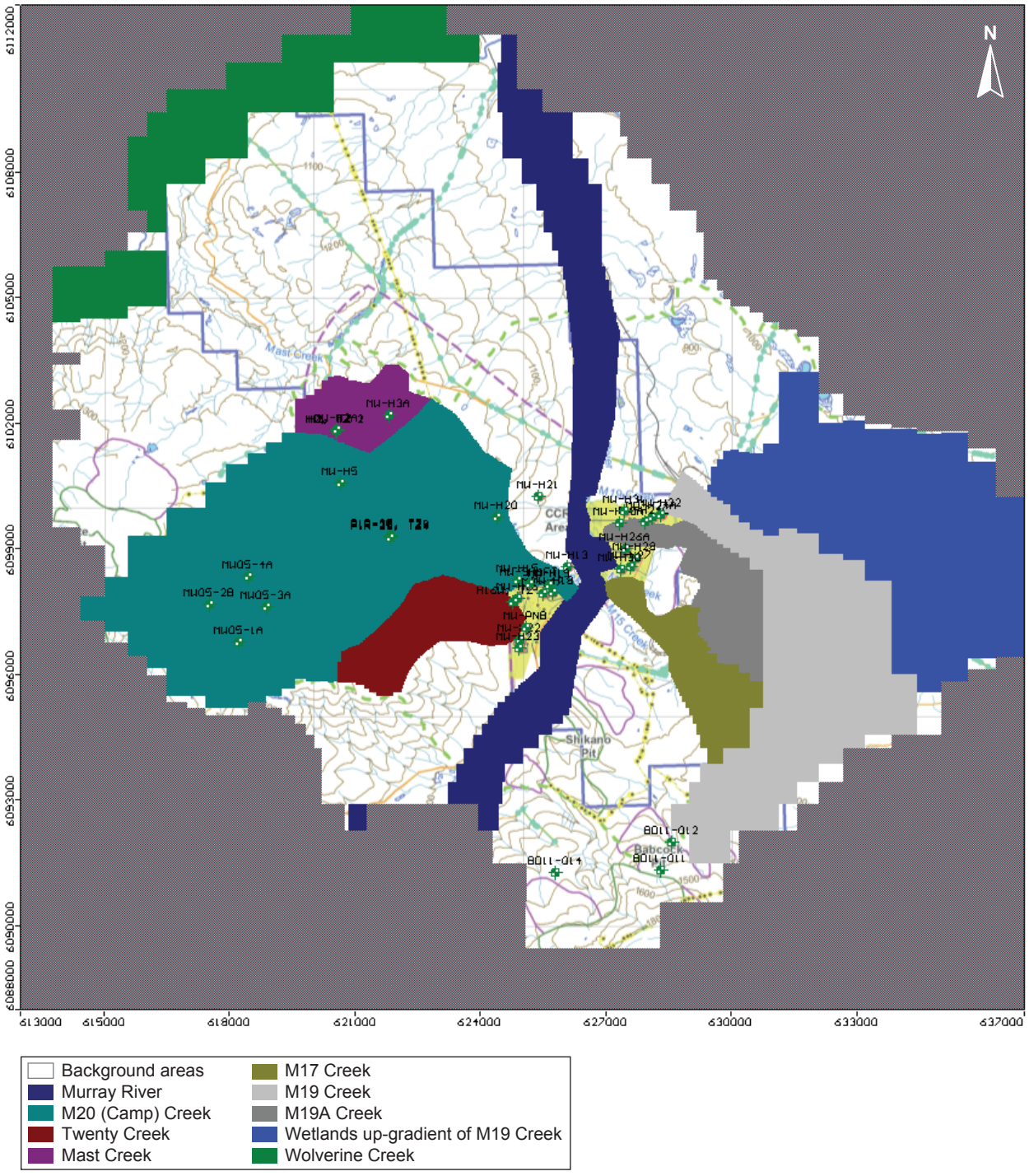

5. HYDROGEOLOGICAL BASELINE MODEL CALIBRATION

Both the model calibration and refinement of the model structure (including redrawing, adding / removing the model components, such as property zones) were carried out concurrently, both processes informing each other. For this reason, the model calibration was performed manually to a successful conclusion – there was no need to resort to automatic calibration (like using PEST or other similar program).

Model was calibrated mainly by adjusting the K values, leaving the recharge rates unchanged during the calibration. The uncertainty of the recharge rates are examined in the sensitivity analysis (see Section 5.3).

5.1 WATER BALANCES

The baseline's model calculated flow mass balance error is zero (the difference between the model calculated inflow and outflow).

The baseline model was calibrated using two classes of measurements – groundwater levels (discussed in the following subsections) and low flow measured in M20 Creek (referred to as Camp Creek).

Stream discharge is monitored at seven hydrometric stations located within the model domain (MH-1 to MH-7). One of them, MH-1, is operated by Water Survey of Canada Hydrometric Station. The other stations are operated by ERM as part of hydrology baseline study (Rescan 2013a; Rescan 2013d). However, only data accumulated at two of those stations, MH-1 (Murray River) and MH-2 (Lower Camp Creek), are sufficient (by the end of 2013) for estimation of a "low-flow", which is assumed to approximate "baseflow".

The value of low-flow for Murray River, 8.3 m^3/sec (station MH-1), was used to calculate recharge to the entire model's domain (see discussion in Section 4.4 – Recharge). The value of low-flow for lower Camp Creek 0.007 m^3/sec (or 605 m^3/day) (station MH-2 – 2 year recurrence: Rescan 2013d, Table 3.3-15) was used to calibrate groundwater discharge to drains representing the Camp Creek. The calibrated model calculates that discharge to be approximately 0.007 m^3/sec (586 m^3/day or 97% of the measured value).

5.2 WATER LEVELS

Table 5.2-1 presents groundwater level data from all the monitoring points (targets) that were used in model calibration, as well as the calibrated vs. measured groundwater elevations at the monitoring points. Figures 5.2-1 and 5.2-2 present locations of those targets within the model domain. Target values for the first 24 monitoring points listed in Table 5.2-1 (Rescan data) were calculated as average of all the collected to date water level measurements. The model was calibrated to three sets of water level targets:

Figure 5.2-1

Location of Groundwater Level Target Wells for Hydrogeological Baseline Model Calibration

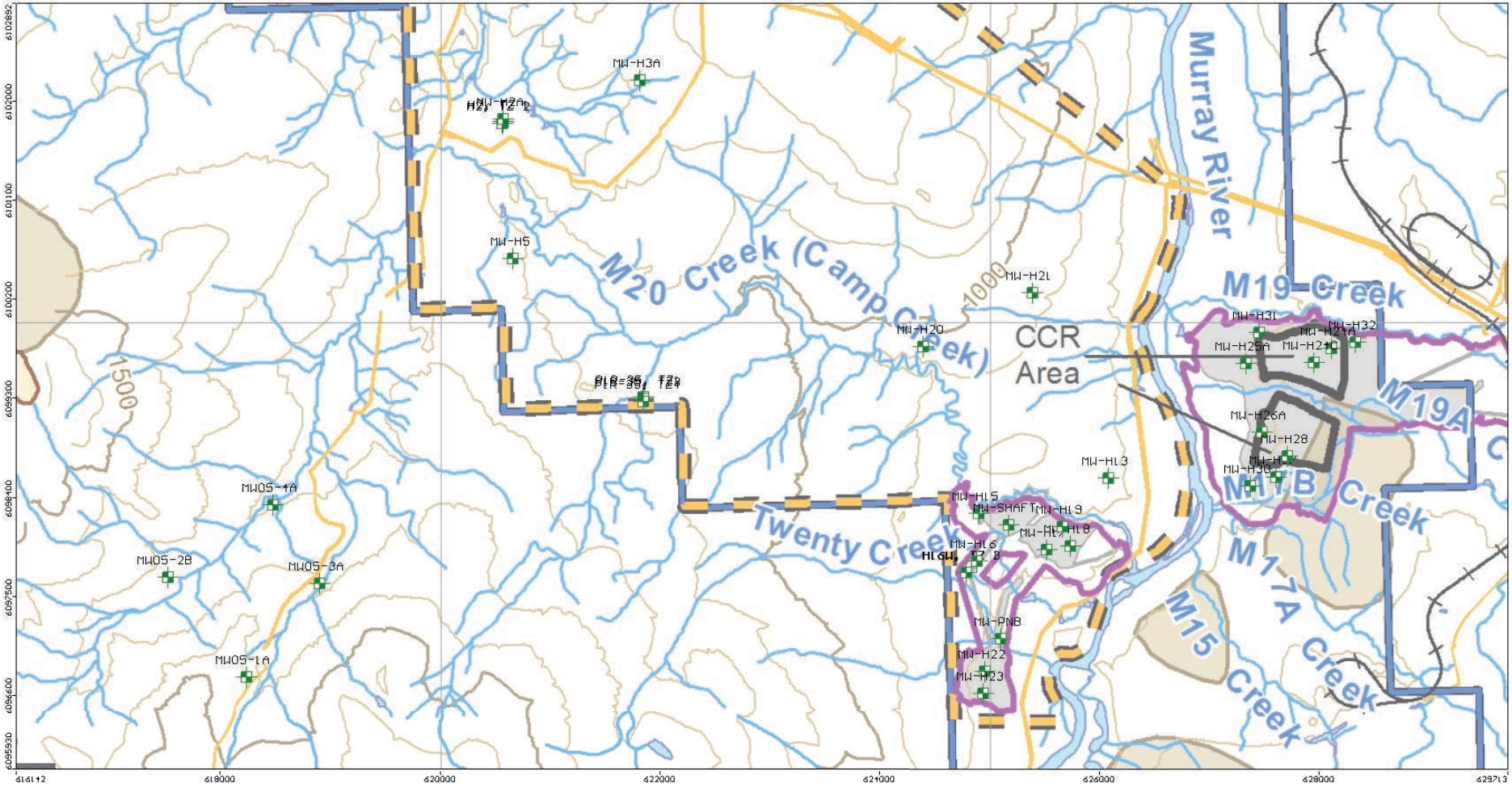

Table 5.2-1. Hydrogeology Baseline Model Calibration Results

Well Name	Easting m	Northing m	Ground Elevation masl	Top of Casing Elevation masl	Elevation of Screen's Midpoint masl	Groundwater Elevation			Depth to Monitoring Point mbgs	Date of Measurement	Source	Formation	Model Layer	Notes	Measured Hydraulic Conductivity m/sec	Calibrated Horizontal Hydraulic Conductivities (K_x) m/sec	K Zone # Set in the Model
						Measured masl	Model Calculated masl	Residual m									
1	2	3	4	5	6	7	8	9	10	11	12	13	14	15	16	17	18
MW-H2A	620575	6101837	1103.581	1104.341	1018.54	1094.21	1113.63	19.42	85.04	2011 - 2012	Rescan 2013c	Hasler Formation	L2	Mudstone / Siltstone	1.5E-07	1.1E-07	3
MW-H3A	621818	6102191.4	1215.26	1215.71	1027.25	1189.01	1189.20	0.19	188.01	7-Jul-11	Rescan 2013c	Boulder Creek Formation	L3	Sandstone		1.0E-08	15
MW-H5	620658	6100571	1101.85	1102.53	1072.82	1102.53	1130.77	28.24	29.03	2011 - 2012	Rescan 2013c	Overburden	L1	Sand and Gravel	2.0E-06	5.0E-06	8
MW-H13	626086.4	6098569	820.31	821.58	752.81	767.46	776.39	8.93	67.5	2011 - 2012	Rescan 2013c	Hasler Formation	L2	Shale		4.0E-06	1
MW-H15	624907	6098253	853.23	854.40	756.18	799.74	839.60	39.86	97.05	2011 - 2013	Rescan 2013c plus July 2013 field event data	Boulder Creek Formation	L2	Sandstone		4.0E-06	1
MW-H16	624891	6097821	836.61	837.47	769.60	777.80	820.23	42.43	67.01	May, Aug 2012	Rescan 2013c	Boulder Creek Formation	L2	Sandstone	6E-9 to 3E-8	1.0E-08	15
MW-H17	625520	6097925	829.30	829.96	822.30	824.28	794.61	-29.67	7	2012 - 2013	Rescan 2013c plus July 2013 field event data	Overburden	L1	Silty Sand/Shale bedrock interface	2.0E-06	5.0E-06	8
MW-H18	625740	6097953	830.88	831.70	818.88	819.69	785.60	-34.09	12	2012 - 2013	Rescan 2013c plus July 2013 field event data	Hasler Formation	L1	Shale	2.0E-06	5.0E-06	8
MW-H19	625663	6098131	832.57	833.34	825.37	829.04	815.25	-13.79	7.2	2012 - 2013	Rescan 2013c plus July 2013 field event data	Hasler Formation	L1	Shale	5.0E-09	1.0E-08	15
MW-H20	624396.9	6099765.8	953.53	954.20	914.11	927.75	977.11	49.36	39.43	2011 - 2012	Rescan 2013c	Boulder Creek Formation	L1	Sandstone	1.5E-08	5.0E-08	2
MW-H21	625390.3	6100258.8	915.70	917.00	864.80	891.05	876.21	-14.84	50.9	2011 - 2012	Rescan 2013c	Hasler Formation	L2	Mudstone		1.0E-08	15
MW-H22	624960	6096815	783.57	784.42	759.97	763.72	776.68	12.96	23.6	2012 - 2013	Rescan 2013c plus July 2013 field event data	Overburden	L1	Silty Sand	1.0E-06	3.0E-05	10
MW-H23	624942	6096618	784.92	785.70	761.30	763.29	774.02	10.73	23.62	2012 - 2013	Rescan 2013c plus July 2013 field event data	Overburden	L1	Sand	3.0E-05	3.0E-05	10
MW-H24A	628116	6099756	831.10	832.00	784.80	814.90	816.63	1.73	46.3	2012 - 2013	Rescan 2013c plus July 2013 field event data	Hasler Formation	L2	Siltstone/Sandstone interface	7.0E-08	1.1E-07	3
MW-H24C	627954	6099625	824.08	825.00	813.38	822.49	819.61	-2.87	10.7	06/31/13	June-July 2013 field event data	Hasler Formation	L2	Mudstone	1.1E-06	1.1E-07	3
MW-H25A	627334	6099615	765.30	766.00	704.80	764.59	761.40	-3.19	60.5	2012 - 2013	Rescan 2013c plus July 2013 field event data	Hasler Formation	L2	Mudstone / Sandstone	4E-7 to 6E-9	7.0E-09	16
MW-H26A	627478	6098990	791.22	792.00	758.02	790.98	789.21	-1.77	33.2	2012 - 2013	Rescan 2013c plus July 2013 field event data	Hasler Formation	L2	Mudstone / Sandstone	2E-6 to 7E-8	1.1E-07	3
MW-H27	627607	6098578	809.53	810.00	772.03	799.64	798.01	-1.63	37.5	7/31/2013	Rescan July 2013 field event data	Hasler Formation	L2	Mudstone / Sandstone	2.0E-07	1.1E-07	3
MW-H28	627715	6098772	818.30	819.00	801.80	806.41	808.79	2.38	16.5	7/31/2013	Rescan July 2013 field event data	Hasler Formation	L2	Mudstone / Sandstone	2.0E-07	1.1E-07	3
MW-H30	627372	6098501	792.27	793.00	779.27	779.36	775.58	-3.78	13	7/31/2013	Rescan July 2013 field event data	Overburden	L2	Silty clay	3.6E-09	7.0E-09	16
MW-H31	627456	6099893	797.32	798.00	768.32	782.30	779.32	-2.97	29	7/31/2013	Rescan July 2013 field event data	Overburden	L2	Silty clay	2.4E-08	7.0E-09	16
MW-H32	628333	6099810	839.63	840.00	811.13	829.23	830.36	1.13	28.5	7/31/2013	Rescan July 2013 field event data	Hasler Formation	L2	Siltstone / Sandstone	2.4E-09	7.0E-09	16
MW-PNB	625101	6097114	777.58	778.85	730.71	765.49	777.48	11.99	46.87	2011 - 2013	Rescan 2013c plus July 2013 field event data	Overburden	L1	Glacial till		3.0E-05	10
MW-Shaft	625176	6098150	845.13	846.03	841.61	841.89	822.41	-19.48	3.52	2011 - 2013	Rescan 2013c plus July 2013 field event data	Overburden	L1	Glacial till		1.2E-05	11
P1R-35 - Test Zone 1	621852	6099308	1083	N/A	447.5	1097.7	1058.5	-39.23	635.5	2010	AMEC 2010	Gates	L9	Sandstone / Mudstone	4.5E-10	1.0E-09	5
P1R-35 - Test Zone 3	621852	6099308	1083	N/A	590.0	1098.9	1078.6	-20.33	493	2010	AMEC 2010	Hulcross	L7	Sandstone / Mudstone	3.0E-08	5.1E-08	6
P1R-35 - Test Zone 4	621852	6099308	1083	N/A	769.5	1098.8	1077.2	-21.64	313.5	2010	AMEC 2010	Hasler / Boulder Creek	L6	Sandstone / Mudstone	2.9E-08	1.0E-08	4
H2 - Test Zone 1	620584	6101836.4	1111.9	N/A	375	1094	1089	-5.43	737	2012	AMEC 2012	Hulcross / Gates	L8	Sandstone / Mudstone	4.5E-09	1.0E-09	5
H2 - Test Zone 2	620584	6101836.4	1111.9	N/A	720	1134	1103	-30.97	392	2012	AMEC 2012	Hasler / Boulder Creek	L5	Sandstone / Mudstone	1.8E-09	1.0E-09	5
H16W - Test Zone 1	624789	6097713	835.5	N/A	-40	831.5	830.4	-1.07	876	2012	AMEC 2012	Gates	L12	Sandstone / Mudstone	6.1E-09	2.0E-09	13
H16W - Test Zone 3	624789	6097713	835.5	N/A	580	815.4	814.3	-1.12	256	2012	AMEC 2012	Hasler	L6	Sandstone / Mudstone	2.7E-08	1.0E-08	4
BD11-011	628313	6091327	1420.18	?	1383.61	1417	1429	12.46	36.57	2011	SRK 2012, Appx B-1, Table 8.2	Overburden	L2	Glacial till		1.0E-08	15
BD11-012	628585	6091997	1281.63	?	1271.51	1273	1284	11.37	10.12	2011	SRK 2012, Appx B-1, Table 8.2	Overburden	L1	Glacial till / bedrock contact		5.0E-06	8
BD11-014	625953	6091270	1256.44	?	1226.75	1228	1239	11.06	29.69	2011	SRK 2012, Appx B-1, Table 8.2	Overburden	L2	Glacial till / bedrock contact		1.0E-08	15
MW05-1a	618240	6096769.9	1422.46	1423.06	1320.49	1416.26	1355.73	-60.53	101.97	Dec-05	Lorax Environmental 2007	Bedrock	L2	Siltstone	8.2E-08	1.0E-08	15
MW05-2b	617523.4	6097674.6	1262.82	1263.42	1237.22	1261.22	1309.21	47.99	25.60	Dec-05	Lorax Environmental 2007	Bedrock	L1	Sandstone	6.7E-07	5.0E-06	8
MW05-3a	618902.2	6097617.5	1291.58	1292.18	1191.60	1299.21	1246.91	-52.30	99.98	Dec-05	Lorax Environmental 2007	Bedrock	L3	Siltstone	6.4E-06	4.0E-06	1
MW05-4a	618477.7	6098334.4	1201.44	1202.04	1121.28	1201.44	1219.72	18.28	80.17	Dec-05	Lorax Environmental 2007	Bedrock	L2	Siltstone	1.1E-07	1.1E-07	3
MW05-4b	618475.4	6098331.8	1201.44	1202.19	1151.76	1199.49			49.685	Dec-05	Lorax Environmental 2007	Bedrock		Slst			
MW05-4c	618473.5	6098328.8	1201.44	1202.43	1190.02	1195.43			11.425	Dec-05	Lorax Environmental 2007	Overburden		Moraine			

Notes:

masl - meters above sea level

N/A - not applicable

AMEC 2010. Memorandum: Packer Testing to Assess Bedrock Permeability Tumbler Ridge, B.C., From T. Kostya, AMEC to J. Luo, Canadian Dehua International Mines Group Inc.

AMEC 2012. Single Well Response Tests: Proposed Murray River Underground Coal Mine, Tumbler Ridge, BC. Submitted to Canadian Dehua International Mines Group Inc. by AMEC Environment and Infrastructure, Kamloops, BC.

Lorax Environmental 2007. Application for an Environmental Assessment Certificate for the Hermann Mine Project submitted by Western Canadian Coal to Bob Hart (British Columbia Environmental Assessment Office) February 2007. Volume 2: Main Document - Part 2, Section 8 – Groundwater, Section 12 – Terrain and Soils.

Rescan 2013. Murray River Coal Project: 2011 to 2012 Hydrogeology Baseline Report. Prepared for HD Mining International Ltd. by Rescan Environmental Services Ltd.: Vancouver, British Columbia, May 2013.

SRK 2012. Quintette Groundwater Technical Assessment Report - Appendix 4-7-A Groundwater Technical Data – Report prepared for Teck Coal Corporation, March 2012.

Figure 5.2-2

Location of Groundwater Level Targets around CCR, North and South Sites for Hydrogeological Baseline Model Calibration

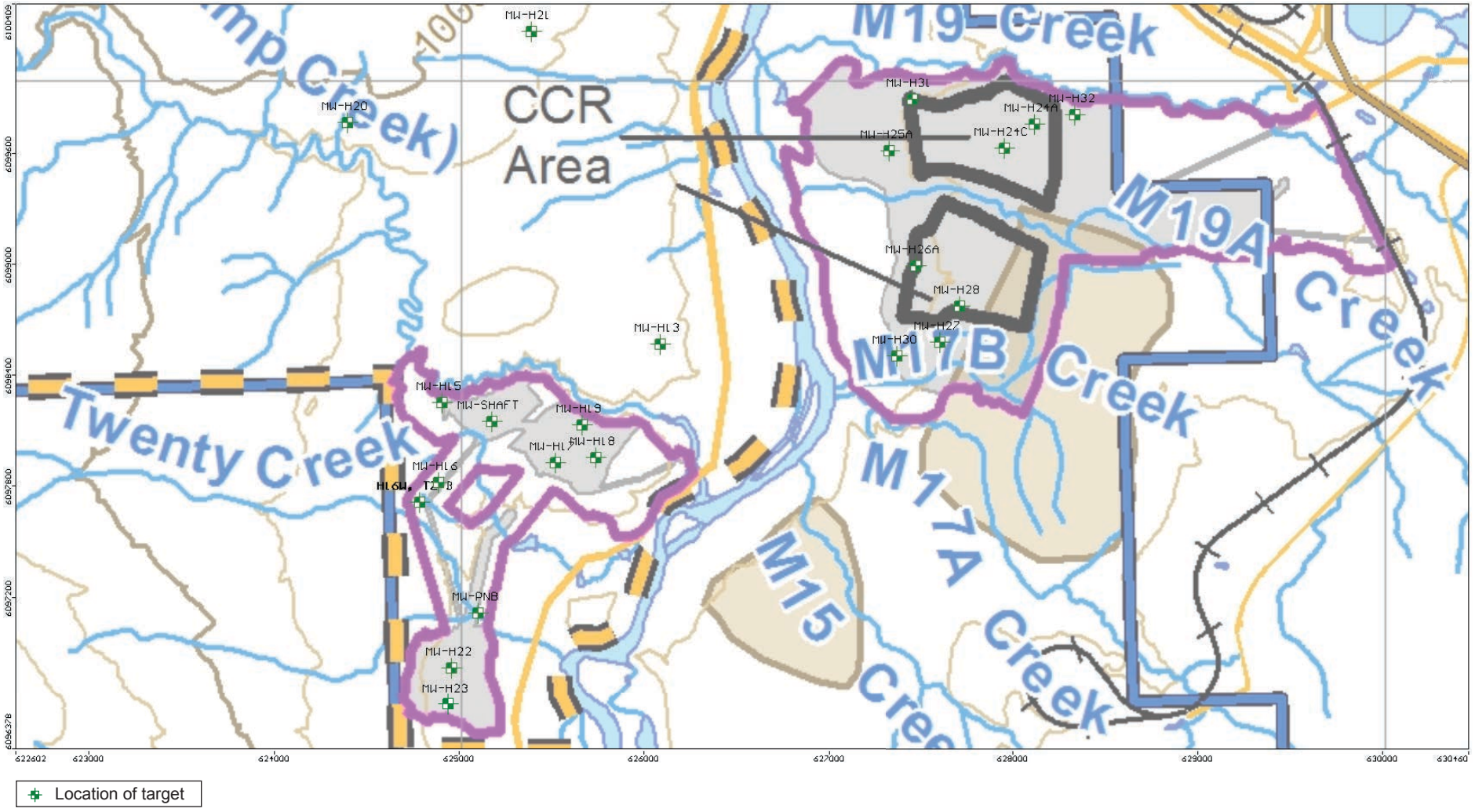

- The entire set of targets;
- Eight targets with deep groundwater level data (collected from zones located at depths ranging from 188 to 876 m below ground surface): MW-H3A, P1R-35 - Test Zone 1, P1R-35 - Test Zone 3, P1R-35 - Test Zone 4, H2 - Test Zone 1, H2 - Test Zone 2, H16W - Test Zone 1, and H16W - Test Zone 3; and
- Nine targets within CCR Site: MW-H24A, MW-H24C, MW-H25A, MW-H26A, MW-H27, MW-H28, MW-H30, MW-H31, MW-H32.

Calibration acceptance criterion adopted for this modelling project was a Normalized Root Mean Square (NRMS) around 5% or less. Typically for an industrial standard of groundwater modeling practice, a model is considered as calibrated and acceptable if the NRMS is less than 10%. Table 5.2-2 lists the calibration statistics for those three sets of targets. Figures 5.2-3, 5.2-4 and 5.2-5 present Calibration Scatter Graph Plots for those three sets of targets.

Table 5.2-2. Calibration Statistics for Hydrogeology Baseline Model

Parameters / Group of Targets	Units of Parameters	Entire Set	Deep Groundwater Set	CCR Site Set
Calibration Statistics:				
Residuals (Max.)	[m]	-60.53	-39.23	-3.79
Residuals (Min.)	[m]	0.19	0.19	1.13
Residual Mean	[m]	-0.80	-14.95	-1.22
Absolute Residual Mean	[m]	18.19	15.00	2.38
Number of Data Points		38	8	9
Standard Error of Estimate	[m]	4.07	5.39	0.78
Root Mean Squared (RMS)	[m]	24.74	20.65	2.52
Normalized RMS	[%]	3.78	5.53	3.90
Correlation Coefficient	[-]	0.99	1.00	1.00
Field Measurements:				
Difference between the highest and lowest elevations of measured water levels within a set of targets	[m]	834.71	373.61	64.64

Figures 5.2-6, 5.2-7 and 5.2-8 show simulated hydraulic head (equipotential line) contour maps in planar view for Layers 1, 2 and 10, and Figure 5.2-9 shows the hydraulic head (equipotential line) contours in cross-sectional view along the model row 260, using the calibrated baseline model computed heads.

Figure 5.2-3

Hydrogeological Baseline Model Calculated Heads vs. Observed Heads – (Entire Dataset)

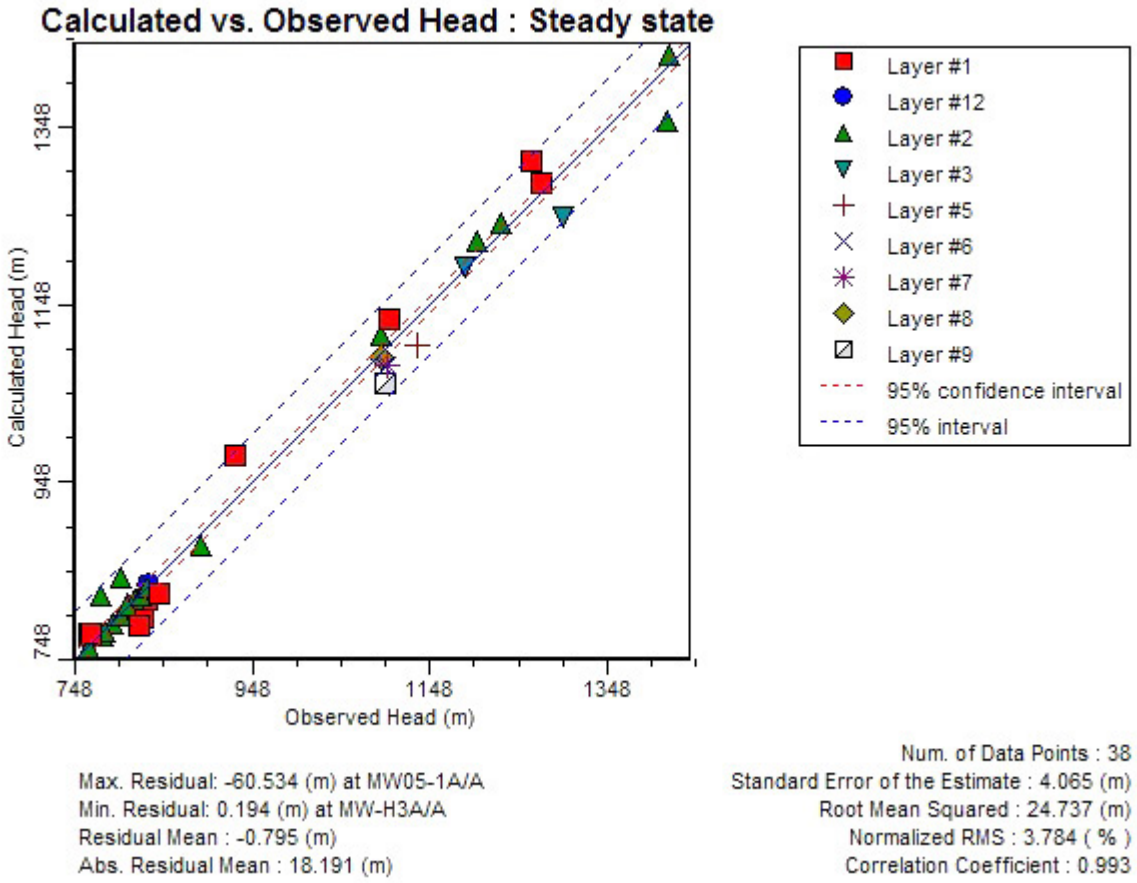

Figure 5.2-4

Hydrogeological Baseline Model Calculated Heads vs. Observed Heads – (Deep Groundwater)

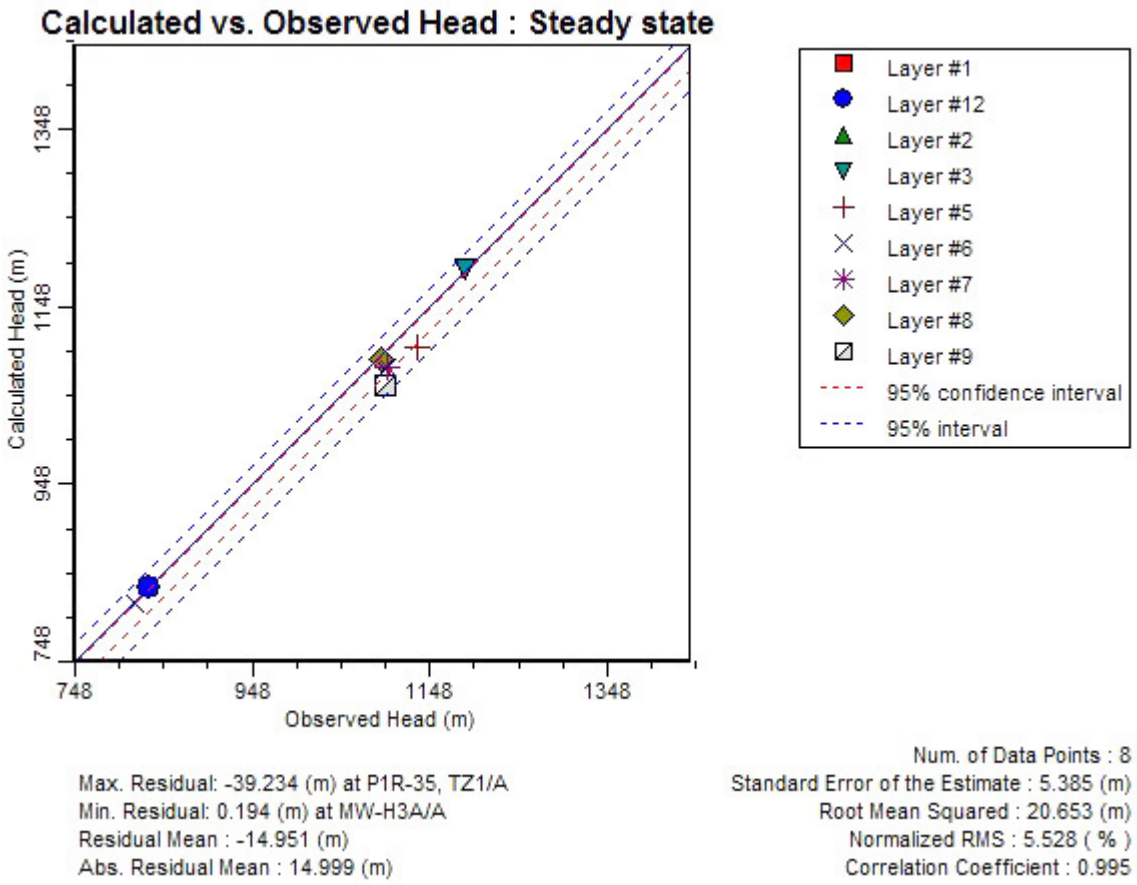

Figure 5.2-5

Hydrogeological Baseline Model Calculated Heads vs. Observed Heads – (CCR Site)

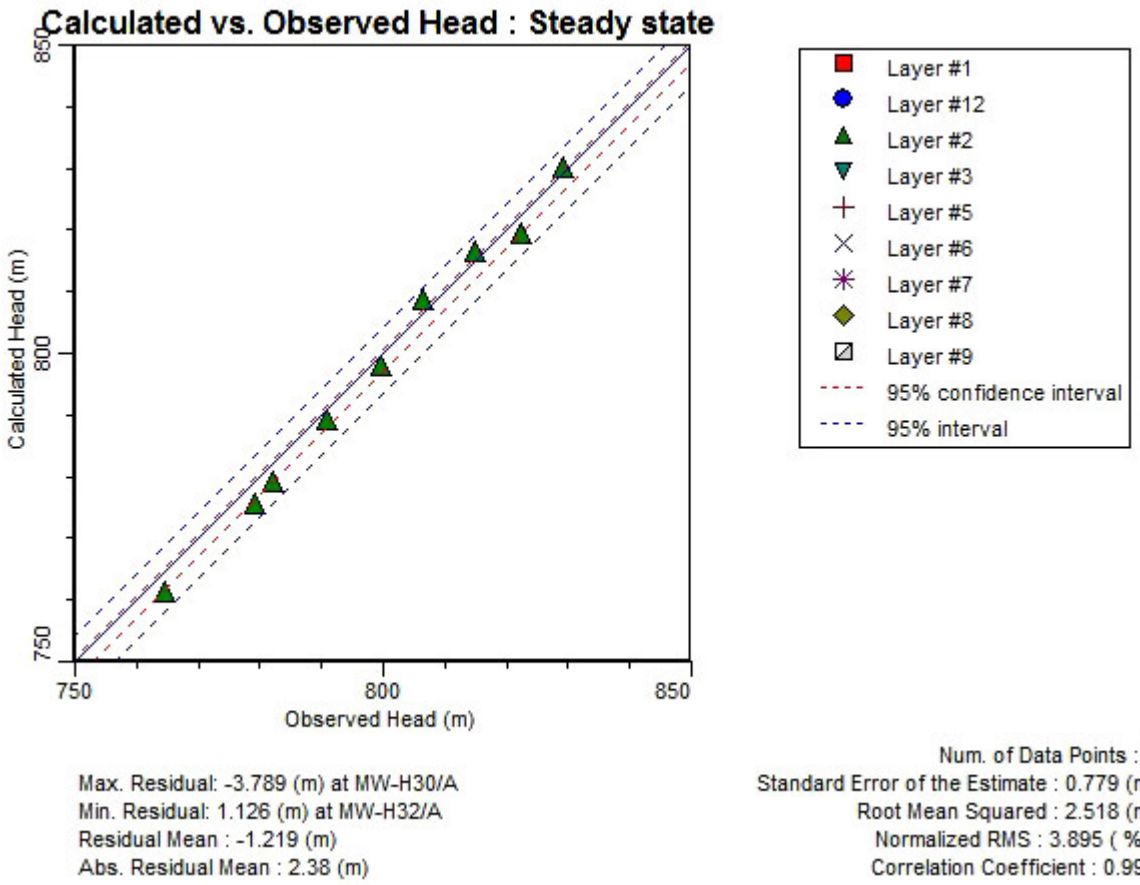

Figure 5.2-6

Simulated Hydrogeological Baseline Hydraulic Head Contours and Groundwater Flow Directions (Plan View, Layer 1)

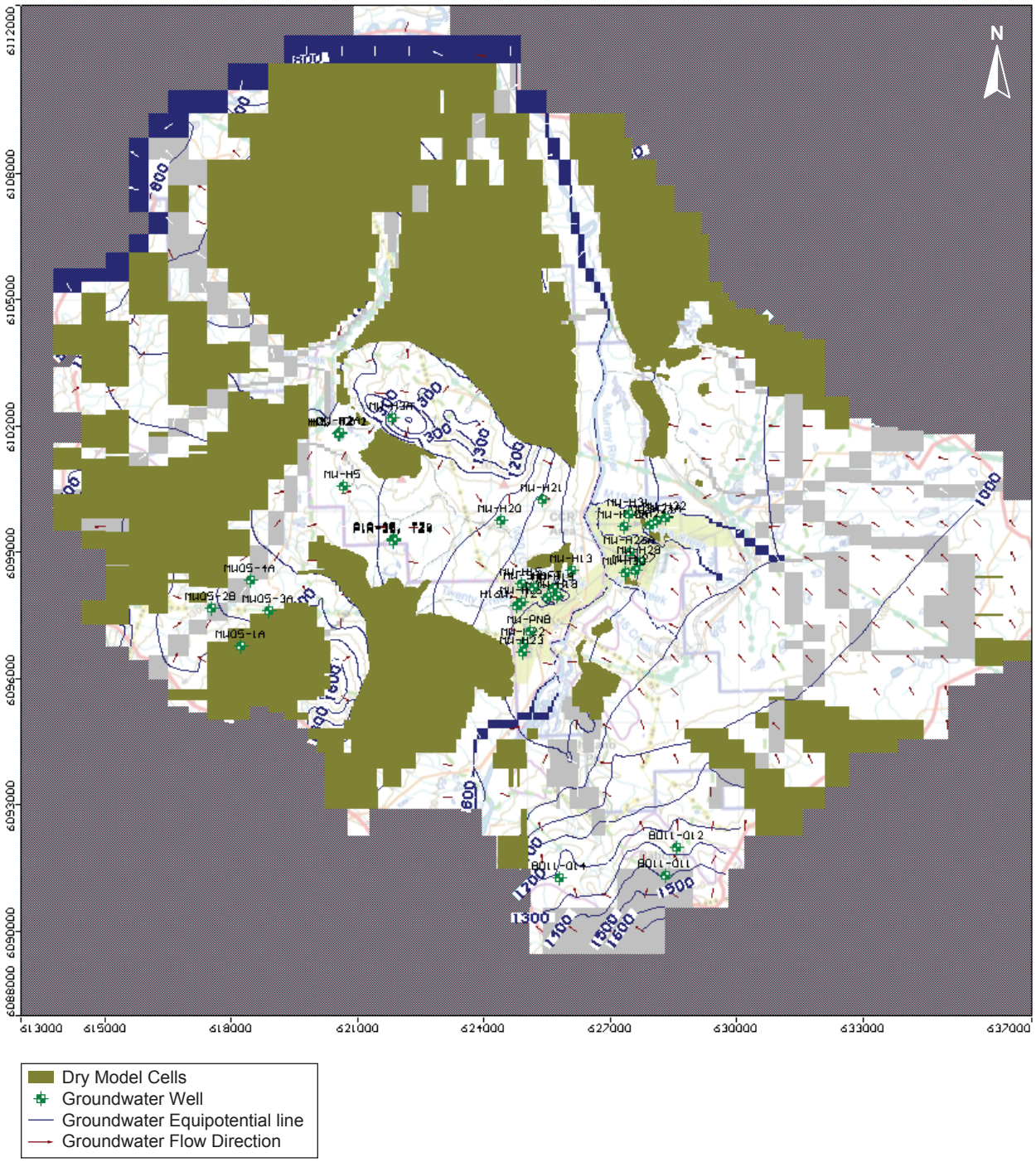

Dry Model Cells
Groundwater Well
Groundwater Equipotential line
Groundwater Flow Direction

Figure 5.2-7

Simulated Hydrogeological Baseline Hydraulic Head Contours and Groundwater Flow Directions (Plan View, Layer 2)

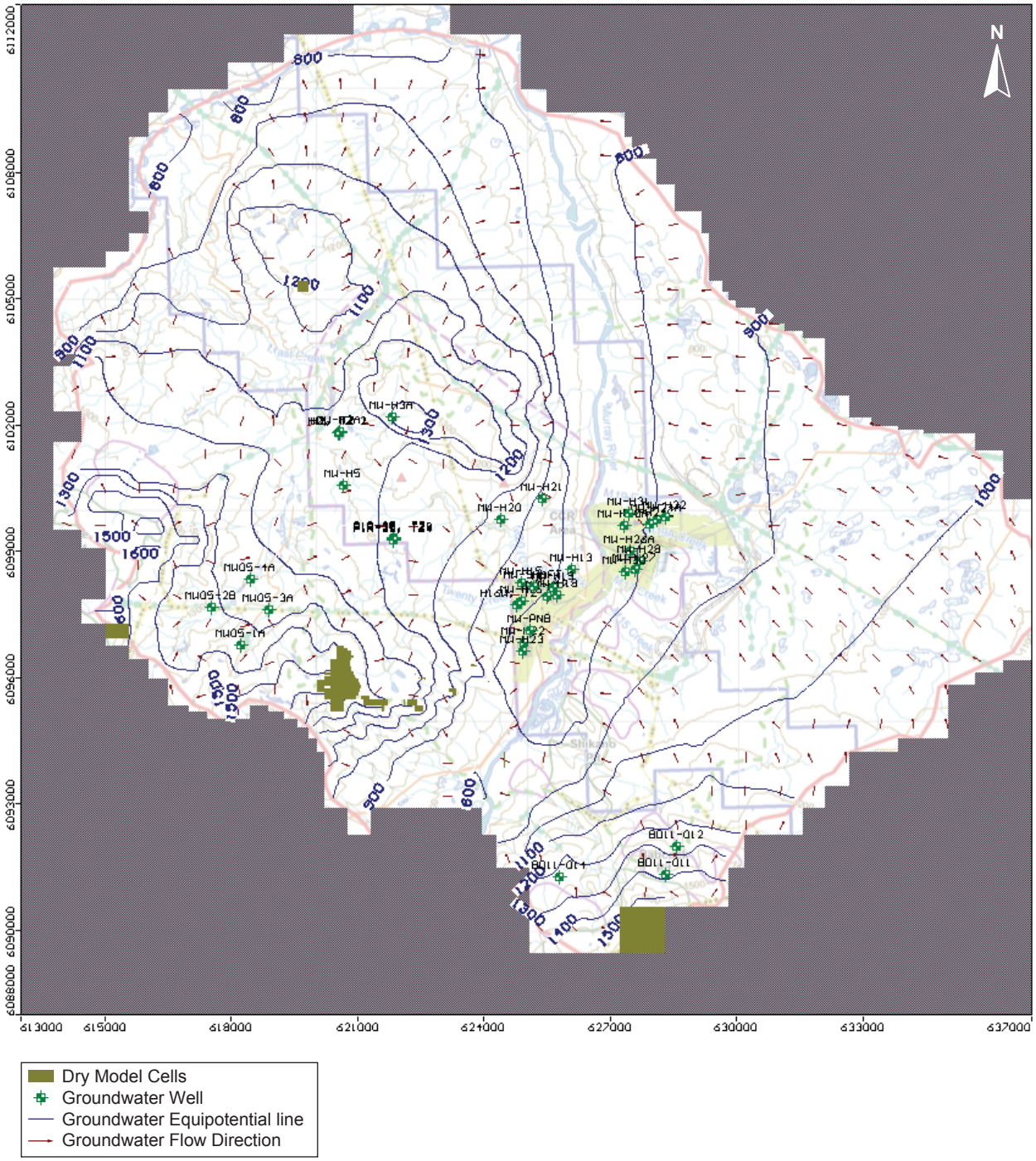

Figure 5.2-8

Simulated Hydrogeological Baseline Hydraulic Head Contours and Groundwater Flow Directions (Plan View, Layer 10)

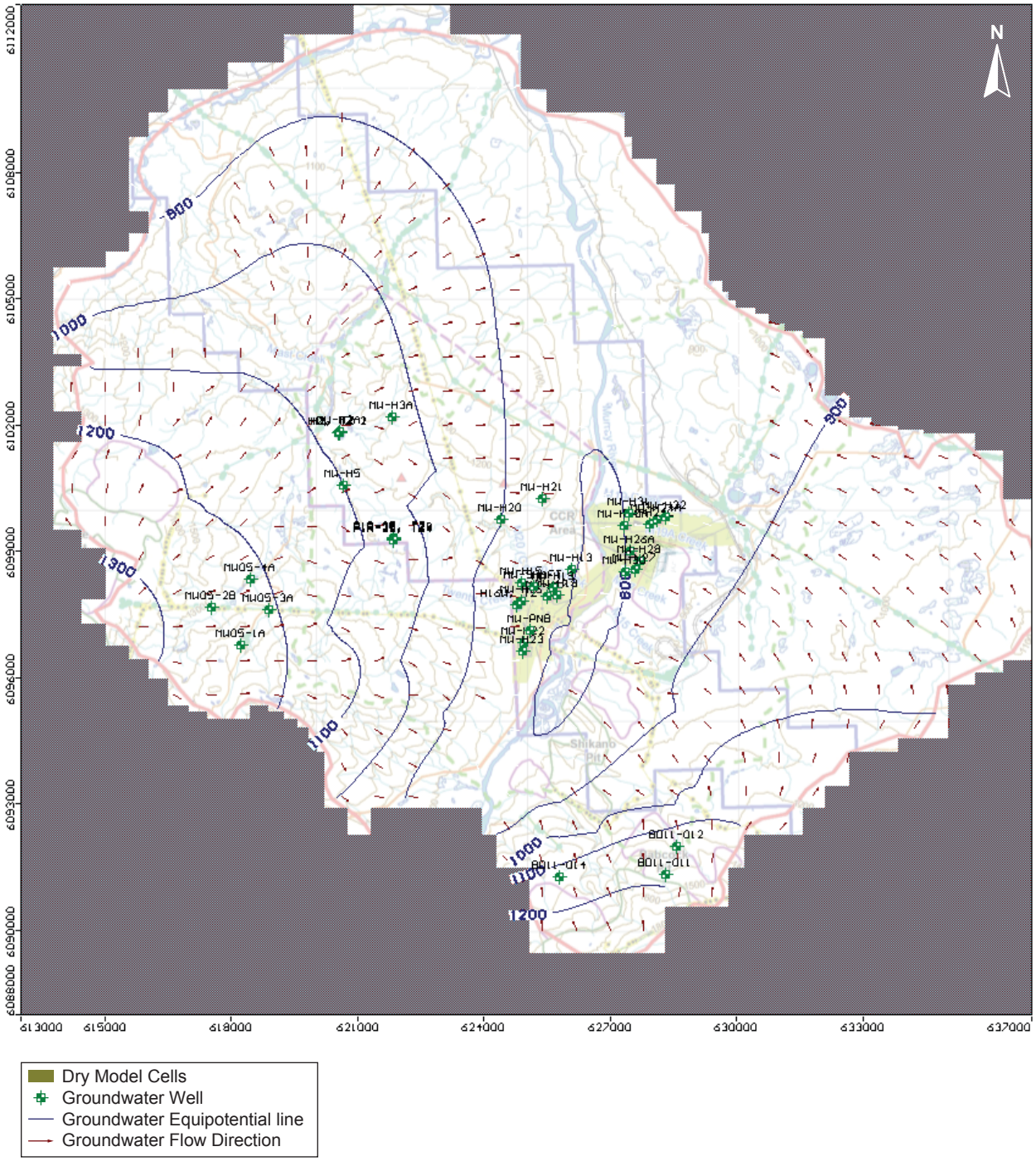

Figure 5.2-9

Simulated Hydrogeological Baseline Hydraulic Head Contours and Flow Directions (Cross-section, Row 225)

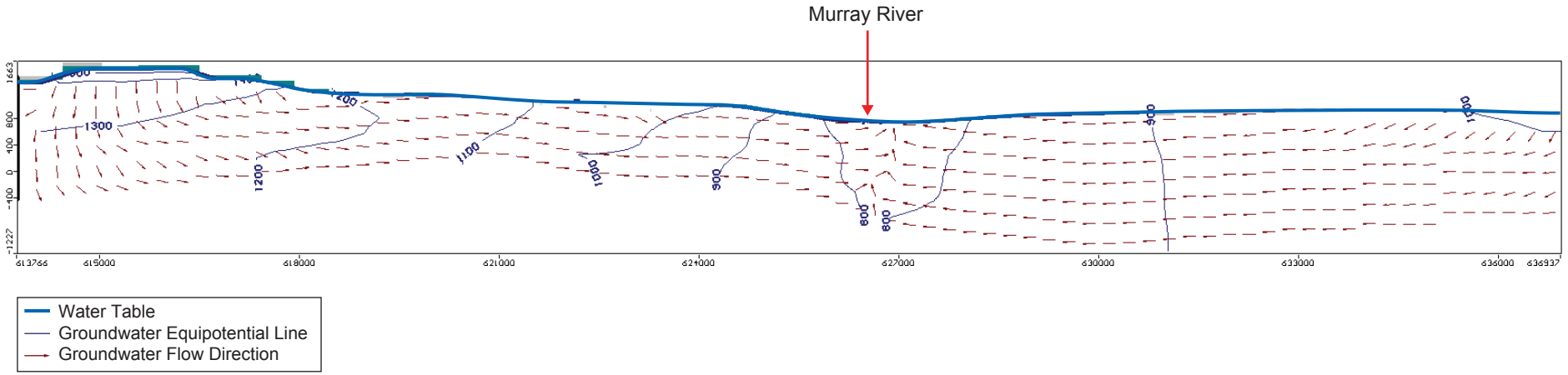

5.3 SENSITIVITY ANALYSES

Sensitivity analyses were performed on the calibrated baseline model to characterize how much changing the value of each of the model input parameters influences the model calibration. Table 5.3-1 documents the scope and results of this sensitivity analysis, while Tables 5.3-2, 5.3-3, 5.3-4 and 5.3-5 summarize and rank the results showing changes of what parameters cause the greatest changes in the measure of model calibration – parameters subject to sensitivity analysis are listed in order of decreasing sensitivity measured as a combined change in normalized RMS (combined results for increasing and decreasing the value of a parameter).

In total, values of twenty parameters were varied during this analysis for five recharge zones and fifteen hydraulic conductivity zones. The values of recharge and hydraulic conductivity used in the calibrated baseline model are associated with considerable uncertainty. It was judged that the actual recharge may vary within a range of +- 25% of the baseline value (derived as explained in Section 4.4 – Recharge). On the other hand, the possible values of hydraulic conductivity were judged to vary over a range of one order of magnitude around the baseline value: it can possibly be ten times larger or ten times smaller than the baseline value.

Discussion of the results of the baseline model sensitivity analysis is organized by the four groups of model targets used in the model calibration.

5.3.1 Entire Model Targets Dataset

Table 5.3-2 shows that model calibration to the entire set of targets is most sensitive to changes in hydraulic conductivity (K) of zones 8, 17 and 2 (in decreasing order of sensitivity). Changing K values by an order of magnitude results in a deterioration of model calibration (measured as normalized RMS) by 222%, 79% and 58%, respectively. K Zone 1 covers most of the model domain area in model Layers 1 and 2, while K Zone 17 is set along Camp Creek and limited areas around underground mine site, close to Murray River. Changing K values by an order of magnitude in either direction (+ or -) results in a drastic model de-calibration. Consequently, it can be safely concluded that the K values used in the calibrated model reasonably represent average hydraulic conductivity of shallow rocks / sediments over most of the model domain area.

K zone 2 covers most of the Hasler Formation represented in the model layers 3, 4 and 5. Again, changing k value in Zone 2 by an order of magnitude results in a very significant model de-calibration, indicating that the calibrated model value reasonably approximates the real average K of the Hasler Formation.

Varying the values of all the other model parameters (K and recharge values) results in a much smaller de-calibration of the model – the model is much less sensitive to changes in those parameters.

Table 5.3-1. Hydrogeology Baseline Model Sensitivity Analysis

Sensitivity Analysis Simulation Number	Parameter (unit)	Zone Color	Base Case Value	Base Case Value's Changing Factor		Lower and Upper Limits of Uncertainty	Calibration to Heads: Entire Model Dataset Norm. RMS %	Entire Model Dataset Residual Mean m	Deep Groundwater Dataset Norm. RMS %	Deep Groundwater Dataset Residual Mean m	CCR Site Dataset Norm. RMS %	CCR Site Dataset Residual Mean m	Calibration to Camp Creek Low-flow: Model Computed Lowflow m^3/day	Computed / Measured %	Ranking of Parameter's Sensitivity: Entire	Deep	CCR	Camp Cr.
															Combined Change in Norm. RMS per Param. %			Combined Change in Flow per Param. %
	Recharge Zone 2 (mm/year)		104				3.78	-0.80	5.53	-16.06	3.91	-1.22	586	97%	16	15	10	8
1				+ 25%	=	130	3.80	-0.09	5.27	-13.87	3.78	-0.90	608	101%				
2				- 25%	=	78	3.77	-1.55	5.80	-16.06	4.15	-1.56	562	93%				
	Recharge Zone 3 (mm/year)		126				3.78	-0.80	5.53	-16.06	3.91	-1.22	586	97%	14	7	15	5
3				+ 25%	=	157.5	3.81	1.40	4.91	-10.04	3.84	-1.10	657	109%				
4				- 25%	=	94.5	3.83	-3.14	8.09	-20.87	3.99	-1.35	513	85%				
	Recharge Zone 4 (mm/year)		155				3.78	-0.80	5.53	-16.06	3.91	-1.22	586	97%	11	5	14	4
5				+ 25%	=	193.75	3.88	-1.18	4.58	-11.30	3.76	2.53	691	114%				
6				- 25%	=	116.25	3.98	-4.32	6.59	-18.82	3.94	-1.26	477	79%				
	Recharge Zone 5 (mm/year)		182				3.78	-0.80	5.53	-16.06	3.91	-1.22	586	97%	20	20	12	17
7				+ 25%	=	227.5	3.78	-0.74	5.53	-14.96	3.82	-0.95	585	97%				
8				- 25%	=	136.5	3.78	-0.87	5.53	-14.96	4.08	-1.49	585	97%				
	Recharge Zone 6 (mm/year)		86				3.78	-0.80	5.53	-16.06	3.91	-1.22	586	97%	19	17	9	14
9				+ 25%	=	107.5	3.78	-0.45	5.51	-14.81	3.73	-0.93	588	97%				
10				- 25%	=	64.5	3.79	-1.17	5.55	-15.11	4.14	-1.53	583	96%				
	Hydraulic Conductivity Zone 2 (m/sec)		5.0E-08				3.78	-0.80	5.53	-16.06	3.91	-1.22	586	97%	3	1	13	3
11				x 10	=	5.0E-07	5.44	-15.14	13.45	-41.97	4.13	-1.17	237	39%				
12				/ 10	=	5.0E-09	4.32	1.96	6.10	-12.94	3.93	-0.98	638	105%				
	Hydraulic Conductivity Zone 3 (m/sec)		1.1E-07				3.78	-0.80	5.53	-16.06	3.91	-1.22	586	97%	17	18	2	16
13				x 10	=	1.1E-06	3.79	-1.53	5.54	-15.03	5.87	-3.57	583	96%				
14				/ 10	=	1.1E-08	3.79	-0.88	5.53	-14.94	5.82	-1.69	586	97%				
	Hydraulic Conductivity Zone 4 (m/sec)		1.0E-08				3.78	-0.80	5.53	-16.06	3.91	-1.22	586	97%	6	5	16	10
15				x 10	=	1.0E-07	4.08	-3.20	8.29	-21.68	3.84	-1.21	556	92%				
16				/ 10	=	1.0E-09	3.95	-1.68	6.92	-19.84	3.92	-1.22	590	97%				
	Hydraulic Conductivity Zone 5 (m/sec)		5.0E-10				3.78	-0.80	5.53	-16.06	3.91	-1.22	586	97%	5	6	18	13
17				x 10	=	5.0E-09	3.85	-0.20	6.18	-11.26	3.90	-1.22	580	96%				
18				/ 10	=	5.0E-11	4.33	-3.37	8.44	-24.65	3.91	-1.22	587	97%				
	Hydraulic Conductivity Zone 6 (m/sec)		5.1E-08				3.78	-0.80	5.53	-16.06	3.91	-1.22	586	97%	7	10	19	18
19				x 10	=	5.1E-07	4.22	-1.31	7.83	-15.70	3.91	-1.22	585	97%				
20				/ 10	=	5.1E-09	3.77	-1.07	5.41	-16.36	3.91	-1.22	586	97%				
	Hydraulic Conductivity Zone 8 (m/sec)		5.0E-06				3.78	-0.80	5.53	-16.06	3.91	-1.22	586	97%	1	2	1	1
21				x 10	=	5.0E-05	No convergence							0%				
22				/ 10	=	5.0E-07	12.18	43.60	13.67	41.08	17.08	7.52	2246	371%				
	Hydraulic Conductivity Zone 9 (m/sec)		1.0E-07				3.78	-0.80	5.53	-16.06	3.91	-1.22	586	97%	15	13	11	12
23				x 10	=	1.0E-06	3.72	1.42	4.67	-6.16	3.62	-0.33	572	95%				
24				/ 10	=	1.0E-08	3.78	-0.78	5.53	-14.96	3.86	-1.12	585	97%				
	Hydraulic Conductivity Zone 10 (m/sec)		3.0E-05				3.78	-0.80	5.53	-16.06	3.91	-1.22	586	97%	10	16	8	9
25				x 10	=	3.0E-04	3.80	-3.24	5.66	-16.22	4.16	-1.42	577	95%				
26				/ 10	=	3.0E-06	4.07	4.29	5.44	-11.94	3.57	0.56	610	101%				
	Hydraulic Conductivity Zone 11 (m/sec)		1.2E-05				3.78	-0.80	5.53	-16.06	3.91	-1.22	586	97%	13	14	5	6
27				x 10	=	1.2E-04	3.78	-3.96	5.83	-16.78	6.08	-2.57	541	89%				
28				/ 10	=	1.2E-06	3.93	1.14	5.27	-13.36	3.92	0.61	624	103%				
	Hydraulic Conductivity Zone 13 (m/sec)		2.0E-09				3.78	-0.80	5.53	-16.06	3.91	-1.22	586	97%	9	8	20	20
29				x 10	=	2.0E-08	3.97	-2.12	7.20	-21.19	3.91	-1.22	585	97%				
30				/ 10	=	2.0E-10	3.95	0.75	6.99	-7.68	3.91	-1.22	586	97%				
	Hydraulic Conductivity Zone 14 (m/sec)		4.0E-07				3.78	-0.80	5.53	-16.06	3.91	-1.22	586	97%	12	12	6	15
31				x 10	=	4.0E-06	3.90	-2.10	6.59	-20.57	3.94	-1.28	584	97%				
32				/ 10	=	4.0E-08	3.82	0.82	5.90	-8.66	3.29	-0.52	587	97%				
	Hydraulic Conductivity Zone 15 (m/sec)		1.0E-08				3.78	-0.80	5.53	-16.06	3.91	-1.22	586	97%	4	4	7	7
33				x 10	=	1.0E-07	3.84	-1.48	4.98	-13.06	3.36	-0.31	564	93%				
34				/ 10	=	1.0E-09	4.85	2.53	9.66	-8.48	4.01	-1.32	612	101%				
	Hydraulic Conductivity Zone 16 (m/sec)		7.0E-09				3.78	-0.80	5.53	-16.06	3.91	-1.22	586	97%	18	19	4	19
35				x 10	=	7.0E-08	3.79	-0.96	5.53	-14.96	6.07	-1.89	586	97%				
36				/ 10	=	7.0E-10	3.78	-0.81	5.54	-14.96	3.87	-1.24	585	97%				
	Hydraulic Conductivity Zone 17 (m/sec)		4.0E-05				3.78	-0.80	5.53	-16.06	3.91	-1.22	586	97%	2	3	3	2
37				x 10	=	4.0E-04	4.86	-12.46	8.71	-27.04	7.15	-2.85	440	73%				
38				/ 10	=	4.0E-06	5.69	14.76	2.67	1.59	3.80	2.25	1102	182%				
	Hydraulic Conductivity Zone 18 (m/sec)		5.0E-09				3.78	-0.80	5.53	-16.06	3.91	-1.22	586	97%	8	9	17	11
39				x 10	=	5.0E-08	4.03	-2.78	7.37	-20.18	3.87	-1.21	567	94%				
40				/ 10	=	5.0E-10	3.90	-0.81	6.56	-15.21	3.92	-1.23	592	98%				

Table 5.3-2. Ranking of Baseline Model Parameters' Sensitivity - Entire Model Dataset

Sensitivity Analysis Simulation Number	Parameter (unit)	Zone Color	Base Case Value's Changing Factor	Calibration to Heads		
				Norm. RMS %	Change in Norm. RMS %	Combined Change in Norm. RMS per Param. (incr. and decr.) %
21	Hydraulic Conductivity Zone 8 (m/sec)		x 10	No conv.		222%
22			/ 10	12.18	222.3%	
37	Hydraulic Conductivity Zone 17 (m/sec)		x 10	4.86	28.5%	79%
38			/ 10	5.69	50.4%	
11	Hydraulic Conductivity Zone 2 (m/sec)		x 10	5.44	43.8%	58%
12			/ 10	4.32	14.2%	
33	Hydraulic Conductivity Zone 15 (m/sec)		x 10	3.84	1.6%	30%
34			/ 10	4.85	28.3%	
17	Hydraulic Conductivity Zone 5 (m/sec)		x 10	3.85	1.7%	16%
18			/ 10	4.33	14.6%	
15	Hydraulic Conductivity Zone 4 (m/sec)		x 10	4.08	8.0%	12%
16			/ 10	3.95	4.4%	
19	Hydraulic Conductivity Zone 6 (m/sec)		x 10	4.22	11.7%	12%
20			/ 10	3.77	0.2%	
39	Hydraulic Conductivity Zone 18 (m/sec)		x 10	4.03	6.6%	9.9%
40			/ 10	3.90	3.2%	
29	Hydraulic Conductivity Zone 13 (m/sec)		x 10	3.97	5.1%	9.5%
30			/ 10	3.95	4.4%	
25	Hydraulic Conductivity Zone 10 (m/sec)		x 10	3.80	0.6%	8.3%
26			/ 10	4.07	7.7%	
5	Recharge Zone 4 (mm/year)		+ 25%	3.88	2.6%	7.8%
6			- 25%	3.98	5.2%	
31	Hydraulic Conductivity Zone 14 (m/sec)		x 10	3.90	3.1%	4.2%
32			/ 10	3.82	1.1%	
27	Hydraulic Conductivity Zone 11 (m/sec)		x 10	3.78	0.1%	4.1%
28			/ 10	3.93	4.0%	
3	Recharge Zone 3 (mm/year)		+ 25%	3.81	0.7%	2.1%
4			- 25%	3.83	1.4%	
23	Hydraulic Conductivity Zone 9 (m/sec)		x 10	3.72	1.7%	1.8%
24			/ 10	3.78	0.1%	
1	Recharge Zone 2 (mm/year)		+ 25%	3.80	0.6%	1.0%
2			- 25%	3.77	0.3%	
13	Hydraulic Conductivity Zone 3 (m/sec)		x 10	3.79	0.3%	0.6%
14			/ 10	3.79	0.2%	
35	Hydraulic Conductivity Zone 16 (m/sec)		x 10	3.79	0.3%	0.4%
36			/ 10	3.78	0.1%	
9	Recharge Zone 6 (mm/year)		+ 25%	3.78	0.0%	0.3%
10			- 25%	3.79	0.3%	
7	Recharge Zone 5 (mm/year)		+ 25%	3.78	0.1%	0.2%
8			- 25%	3.78	0.1%	

Table 5.3-3. Ranking of Model Parameters' Sensitivity - Deep Groundwater Dataset

Sensitivity Analysis Simulation Number	Parameter (unit)	Zone Color	Base Case Value's Changing Factor	Calibration to Heads		
				Norm. RMS %	Change in Norm. RMS %	Combined Change in Norm. RMS per Param. (incr. and decr.) %
11	Hydraulic Conductivity Zone 2 (m/sec)		x 10	13.45	143.1%	153%
12			/ 10	6.10	10.3%	
21	Hydraulic Conductivity Zone 8 (m/sec)		x 10	No conv.		147%
22			/ 10	13.67	147.3%	
37	Hydraulic Conductivity Zone 17 (m/sec)		x 10	8.71	57.6%	109%
38			/ 10	2.67	51.8%	
33	Hydraulic Conductivity Zone 15 (m/sec)		x 10	4.98	10.0%	85%
34			/ 10	9.66	74.6%	
15	Hydraulic Conductivity Zone 4 (m/sec)		x 10	8.29	49.9%	75%
16			/ 10	6.92	25.1%	
17	Hydraulic Conductivity Zone 5 (m/sec)		x 10	6.18	11.7%	64%
18			/ 10	8.44	52.6%	
3	Recharge Zone 3 (mm/year)		+ 25%	4.91	11.2%	57%
4			- 25%	8.09	46.2%	
29	Hydraulic Conductivity Zone 13 (m/sec)		x 10	7.20	30.1%	57%
30			/ 10	6.99	26.4%	
39	Hydraulic Conductivity Zone 18 (m/sec)		x 10	7.37	33.3%	52%
40			/ 10	6.56	18.5%	
19	Hydraulic Conductivity Zone 6 (m/sec)		x 10	7.83	41.6%	44%
20			/ 10	5.41	2.1%	
5	Recharge Zone 4 (mm/year)		+ 25%	4.58	17.2%	36%
6			- 25%	6.59	19.2%	
31	Hydraulic Conductivity Zone 14 (m/sec)		x 10	6.59	19.2%	26%
32			/ 10	5.90	6.6%	
23	Hydraulic Conductivity Zone 9 (m/sec)		x 10	4.67	15.6%	16%
24			/ 10	5.53	0.0%	
27	Hydraulic Conductivity Zone 11 (m/sec)		x 10	5.83	5.4%	10%
28			/ 10	5.27	4.6%	
1	Recharge Zone 2 (mm/year)		+ 25%	5.27	4.7%	9.6%
2			- 25%	5.80	4.9%	
25	Hydraulic Conductivity Zone 10 (m/sec)		x 10	5.66	2.3%	3.9%
26			/ 10	5.44	1.6%	
9	Recharge Zone 6 (mm/year)		+ 25%	5.51	0.4%	0.8%
10			- 25%	5.55	0.4%	
13	Hydraulic Conductivity Zone 3 (m/sec)		x 10	5.54	0.2%	0.3%
14			/ 10	5.53	0.1%	
35	Hydraulic Conductivity Zone 16 (m/sec)		x 10	5.53	0.0%	0.1%
36			/ 10	5.54	0.1%	
7	Recharge Zone 5 (mm/year)		+ 25%	5.53	0.1%	0.1%
8			- 25%	5.53	0.0%	

Table 5.3-4. Ranking of Model Parameters' Sensitivity - CCR Dataset

Sensitivity Analysis Simulation Number	Parameter (unit)	Zone Color	Base Case Value's Changing Factor	Calibration to Heads		
				Norm. RMS %	Change in Norm. RMS %	Combined Change in Norm. RMS per Param. (incr. and decr.) %
21	Hydraulic Conductivity Zone 8 (m/sec)		x 10	No conv.		337%
22			/ 10	17.08	336.8%	
13	Hydraulic Conductivity Zone 3 (m/sec)		x 10	5.87	50.0%	99%
14			/ 10	5.82	48.7%	
37	Hydraulic Conductivity Zone 17 (m/sec)		x 10	7.15	82.9%	86%
38			/ 10	3.80	2.7%	
35	Hydraulic Conductivity Zone 16 (m/sec)		x 10	6.07	55.2%	56%
36			/ 10	3.87	0.9%	
27	Hydraulic Conductivity Zone 11 (m/sec)		x 10	6.08	55.4%	56%
28			/ 10	3.92	0.2%	
33	Hydraulic Conductivity Zone 14 (m/sec)		x 10	3.36	14.1%	17%
34			/ 10	4.01	2.7%	
31	Hydraulic Conductivity Zone 15 (m/sec)		x 10	3.94	0.8%	17%
32			/ 10	3.29	15.8%	
25	Hydraulic Conductivity Zone 10 (m/sec)		x 10	4.16	6.4%	15%
26			/ 10	3.57	8.8%	
9	Recharge Zone 6 (mm/year)		+ 25%	3.73	4.7%	11%
10			- 25%	4.14	5.9%	
1	Recharge Zone 2 (mm/year)		+ 25%	3.78	3.4%	9.5%
2			- 25%	4.15	6.1%	
23	Hydraulic Conductivity Zone 9 (m/sec)		x 10	3.62	7.5%	8.9%
24			/ 10	3.86	1.4%	
7	Recharge Zone 5 (mm/year)		+ 25%	3.82	2.3%	6.5%
8			- 25%	4.08	4.2%	
11	Hydraulic Conductivity Zone 2 (m/sec)		x 10	4.13	5.5%	6.1%
12			/ 10	3.93	0.6%	
5	Recharge Zone 4 (mm/year)		+ 25%	3.76	4.0%	4.7%
6			- 25%	3.94	0.7%	
3	Recharge Zone 3 (mm/year)		+ 25%	3.84	1.8%	3.9%
4			- 25%	3.99	2.1%	
15	Hydraulic Conductivity Zone 4 (m/sec)		x 10	3.84	1.8%	2.0%
16			/ 10	3.92	0.2%	
39	Hydraulic Conductivity Zone 18 (m/sec)		x 10	3.87	1.0%	1.2%
40			/ 10	3.92	0.1%	
17	Hydraulic Conductivity Zone 5 (m/sec)		x 10	3.90	0.4%	0.4%
18			/ 10	3.91	0.1%	
19	Hydraulic Conductivity Zone 6 (m/sec)		x 10	3.91	0.1%	0.2%
20			/ 10	3.91	0.1%	
29	Hydraulic Conductivity Zone 13 (m/sec)		x 10	3.91	0.1%	0.2%
30			/ 10	3.91	0.1%	

Table 5.3-5. Ranking of Model Parameters' Sensitivity - Calibration to Camp Creek Low-flow

Sensitivity Analysis Simulation Number	Parameter (unit)	Zone Color	Base Case Value's Changing Factor	Calibration to Camp Creek Low-flow		
				Computed Flow with Adjusted Parameter %	Change in Flow Compared to Baseline Model %	Combined Change in Flow per Param. (incr. and decr.) %
21	Hydraulic Conductivity Zone 8 (m/sec)		x 10	No conv.		283%
22			/ 10	2246	283.2%	
37	Hydraulic Conductivity Zone 17 (m/sec)		x 10	440	24.9%	113%
38			/ 10	1102	88.1%	
11	Hydraulic Conductivity Zone 2 (m/sec)		x 10	237	59.6%	68%
12			/ 10	638	8.8%	
5	Recharge Zone 4 (mm/year)		+ 25%	691	18.0%	37%
6			- 25%	477	18.5%	
3	Recharge Zone 3 (mm/year)		+ 25%	657	12.2%	25%
4			- 25%	513	12.5%	
27	Hydraulic Conductivity Zone 11 (m/sec)		x 10	541	7.7%	14%
28			/ 10	624	6.5%	
33	Hydraulic Conductivity Zone 15 (m/sec)		x 10	564	3.8%	8.1%
34			/ 10	612	4.4%	
1	Recharge Zone 2 (mm/year)		+ 25%	608	3.8%	7.9%
2			- 25%	562	4.1%	
25	Hydraulic Conductivity Zone 10 (m/sec)		x 10	577	1.5%	5.7%
26			/ 10	610	4.2%	
15	Hydraulic Conductivity Zone 4 (m/sec)		x 10	556	5.1%	5.7%
16			/ 10	590	0.6%	
39	Hydraulic Conductivity Zone 18 (m/sec)		x 10	567	3.3%	4.3%
40			/ 10	592	1.0%	
23	Hydraulic Conductivity Zone 9 (m/sec)		x 10	572	2.4%	2.5%
24			/ 10	585	0.1%	
17	Hydraulic Conductivity Zone 5 (m/sec)		x 10	580	1.0%	1.2%
18			/ 10	587	0.2%	
9	Recharge Zone 6 (mm/year)		+ 25%	588	0.3%	0.9%
10			- 25%	583	0.6%	
31	Hydraulic Conductivity Zone 14 (m/sec)		x 10	584	0.3%	0.5%
32			/ 10	587	0.2%	
13	Hydraulic Conductivity Zone 3 (m/sec)		x 10	583	0.5%	0.5%
14			/ 10	586	0.0%	
7	Recharge Zone 5 (mm/year)		+ 25%	585	0.2%	0.4%
8			- 25%	585	0.2%	
19	Hydraulic Conductivity Zone 6 (m/sec)		x 10	585	0.2%	0.3%
20			/ 10	586	0.1%	
35	Hydraulic Conductivity Zone 16 (m/sec)		x 10	586	0.1%	0.3%
36			/ 10	585	0.2%	
29	Hydraulic Conductivity Zone 13 (m/sec)		x 10	585	0.2%	0.2%
30			/ 10	586	0.0%	

5.3.2 Deep Groundwater Targets Dataset

Table 5.3-3 shows that model calibration to the set of deep groundwater targets is most sensitive to changes in hydraulic conductivity (K) of zones 2, 8 and 17 (in decreasing order of sensitivity). Those are the same most sensitive parameter zones as listed for the entire model target dataset (discussed above). However, those same zones are listed here in a different order. Since all of the targets in this target group are located within deeper bedrock, the model calibration is most sensitive to parameter changes in the deepest of the three sensitive zones – Zone 2. However, the deeper portion of the model is sensitive to changes in a much larger number of parameters, compared to the entire model (which is primarily sensitive to changes on only three parameters). Model de-calibration larger than 50% is caused by changes in nine parameters: K in Zones 2, 8, 17, 15, 4, 5, recharge in Zone 3, K in Zones 13 and 18.

The differences between conclusions for the entire model vs. deeper part of the model are easy to explain: most of the targets of the entire model dataset are located in shallow formations and, thus, model calibration responds primarily to changes in parameters assigned to shallow layers – K for Zones 8 and 17. On the other hand, calibration of the deeper part of the model is more sensitive to the entire model set-up.

5.3.3 CCR Site Targets Dataset

Table 5.3-4 shows that model calibration to the CCR set of targets is most sensitive to changes in hydraulic conductivity (K) of zones 8, 3, 17, 16 and 11 (in decreasing order of sensitivity). Changing K values by an order of magnitude results in a deterioration of model calibration (measured as normalized RMS) by more than 50%. All those K zones represent shallow, unconsolidated formations encountered around the CCR Site. Thus, this part of the model is not sensitive to any parameters representing deeper parts of the model domain. Also, changes in recharge within reasonable limits (+-25%) do not result in a significant de-calibration of the CCR Site part of the model due to the fact that the CCR site is located in the local groundwater discharge zone adjacent to Murray River.

5.3.4 Flow in Camp Creek

Table 5.3-5 shows that model calibration to the measured flow (estimated would be a more correct description of this parameter) flow in Camp Creek is most sensitive to changes in hydraulic conductivity (K) of zones 8, 17 and 2. Those are the same parameters and listed in the same order as for the entire model water level target dataset. Thus, the conclusions of this part of analysis are the same as discussed above.

6. PREDICTIVE MODEL SIMULATIONS AND RESULTS

This section describes the methodology and the results of predictive model simulations of the conditions of groundwater system during the mine operations and after the mine closure (the post closure period). The objective of those simulations was to predict the impacts of mining activities on groundwater quantity and quality in the study area.

Two different kinds of predictive model simulations were completed as part of this groundwater modelling project: 1) dewatering of the underground mine (discussed in Section 6.1), and 2) contaminant transport at the CCR Site (discussed in Section 6.2). Several model scenarios were developed from the calibrated baseline model to simulate groundwater impacts caused by the proposed mine.

All the model scenarios set for predictive simulations were derived from the calibrated baseline model described in the previous sections of this report. All the flow boundaries and aquifer properties were left as in the calibrated baseline model, except for modifications described below.

6.1 SIMULATIONS OF UNDERGROUND MINE DEWATERING

6.1.1 Model Set-up for Mine Dewatering Simulations

The calibrated baseline model has been modified in order to simulate dewatering of the underground mine. The following modifications were made to prepare the model for predictive simulations of dewatering:

- Drains were set in the model layer 10 (L10 – representing J Coal Seam and other coal seams that are proposed to be mined) covering the areas of the planned mining in Blocks 1, 2, 3 and 4 (see Figures 1.1-3 and 6.1-1)
- Two additional hydraulic conductivity zones were created: Zone 19 in model layer 10 (L10) to represent increased hydraulic conductivity of the mined out parts of the rock formation; Zone 20 in the model layers 9, 10 and 11 (L9, L10 and L11) encapsulating the mined out parts of the rock formation (from the sides, from below and from above) to represent increased hydraulic conductivity of the rock around the mined out cavities as a result of decompression fracturing (see Figures 6.1-2, 6.1-3 and 6.1-4).

The drains are set in model layer L 10 representing J Coal Seam within Gates Formation. Although coal seams other than J Coal Seam will also be subject to mining, those seams are located at depths not much different from J Seam - hundreds of meters below ground surface. Their combined thickness is estimated not to exceed the thickness of 20 m for the model layer L10.

Several scenarios of the model were developed to simulate different situations for underground mine dewatering, as listed in Table 6.1-1. That table explains what parameters were changed, compared to the calibrated baseline model. Figure 6.1-5 shows the model budget zones assigned in the model Layer 10 in order to calculate the groundwater discharge (inflow) into the underground mine zones.

Figure 6.1-1

Drains Set in Model Layer 10

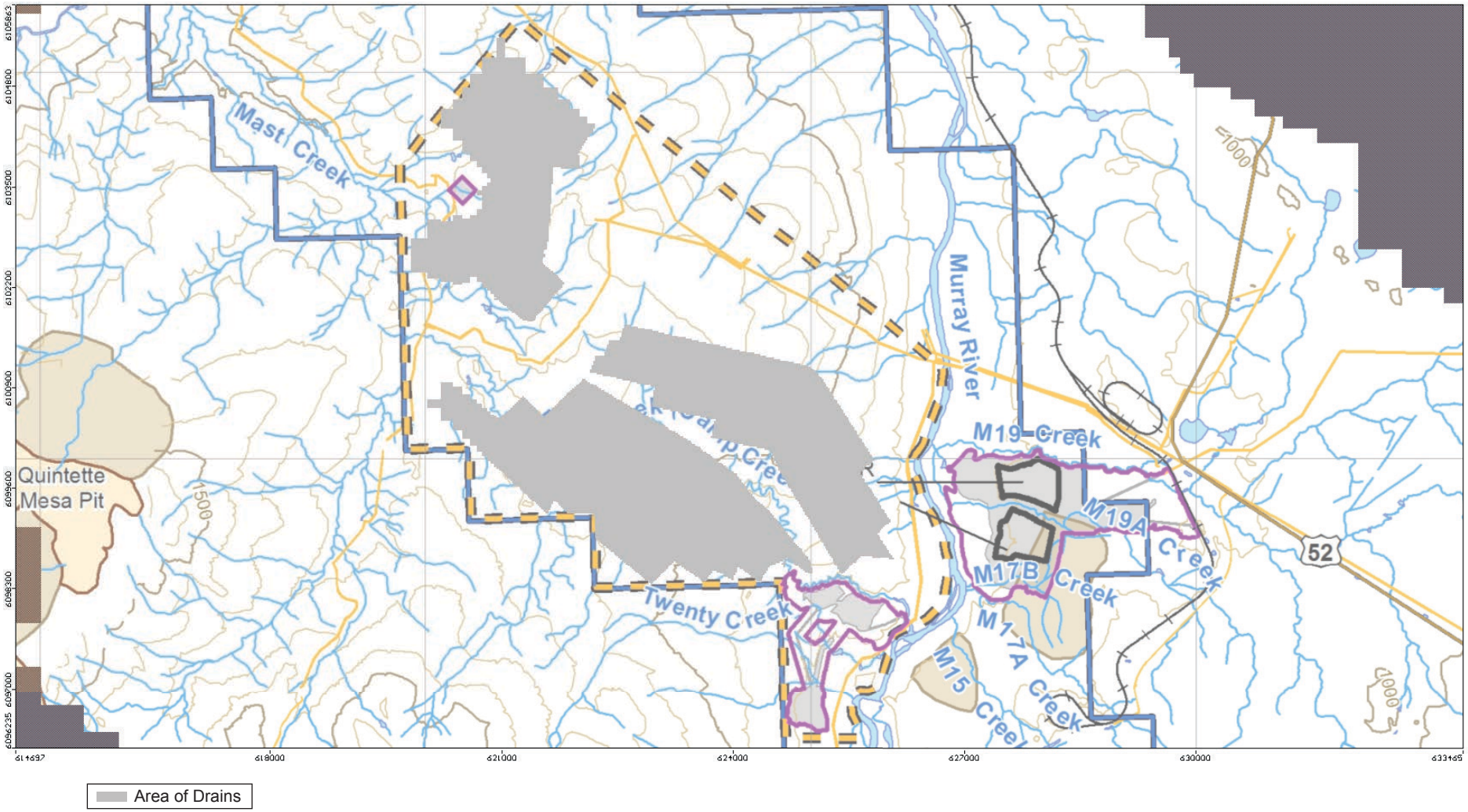

Figure 6.1-2

Hydraulic Conductivity Zones Set in Model Layer 9 for Mine Predictive Simulations

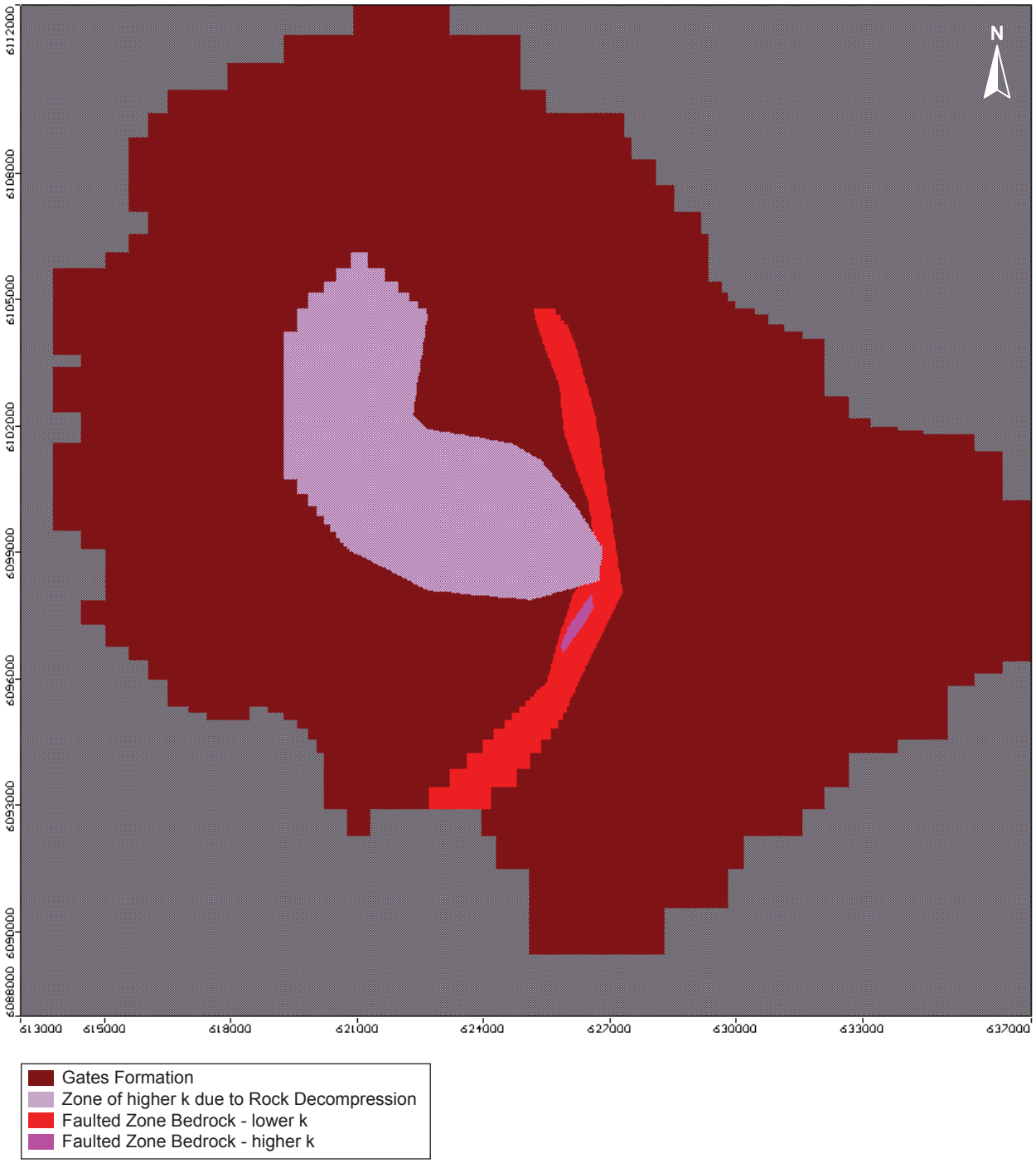

Figure 6.1-3

Hydraulic Conductivity Zones Set in Model Layer 10 for Mine Predictive Simulations

Figure 6.1-4

Hydraulic Conductivity Zones Set in Model Layer 11 for Mine Predictive Simulations

Figure 6.1-5

Hydrogeological Mine Predictive Model Budget Zones set in Model Layer 10

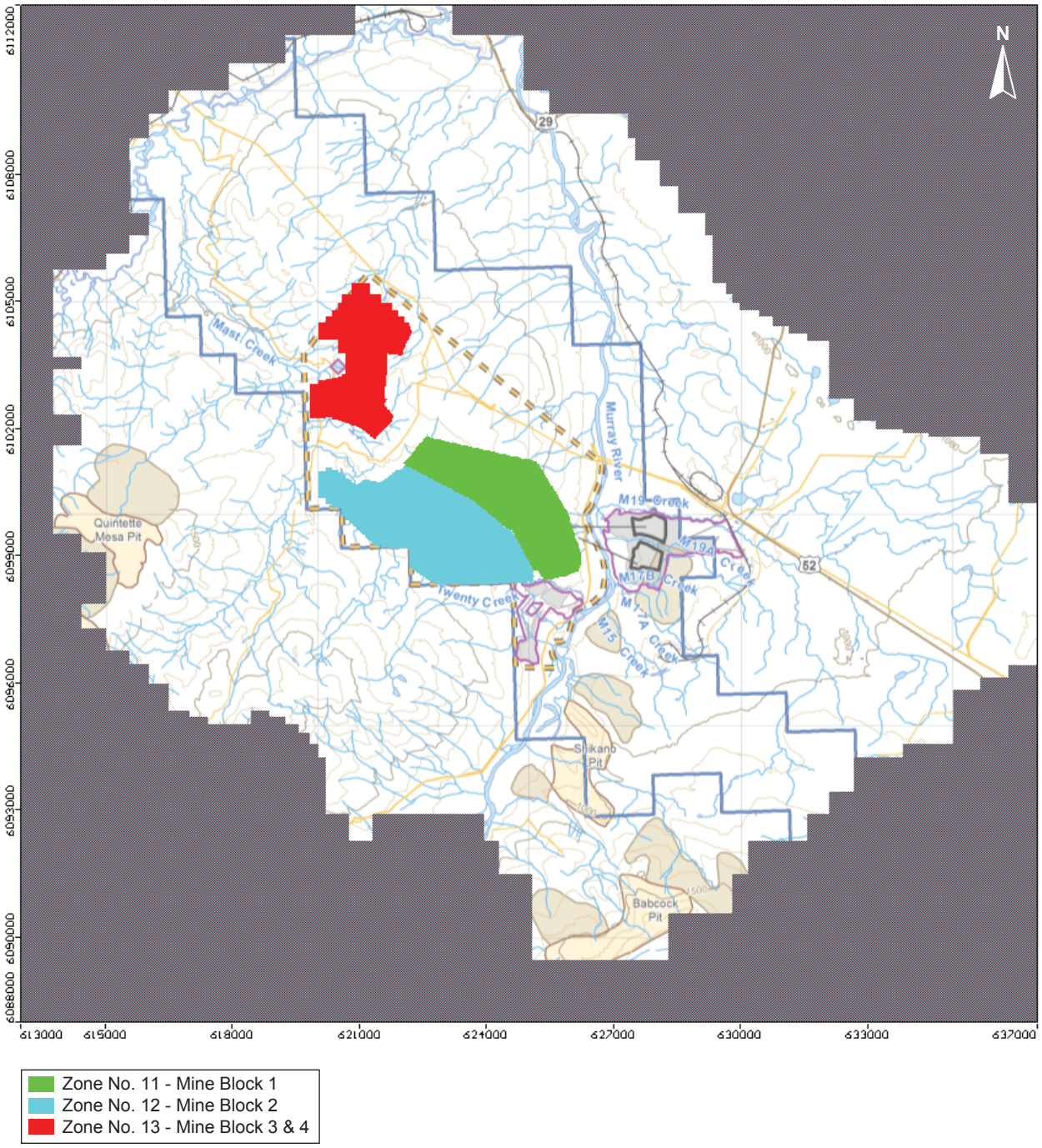

Table 6.1-1. List of the Murray River Groundwater Model Scenarios for Mine Dewatering Simulations

Scenario Name	Description of the Scenario	Modifications from the Calibrated Baseline Model	Model Predictions	Discharge to Mine Zones					Model Mass Balance Error
				Mine Block 1 (m^3/day)	Mine Block 2 (m^3/day)	Mine Blocks 3 and 4 (m^3/day)	All Mine Blocks (m^3/day)	All Mine Blocks (L/sec)	
Base Case Scenarios									
Base Case - Entire Mine Dewatering	Base case model for simulating mine dewatering	Set drains within the mine footprint; K for Zone No. 19 = 1E-5 m/s; K for Zone No. 20 = 1E-8 m/s;	Groundwater inflow rate into mine = 22 L/sec; 3.5% reduction in groundwater discharge to M20 Camp Creek; max drawdown <2.5 m	715	538	638	1891	22	-0.07%
Base Case - Block 1 Mine Dewatering	Base case model for simulating mine dewatering from Mine Block No. 1 only	Set drains only within the footprint of mine block No. 1;	Groundwater inflow rate into mine = 10 L/sec	892	NA	NA	892	10	0.00%
Wetter Climate Scenario	Model developed from base case model to simulate wetter climate scenario	Recharge in all model recharge zones increased by 25%, compared to baseline model	Groundwater inflow rate into mine = 23 L/sec	798	542	642	1982	23	-0.04%
Lower Permeability Scenario	Model developed from base case model to simulate lower hydralic conductivity scenario	K for Zone No. 19 = 1E-6 m/s; K for Zone No. 20 = 1E-8 m/s;	Groundwater inflow rate into mine = 22 L/sec	716	536	629	1881	22	-0.06%
Upper Case Scenarios									
Upper Case - Entire Mine Dewatering	Model developed from base case model to simulate high hydraulic conductivity scenario	K for Zone No. 5 = 5E-9 m/s;	Groundwater inflow rate into mine = 69 L/sec; 15% reduction in groundwater discharge to M20 Camp Creek; max drawdown 11.5 m	1721	2026	2256	6002	69	-0.02%
Upper Case - Block 1 Mine Dewatering	Model developed from base case model to simulate high hydraulic conductivity scenario for Mine Block No. 1 only	Set drains only within the footprint of mine block No. 1; K for Zone No. 5 = 5E-9 m/s; K for Zone No. 19 = 1E-5 m/s; K for Zone No. 20 = 1E-8 m/s	Groundwater inflow rate into mine = 35 L/sec	3056	NA	NA	3056	35	-2.23%
Uppermost Case Scenarios									
Uppermost Case 1 - Entire Mine Dewatering	Model developed from base case model to simulate very high hydraulic conductivity scenario	K for Zone No. 5 = 1E-8 m/s;	Groundwater inflow rate into mine = 91 L/sec; 22% reduction in groundwater discharge to M20 Camp Creek; max drawdown 14.5 m	2189	2650	2998	7837	91	-0.04%
Uppermost Case 2 - Entire Mine Dewatering	Model developed from base case model to simulate very high hydraulic conductivity scenario	K for Zone No. 5 = 2E-8 m/s; K for Zone No. 20 = 4E-8 m/s;	Groundwater inflow rate into mine = 148 L/sec; 26% reduction in groundwater discharge to M20 Camp Creek; max drawdown 19.5 m	3867	3710	5172	12748	148	-0.08%

All the model scenarios set for simulating mine dewatering were run using MODFLOW-Surfact 3.0 program (HydroGeologic Inc. 1996). PCG4 Solver was used to obtain the solutions with the following configuration of the engine parameters:

- Head change criterion = 10; and
- Relative closure criterion = 10

6.1.2 Limited Sensitivity Analysis of the Model Constructed to Simulate Mine Dewatering

The values of two groups of parameters were varied to evaluate changes in model predictions: hydraulic conductivity of zones 5 & 19 and values of recharge. Hydraulic conductivity of Zone 5 (which encapsulates the simulated mine) was found to be the most sensitive parameter with regard to the model-predicted groundwater discharge into the mine and water table drawdowns. Increasing groundwater recharge by 25% (applied to water table to simulate wet climate conditions) did not result in a significant change of groundwater discharge into the mine and water table drawdowns, compared to the base case model.

6.1.3 Predictions of Mine Dewatering Inflows and Effects

6.1.3.1 Base Case Scenarios

Two base case model scenarios were constructed to simulate the mine dewatering of the entire underground mine (including all of the four blocks) and the Mine Block No. 1 only, respectively (listed in the upper part of Table 6.1-1). Model simulating those scenarios predicted relatively lower groundwater inflow rates into the mine and low water table drawdowns. The calculated groundwater inflow rate in the base case is 1,891 m^3/day for the entire mine dewatering (with the assumption of all of the four blocks are being dewatered simultaneously to their maximum extents), and 892 m^3/day for Mine Block No. 1 dewatering only. Maximum water table drawdowns are less than 2.5 m when the entire mine is dewatered with the assumption that all the four blocks are dewatered simultaneously to their maximum extents (see Figure 6.1-6). The reduction of groundwater discharge into M20 Camp Creek is 3.5% of the estimated baseflow in that Creek, under the condition that the entire mine is dewatered.

6.1.3.2 Wetter Climate Scenario

This model scenario was constructed from base case scenario by increasing recharge in all the model recharge zones by 25%, in order to evaluate the effects of the recharge under the wetter climate condition upon the model simulated groundwater flow and its predictions (Table 6.1-1). The calculated groundwater inflow rate in the wetter climate scenario is about 5% higher compared to the base case scenario - 1,982 m^3/day vs 1,891 m^3/day for the entire mine dewatering (with the assumption of all of the four blocks are being dewatered simultaneously to their maximum extents). The changes in discharge to M20 Camp Creek and to water table drawdowns, relative to base case scenario, are minimal.

Figure 6.1-6

Map of Water Table Drawdown Caused by Mine Dewatering – Base Case Scenario

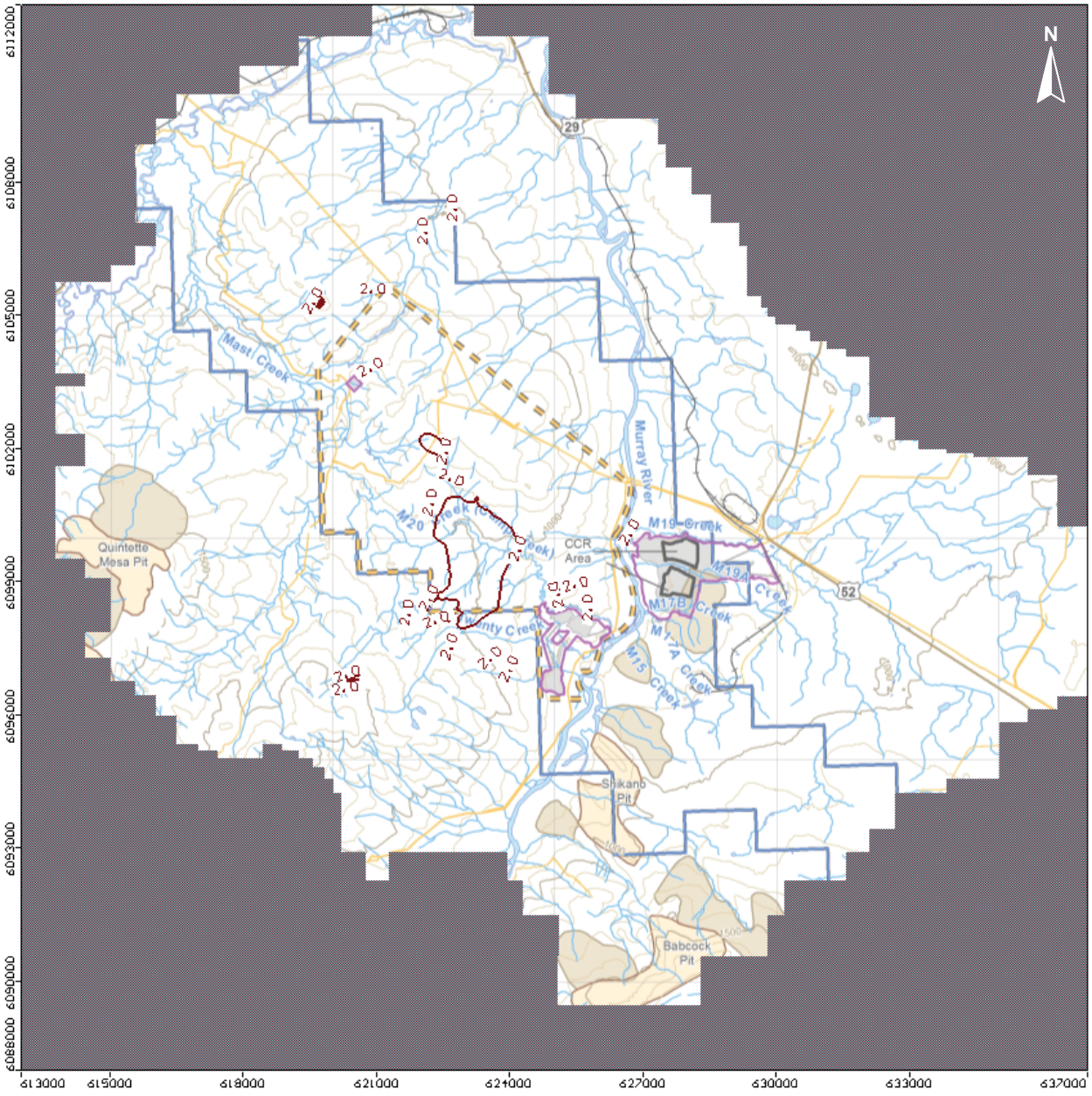

6.1.3.3 Lower Permeability Scenario

This model scenario was constructed from base case scenario by lowering hydraulic conductivity of Zone No. 19 (encapsulating the mine) by one order of magnitude (from 1 x 10^{-5} m/sec to 1 x 10^{-6} m/sec). This scenario allows to evaluate the effects of uncertainty associated with the assumed permeability of that zone on the model prediction (of groundwater inflow into the mine zones) (Table 6.1-1). The calculated groundwater inflow rate in this lower permeability scenario is slightly lower than the rate calculated in the base case scenario, about 0.5% lower - 1,881 m^3/day vs 1,891 m^3/day for the entire mine dewatering (with the assumption of all of the four blocks are being dewatered simultaneously to their maximum extents). The changes in discharge to M20 Camp Creek and to water table drawdowns, relative to base case scenario, are minimal.

6.1.3.4 Upper Case Scenarios

Two upper case model scenarios were prepared for predictive simulations of the mine dewatering of the entire underground mine (including all of the four blocks) and the Mine Block No. 1 only, respectively, with higher hydraulic conductivities. In these scenarios, the hydraulic conductivity of the Zone No. 5 (encapsulating the mine) was increased tenfold (from 5 x 10^{-10} m/sec to 5 x 10^{-9} m/sec), in comparison with the base case model. They predict the higher groundwater inflow rates into the mine (6,002 m^3/day vs 1,891 m^3/day) and larger water table drawdowns (11.5 m in the upper case vs. 2.5 m in the base case, see Figure 6.1-7) for the entire mine dewatering (with the assumption of all of the four blocks are being dewatered simultaneously to their maximum extents), in comparison with the predictions of the base case and lower permeability case model scenarios (Table 6.1-1). These upper case models calculated groundwater inflow rates were used as an input for base case water quantity and quality modelling for conservative purpose (ERM 2014c).

6.1.3.5 Uppermost Case Scenarios

Two model scenarios were set as the uppermost case. In those model scenarios, hydraulic conductivity of the Zone No. 5 was increased twenty and forty times (from 5 x 10^{-10} m/sec to 1 x 10^{-8} and 2 x 10^{-8} m/sec), in comparison with the base case model.

The uppermost case model scenarios predict not only the much higher groundwater discharge rates into the mine (from 7,837 to 12,748 m^3/day, Table 6.1-1), but also the much larger water table drawdowns (from 14.5 to 19.5 m), with the assumption that the entire mine of all of the four blocks is dewatered simultaneously to their maximum extents. The loss of groundwater discharge to M20 Camp Creek varies from 22% to 26% of the estimated baseflow).

Continuing increasing hydraulic conductivity of the Zone No. 5 beyond the value used in the uppermost case scenario would result in de-calibrating the model and de-calibrated models should not be used for making predictions.

6.1.3.6 Calculating Changing-with-Time Groundwater Mine Seepage Rates for Water Use Planning

The model provided steady-state rates of groundwater seepage into the mine were used to estimate how those rates will change with time during the mine operations. Those calculations are important

for water quality modelling and for planning of water management at the project site (ERM Rescan 2014c). The calculations were completed using the following assumptions:

- For baseline and upper case scenarios it was assumed that by the end of year -4 (completion of bulk sample), the inflow rate will be 1/3rd of the inflow rate at the end of year 3;
- For the base case and upper case scenarios, the flow at the end of year 3 was assumed equal to the one calculated by the groundwater model that was set up to simulate dewatering from Block 1 area only;
- For the uppermost case scenario the flow at the end of year 3 was calculated using a proportion of the model-calculated inflow rates at the end of mining operations for: (1) the base case and the (2) uppermost case (calculated by the steady-state model simulating dewatering the entire area of the mine);
- The increase in inflow from year -4 to year 3 was assumed to be linear;
- The increase in inflow from year 3 to year 25 (the end of mining operations) for base case and uppermost case was calculated by multiplying the inflow rates calculated for the upper case scenario by the ratio of the model-calculated final inflow rates for the upper case and the uppermost case (calculated by the steady-state model simulating dewatering the entire area of the mine).

Inflow into the mine for the upper case scenario between year 3 and 25 was calculated, in turn, using the following set of assumptions:

- Inflow into mine Block1 decreases linearly from the value calculated by the upper case model for mining Block 1 only" to the value calculated by the steady-state model (upper case model for the entire mine) for the Budget zone covering only Block 1 of the mine;
- Inflow rates in Blocks 2, 3 and 4 increase linearly with years of mining until they reach the maximum predicted by the steady-state model simulating the entire mine for each mine block (each block has assigned to it a separate budget zone).
- Inflow rates into Blocks 3 and 4 are equal.

The results of those calculations are presented in Table 6.1-2. Figure 6.1-8 shows increase in groundwater mine seepage rate for the upper case scenario and the estimated water use by the underground mine. As Table 6.1-2 indicates, groundwater seepage rates will produce sufficient amount of water for the underground mine operations' use for both the upper- and uppermost case. However, seepage rates will not satisfy the underground mine's water needs according to the groundwater model base case scenario.

The groundwater model's upper case scenario results were used as a base case scenario in water quantity and water quality modelling (ERM Rescan 2014c).

Figure 6.1-7

Map of Water Table Drawdown Caused by Mine Dewatering – Upper Case Scenario

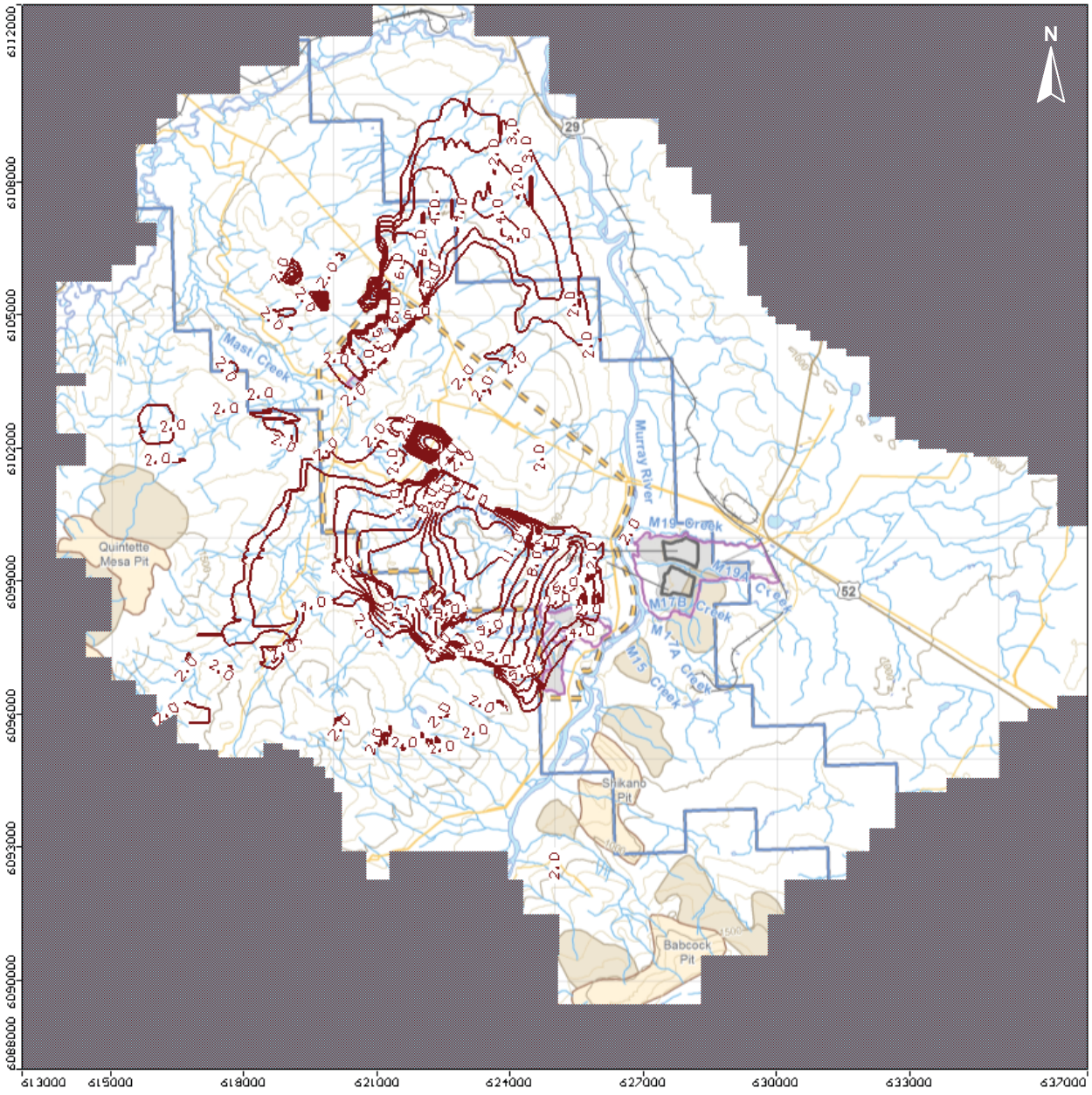

Figure 6.1-8

Estimated Changing-with-Time Groundwater Seepage Rates vs. Water Use

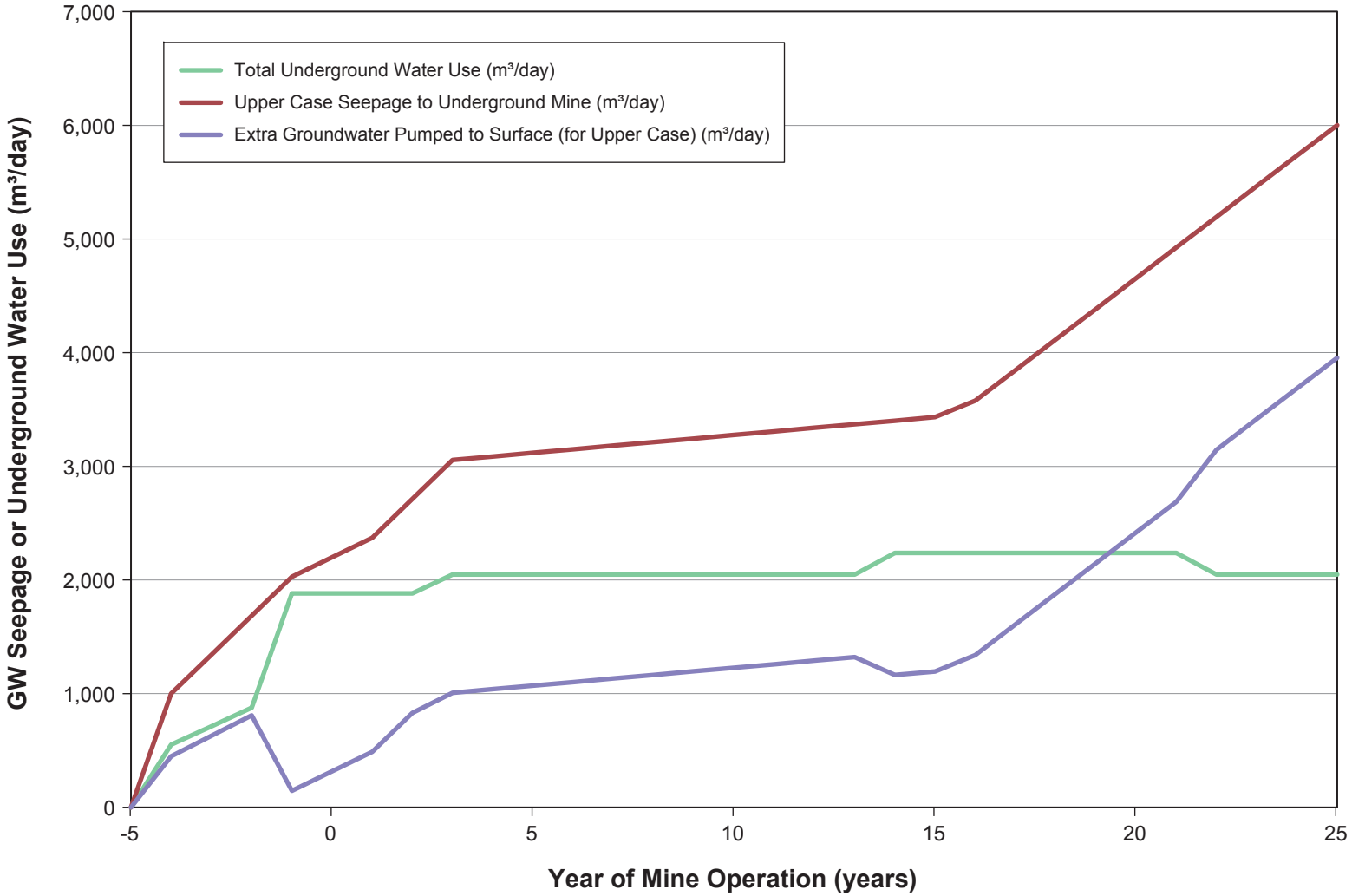

Table 6.1-2. Estimated Changing-with-Time Groundwater Mine Seepage Rates vs. Water Use

Date		Underground Water Consumption[1] (m^3/day)	Underground Evaporation[2] (m^3/day)	Total Underground Water use[3] (m^3/day)	Base Case Seepage to Underground Mine (m^3/day)	Upper Case Seepage to Underground Mine (m^3/day)	Uppermost Case Seepage to Underground Mine (m^3/day)	Extra Groundwater Pumped to Surface (for Upper Case) (m^3/day)
End of Year -5, (Bulk Sample)	12/31/2013	0	0	0	0	0	0	0
End of Year -4, (Bulk Sample)	12/31/2014	390	162	552	324	1,000	2,186	448
End of Year -3, (Construction)	12/31/2015	550	162	712	419	1,343	2,914	631
End of Year -2, (Construction)	12/31/2016	715	162	877	513	1,685	3,643	808
End of Year -1, (Construction)	12/31/2017	1,721	162	1,883	608	2,028	4,372	145
End of Year 1, (Operation)	12/31/2018	1,721	162	1,883	703	2,371	5,100	488
End of Year 2, (Operation)	12/31/2019	1,721	162	1,883	797	2,713	5,829	830
End of Year 3, (Operation)	12/31/2020	1,886	162	2,048	892	3,056	6,558	1,008
End of Year 4, (Operation)	12/31/2021	1,886	162	2,048	973	3,087	6,558	1,039
End of Year 5, (Operation)	12/31/2022	1,886	162	2,048	983	3,119	6,624	1,071
End of Year 6, (Operation)	12/31/2023	1,886	162	2,048	993	3,150	6,691	1,102
End of Year 7, (Operation)	12/31/2024	1,886	162	2,048	1,002	3,182	6,758	1,134
End of Year 8, (Operation)	12/31/2025	1,886	162	2,048	1,012	3,213	6,824	1,165
End of Year 9, (Operation)	12/31/2026	1,886	162	2,048	1,022	3,244	6,891	1,196
End of Year 10, (Operation)	12/31/2027	1,886	162	2,048	1,032	3,276	6,958	1,228
End of Year 11, (Operation)	12/31/2028	1,886	162	2,048	1,042	3,307	7,025	1,259
End of Year 12, (Operation)	12/31/2029	1,886	162	2,048	1,052	3,339	7,091	1,291
End of Year 13, (Operation)	12/31/2030	1,886	162	2,048	1,062	3,370	7,158	1,322
End of Year 14, (Operation)	12/31/2031	2,075	162	2,237	1,072	3,402	7,225	1,165
End of Year 15, (Operation)	12/31/2032	2,075	162	2,237	1,082	3,433	7,291	1,196
End of Year 16, (Operation)	12/31/2033	2,075	162	2,237	1,127	3,577	7,598	1,340
End of Year 17, (Operation)	12/31/2034	2,075	162	2,237	1,212	3,847	8,170	1,610
End of Year 18, (Operation)	12/31/2035	2,075	162	2,237	1,297	4,116	8,743	1,879
End of Year 19, (Operation)	12/31/2036	2,075	162	2,237	1,382	4,386	9,315	2,149
End of Year 20, (Operation)	12/31/2037	2,075	162	2,237	1,467	4,655	9,888	2,418
End of Year 21, (Operation)	12/31/2038	2,075	162	2,237	1,552	4,925	10,460	2,688
End of Year 22, (Operation)	12/31/2039	1,886	162	2,048	1,637	5,194	11,033	3,146
End of Year 23, (Operation)	12/31/2040	1,886	162	2,048	1,721	5,464	11,605	3,416
End of Year 24, (Operation)	12/31/2041	1,886	162	2,048	1,806	5,733	12,178	3,685
End of Year 25, (Operation)	12/31/2042	1,886	162	2,048	1,891	6,002	12,748	3,954

[1] *Based on information received from from HD Mining on April 28, 2014*

[2] *Based on information received from HD Mining on April 22, 2014*

[3] *Sum of the previous two columns*

Projected underground water use higher than the estimated rate of groundwater inflow into the mine

6.1.4 Predictions of Post-mine Flooding and Water Table Recovery

After the mine operations are completed, groundwater will be allowed to fill in the post-mine voids and, then, water table will be gradually recovering to pre-mining levels.

The volume of the post-mine underground voids was calculated using the planned panel heights (partly 5.1 m, partly 2.1m), widths (220m) and lengths. The total calculated volume is 113,104,134 m^3. The model calculated rates of groundwater inflow into the mine were used to calculate the time needed to completely flood the post-mine voids with groundwater. The results for the base case , the upper case and the uppermost case are 164 years, 52 years and 24 years, respectively, under the assumption that the entire mine zone of all the four mine blocks are mined out completely before the flooding. These calculations also conservatively assume that the voids would not be filled with rock collapsed from the ceiling or backfilled from the waste rock from the later mine phases and that the flooding will start only after all mining has been completed (not during mining operations).

Once the post-mine voids are filled with groundwater, water levels in the groundwater system affected by mine operations will start recovering. Figure 6.1-9 shows the model calculated progress of water table recovery with time (starting from the moment the mine is fully flooded) at the monitoring well MW-H20. This well is located close to the model calculated area of maximum water table drawdown (caused by mine dewatering) near the center of the mine blocks 1 and 2.

As Figure 6.1-9 shows, it will take 40 years for water table near MW-H20 to reach 80% recovery toward the pre-mining level. Those years are counted from the moment the mine voids are completely flooded by groundwater, which according to the above presented calculation will take 164 years, 52 years and 24 years for the base case, the upper case and the uppermost case, respectively.

The results of transient model indicate that the predictions of water table drawdown made with the use of a steady-state model are conservative. According to the information ERM has at the moment of writing this report, the mine operations are planned to be carried out for 25 years. Inspection of Figure 6.1-9 (Decreasing Drawdown vs. Time) reveals that at year 25 the groundwater levels will recover 60% from the maximum drawdown. By analogy, it can be estimated that after 25 years of mine dewatering operations drawdowns will reach about 60% of the maximum drawdown predicted by the steady-state model.

Another layer of conservatism stems from the assumption that the mine dewatering will be carried out from the entire planned mine area right from the start. In reality, the mine will be opened in the Bulk Sample area, then, the mining operations will progressively move through the areas of Blocks 1, 2, 3 and 4. Thus, the cone of depression will grow considerably slower, compared to that developing in response to dewatering form the entire mine area right from the start.

It can be argued that the conservative manner in which the model was set to calculate drawdowns represents a counterbalance to many uncertainties associated with the model set-up.

Figure 6.1-9

Decreasing Drawdown vs. Time – Base and Upper Case Scenarios

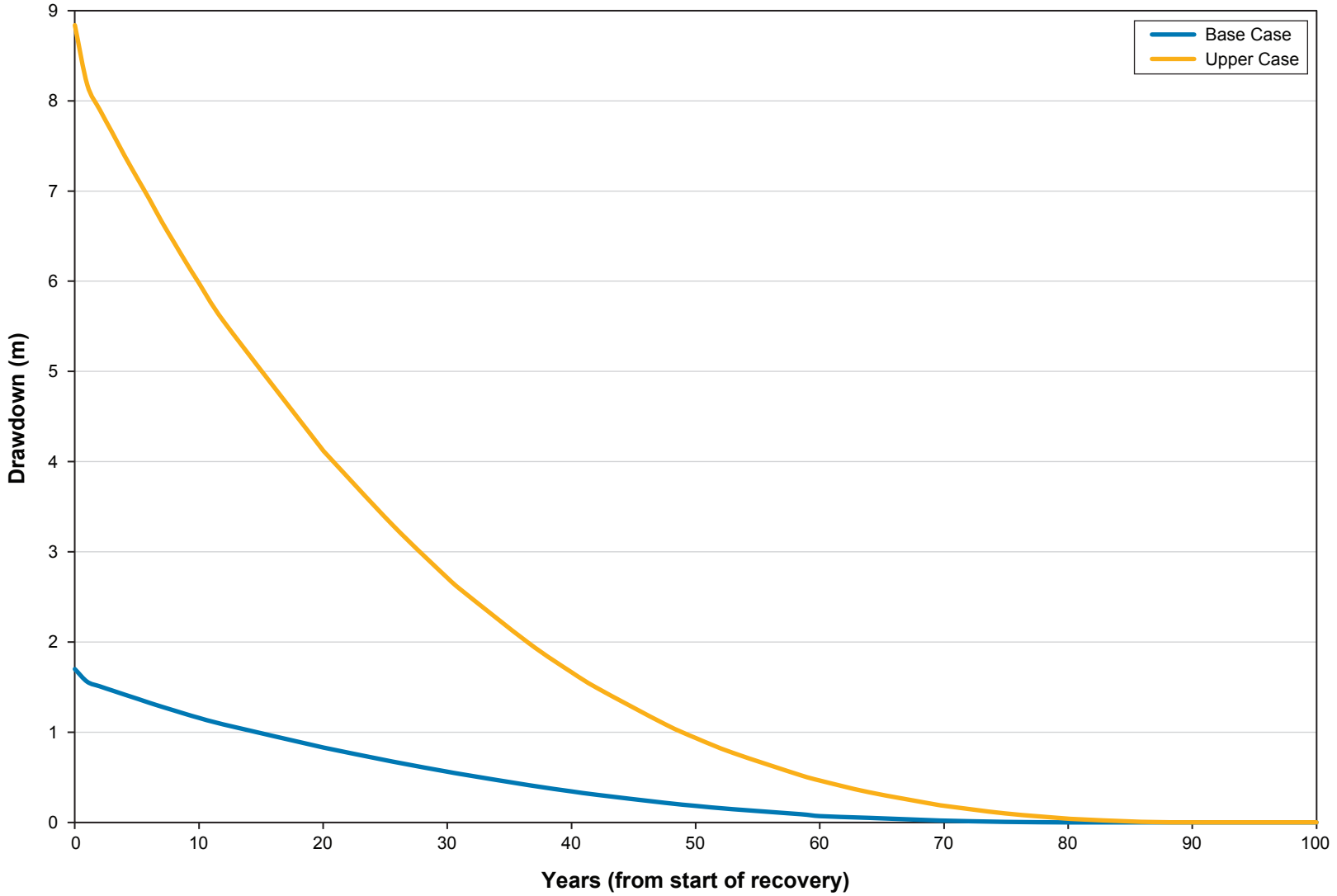

6.1.5 Predictions of Mine-contact Groundwater Travel Time to Murray River after Closure

At a certain point of post-mining groundwater level recovery, hydraulic gradients will reverse - from pointing toward the mine to pointing toward the regional discharge areas along the rivers. At that point, groundwater which comes into contact with the post-mine cavities (contact groundwater) will start migrating toward- and, ultimately, discharging into the rivers.

Two model scenarios were developed for MODPATH program simulations to **help** estimate groundwater travel time from the post-mine voids to the rivers. Both scenarios assume steady-state, pre-mining groundwater levels. Hydraulic conductivities set for those simulations correspond to those set in the mine-dewatering-simulations for the base case- and uppermost case scenarios (discussed in Sections 6.1.3.1 and 6.1.3.5).

Those simulations show that most of the contact water will be discharging to Murray River along its reach closest to the mine. The travel time of contact water varies depending on the distance from the **r**iver and the model scenario. As expected, the shortest estimated travel times are for the groundwater that contacts the post-mine voids on the eastern edge of the mine block No. 1 – the area closest to the **r**iver. The calculated times are 400 and 1,000 years for the uppermost case and the base case scenarios, respectively.

Only a small portion of contact water could be possibly discharging into Wolverine River - water contacting the northwestern parts of the mine blocks No. 3 and 4. The model calculated travel times for the pathlines ending in that River are measured in **tens** of thousands of years.

Calculation of a minimum time between the mine closure and the moment when any contact water discharges to the Murray River also has to account for the time of mine flooding and the time of the cone of depression recovery. The calculated minimum times are about 460 years and 1,200 years (for the model scenarios using hydraulic conductivities set in the uppermost and base case scenarios, respectively).

Some small portion of the contact water will travel along the abandoned **declines**. **G**roundwater is expected to migrate somewhat faster **along these paths**. **However, it is not possible** to estimate the travel time for that water without detailed analysis that would have to be based on several additional assumptions and very limited data**.**

6.2 SIMULATIONS OF SOLUTE TRANSPORT FROM CCR NORTH AND SOUTH PILES

6.2.1 Selection of Modelling Programs

Three different programs were used to simulate groundwater flow and solute transport around the CCR Site: MODFLOW 2000, MODPATH and MT3DMS.

Groundwater flow was simulated using the U.S. Geological Survey MODFLOW 2000 program (Mehl and Hill 2001). PCG Solver was used to obtain the solution with the following configuration of the engine parameters:

- Head change criterion = 0.01 m; and
- Residual criterion = 0.01 m

The latest U.S. Geological Survey version of MODPATH program (Pollack, 1994), was used to simulate groundwater flow particle-tracking "pathlines" migrating from the proposed North and South CCR Piles.

MT3DMS v. 5.2 program was selected for simulating solute transport from the North and South Piles at CCR Site to the neighboring surface waters, where the potentially impacted groundwater (by operations of CCR piles) will be discharging. The implicit Generalized Conjugate Gradient (GCG) solver with the upstream weighting finite difference solution method within the MT3DMS package was used to solve the solute transport in groundwater (Zheng and Wang 1999). The parameters for the transport solver were set as follows:

- relative convergence criterion of concentration: 0.0001 mg/L
- initial timestep size: 0.1
- maximum timestep size: 90 days
- timestep multiplier: 1.1

6.2.2 Boundary Conditions

All the model flow boundary conditions were set identical to those in the baseline model (discussed in Section 4), except for adding:

- two recharge zones covering the footprints of the CCR North and South Piles; and
- surface water drains on south and west sides of the CCR North and South Piles.

The CCR Site was designed to accommodate two mine coal reject storage areas, North Pile and South Pile,that will be used to store the rejects. It is estimated that for most of the CCR Site operations only the North Pile will be receiving the rejects, while the South Pile would be receiving rejects toward the end of the mine operations. Both the North and South CCR Piles were designed to be constructed with the use of very low permeability geomembrane liners.

Recharge values applied to the North and South CCR Pilezones were calculated conservatively assuming that 5% of the area of geomembrane liners (that will be placed at the bottom of each pile) will fail. Thus, approximately 5% of the water infiltrating into the pile material will escape through its bottom. This calculation conservatively assumes that the drains to be placed above the liner will not intercept any of the escaping water (leachate).

The values of the rates of water infiltration into the pile material were provided by Ausenco (per Ausenco presentation to ERM - March 8, 2014). Ausenco, the designer of the CCR Piles, developed a flux model for the CCR Site using SEEP/W model. Recharge values calculated based on infiltration and 5% liner failure are 6 mm/year for the North Pile and 7 mm/year for the South Pile in the Base Case.

A recharge concentration equal to 1 (one) was set for the recharge zones assigned to the CCR Piles. This kind of a setup results in the model calculating a fraction of a concentration of leachate originating at the pile reaching any given point down-gradient from the pile, at a given time.

6.2.3 Simulation Period, Initial Conditions and Time Stepping

Initial heads set in the MODFLOW predictive model (ran prior to MT3DMS simulation) were calculated by a baseline flow model.

MT3DMS transport model simulation time was set to 200 years, with requested model outputs for days: 30, 90, 180, 365, 1,825 (5 years), 3,650 (10 years), 10,950 (30 years), 18,250 (50 years), 36,500 (100 years) and 73,000 (200 years).

6.2.4 Sensitivity and Uncertainty Analysis

Four scenarios of the model were set up and ran for the CCR site operation and post-closure to evaluate how uncertainty associated with hydraulic conductivity and climate change may influence predictions of the transport model (see Table 6.2-1):

- Base case scenario was set using baseline model adjusted as discussed in Section 6.2.2.
- Wetter climate scenario was set by increasing recharge applied to all recharge zones except CCR Zones, by 25%, compared to the baseline model. Recharge to water table from below the North and South Piles were increased per Ausenco's model results (Ausenco presentation to ERM - March 8th, 2014) to: 17 and 20 mm/year for the North and South Piles, respectively. Such setup assumes that 1-in-100 years wet year conditions would prevail for a period of 200 years.
- Higher permeability scenario was set by increasing hydraulic conductivity values of zones 3, 8 and 17 (the most sensitive parameters with regard to calibration of baseline model using targets located within the CCR area) by a factor of 3.
- Lower permeability scenario was set by decreasing hydraulic conductivity values of zones 3, 8 and 17 by a factor of 3.

Table 6.2-1. List of the Murray River Groundwater Model Scenarios for CCR Site Solute Transport Simulations

Model File Name	Description of the Scenario	Recharge Rate (mm/year)	
		North Pile	South Pile
CCR Facility Operation			
Base Case	Base case model for simulating solute transport from CCR Piles	6	7
Wetter Climate Scenario	Model developed from base case model to simulate wet climate scenario	17	20
Higher Permeability Scenario	Model developed from base case model to simulate high hydraulic conductivity scenario	6	7
Lower Permeability Scenario	Model developed from base case model to simulate low hydraulic conductivity scenario	6	7

(continued)

Table 6.2-1. List of the Murray River Groundwater Model Scenarios for CCR Site Solute Transport Simulations (completed)

Model File Name	Description of the Scenario	Recharge Rate (mm/year)	
		North Pile	South Pile
CCR Facility Post-closure			
Base Case	Model developed from base case model to simulate CCR Site post-colsure conditions	0.01	0.01
Wetter Climate Scenario	Model developed from base case model to simulate CCR Site post-colsure conditions under wet climate scenario	0.03	0.03
Higher Permeability Scenario	Model developed from base case model to simulate CCR Site post-colsure conditions under high hydraulic conductivity scenario	0.01	0.01
Lower Permeability Scenario	Model developed from base case model to simulate CCR Site post-colsure conditions under low hydraulic conductivity scenario	0.01	0.01

6.2.5 Contaminants of Concern (CoC)

Contaminants of concern were identified via geochemical modelling of the CCR piles. The model was used to simulate transport of a generic contaminant species leaving the CCR piles as solutes at an arbitrarily set unit concentration equal to 1. The model calculated what fraction of the source concentration would reach any of the seventeen monitoring points set in the model down-gradient from the pile and any given time. Given a concentration of an identified contaminant of concern at the source (CCR pile), this fraction is used to calculate contaminant (solute) concentration at a given down-gradient point at a given time for water quality modelling.

6.2.6 Sources and Sinks of CoC

CCR North and South Piles are the only sources of contaminants migrating through the groundwater system simulated in this model. The groundwater quality sampling data collected up to May 2014 shows no evidence that the Tech's Quintette Pile located up-gradient of the CCR Site was the source of any significant groundwater contamination.

6.2.7 Applicable Transport Processes

The complex geochemical and biogeochemical processes such as biodegradation or adsorption/absorption to the geological materials (resulting in retardation of transport) were not simulated. Thus, two conservative assumptions were made for solute transport simulations:

- Solutes do not degrade while migrating from the source (CCR piles) to receptor points; and
- Solute movement is not retarded.

These assumptions likely result in an over-prediction of solute concentrations reaching receiving surface waters (for organic substances) and over-estimating contaminant mass fluxes. If transport of solutes is retarded compared to groundwater flow, solute mass is discharging to surface waters at

slower rates, compared to non-retarded solutes. This is particularly the case for metals as transport of metals is strongly retarded, especially in an environment with negatively charged clay minerals, as observed beneath the CCR Site.

The only solute transport processes simulated by the model were advection, mixing with up-gradient, non-contaminated groundwater and dispersion. Both advection and dispersion were simulated for solute transport using effective porosity.

As no site-specific, field test data is available, dispersivity was set in the model to a value of 10 m by referring to the literature (Gelhar et al. 1992; Li 1995; Shapiro 2001; Schulze-Makuch 2005; Zhou et al. 2007; Niemann and Rovey 2009). Dispersivity is a scale-dependent parameter used to characterize the dispersive solute transport in porous and fractured bedrock media. Laboratory and field experiments found that dispersivity generally increases with scale and with increasing heterogeneity of the transport medium. According to Gelhar et al. (1992) and Schulze-Makuch (2005), the reliable field measured dispersivity values range from 0.01 m to 100 m for transport over a distance of up to 100 m within both unconsolidated and consolidated geological materials.

6.2.8 Predictions of the Effects of CCR Facility Operation

Figure 6.2-1 presents the Base Case model simulated contaminant plumes originating from the CCR Piles at year 30, under the assumption that both the Piles are full and occupy the entire areas of the footprints. This is considered to be very conservative. After 30 years of operations, the CCR Piles will be closed, capped and the contaminant plumes originating from the piles will start dissipating. The extent of the plumes is defined with a concentration contour interval of 10% of the concentration of the source (the CCR Piles) and a cut-off contour line of 1% of the concentration at the source (the CCR Piles). As the figure demonstrates, the model calculated 30-year plume will not reach Murray River and will be discharging into M19A and M19 Creeks. The plumes' extents calculated by the model for different scenarios are very similar.

Figure 6.2-2 presents the Base Case model simulated pathlines of groundwater flow particle-tracking from the CCR Piles to the receiving creeks, while Figure 6.2-3 presents a network of wells that are proposed to be installed to monitor groundwater contamination originating at the CCR Piles. Several of those monitoring points were set along the M19 and M19A creeks and Murray River.

Figures 6.2-4a, b, c, d through 6.2-7a, b, c, d show graphs of solute concentrations vs. time at all seventeen monitoring points set in the Base Case model. The plotted concentration is a fraction of the concentration at the source – CCR Piles. All of those monitoring points, except OBS-1, 2, 3 and 4, were set along the M19 and M19A creeks and Murray River (see Figure 6.2-3 - Proposed Long-term Groundwater Monitoring Wells Network at the CCR Site).

Inspection of the Figures 6.2-4a, b, c and d reveals that according to the base case model scenario groundwater solute concentrations at the monitoring points will reach maximum 30 years after the start of CCR Piles' operations (assuming the piles are full) and, then, quickly decrease after the Piles capping and closure. The maximum concentration among the set monitoring points was model calculated for OBS-17 located right next to M19A Creek – 9.4% of the concentration at the source at the end of full operation of the CCR Piles. The 30-year concentrations calculated for other points are 3% or less at the end of full operation of the CCR Piles. The concentrations during the post-closure period gradually decrease.

Figure 6.2-1

Groundwater Contaminant Plumes Originating from CCR Piles at Time 30 Year – Base Case Scenario

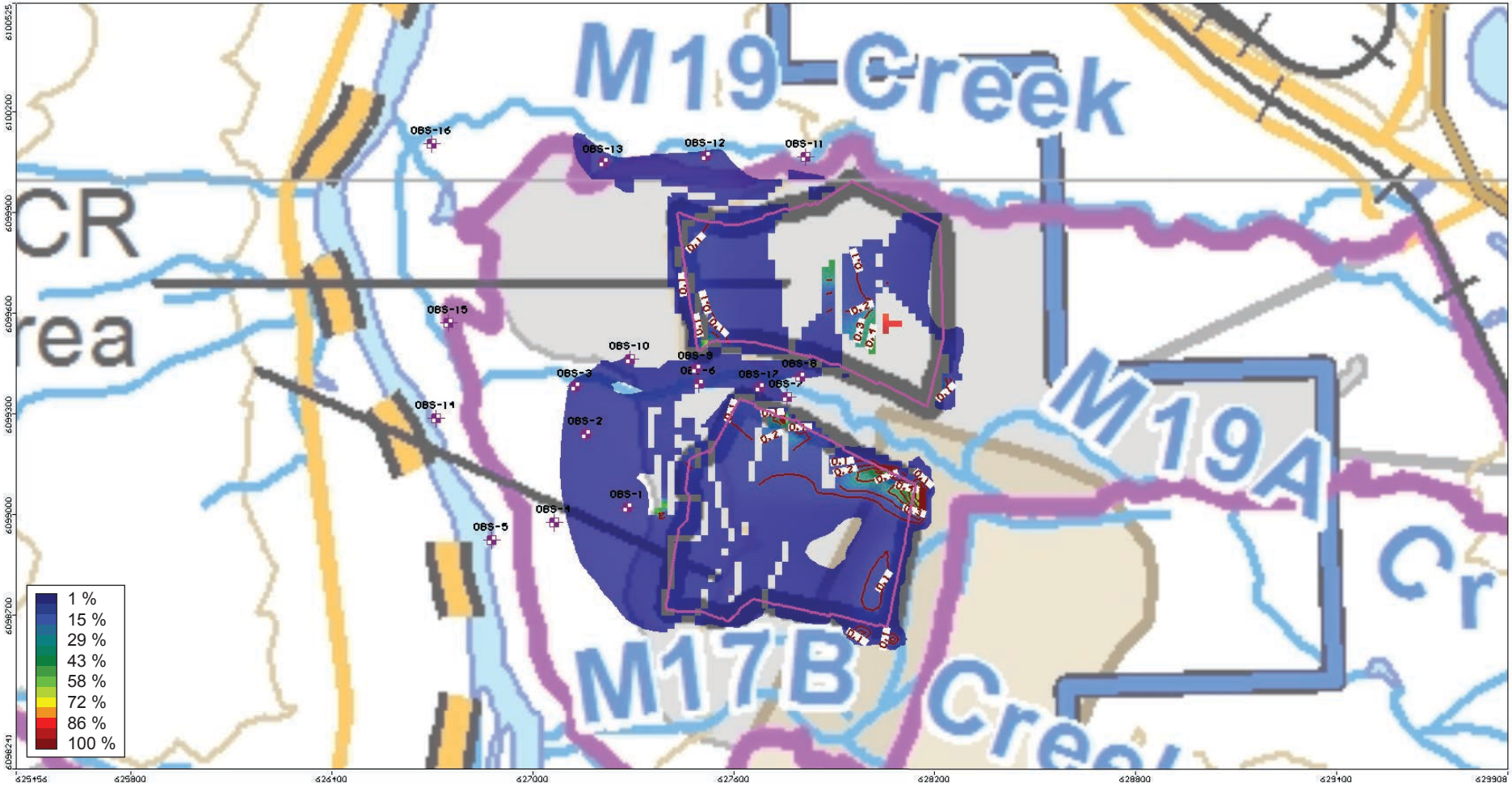

Figure 6.2-2

Groundwater Flow-paths from CCR Piles to Receiving Creeks – Base Case Scenario

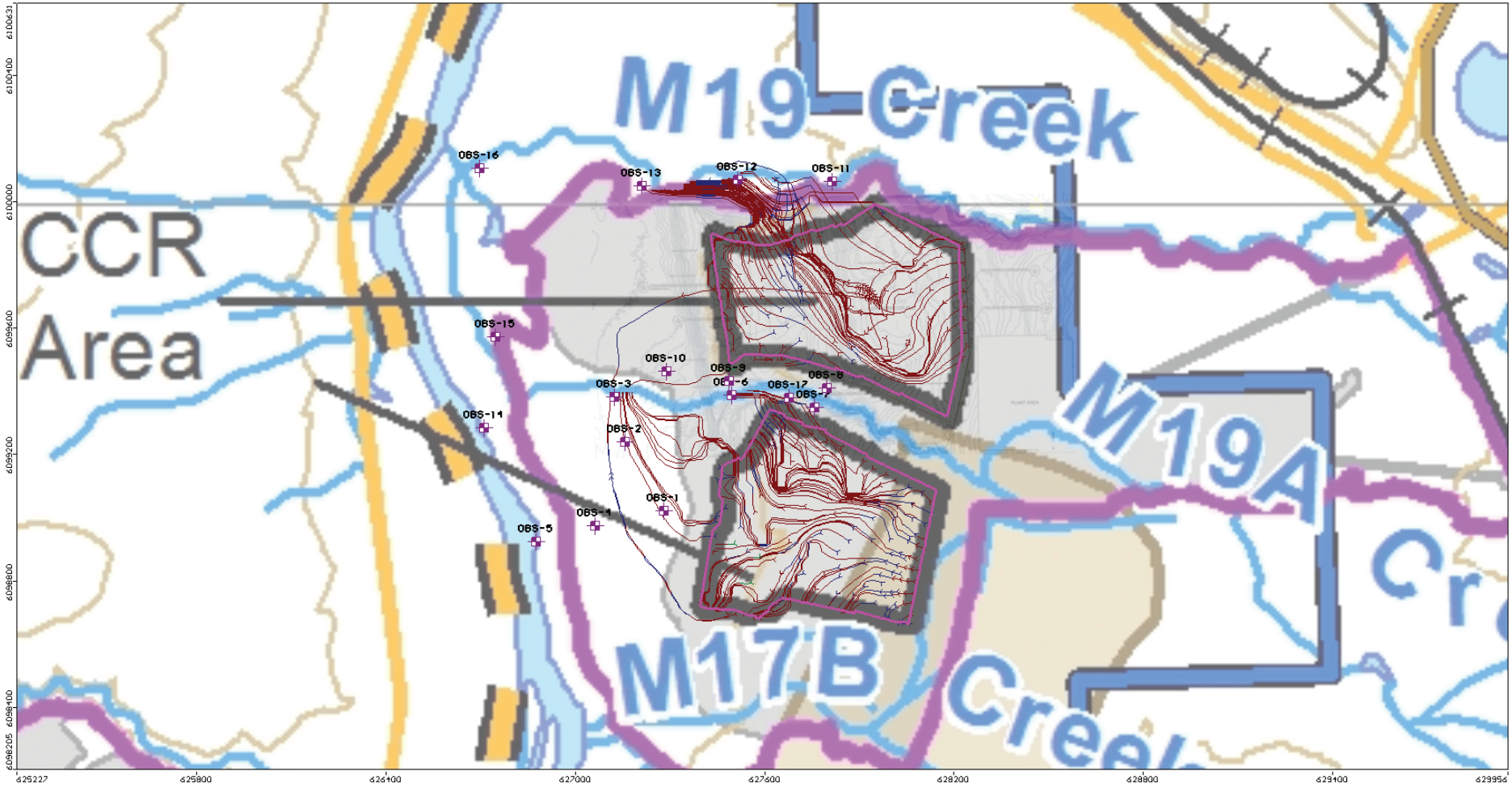

Note: Time markers on pathline every 10 years.

Figure 6.2-3

Proposed Long-term Groundwater Monitoring Wells Network at the CCR Site

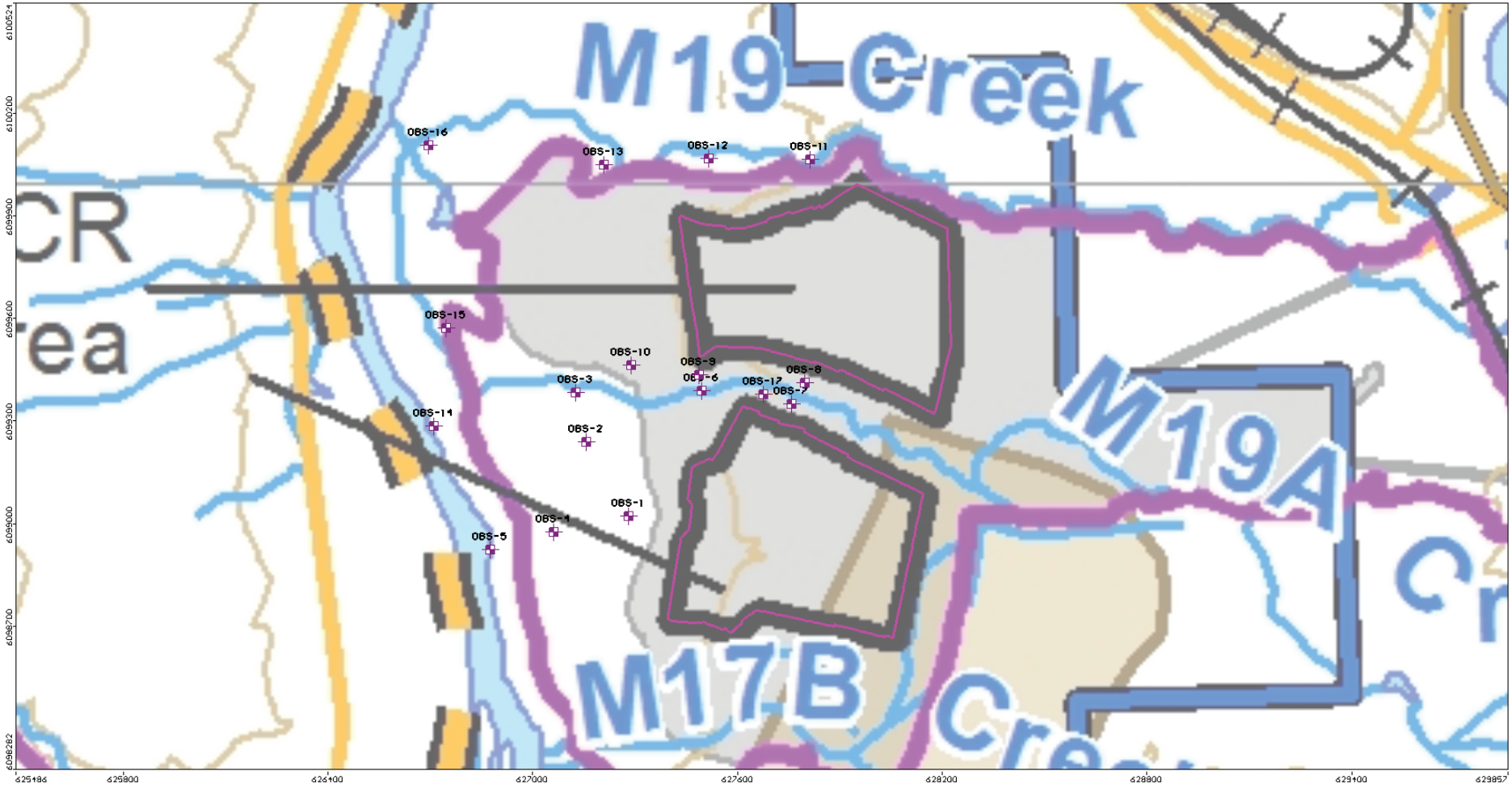

Proposed Monitoring Well

Figure 6.2-4a

Concentration vs. Time at North Pile Monitoring Points – Base Case Scenario

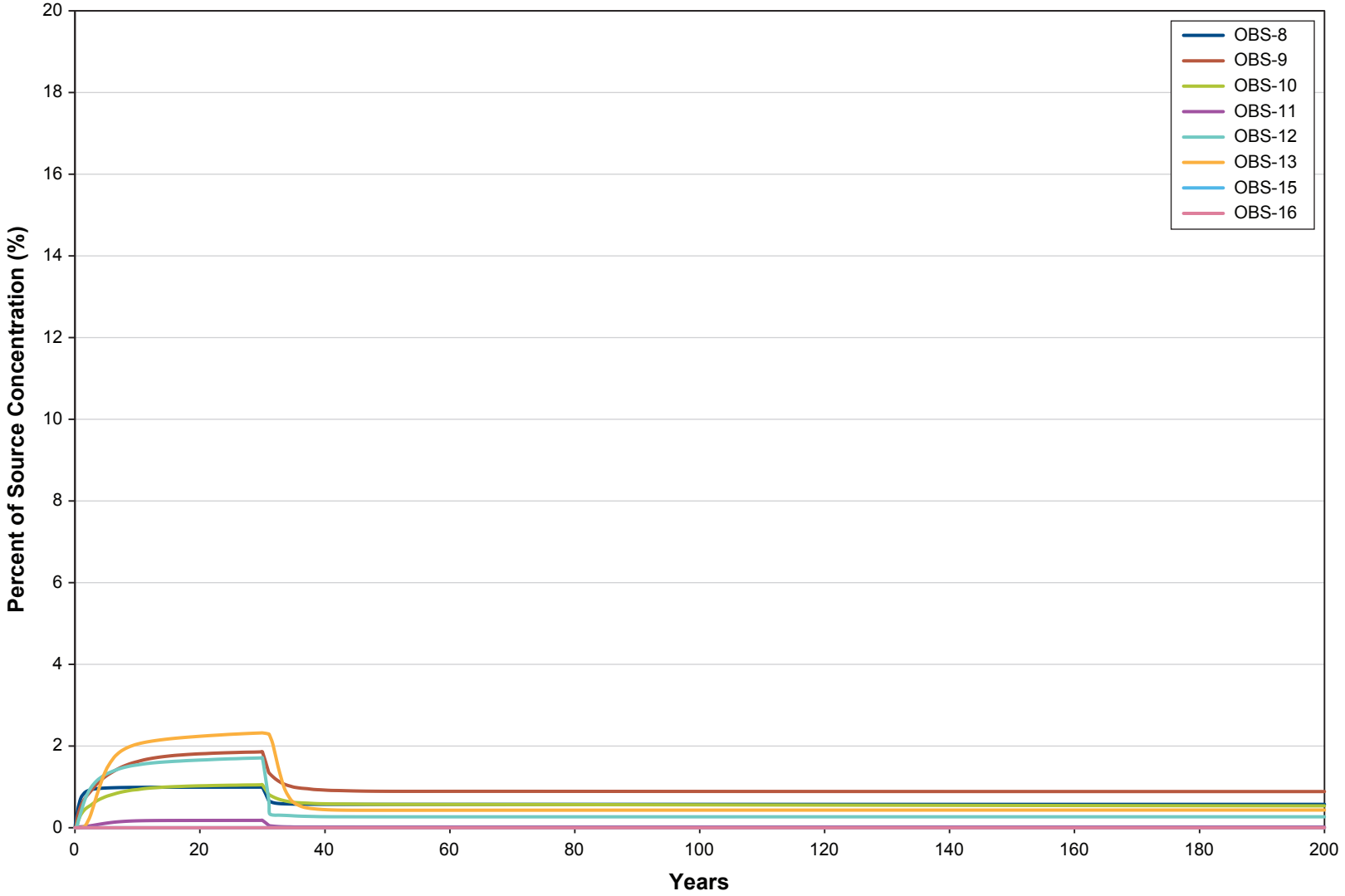

Figure 6.2-4b

Concentration vs. Time at South Pile Monitoring Points next to Creek and River – Base Case Scenario

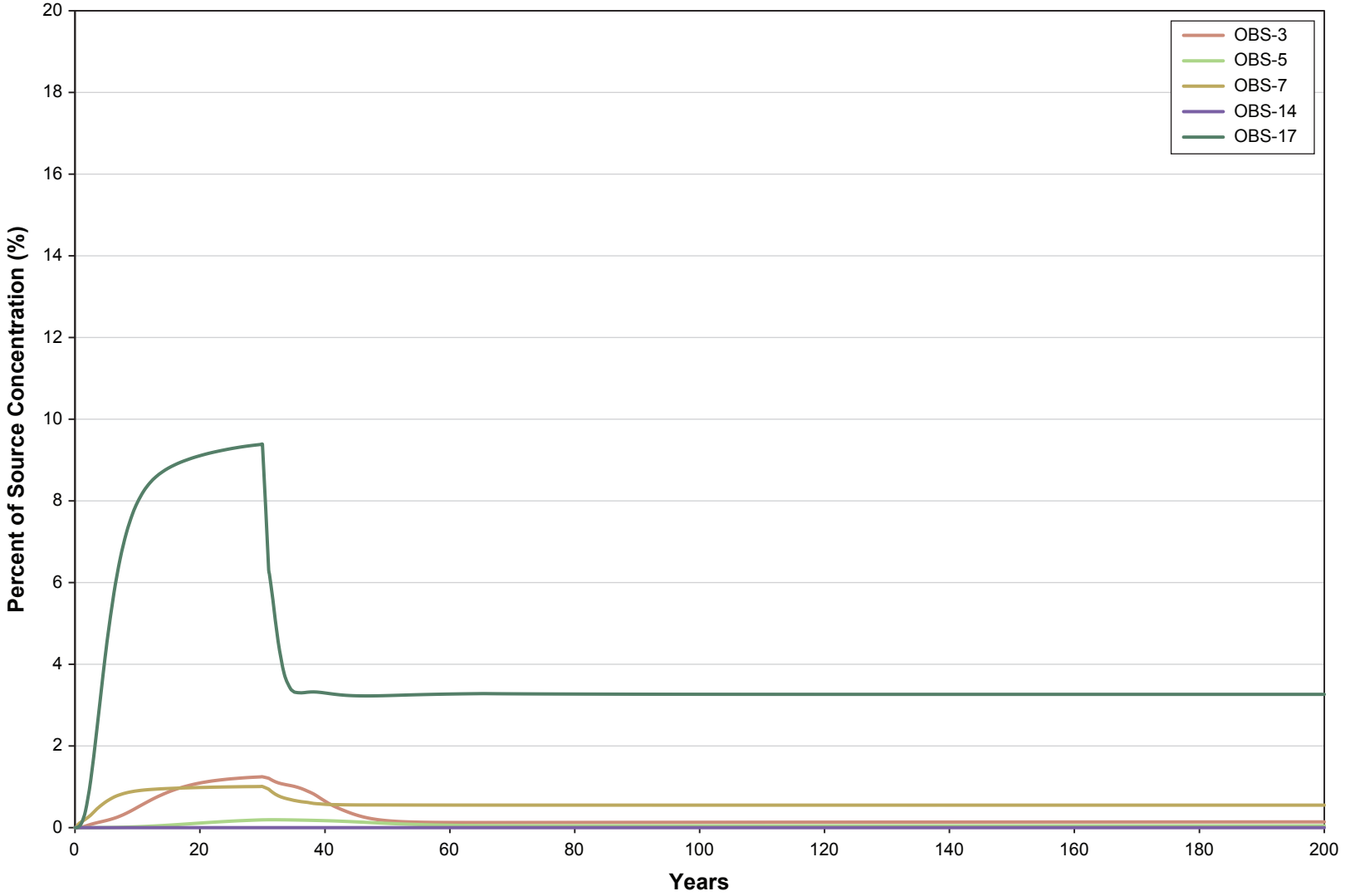

Figure 6.2-4c

Concentration vs. Time - South Pile Plume Profile No. 1 – Base Case Scenario

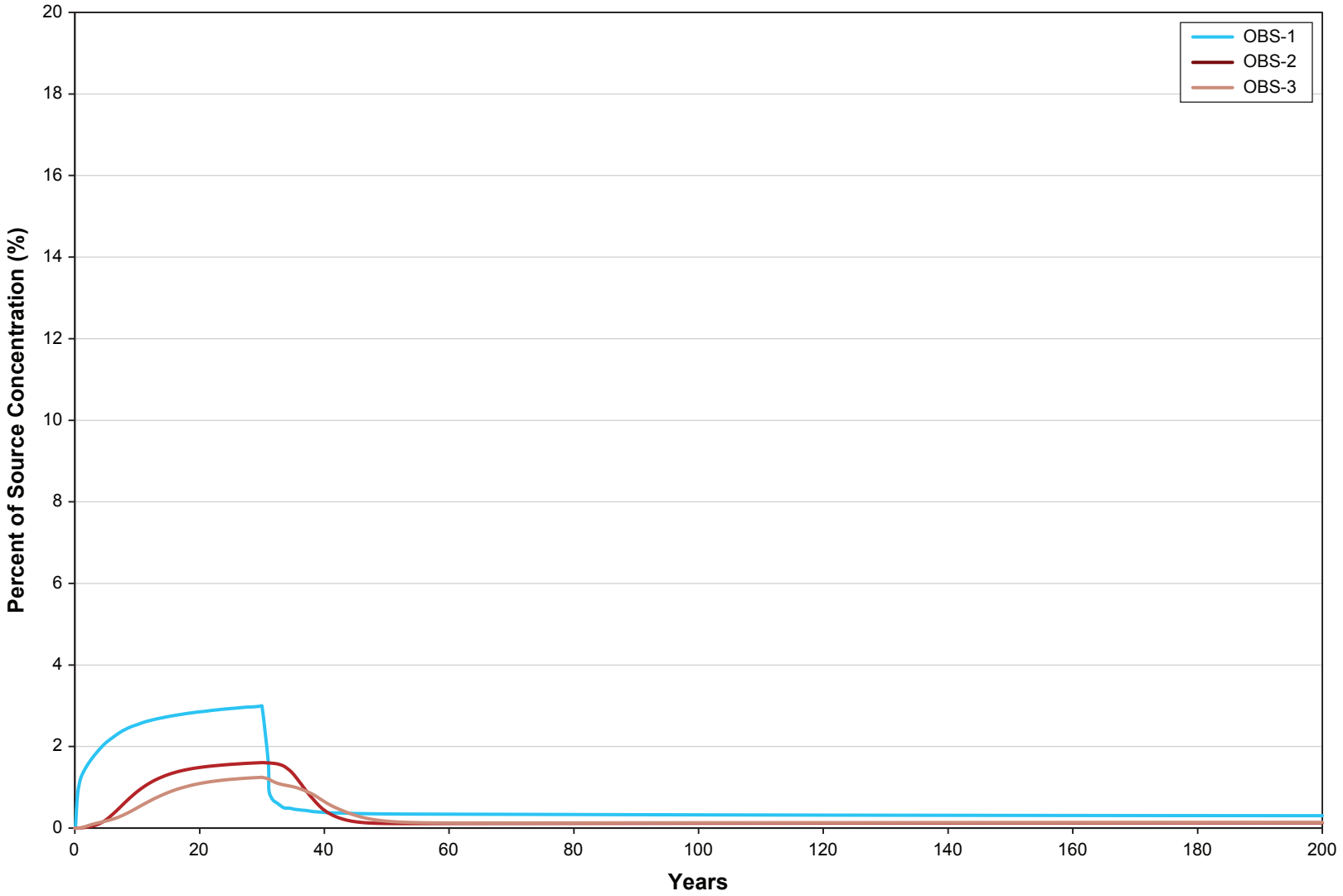

Figure 6.2-4d

Concentration vs. Time - South Pile Plume Profile No. 2 - Base Case Scenario

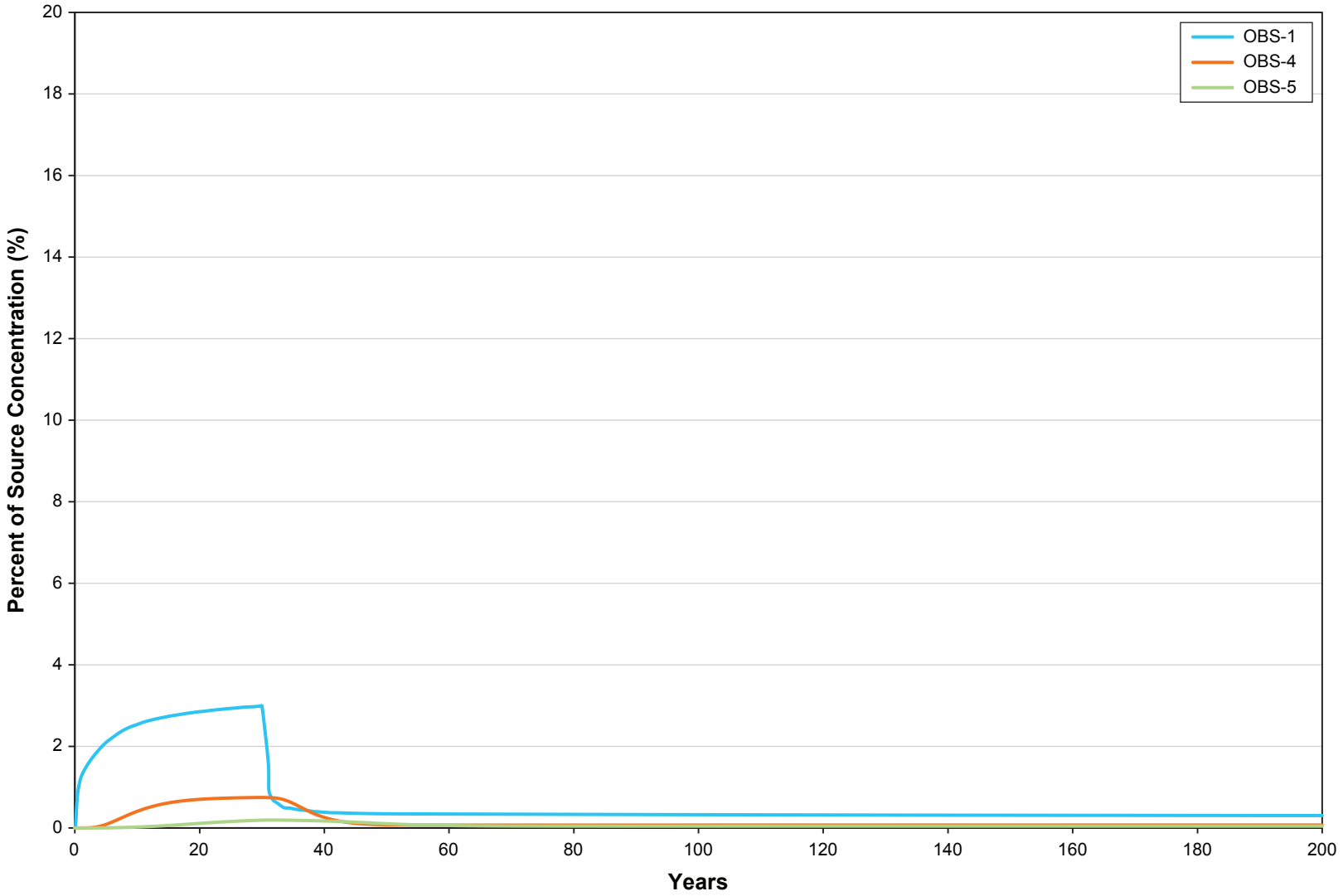

Figure 6.2-5a

Concentration vs. Time at North Pile Monitoring Points – Wetter Climate Scenario

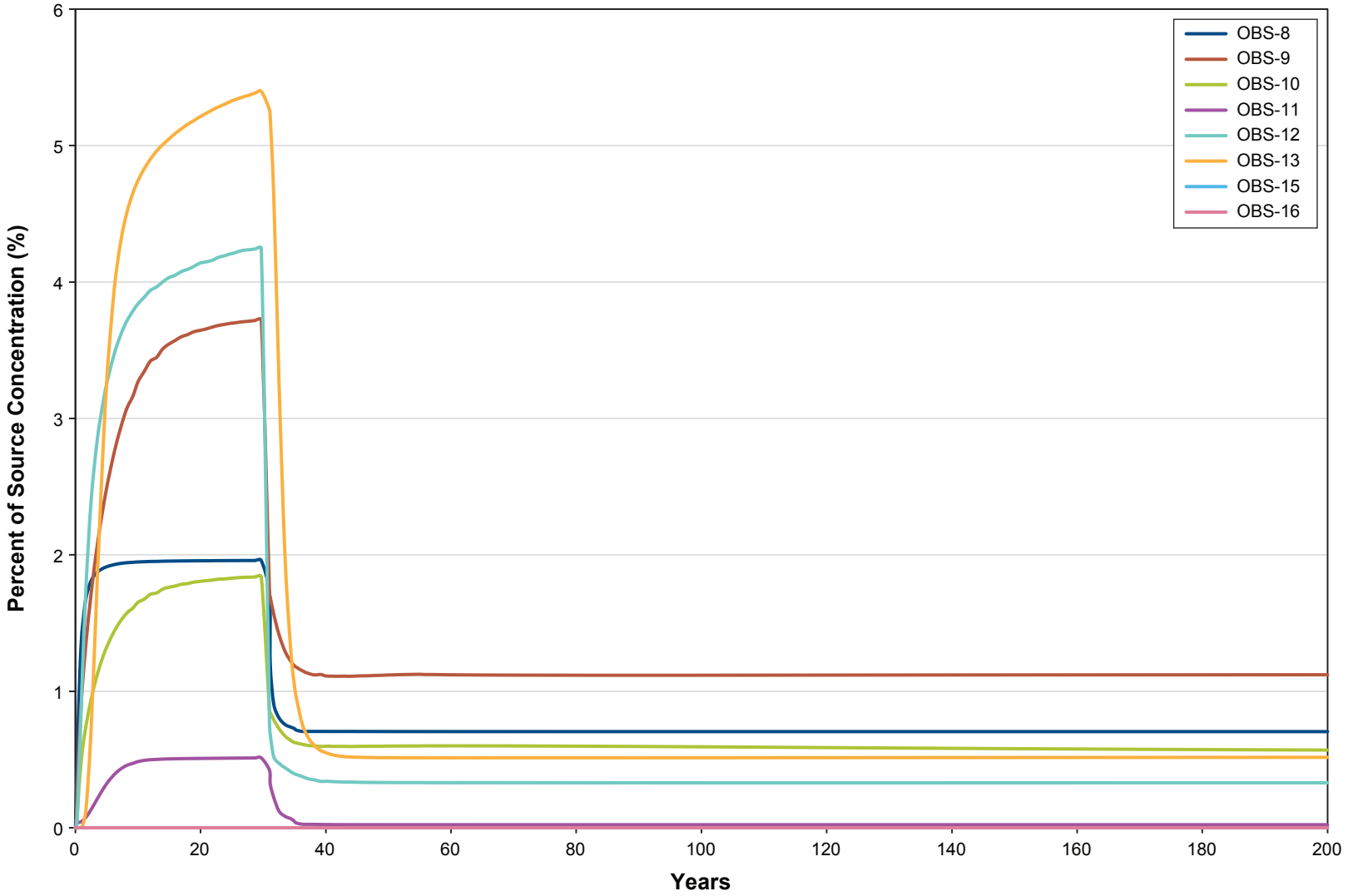

Figure 6.2-5b

Concentration vs. Time at South Pile Monitoring Points next to Creek and River – Wetter Climate Scenario

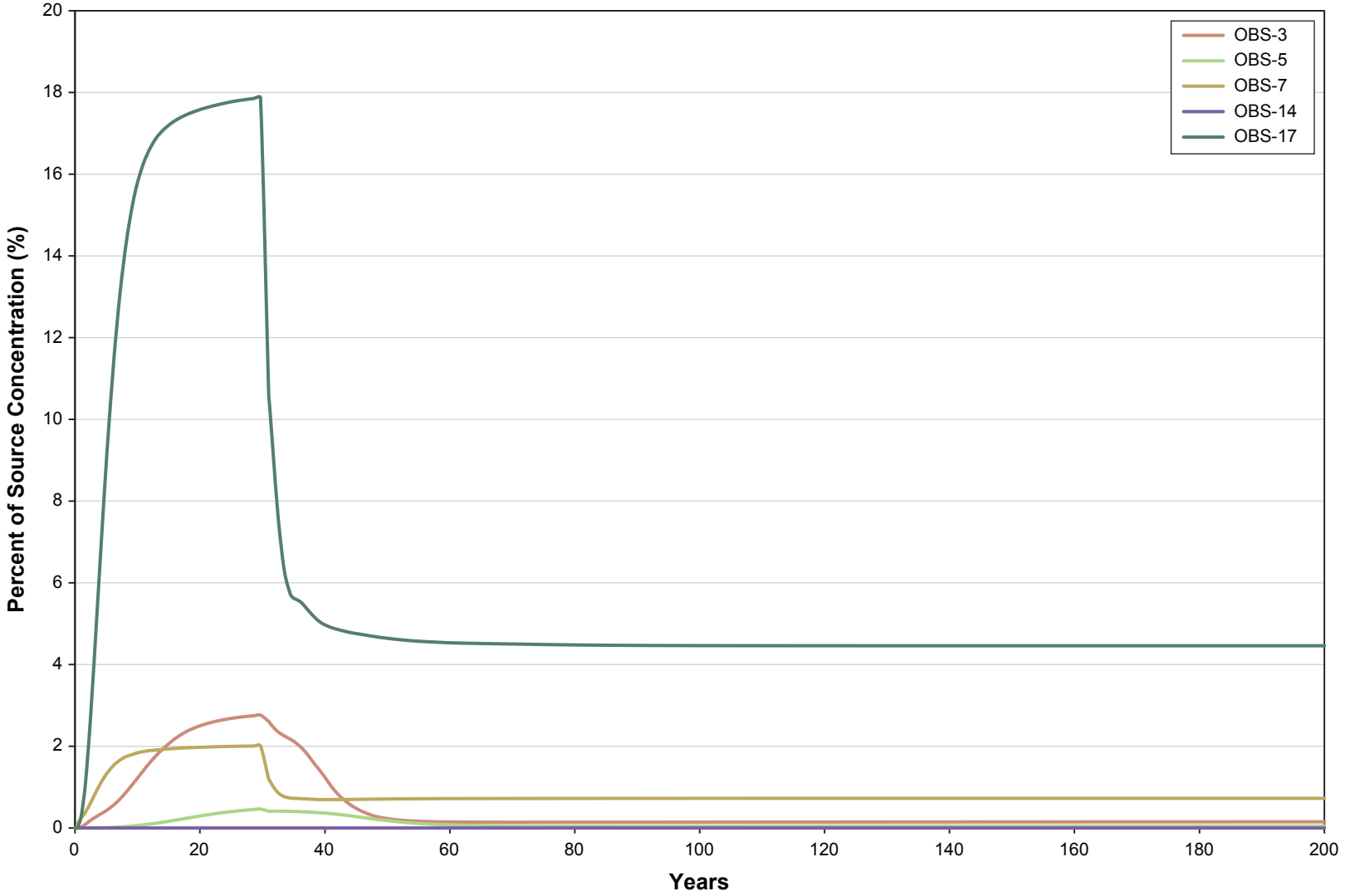

Figure 6.2-5c

Concentration vs. Time - South Pile Plume Profile No. 1 - Wetter Climate Scenario

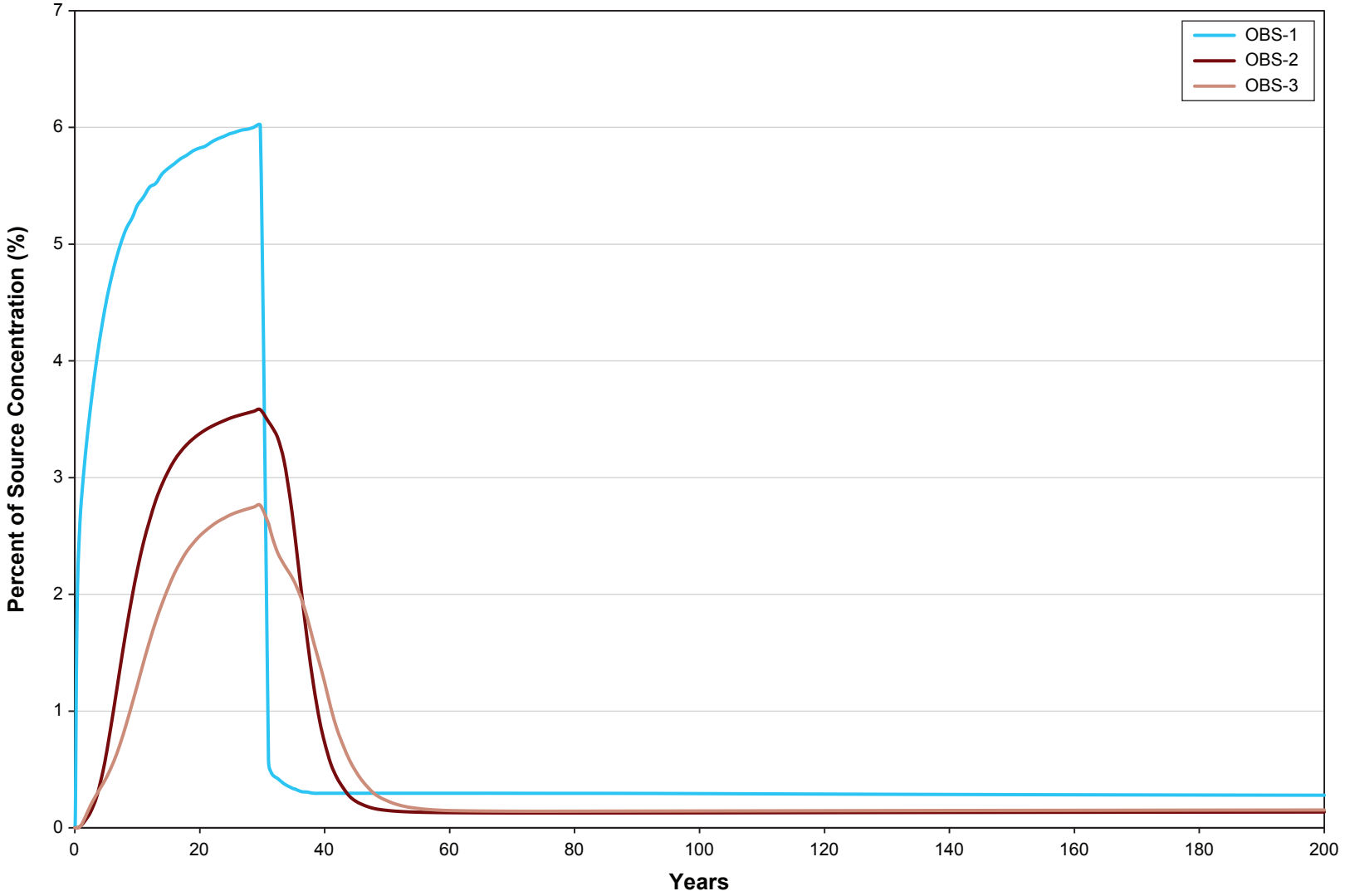

Figure 6.2-5d

Concentration vs. Time - South Pile Plume Profile No. 2 - Wetter Climate Scenario

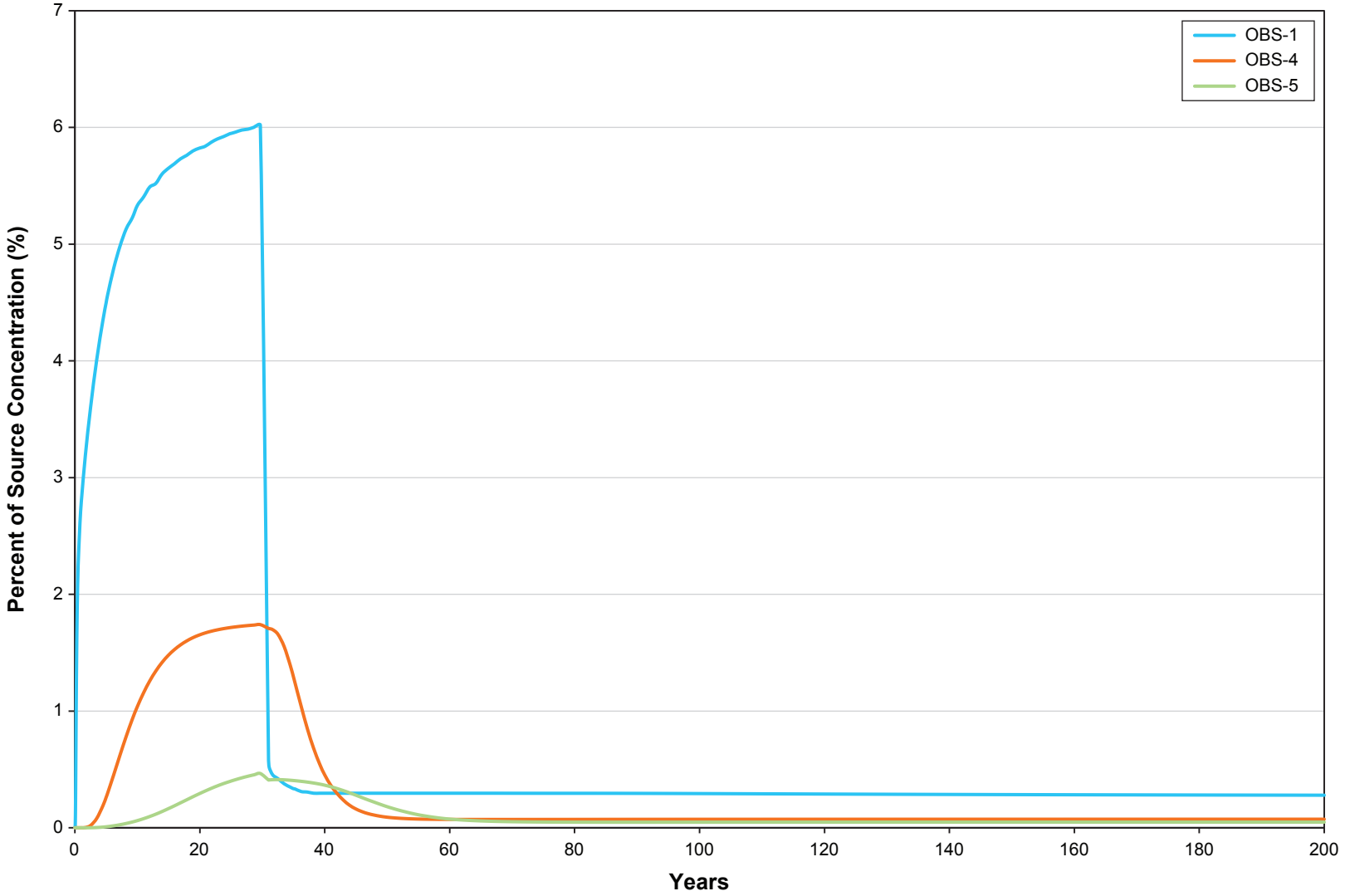

Figure 6.2-6a

Concentration vs. Time at North Pile Monitoring Points – Higher Permeability Scenario

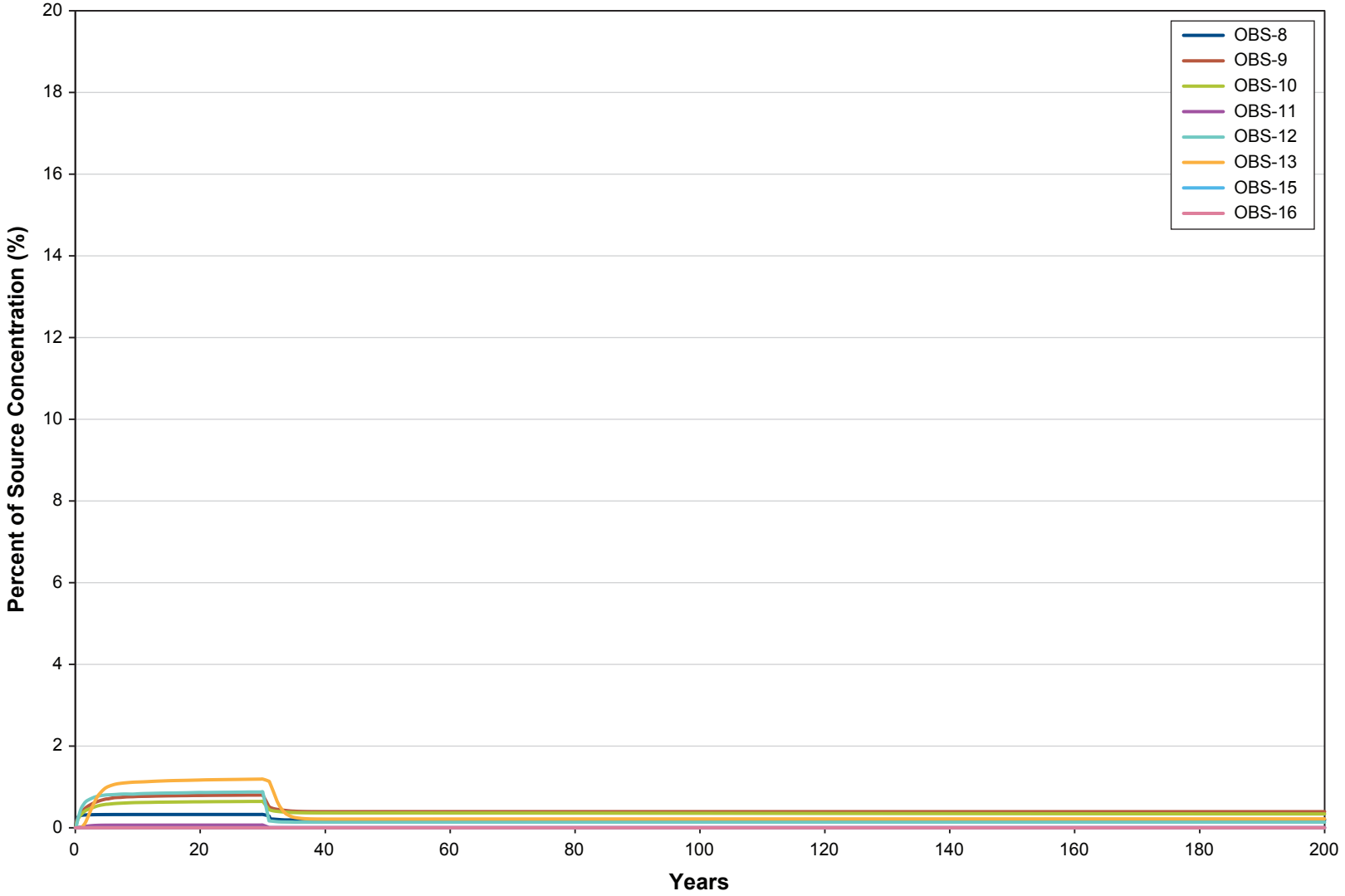

Figure 6.2-6b

Concentration vs. Time at South Pile Monitoring Points next to Creek and River – Higher Permeability Scenario

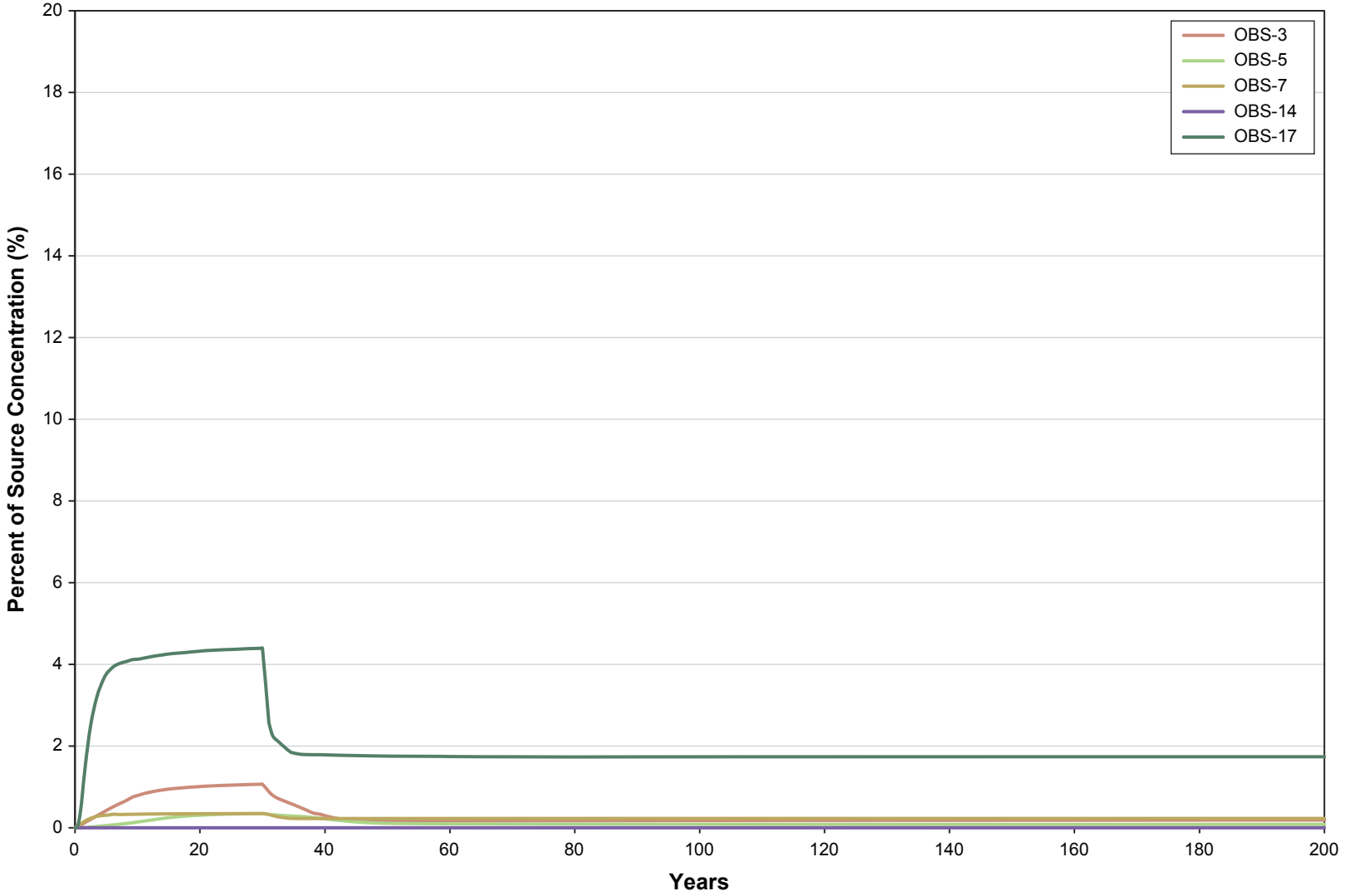

Figure 6.2-6c

Concentration vs. Time - South Pile Plume Profile No. 1 – Higher Permeability Scenario

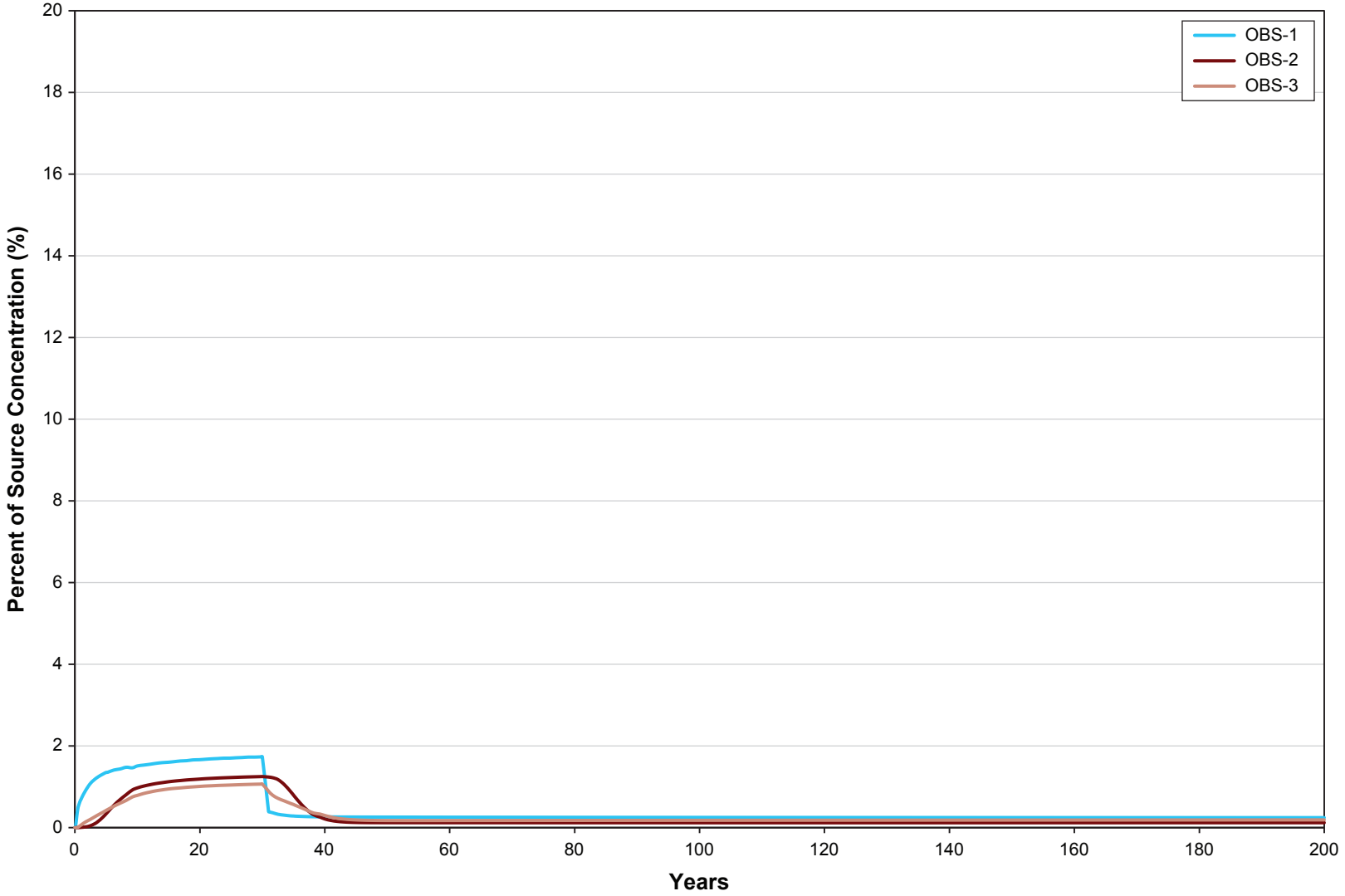

Figure 6.2-6d

Concentration vs. Time - South Pile Plume Profile No. 2 – Higher Permeability Scenario

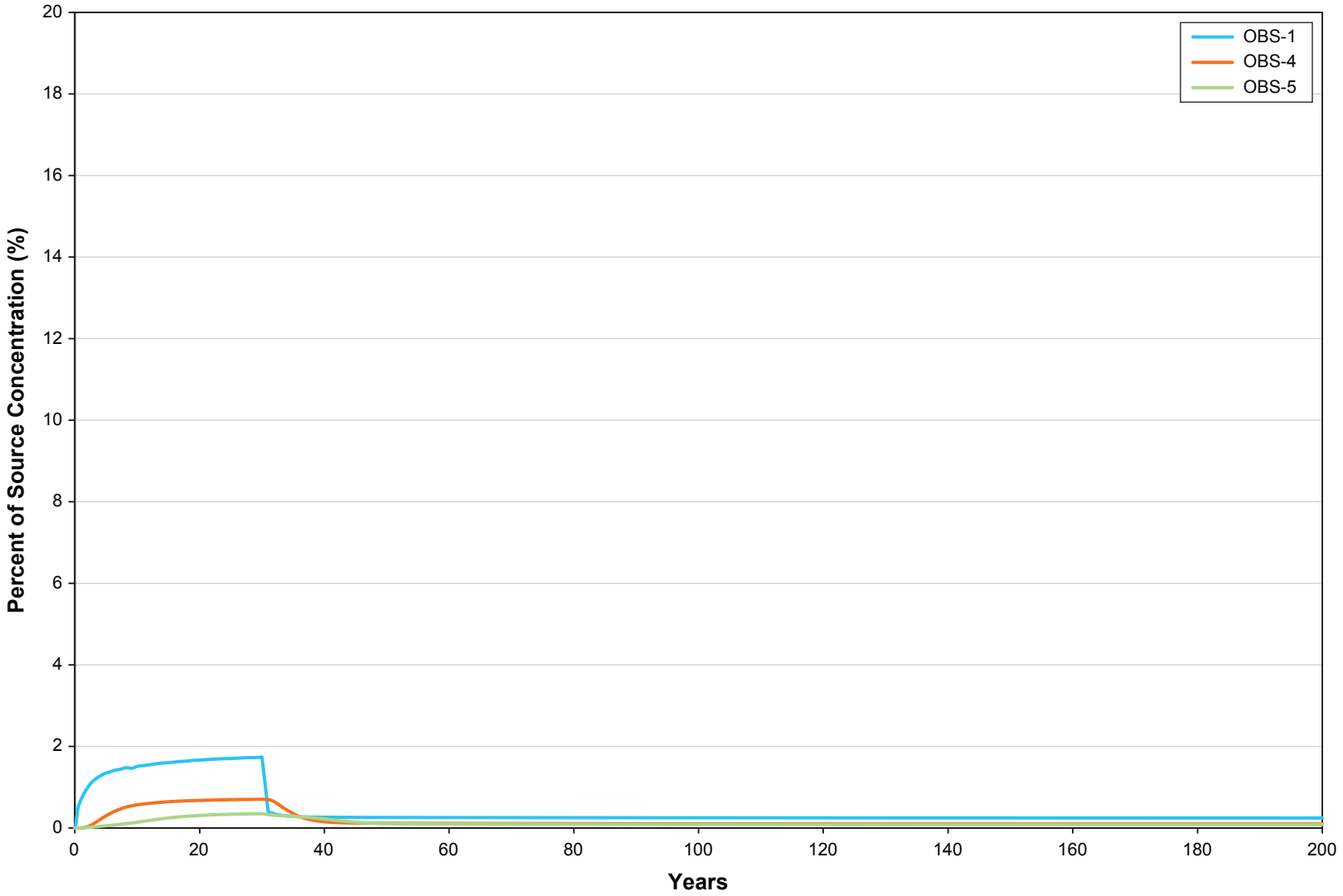

Figure 6.2-7a

Concentration vs. Time at North Pile Monitoring Points – Lower Permeability Scenario

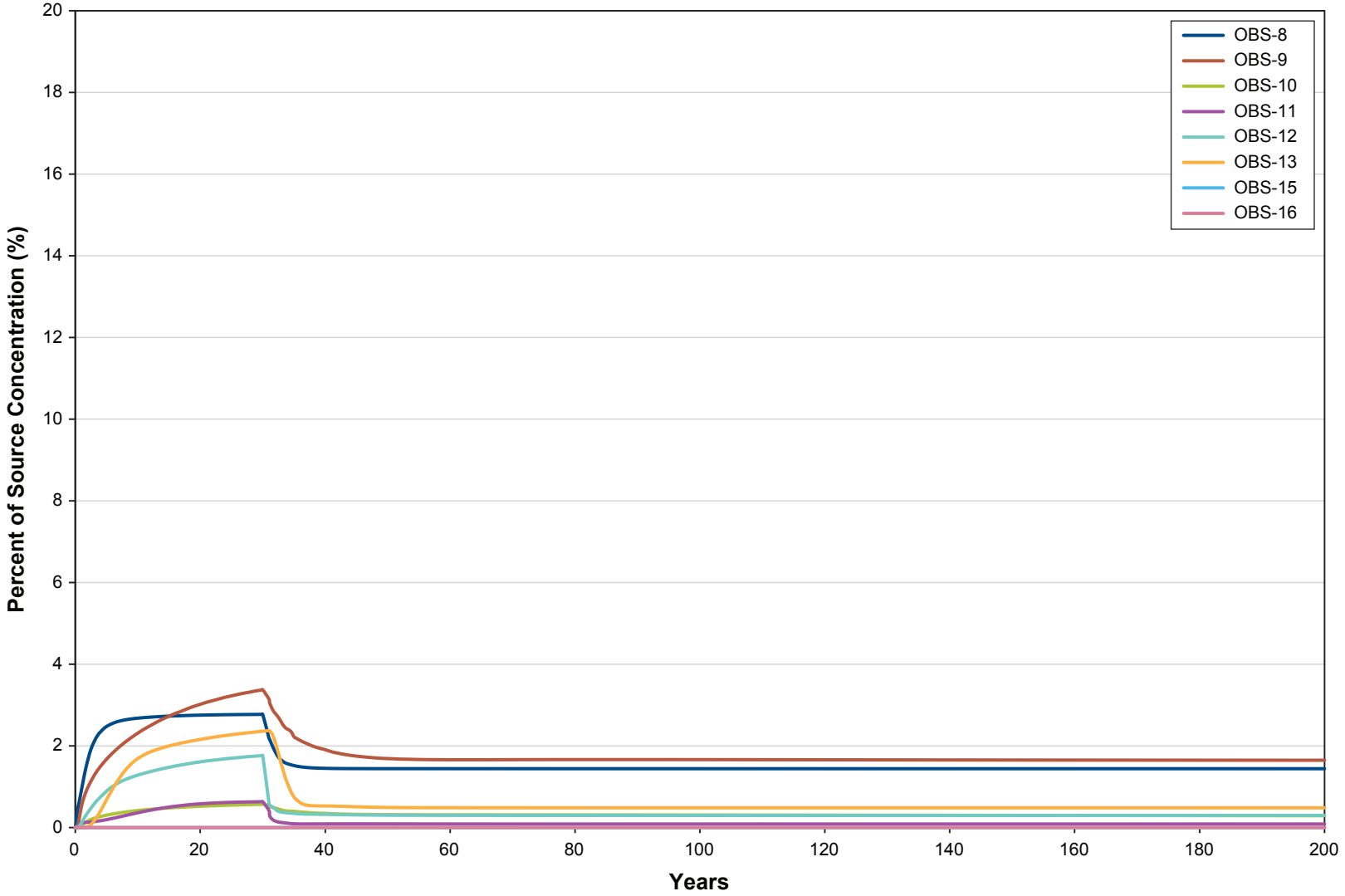

Figure 6.2-7b

Concentration vs. Time at South Pile Monitoring Points next to Creek and River – Lower Permeability Scenario

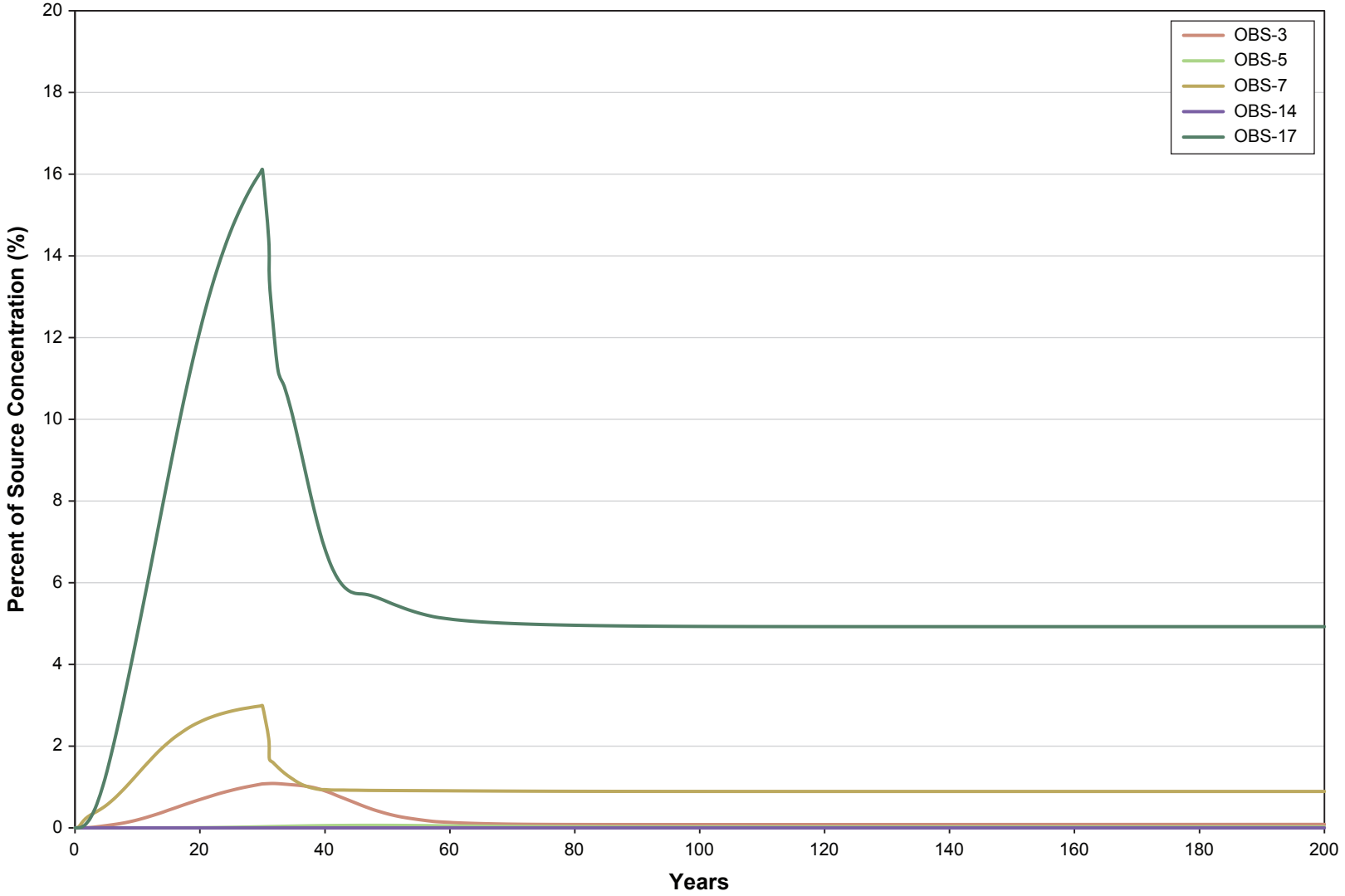

Figure 6.2-7c

Concentration vs. Time - South Pile Plume Profile No. 1 – Lower Permeability Scenario

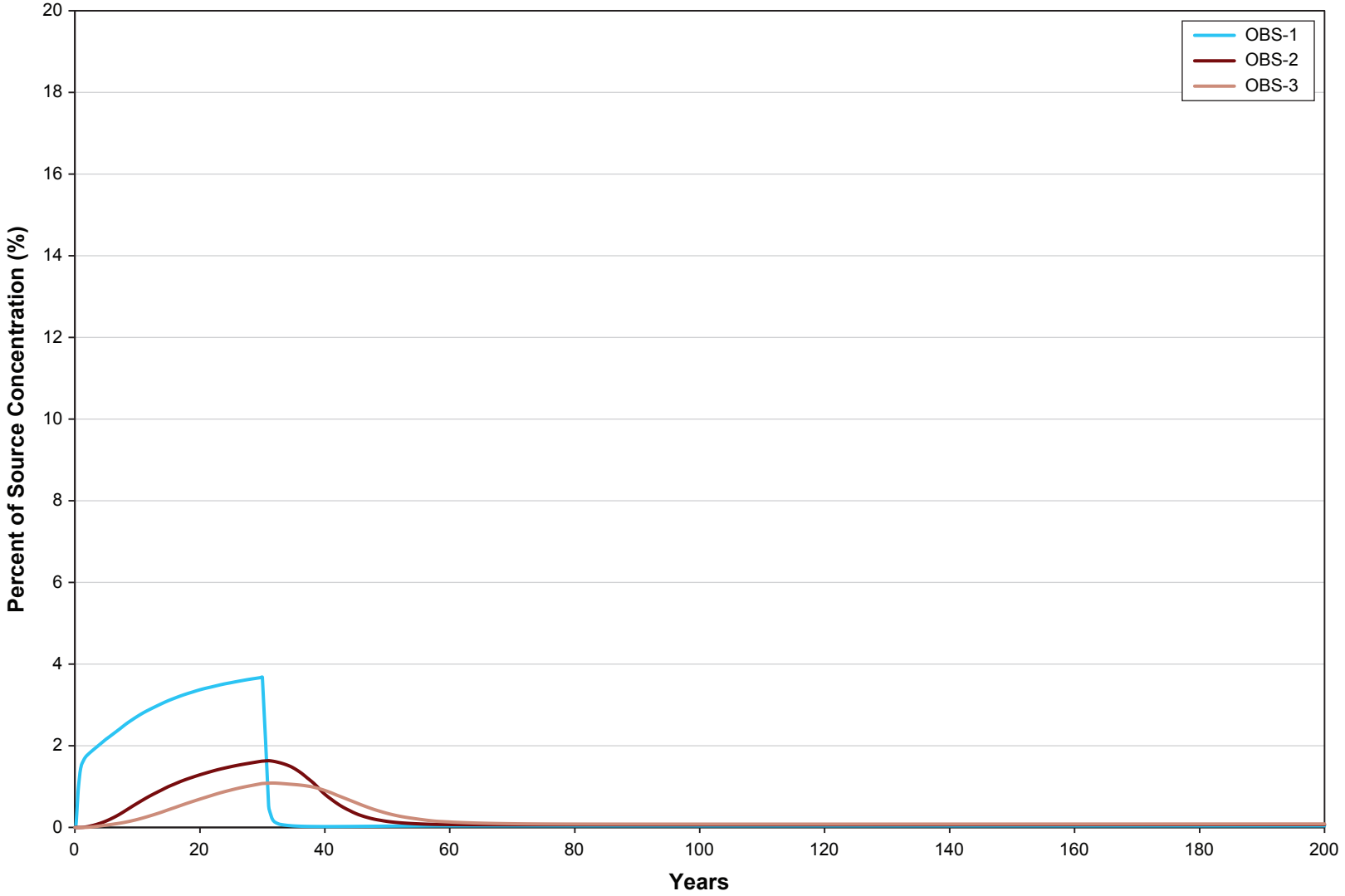

Figure 6.2-7d

Concentration vs. Time - South Pile Plume Profile No. 2 – Lower Permeability Scenario

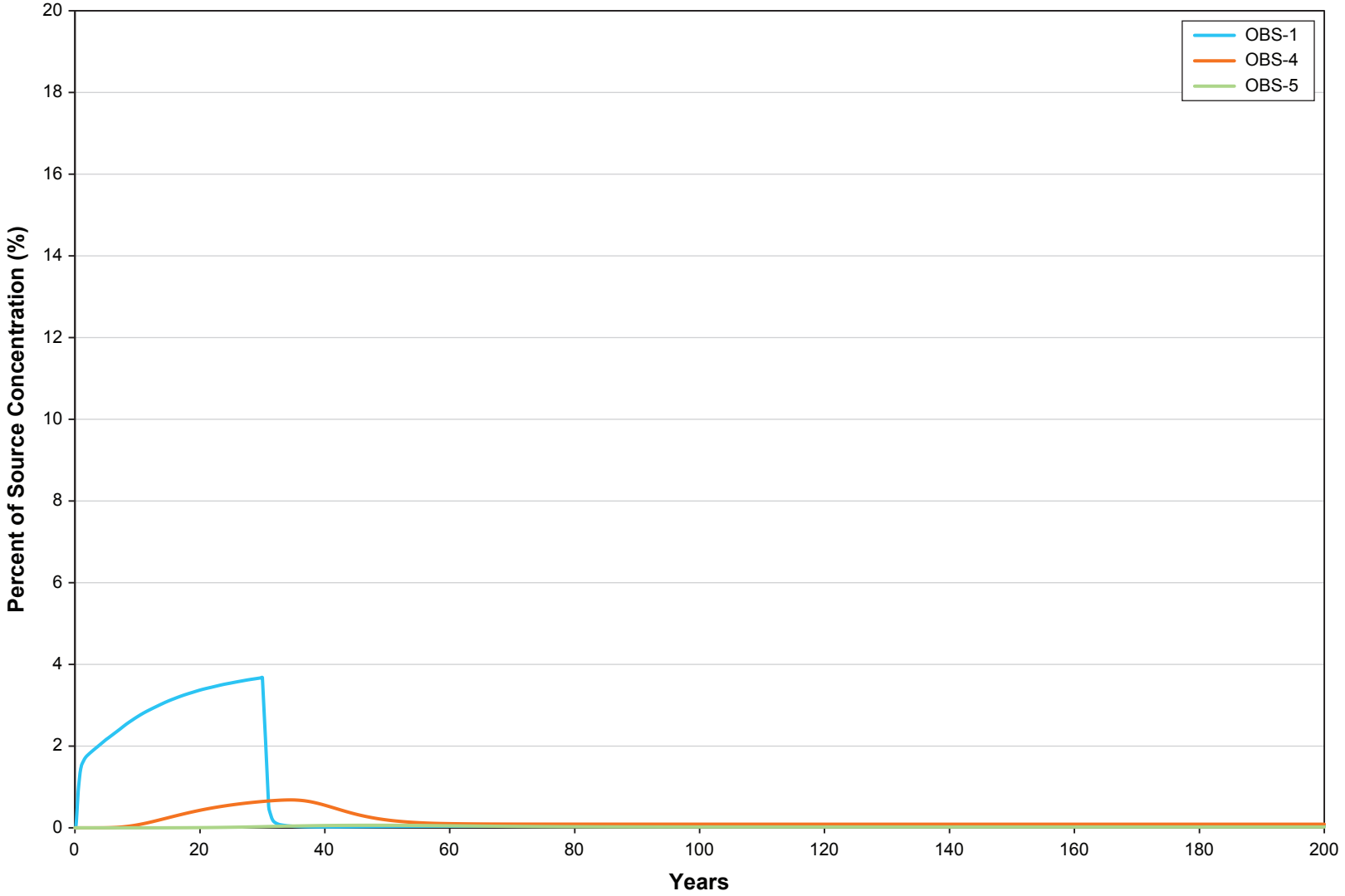

Wetter climate scenario predicts that the maximum concentration will reach 18% at OBS-17 at the end of full operation of the CCR Piles. The concentrations calculated for other points are 6% or less at the end of full operation of the CCR Piles. The concentrations during the post-closure period gradually decrease.

Higher permeability scenario predicts that the maximum concentration will reach 4.4% at OBS-17 at the end of full operation of the CCR Piles. The concentrations calculated for other points are 1.7% or less at the end of full operation of the CCR Piles. The concentrations during the post-closure period gradually decrease.

Finally, lower permeability scenario predicts that the maximum concentration will reach 16% at OBS-17 at the end of full operation of the CCR Piles. The concentrations calculated for other points are 3.6% or less at the end of full operation of the CCR Piles. The concentrations during the post-closure period gradually decrease.

Those model predictions are based on a conservative assumption that 5% of the entire area of synthetic liners (to be installed under each of the CCR Piles) will fail completely. This is considered unlikely. A 2% value is judged more realistic. This conservatism offsets the uncertainty associated with the 10 m value of the dispersivity used in the model.

The Murray River Project Groundwater Model was also used to analyze the impact of CCR South Pile constructed without a synthetic liner at its bottom. Under this alternative design, leachate plume originating from the South Pile would be controlled by installation of a network of drains placed below the Pile. The model simulations showed that the rates of plume interception by the drainage network would range from 51.9% to 95.8%, depending on the model scenarios. The model calculated maximum concentration (as OBS-17) would reach at year 30 about 40% of the concentration at the CCR source at the end of full operation of the CCR Piles. Those model results in part influenced a redesign of the South CCR Pile to include the use of a synthetic liner.

7. MODEL LIMITATIONS

As of June 2014, all the values of hydraulic conductivity were derived from slug and packer tests (one exception is a pump test preformed on one deep borehole, H2). These tests could underestimate the large-scale bulk permeability of the materials. No test data are available for characterization of anisotropy of the materials. The anisotropy ratios (horizontal vs. vertical) were assumed based on the professional judgment, the previous project experience, and the industry standard practice.

It has been widely accepted in the groundwater modelling practice for large-scale mining and resources development that the "equivalent porous medium approach" can be used to represent fractured bedrock for characterization of bulk permeability. However, this approach has limitations with respect to representing discrete flow pathways such as along fractures and faults. The bedrock formations found in the mine area contain a number of regional and less extensive faults. This limitation has implications for accurate simulation of groundwater flow at the small site scale, but it is not expected to drastically affect accuracy of the simulation results at the large scale for this Project.

The main perceived uncertainties associated with the conceptual model, model parametrization and, consequently, model predictions of the mine dewatering impacts stem from the following information shortages:

- a limited database characterizing deep groundwater conditions;
- lack of data on hydrogeological significance of the faults present in the rock formations above and around the mine; and
- difficulty associated with estimating the magnitude of mining-caused subsidence and altering of bulk hydraulic properties of the rock formations above and around the mine that subsidence may cause.

The first source of model uncertainties can be addressed by drilling additional deep boreholes and their hydraulic testing and sampling, as well as the information to be collected during the bulk sampling. Monitoring conducted during bulk sampling will produce a significant amount of important data.

The other two sources of uncertainties may be addressed after the actual mine operations are started. Those uncertainties can be decreased with time via systematic monitoring of groundwater levels, discharge in M20 Creek, and the rate of groundwater inflow into the mines, once the mine starts operations.

It is ERM's professional judgment that uncertainties associated with solute transport model version developed for evaluating the CCR Site are associated mainly with a high heterogeneity of the overburden soils in the area of CCR Piles. However, because both CCR Piles will be constructed using a synthetic liner at its bottom and also being covered on the top after their closure, the risks associated with the Piles' operation are limited and the possible impacts will be detected by systematic monitoring that may be carried out using the proposed network of the monitoring wells.

8. CONCLUSIONS AND RECOMMENDATIONS

Dewatering of the underground mine will result in a long-term lowering of water table above the mine and some loss in M20 Creek's baseflow. Those effects are predicted to be more significant when using the upper case and uppermost case scenarios of the model. Such effects should be closely monitored after the mine starts operations. The proposed monitoring activities include monitoring: (1) water levels in the wells, (2) discharge in M20 Creek, (3) subsidence and (4) rates of groundwater inflow into the mine.

The model predicted rates of groundwater inflow into the mine range from 1,891 m^3/day (for base case scenario) to 12,748 m^3/day (for uppermost case scenario 2). This uppermost case value is similar to 13,152 m^3/day, a conservatively calculated value for the "first prospecting area", as provided by the No.173 Prospecting Party of China National Administration of Coal Geology.

Those model calculated inflow rates represent steady-state conditions reached when the cone of depression matures. At the start of dewatering the inflow rates are typically higher due to higher hydraulic gradients around the dewatering area. Consequently, the model calculated rates underestimate the rates that could be expected if the entire mine were to be open right at the start of the mine operations. However, in reality, mining operations will develop gradually. In addition, during late phases of the mining, part of the previously mined out areas may be allowed to flood.

Maximum model predicted drawdowns caused by underground mine dewatering range from 2.5 m (for base case scenario) to 19.5 m (for uppermost case scenario 2).

After the mining operations are finished, it is conservatively estimated that filling the post-mine voids with naturally infiltrating groundwater will take from 24 years (for uppermost case scenario) to 164 years (for base case scenario). Once the post-mine voids are completely filled, groundwater levels lowered by mine dewatering will start recovering. The model calculations show that it will take 40 years for water table to reach 80% recovery toward the pre-mining levels. Those 40 years need to be added to the time required for post-mine void filling up with groundwater to estimate the time required for water table recovery.

The minimum times for the contact groundwater water (groundwater contacting the post-mine voids) to travel between the mine and the Murray River are calculated to range from 460 to 1,200 years, depending on the model scenario.

The range of the results generated from different model scenarios illustrate uncertainties associated with the model predictions, given available information and data. Some of these uncertainties can be significantly reduced by drilling additional deep boreholes and their hydraulic testing and sampling, as well as collecting information during the bulk sampling phase of this project.

Other uncertainties can be decreased in time via systematic monitoring of groundwater levels, discharge in M20 Creek, and the rate of groundwater inflow into the mines, once the mine starts operations.

The model pathline simulations show that groundwater flowing through the area of the CCR Piles discharges a short distance to the neighboring creeks. Due to this short distance, groundwater travel time from the edges of the CCR South Pile to the M19A Creek will be less than 10 years.

The model simulations of solute transport from the CCR Piles show that groundwater solute concentrations will reach their maximum 30 years after the start of the Piles' operations and, then, quickly decrease after the Piles' capping and closure. The maximum base case model calculated solute concentration reaching the nearby creeks is 9.4% of the concentration at the source (CCR Piles). The concentrations in other parts of the solute plume reaching the creeks are calculated to be about 3%. The maximum concentrations calculated by the other model scenarios range from 4.4% (for high permeability scenario) to 18% (for the wetter climate scenario).

The low value for high permeability scenario is explained by mixing of source water with groundwater entering the CCR Pile's footprint area from the up-gradient direction at a higher rate (compared to rates for lower permeability scenarios). The high value for wetter climate is caused by the higher rate of source loading (the rate of leachate migrating to groundwater from the bottom of CCR Pile) for that scenario, compared to the other scenarios. Those model predictions are based on a conservative assumption that a 5% of the entire area of synthetic liners (to be installed under each of the CCR Piles) will fail completely. This is considered unlikely. A 2% value is judged more realistic. Another conservative assumption is that both CCR Piles are full right at start of the 30-year long operation. In fact the South Pile may be opened only during the latest phases of the mine operations.

It is ERM's professional judgment that uncertainties associated with solute transport model version developed for evaluating the CCR Site are associated mainly with a high heterogeneity of the overburden soils in the area of CCR Piles. However, because both CCR Piles will be constructed using a synthetic liner at its bottom and also being covered on the top after the closure, the risks associated with the Piles' operation are limited. The possible impacts will be detected by systematic monitoring that may be carried out using the proposed network of the monitoring wells.

As the coal mine project progresses and new monitoring data are collected, the Murray River Groundwater Model can be adjusted, refined, re-calibrated and used in a predictive mode to assist in the planning of further mine operations.

REFERENCES

AMEC 2010. *Memorandum: Packer Testing to Assess Bedrock Permeability* Tumbler Ridge, B.C., From T. Kostya, AMEC to J. Luo, Canadian Dehua International Mines Group Inc.

AMEC. 2012. *Single Well Response Tests: Proposed Murray River Underground Coal Mine*, Tumbler Ridge, BC. Submitted to Canadian Dehua International Mines Group Inc. by AMEC Environment and Infrastructure, Kamloops, BC.

AMEC. 2013. *Mine Inflow Design Parameters – Proposed Bullmoose Underground Coal Mine*, Tumbler Ridge, BC. Submitted to Canadian Dehua International Mines Group Inc. by AMEC Environment & Infrastructure, 13 February 2013.

ASTM. 1996. *Americal Society of Civil Engineers Hydrology Handbook*. ASCE Manuals and Reports on Engineering Practice No. 28.

BGC. 2009. TML, *Prosperity Gold-Copper Project Numerical Hydrogeologic Analysis - Final Report*, Prepared for Taseko Mines Ltd. by BGC Engineering Inc. June 12, 2009.

BC MOE. 2012. *Guidelines for Groundwater Modelling to Assess Impacts of Proposed Natural Resource Development Activities*, Prepared by Dr. Christoph Wels et al. for British Columbia Ministry of Environment, Water Protection & Sustainability Branch. April 2012.

Cho, H. J. 2009. Memo: *Update of MODFLOW model of Davidson Project*. Prepared on behalf of Rescan Environmental Services Ltd.

Davis, J. H. 2003. *Fate and transport modelling of selected chlorinated organic compounds at Hangar 1000*, U.S. Naval Air Station, Jacksonville, Florida. Tallahassee, FLA: US Geological Survey.

Domenico, P.A. and M.D. Mifflin, 1965. Water from low-permeability sediments and land subsidence, *Water Resources Research*, vol. 1, no. 4., pp. 563-576.

Dorsch, J. and T. J. Katsube. 1996. *Effective porosity and pore-throat sizes of mudrock saprolite from the Nolichucky shale within Bear Creek valley on the Oak Ridge Reservation: Implications for contaminant transport and retardation through matrix diffusion*. Oak Ridge National Laboratory, Department of Energy, Oak Ridge, Tennesse, USA.

ERM Rescan. 2014a. *Murray River Coal Project: 2011-2013 Hydrology Baseline Report.* Prepared for HD Mining International Ltd. by ERM Rescan: Vancouver, British Columbia, March 2014.

ERM Rescan. 2014b. *Murray River Coal Project: Cumulative Hydrogeology Baseline Report.* Prepared for HD Mining International Ltd. by Rescan Environmental Services Ltd.: Vancouver, British Columbia, June 2014.

ERM Rescan. 2014c. *Murray River Coal Project: Water Quantity and Quality Modelling Report*. Prepared for HD Mining International Ltd. by Rescan Environmental Services Ltd.: Vancouver, British Columbia, June 2014.

Fetter, C. W. 2001. *Applied hydrogeology*. Fourth Edition. New Jersey: Prentice Hall.

Freeze, R. A. and J. A. Cherry. 1979. Groundwater. Upper Saddle River, NJ: Prentice Hall.

Garber J. 2011. Tectonic History of British Columbia: Historical and Current Influences on the Chilko-Chilkotin-Frasier River System. Chapter 1 of Ecogeomorphology of the CCR – Field Guides, *Ecogeomorphology of British Columbia* (https://www.geology.ucdavis.edu/~shlemonc/trips/CCR_11/fieldguide.htm, University of California, website last updated September 2011).

Gelhar, L. W., C. Welty, and K. R. Rehfeldt (1992). A critical review of data on field-scale dispersion in aquifers, *Water Resour. Res.*, 28(7), 1955–1974, doi:10.1029/92WR00607.

Gleeson, T. and A. H. Manning. 2008. Regional groundwater flow in mountainous terrain: Three-dimensional simulations of topographic and hydrogeologic controls. *Water Resour. Res.*, 44, W10403, doi:10.1029/2008WR006848.

Golder Associates. 2013a. *Vertical Shaft Pilot Hole Data Report – Draft*. HD Mining International Ltd. Murray River Coal Project, Tumbler Ridge, British Columbia, Canada, March 21, 2013.

Golder Associates. 2013b. *Hehua Wapiti River Project – Hydrogeological In-situ Testing Program*. Submitted to Canadian Dehua International Mines Group Inc. by Golder Associates, July 4, 2013.

Harbaugh, A. W., E. R. Banta, M. C. Hill, and M. G. McDonald. 2000. MODFLOW-2000, The U.S. Geological Survey Modular Ground-Water Model – User Guide to the Modularization Concepts and the Ground-Water Flow Process. *U.S. Geological Survey, Open File Report* 00-92, 130 p. Reston, Virginia.

Huiyong Holding Group. 2011. *Coal Exploration Report for the First Prospecting Area of the Murray River Coal Property in Northeastern British Columbia, Canada*, No.173 Prospecting Party of China National Administration of Coal Geology, July 2011.

HydroGeoLogic Inc. 1996. *MODFLOW-SURFACT ver. 3.0 User's Manual*. A three dimensional fully integrated finite difference code for simulating fluid flow and transport of contaminant in saturated-unsaturated porous media. Herndon, VA 20170, USA.

Johnson, A.I. 1967. Specific yield — compilation of specific yields for various materials. *U.S. Geological Survey Water Supply Paper* 1662-D. 74 p.

Jones, P. M. 2002. Characterization of ground-water flow between the Canisteo mine pit and surrounding aquifers, Mesabi Iron Range, Minnesota. Mounds View, Minnesota: U.S. Geological Survey, *Water Resources Investigations Report* 02-4198.

Larry, B., H. Amy, B. Phillip, and H. Mike. 2005. Hydrogeologic investigation of the gold reserve incorporated Brisas del Cuyuni Concession in southeast Venezuela. Oviedo, Spain: Proceedings of the *9th International Mine Water Congress*.

Li, H. 1995. Effective porosity and longitudinal dispersivity of sedimentary rocks determined by laboratory and field tracer tests. *Environmental Geology*, 25:71-85.

Lorax Environmental 2007. *Application for an Environmental Assessment Certificate for the Hermann Mine Project* submitted by Western Canadian Coal to Bob Hart (British Columbia Environmental Assessment Office) February 2007. Volume 2: Main Document - Part 2, Section 8 – Groundwater, Section 12 – Terrain and Soils.

Loukas, A. and M.C. Quick. 1993. Rain Distribution in a Mountainous Watershed. *Nordic Hydrology*, 24(4): 225 – 242.

Lyford, F. P., C. S. Carlson, C. J. Brown, and J. J. Starn. 2007. *Hydrogeologic setting and ground-water flow simulations of the Pomperaug River Basin Regional Study Area*, Connecticut. Reston, VA: US Geological Survey.

Mahajan O.P and P.L. Walker Jr. 1978. *Porosity of Coal and Coal Products*. Coal Research Section of the Pensylvania State University. PSU-TR-7. March 1978.

Malkki, E. 2003. Groundwater flow conditions in the coastal bedrock area of the Gulf of Finland. *Geological Quarterly*, 47(3): 299-306.

Mehl, S.W., and Hill, M.C., 2001. MODFLOW-2000, The U.S. Geological Survey Modular Ground-Water Model - User Guide To The Link-AMG (LMG) Package For Solving Matrix Equations Using An Algebraic Multigrid Solver. *U.S. Geological Survey Open-File Report* 01-177.

Morris, D.A. and A.I. Johnson. 1967. Summary of hydrologic and physical properties of rock and soil materials as analyzed by the Hydrologic Laboratory of the U.S. Geological Survey. *U.S. Geological Survey Water-Supply Paper* 1839-D, 42p.

Niemann, W. L. and Rovey, C. W. 2009. A systematic field-based testing program of hydraulic conductivity and dispersivity over a range in scale. *Hydrogeology Journal*, 17: 307-320.

No. 173 Prospecting Party of China National Administration of Coal Geology. 2011. *Coal Exploration Report for the First Prospecting Area of the Murray River Coal Property in Northeastern British Columbia, Canada*. Compiled for Huiyong Holding Group Co., Ltd. by No. 173 Prospecting Party of China National Administration of Coal Geology July 2011.

Norwest Corporation. 2010. *Geology and Coal Resources of the Murray River Coal Property*, Peace River Coalfield, British Columbia. Submitted to Canadian Dehua International Mines Groun Inc., June 30, 2010.

Pollak, D.W. 1994. User's Guide for MODPATH/MODPATH-PLOT, Version 3: A Particle tracking post-processing package for MODFLOW, the U.S. Geological Survey finite-difference ground-water flow model: *US Geological Survey Open-File Report* 94-464, 6ch.

Rescan. 2009a. *Morrison Copper/Gold Project Hydrogeological Modelling Report*. Prepared for Pacific Booker Minerals Inc. by Rescan Environmental Services Ltd.

Rescan. 2009b. *Update of MODFLOW Model of Davidson Project*. Memorandum by H. Jean Cho, Ph.D., P.Eng., March 4, 2009.

Rescan. 2011. *Murray River Coal Project: 2011 Terrain and Soils Baseline Report: 2011-2012.* Prepared for HD Mining International Ltd. by Rescan Environmental Services Ltd.: Vancouver, British Columbia, November 2011.

Rescan. 2013a. *Murray River Coal Project: Hydrology Cumulative Baseline Report: 2011-2012.* Prepared for HD Mining International Ltd. by Rescan Environmental Services Ltd.: Vancouver, British Columbia, May 2013.

Rescan. 2013b. *Murray River Coal Project: 2011-2012 Cumulative Meteorology Baseline.* Prepared for HD Mining International Ltd. by Rescan Environmental Services Ltd.: Vancouver, British Columbia, May 2013.

Rescan. 2013c. KSM Project. *Updated Hydrogeology Modelling Report*, June 2013. Prepared for Seabridge Gold Inc. by Rescan Environmental Services Ltd.

Rescan. 2013d. *Murray River Hydrometeorology Report* - Memorandum to Jason Rempel authored by Ali Naghibi, Ph.D., P.Eng., Natasha Cowie, M.Sc. and David Luzi, M.Sc. Rescan – an ERM Company, August 30, 2013.

Schulze-Makuch, D. 2005. Longitudinal dispersivity data and implications for scaling behaviour. *Ground Water*, Vol. 43, No. 3, Pages 443-456.

Schlumberger. 2008. *Visual MODFLOW Premium Version 4.3*. Schlumberger Water Services.

Shapiro, A. M. 2001. Effective matrix diffusion in kilometre-scale transport in fractured crystalline rock. *Water Resources Research* 37(3): 507-522.

SRK. 2012. *Quintette Groundwater Technical Assessment Report* - Appendix 4-7-A Groundwater Technical Data – Report prepared for Teck Coal Corporation, March 2012.

Stone, D. B. and R. C. Fontaine. 1998. Simulation of groundwater fluxes during open-pit filling and under steady state pit lake conditions. Proceedings of *1998 Conference on Hazardous Waste Research*, Snowbird, Utah, USA.

Tòth, J.A. 1962. A Theory of Ground-Water Motion in Small Drainage Basins in Central Alberta, Canada. In: *Journal of Geophysical Research*, 67, No. 11, pp: 4375-87.

Van der Leeden F., F.L. Troise and D.K. Todd. 1990. *The Water Encyclopedia*. Second Edition, Lewis Publishers.

Water Management Consultants. 2008. Analytical methods and numerical models, appendix V of *MT. Milligan Copper-Gold Project Environmental Assessment*.

Wels, C., L. Findlater, and C. McCombe. 2006. *Assessment of groundwater impacts at the historic Mount Morgan Mine Site, Queensland, Australia*. Paper presented at Proceedings of the 7th ICARD (International Conference on Acid Rock Drainage), St Louis, MO.

Wels, C. and L. L. Findlater. 2009. *Groundwater modelling as a tool for closure planning: prediction of zinc transport for alternative cover scenarios*. Securing the Future and 8th ICARD (International Conference on Acid Rock Drainage), Skelleftea, Sweden.

Zheng, C. and P. P. Wang. 1999. *MT3DMS: A modular three-dimensional multispecies transport model for simulation of advection, dispersion and chemical reactions of contaminants in groundwater systems: Documentation and user's guide*. Vicksburg, Mississippi: U. S. Army Corps of Engineers, U. S. Army Engineer Research and Development Center.

Zhou, Q., H. H. Liu, F. J. Molz, Y. Zhang, and G. S. Bodvarsson. 2007. Field-scale effective matrix diffusion coefficient for fractured rock: results from literature survey. *Journal of Contaminant Hydrogeology*, 93:161-187.

Appendix A

Murray River Geologic Model Memorandum

Memorandum

Refer to File No.: \\server04\publishing\Murray River\2014 Geology Model Memo\0.3 MUR_GC_Geology Model.docx

Date: June 04, 2014

To: Piotr Rzepecki

From: Mark Nelson

Cc: Kelsey Norlund, Jason Rempel

Subject: **Memorandum: Murray River Geological Model**

A three dimensional (3D) geology model of the stratigraphy above and hosting the coal seams at the Murray River Project was not available to provide cross sections incorporating hydrogeology data. Seismic interpretations were matched to and modified by down hole geology to generate a 3D geology model that can be cut to produce various visualizations of the data.

This 3D geology model was generated to allow for visualization of overall structure within the Murray River Project area. The model is not detailed enough to act aid in any resource or reserve estimation as the error on faults and lithological contacts exceeds ±10m.

1. METHODOLOGY

The geology model was generated by blending seismic interpreted cross sections generated by HD Mining (No. 173 Prospecting Party of China National Administration of Coal Geology 2011) with stratigraphic interpretations presented in exploration drill logs.

1.1 Limitations

The stratigraphic interpretations do not differentiate between units above the Boulder Creek Formation. All material above Boulder Creek Formation is logged as Hasler Formation. The thickness of the material indicates that some of the material should belong to overlying units (Dunvagen, Cruiser, or Goodrich Formations).

The complexity of the shape of the overlying, undifferentiated material and its uncertain origin made modelling the material difficult and resulted in its exclusion from the final 3D model.

Faults interpreted from the seismic survey did not always match the exploration drill logs. Additionally not all faults were presented in all the HD Mining cross sections. It was assumed that faults interpreted from the seismic survey were large or persistent enough that they should appear in all cross sections. When faults were inferred between sections they were labelled as inferred. An example of this reinterpretation is presented in Figure 1.1-1.

Deep drill holes or seismic survey results do not extend under the proposed Coarse Coal Reject site to the west of the Murray River. Consequently the geological model does not cover that region.

Appendix A contains notes made during the interpretation process.

Figure 1.1-1

Comparison Between Seismic and Exploration Interpreted Geology

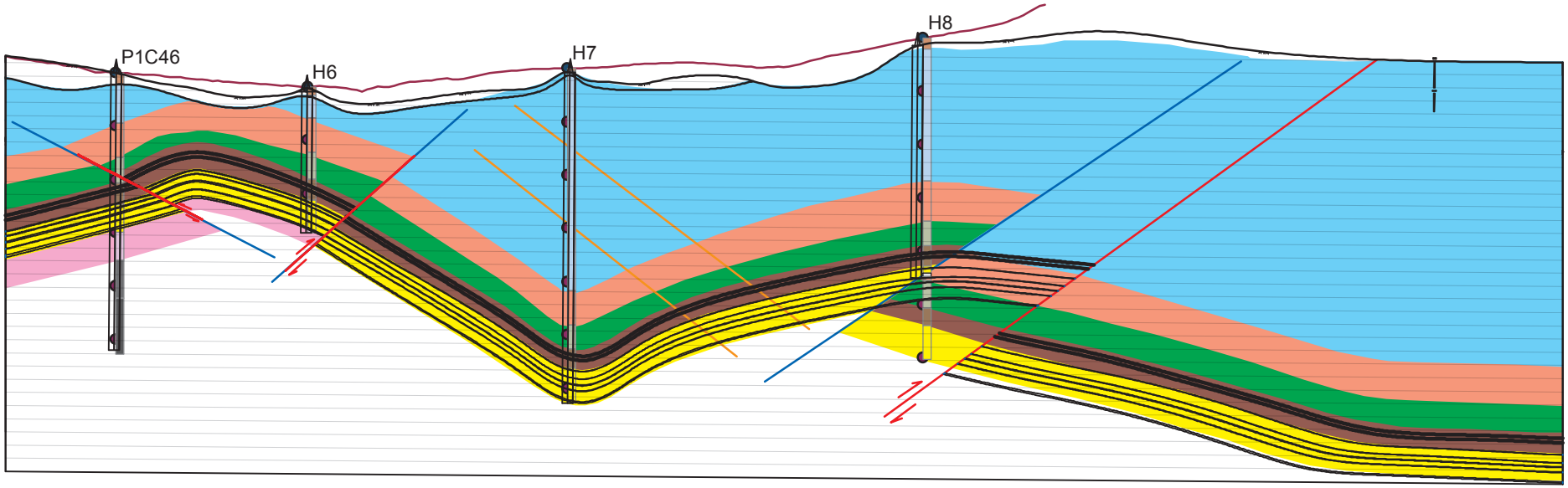

1.2 Process

A summary of the process is listed below:

1. Import location and down hole stratigraphy information of exploration and hydrogeology drill holes.
2. Choose eight cross section locations that closely match the seismic interpreted sections and plot preliminary cross sections displaying topography, drill hole trace, and down hole stratigraphy.
3. Import the eight seismic interpreted cross sections generated by HD Mining (No. 173 Prospecting Party of China National Administration of Coal Geology 2011).
4. Georeference the eight seismic interpreted cross sections in the preliminary drill hole cross sections so that they are hanging in 3D space correctly.
5. Compare the seismic interpreted stratigraphy and the down hole stratigraphy sections to determine discrepancies between interpreted and logged coal seams and faults.
6. Adjust seismic interpreted faults to account for potential faults in the exploration drill logs. Add new interpreted faults not present in the seismic interpretations. The new interpreted faults were added to the geology model to help the software interpolate between sections.
7. Digitize geology in each section using the shape of the seismic interpreted coal seams as a guide for the form of the stratigraphic contacts.
8. When each section was complete the geology was interpolated between sections to create volumes.

2. RESULTS

The primary result of the modelling exercise was the generation of a 3D geology model. The extent of three cross sections through the model are presented in Figure 2-1. Three cross sections are presented in Figures 2-2 to 2-4 and a 3D perspective of the geologic cross sections used to generate the 3D model are presented in Figure 2-5.

Figure 2-1

Plan Map Illustrating Extents of Cross Sections

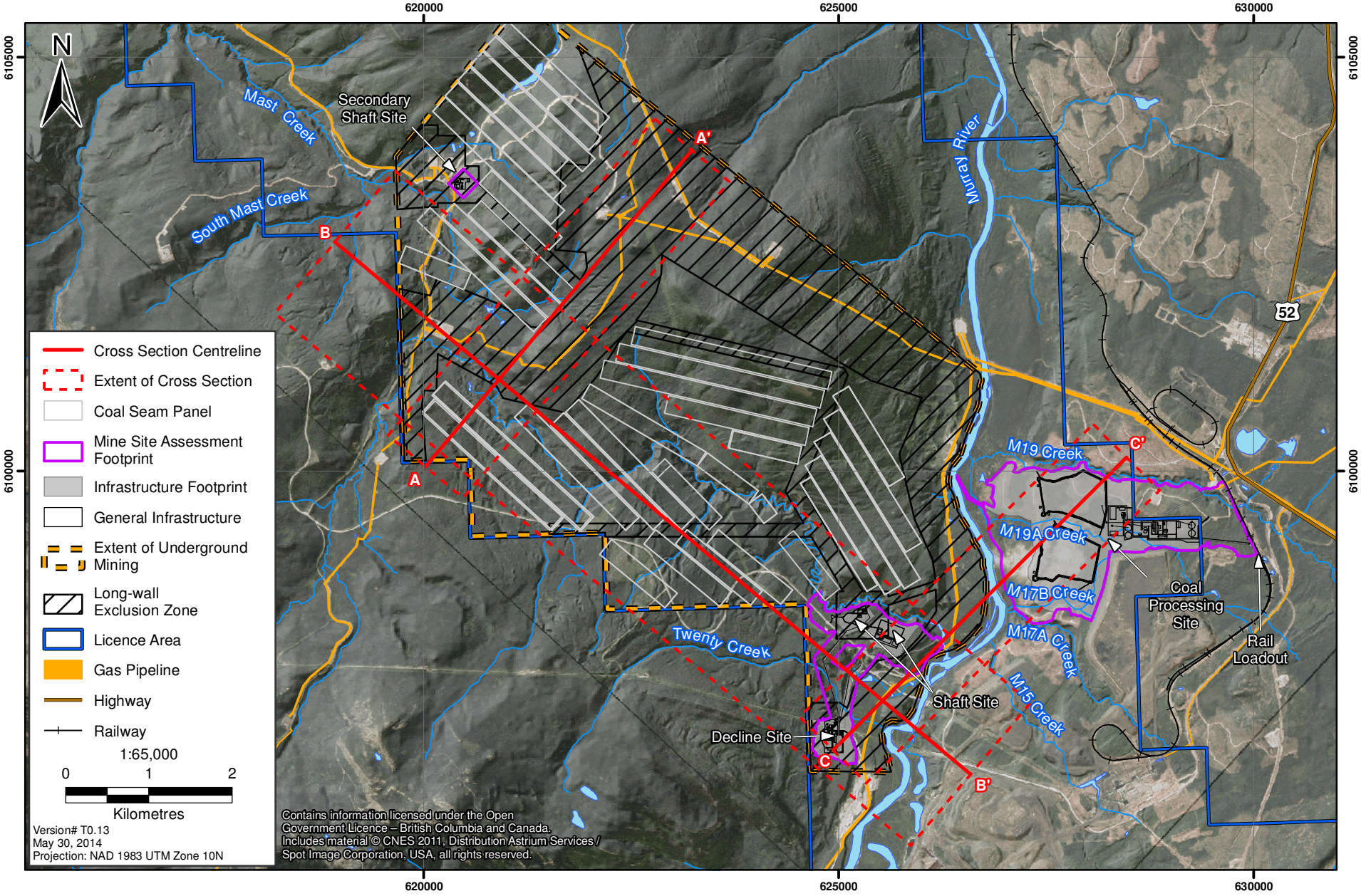

Figure 2-2
Cross Section A-A'

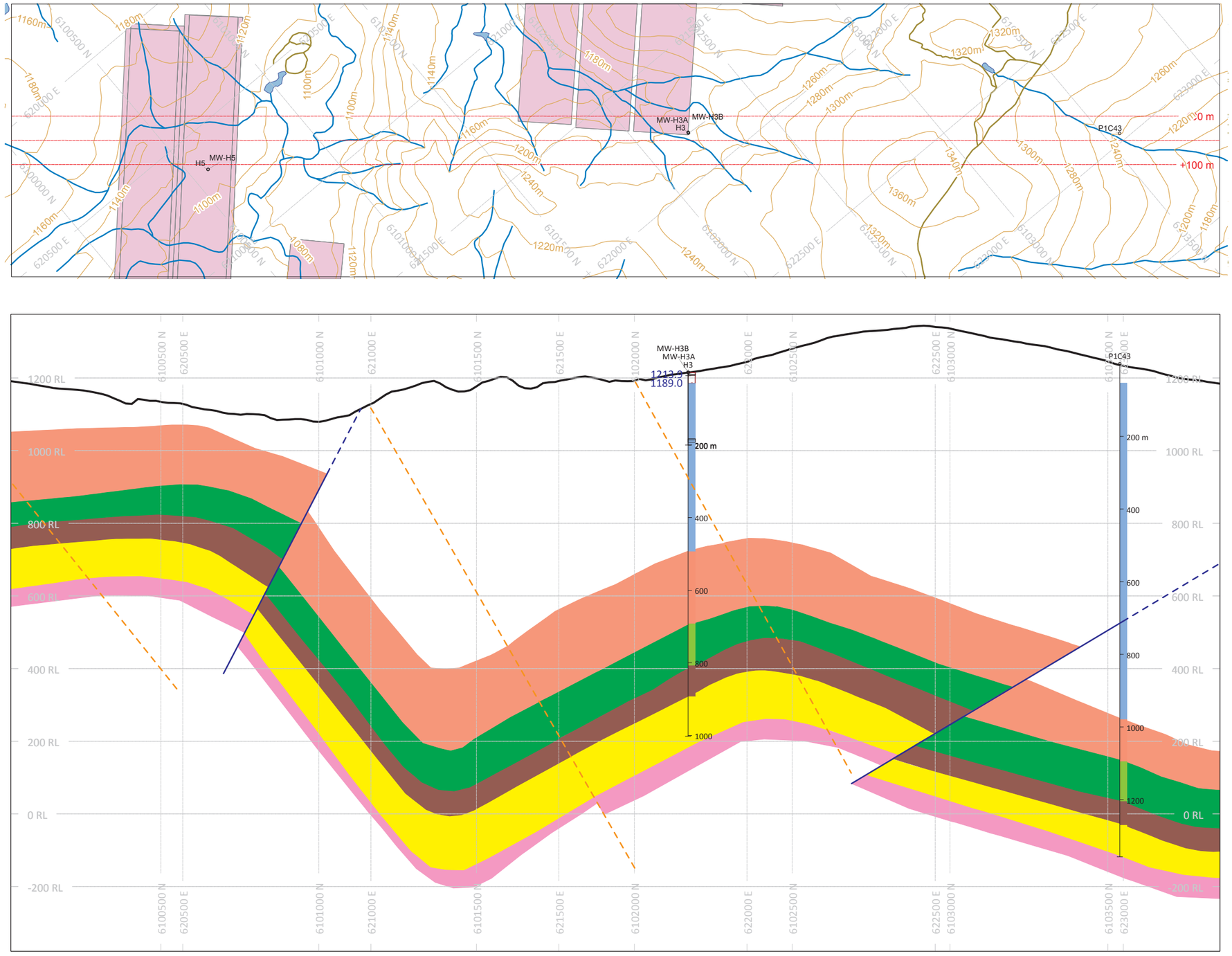

HOLES PLOTTED

TOTAL 4

H3 MW-H3A MW-H3B P1C43

- Contours
- Transportation
- Stream
- Coal Seam Panel
- Water Wetlands
- Powerline
- Conveyor
- Structure
- Concrete Paving
- Coarse Coal Reject Pile
- Pad
- Pond
- Collection Pipe
- Diversion Channel
- Topography
- Overburden
- Hasler and undifferentiated
- Boulder Creek
- Hulcross
- Upper Gates
- Middle Gates
- Lower Gates
- Hydrogeology Well
- 777.8 Water Table
- Fault, Interpretted from Geophysics
- Fault, Inferred

SECTION SPECS:

REF. PT. E, N	621650 m	6101940 m
EXTENTS	5000 m	1754 m
SECTION TOP, BOT	1375 m	-378.5 m
TOLERANCE +/-	100 m	
VERTICAL EXAG.	1.5 m	

SCALE
(m)
-100 0 100 200 300 400 500
NAD83 / UTM zone 10

AZIMUTH = 45°
N
W E
S

Figure 2-3
Cross Section B-B'

DRAFT

ERM

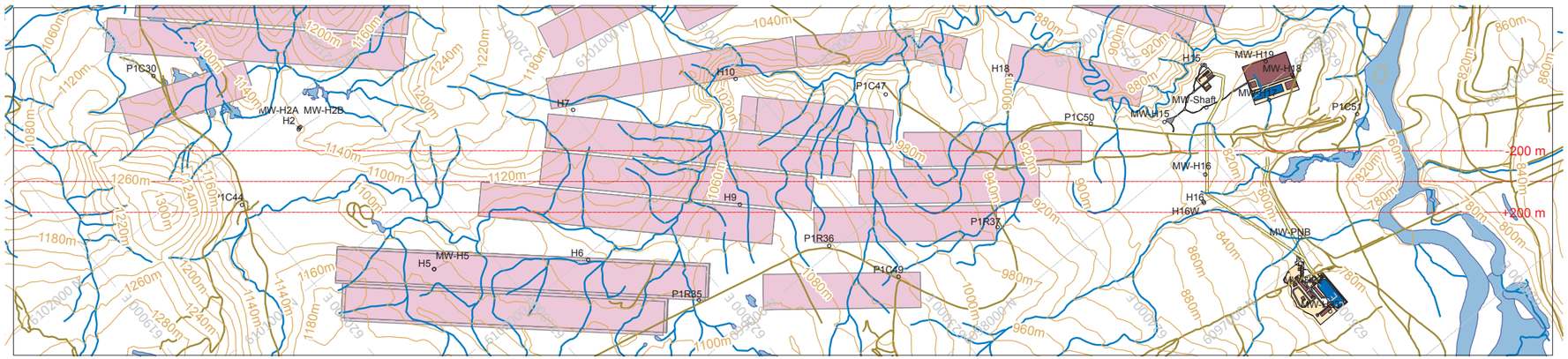

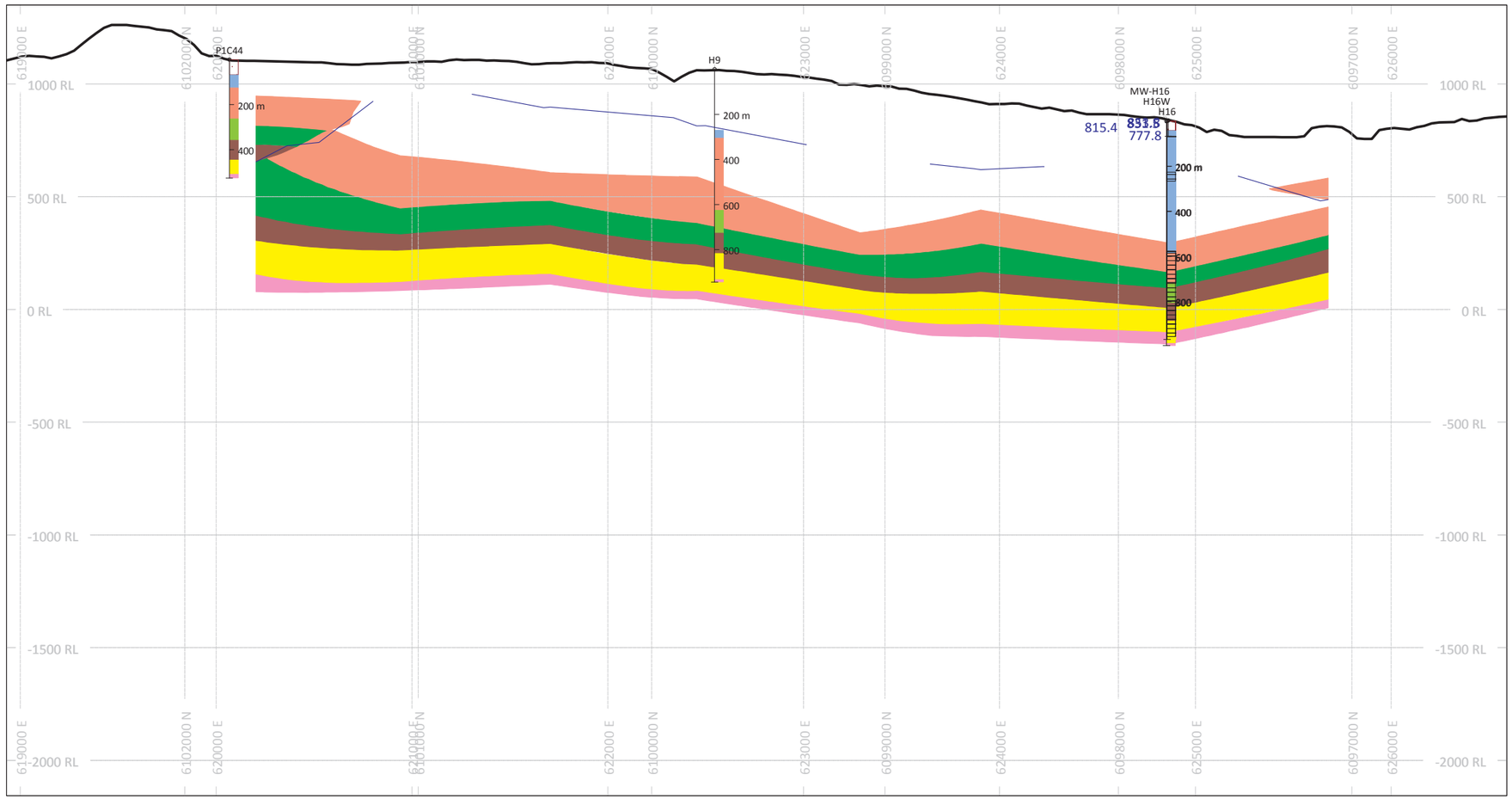

HOLES PLOTTED

TOTAL 5

H16 P1C44 | H16W | H9 | MW-H16

- Contours
- Transportation
- Stream
- Coal Seam Panel
- Water Wetlands
- Powerline
- Conveyor
- Structure
- Concrete Paving
- Coarse Coal Reject Pile
- Pad
- Pond
- Collection Pipe
- Diversion Channel
- Topography
- Overburden
- Hasler and undifferentiated
- Boulder Creek
- Hulcross
- Upper Gates
- Middle Gates
- Lower Gates
- Hydrogeology Well
- 777.8 Water Table
- Fault, Interpretted from Geophysics
- Fault, Inferred

SECTION SPECS:

REF. PT. E, N	622760 m	6099550 m
EXTENTS	10000 m	3508 m
SECTION TOP, BOT	1351 m	-2157 m
TOLERANCE +/-	200 m	
VERTICAL EXAG.	1.5 m	

SCALE
(m)
-200 0 200 400 600 800 1000
NAD83 / UTM zone 10

AZIMUTH = 130°
N W E S

Figure 2-4
Cross Section C-C'

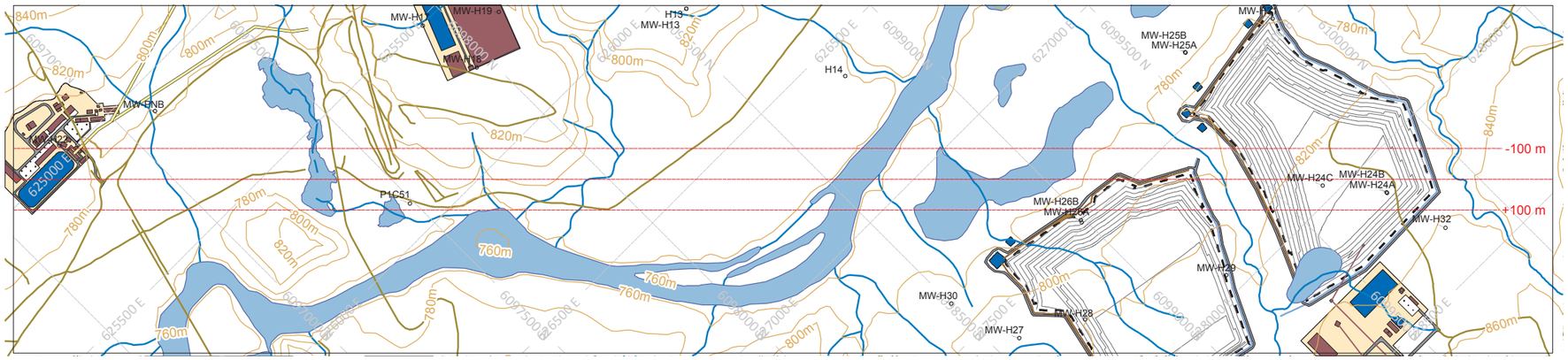

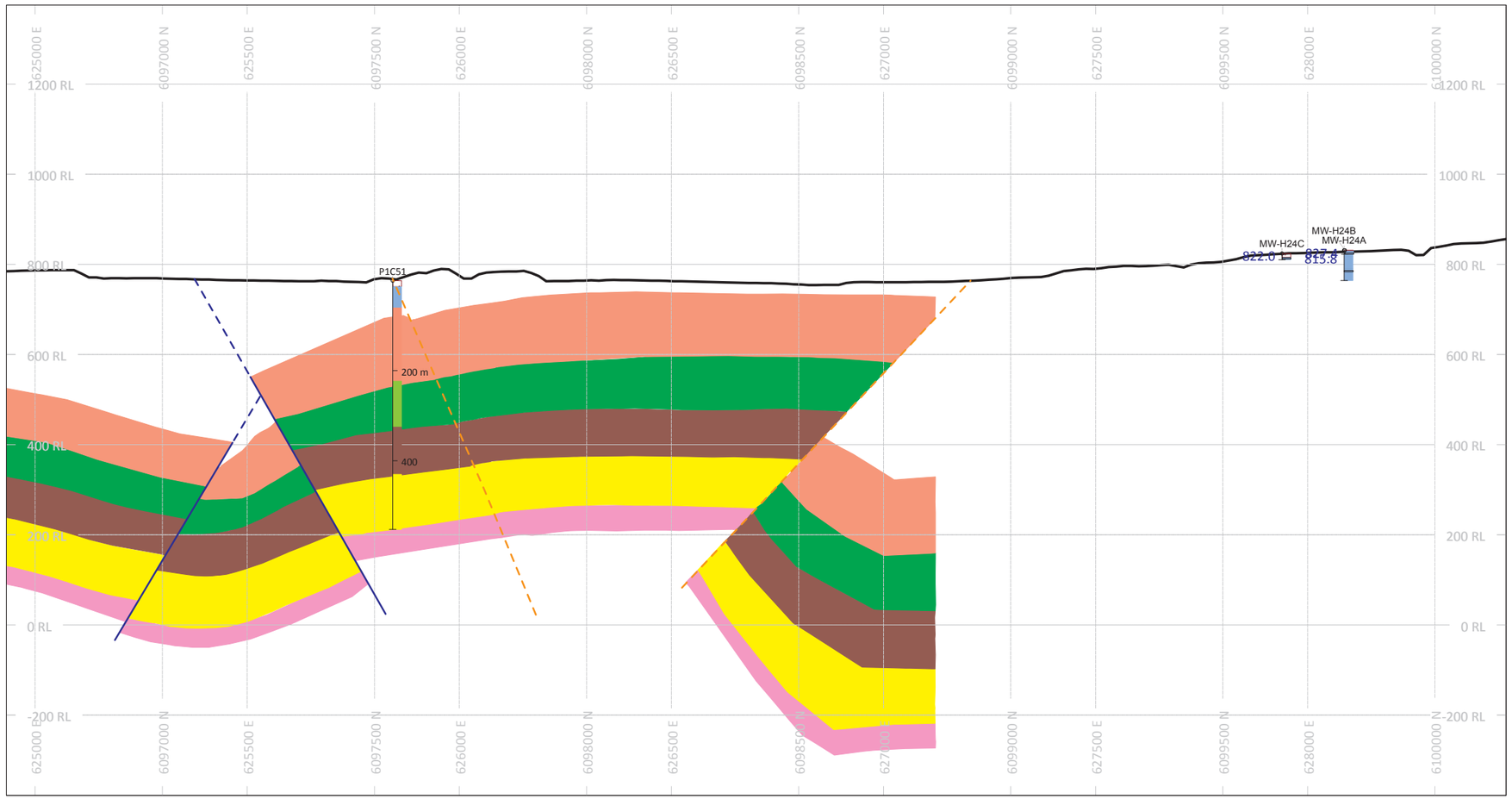

HOLES PLOTTED

TOTAL 4

MW-H24A MW-H24B MW-H24C P1C51

- Contours
- Transportation
- Stream
- Coal Seam Panel
- Water Wetlands
- Powerline
- Conveyor
- Structure
- Concrete Paving
- Coarse Coal Reject Pile
- Pad
- Pond
- Collection Pipe
- Diversion Channel

- Topography
- Overburden
- Hasler and undifferentiated
- Boulder Creek
- Hulcross
- Upper Gates
- Middle Gates
- Lower Gates
- Hydrogeology Well
- 777.8 Water Table
- Fault, Interpretted from Geophysics
- Fault, Inferred

SECTION SPECS:

REF. PT. E, N	626700 m	6098400 m
EXTENTS	5000 m	1754 m
SECTION TOP, BOT	1375 m	-378.5 m
TOLERANCE +/-	100 m	
VERTICAL EXAG.	1.5 m	

SCALE
(m)
-100 0 100 200 300 400 500
NAD83 / UTM zone 10

AZIMUTH = 45°
N
W E
S

Figure 2-5

3D Perspective View of Geologic Cross Sections

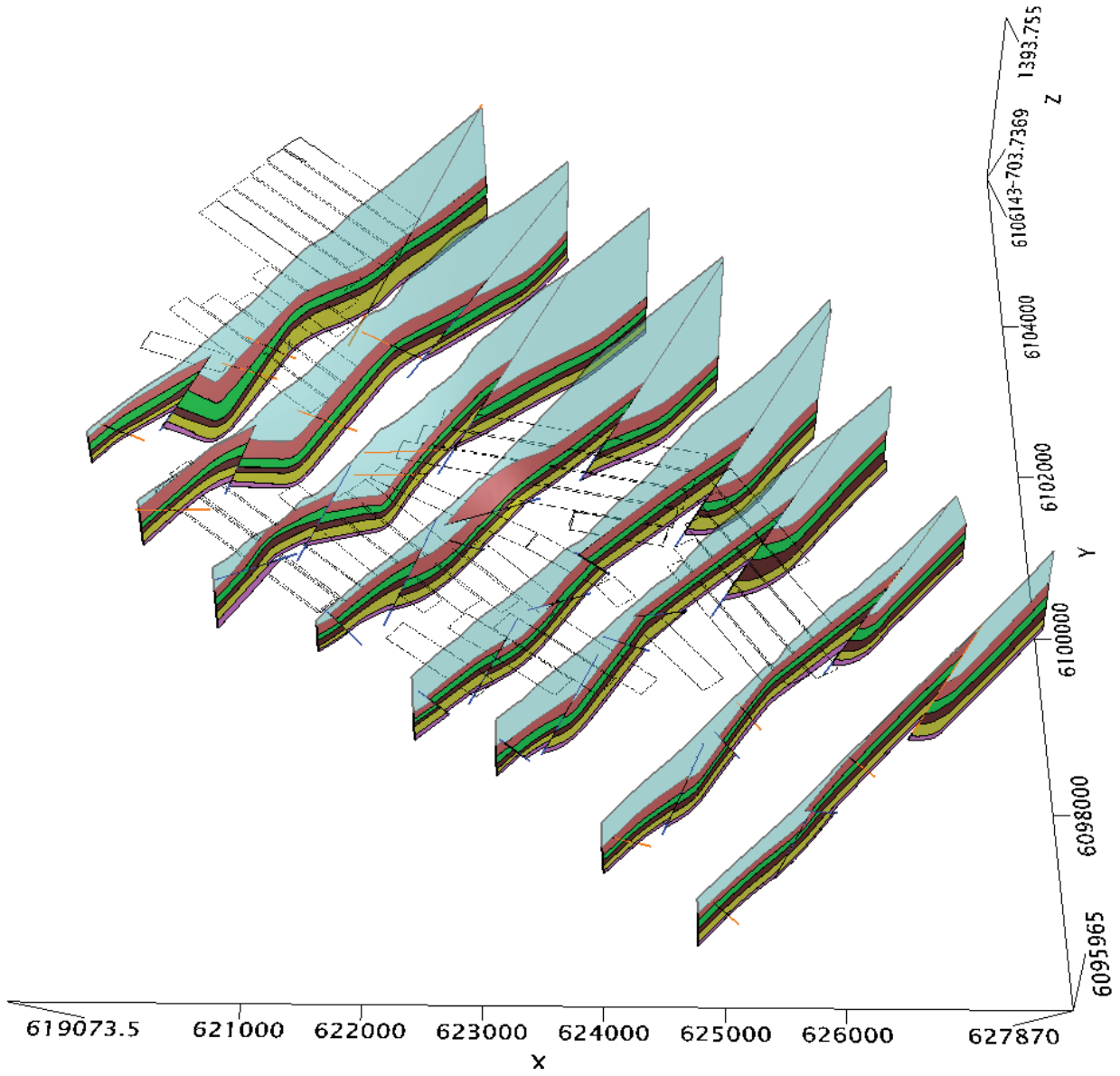

Prepared By:

Mark Nelson M.Sc. P.Geo., Consultant
ERM Rescan

REFERENCES

No. 173 Prospecting Party of China National Administration of Coal Geology. 2011. *Coal Exploration Report for the First Prospecting Area of the Murray River Coal Property in Northeastern British Columbia, Canada*. Compiled for Huiyong Holding Group Co., Ltd. by No. 173 Prospecting Party of China National Administration of Coal Geology July 2011:

APPENDIX A

— Notes —

- **Section 09**: no fault adjustments
- **Section 08**: near PIC48 – fault moved down due to repeating lithology in exploration drill logs AND slickenlines mentioned. No breccia/slickenlines mentioned at location of HD interpreted fault location
- **Section 07**: near PIR37 – moved fault up as thickened Boulder Creek and exploration logs indicate polished bedding plane and fractures ~600m down hole
  - near H21 – moved fault down as exploration log indicated bedding plane changes and broken rock at ~740m (Middle Gates)
- **Section 06**: no adjustments
- **Section 05**: near H9 – moved fault down from ~336 to ~420m because thickening of Boulder Creek and exploration logs indicate slickenlines between 426 and 460m. Fractures noted at ~330m
  - near H10 (middle) – moved fault up ~100m as thickened Boulder Creek and exploration log indicates bedding faults at ~480m and no fault fracture info at ~600m
- **Section 04**: not provided
- **Section 03**: near H8 – moved fault up ~450m because exploration log indicated fault unit at ~880m
  - did not modify (add) extra faults on H8 to account for thickening of Hasler Formation. I expect thick Hasler is due to incorrect core logging and should be Dunvegan or other overlying stratigraphy.
  - near H7 – added fault to intersect at ~300m based on exploration log broken core at ~300m and thickened Hasler and evidence of fault in Section 04
- **Section 02**: near PIC43 – moved fault down ~470m, thickening of Hasler with slickenlines mentioned in exploration logs between 680-740m and not in top 100m
  - no additional fractures added to PIC43 because probably incorrect stratigraphy, however broken core is noted in H3 between 200-290m so there is potential, although nothing noted in Section 03
  - near H3 – added fault, thickened Hasler and exploration log with broken core at ~200m and also present in Section 03 and 05. The fault seems out of sequence spatially with Section 03 and 05.
- **Section 01**: near H2 – fault adjusted/extended to account for slickenlines at ~100m. Hasler is still very thickened. Compressional fault noted in exploration log at 425m so a new fault added en echelon to existing